UNIVERSITY OF SOUTHAMPTON

FACULTY OF ENGINEERING, SCIENCE AND MATHEMATICS

School of Engineering Sciences

Combined Musculoskeletal and Finite Element Modelling of Total Hip Replacement to Account For Surgical And Patient Related Factors

by

Catherine Jane Manders

Thesis for the degree of Doctor of Philosophy

September 2010

UNIVERSITY OF SOUTHAMPTON

ABSTRACT

FACULTY OF ENGINEERING, SCIENCE AND MATHEMATICS
SCHOOL OF ENGINEERING SCIENCES

Doctor of Philosophy

COMBINED MUSCULOSKELETAL AND FINITE ELEMENT MODELLING OF TOTAL HIP REPLACEMENT TO ACCOUNT FOR SURGICAL AND PATIENT RELATED FACTORS

By Catherine Jane Manders

Muscle and hip contact forces were predicted using a musculoskeletal model which was combined with a finite element model to calculate the primary stability in a cementless total hip replacement stem. Similarities were found between the kinematics measured in the healthy subjects from this study and measurements published in the literature. The predicted hip contact forces were also similar to measured hip forces from the literature. Once good comparison with literature forces had been established the potential for using the combined modelling process to study surgical and patient related variability was investigated. The hip contact force varied between the modelled healthy subjects by more than four times body weight at toe off and the combined abductor muscle force was found to vary by more than two times body weight. The load cases predicted in the musculoskeletal models were used in a finite element model of an implanted cementless hip stem and variation was also found in the strain and micromotion at the bone-implant interface. Total hip replacement patients were compared to the healthy subjects and the hip contact force at toe off was found to be lower in the patients. At the first peak in hip contact force, the patients' hip contact and abductor forces were higher than the healthy subjects and this lead to higher femoral strain and micromotion. The study also investigated manipulating the musculoskeletal model to simulate post-surgical total hip replacement patients either by reducing the strength of specific muscles or by adjusting the hip centre of rotation. Adjusting muscle strengths to model surgical techniques did not produce substantial differences between models of different surgical approaches and the motion capture models were deemed to provide better insight into post-surgery behaviour. The scenarios modelling changes to the hip centre found that the displacement affects the hip contact and abductor muscle forces. However it is of a similar magnitude to the variation predicted between patients and has a lower reliability. This study found that using motion capture in association with combined musculoskeletal and finite element modelling produced reasonable variation between subjects which could be used to provide more detailed models for preclinical testing of total hip replacements. Further study should focus on using motion capture data in order to drive future finite element analysis and potentially improve the loading scenarios for preclinical testing.

Contents

List of tables

List of figures

Declaration of authorship

I, Catherine Jane Manders, declare that the thesis entitled:

Combined Musculoskeletal and Finite Element Modelling of Total Hip Replacement to Account For Surgical And Patient Related Factors

and the work presented in the thesis are both my own, and have been generated by me as the result of my own original research. I confirm that:

- this work was done wholly or mainly while in candidature for a research degree at this University;
- where any part of this thesis has previously been submitted for a degree or any other qualification at this University or any other institution, this has been clearly stated;
- where I have consulted the published work of others, this is always clearly attributed;
- where I have quoted from the work of others, the source is always given. With the exception of such quotations, this thesis is entirely my own work;
- I have acknowledged all main sources of help;
- where the thesis is based on work done by myself jointly with others, I have made clear exactly what was done by others and what I have contributed myself;
- parts of this work have been published as:

Manders, C., New, A. M. and Rasmussen, J. (2008) *Validation of Musculoskeletal Gait Simulation for Use in Investigation of Total Hip Replacement*. 16th Congress of the European Society of Biomechanics, Lucerne, Switzerland.

Manders, C. and Taylor, M. (2010) *How Does the Position of a Hip Replacement Affect the Femoral Strain? Journal of Biomechanics 43* (Supplement 1): S47-S47.

Manders, C. J. and New, A. M. (2009) *Effect of Surgical Approach on Femoral Strain Distribution after Total Hip Replacement.* 55th Annual Meeting of the Orthopaedic Research Society, Las Vegas, NV.

Signed: ……..

Date:…….

Acknowledgements

I would like to thank Depuy International and the School of Engineering Sciences, University of Southampton for the financial support of this work. The Institute of Mechanical Engineers and the Royal Academy of Engineers also provided funding to enable me to visit the AnyBody Research Group, Aalborg University. The AnyBody Research Group and AnyBody Technology company, in particular Prof. John Rasmussen, were really helpful when I visited them early in my project and they have continued to provide help and support throughout the project on any problems with the AnyBody modelling. I would like to thank Prof. Cathy Holt and Dr Gemma Whatling for their motion capture data of total hip replacement patients and healthy subjects. Thanks also go to Peter Worsely, who also provided motion capture data and invaluable help with the AnyBody system and general motion capture information.

I would like to thank my supervisors, past and present, Dr Andrew New and Prof. Mark Taylor for all their help and support through this project. Dr Andrew New was superb starting me off down this path and a big thank you to Prof. Mark Taylor for sorting out all my problems over the last couple of years in particular helping me to focus the work and patiently proofreading my thesis many times over. I would also like to thank my other proofreaders, my parents and particularly my husband Jon, who have listened to me struggling with the writing and just sat down and read through it for me. I would also like to thank all the members of the Bioengineering Sciences Research group at Southampton who have provided helpful insights into my work or just been there to commiserate with when things didn't go to plan. Thank you.

Glossary of terms and abbreviations

Anisotropic	Material properties vary depending on the orientation of the specimen.
Antagonistic muscle	Muscle that opposes the action of another muscle.
Anthropometric data	The physical dimensions of parts of the body.
BMI	Body Mass Index.
BW	Body weight.
Cancellous bone	Low density spongy bone that makes up the majority of the bone volume.
Contralateral	On the other side of the body. For example the left hip would be the contralateral hip in a patient with a right hip replacement.
Cortical bone	Compact bone that makes up the outer shell of the bone.
CT	Computer tomography.
DOF	Degrees of freedom.
EMG	Electromyography.
FE	Finite element.
FO	Femoral offset.
Forward dynamics	Motion calculated from forces.
HA	Hydroxylapatite.
Haemotoma	A collection of blood caused by internal bleeding.
Heterotrophic bone	Bone that cannot synthesize metabolic products and therefore acts as a parasite to surrounding bone.
HHC	Horizontal hip centre.
Hip dysplasia	Hereditary disease in which the femoral head has only a loose fit in a misshapen acetabulum.
HS	Heel strike, in reference to the point in the gait cycle when the heel first hits the ground.
HU	Hounsfield Unit. Unit of relative density measured by a computer tomography scan.
Inverse dynamics	Internal forces calculated from motion.
Isometric contraction	A muscle contraction producing force with no appreciable change in length, unlike concentric or eccentric contractions where the muscle shortens or lengthens.
Laceration	Cut or wound, soft tissue broken, covers all degrees of wound from superficial to deep.
MA	Muscle moment arm.

ML	Muscle length.
Muscle activity	The force in the muscle divided by the muscle strength.
Muscle force	This is calculated by musculoskeletal recruitment criteria or measured indirectly using EMG.
Muscle peak isometric strength	The largest force the muscle is capable of producing is the muscle strength at its optimum muscle fibre length.
Muscle strength	The potential force the muscle could produce at a particular length. This is the value that Hill's muscle model calculates.
Musculoskeletal	Relating to or involving the muscles and the skeleton.
Osteoarthritis	A disease where the cartilage becomes damaged and the underlying bone thickens due to the body's attempt to heal. The thickened bone often contains rough patches which catches the membrane surrounding the joint inflaming them causing pain and reduced function.
PCSA	Physiological cross-sectional area of a muscle.
Resorption of bone	The process which results in loss of bone by absorption into the body.
RSA	Radiostereometric analysis.
THR, THA	Total hip replacement, Total hip arthroplasty.
TO	Toe off, in reference to the point in the gait cycle when the foot leaves the ground.
Trabecular bone	See cancellous bone
Trochanteric bursitis	Inflammation of the synovial sacs around the trochanter.
VHC	Vertical hip centre.

1. Introduction

Total hip arthroplasty is used as a last resort to alleviate pain and restore joint function to the hip joint if non-surgical interventions have been exhausted. There were approximately 65,000 total hip replacements conducted in England and Wales in 2008 (National Joint Registry 2009) and historical data suggests that approximately 95% of those will be successful at 10 years (Kärrholm et al. 2008). Unfortunately for the patients with failed hip arthroplasty the revision surgery to replace their prosthesis has a lower rate of success than primary surgery (Kärrholm et al. 2008) . The patient group undergoing total hip arthroplasty now includes younger and more active patients who require a broad range of motion and a longer service lifetime for the replacement joint. The rise in the number of obese patients is also increasing the loads on the prosthesis. As the demands on the artificial joint increase, better testing of the current and new designs is needed.

Total hip replacements are tested for strength, fatigue and wear properties in the laboratory and clinical studies compare different designs, as well as patient and surgical related factors. However this testing can be expensive, slow to produce useful results and can lack the flexibility to alter parameters easily and ethically. Computational analysis can quickly and flexibly test hip prostheses; however only reliable models and input conditions can produce useful resulting analyses. Finite element modelling is a method commonly used in computational analysis and the models have improved since it was first employed to investigate hip replacements (Section 3.2). Models of bone and implant geometry are more physiological and representative as techniques such as computer tomography (CT) scans are used to generate models. New modelling methods such as adaptive and probabilistic models have allowed finite element models to move from generic static tests to investigate some of the changes that occur in the bone and consider a larger population of patients. The geometry and material properties in finite element models can be extremely detailed (Wong et al. 2005; Schileo et al. 2008; Schileo et al. 2008; Taddei et al. 2008). However, despite the increase in complexity of the finite element models

the applied forces have remained relatively simple. Studies have shown that the forces applied to finite element models also need to be complex to provide physiological strain patterns in the bone (Duda et al. 1998). Probabilistic modelling has recently been used to analyse geometry and implant position variability (Bryan et al. 2009; Dopico-González et al. 2010) and there is a need to improve the loading conditions for these probabilistic models. In particular, the range of potential forces which could affect an implanted hip, either due to surgical or patient related factors, needs to be established to provide meaningful statistical analysis. Only a simplified set of forces are applied to the models compared to the complex physiological load case, and despite changes to the implant position, the load across the hip remains unchanged in these studies (Dopico-González et al. 2010). Detailed understanding of the strain and micromotion at the interface between the implant and bone is important because they have been used to investigate the primary stability of the implant and the risk of implant migration leading to aseptic loosening. A reduction in the primary stability of the implant increases the risk of revising the hip arthroplasty and the stress at the bone-implant interface has been shown to correlate to the lifetime of the arthroplasty (Taylor et al. 1995).

Joint contact forces have been measured using instrumented joint prostheses (Rydell 1966; Brand et al. 1994; Bergmann et al. 2001), but these studies have only considered a limited number of patients (Section 2.5.1). Muscle forces have not been measured in the body and although some studies have tried to correlate the electrical signal from the muscle to the force it generates (Delp and Loan 1995) it is difficult to calibrate or verify the technique (Erdemir et al. 2007) (Section 2.5.2). Musculoskeletal modelling can be used to predict joint and muscle forces from measured gait patterns (Chapter 3.1). Since this is a non-invasive technique it can be used with a larger number of people, both with and without hip replacements, and the calculated muscle and joint forces have been used in finite element modelling (Section 3.2).

This research has investigated scenarios in which finite element modelling of total hip replacements could be improved by using musculoskeletal modelling to produce joint and muscle forces. A modelling process was created by applying muscle and hip contact forces, predicted by a musculoskeletal model, to a finite element analysis of an implanted hip. Before the hip and joint replacement were analysed, the anatomy and physiology of the hip were investigated. Some studies have measured forces across the hip, although only when the joint had been artificially replaced. These measured loads are important when testing joint replacements, either directly as applied loads or as a comparison to predicted forces. Several diseases affect movement at the hip and in extreme cases surgical intervention is required to replace the joint. Joint replacement surgery has been performed for many years and studies have shown that the range of joint replacement options can affect the lifetime and likely causes of failure of the artificial joint and therefore were researched for this study. Previous studies have also investigated the forces across the hip by modelling the anatomy and recording the movement of the body. These musculoskeletal models have had some success in predicting muscle and joint contact forces and this research has reviewed several studies and their methods. Computational models have also been used to analyse the relative potential lifetimes of hip replacement designs and scenarios, by calculating the potential affect of the joint loads on the likely failure methods. A review of the studies investigating cementless hip replacement designs, which have similar main failure type, has been conducted to find the current state of the computational analysis field.

2. Review of the hip joint

2.1. Anatomy

The joint at the hip is a ball and socket comprising the pelvis, made up of the ilium, ischium and pubis bones, and the femur (Gray 1918) (Figure 1). The femoral head acts as a ball within the socket of the acetabulum which is formed at the joint between the three pelvis bones. This allows the joint all three rotational degrees of freedom restricted only by the capsular ligaments and the depth of the cup (Van Wynsberghe et al. 1995). The hip is a synovial joint; both of the articulating surfaces are covered with cartilage and the joint is contained within the hip joint capsule. The inner layer of the capsule is the synovial membrane which produces synovial fluid to lubricate the joint (Van Wynsberghe et al. 1995).

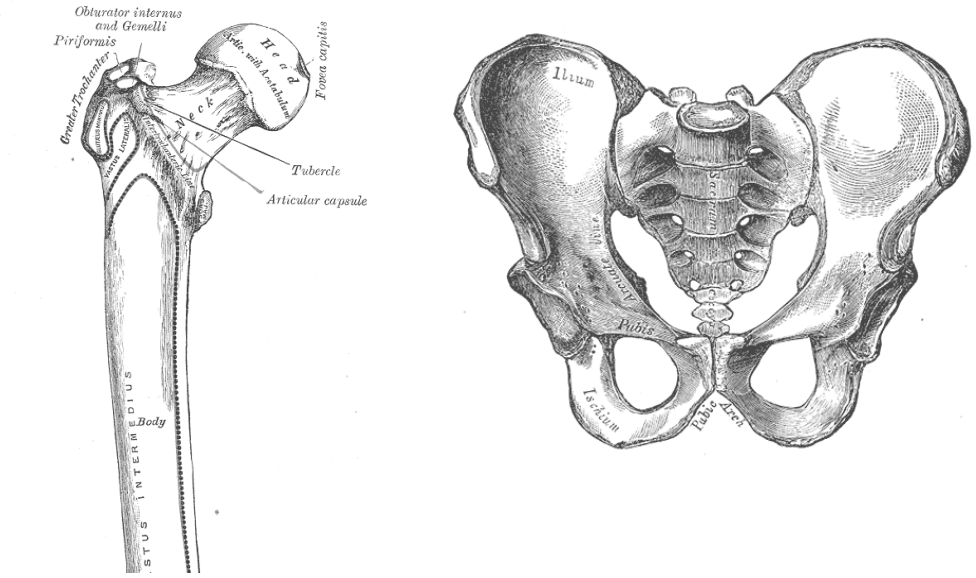

Figure 1: The femur and pelvis bones (Gray 1918).

The hip joint allows rotation in all three axes but does not allow translation between the femur and pelvis. For the purpose of this study the y-axis lies parallel to the length of the femur shaft, the z-axis lies at 90° to the femoral shaft in the direction from the femoral head to the greater trochanter and the x-axis is the product of the two other axes (Figure 2).

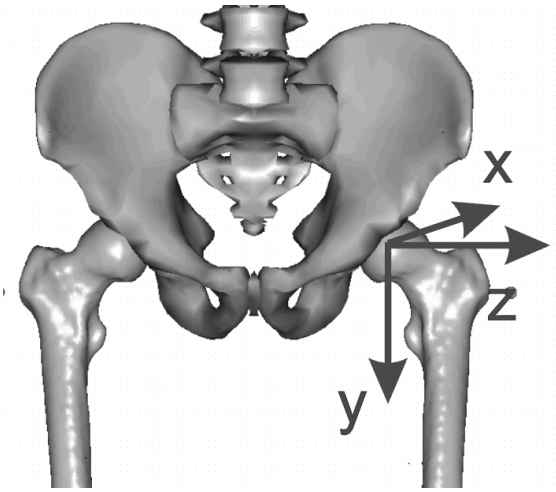

Figure 2: Coordinate system of the left hip. Positive x-axis in posterior direction, positive y-axis in distal direction and positive z-axis in lateral direction.

2.2. Osteology

The limbs are mainly made of "long bones" which comprise a shaft or diaphysis and two extremities which are known as the epiphyses (Figure 3). Long bones are anisotropic and the Young's modulus along the bone axis is approximately 17.4GPa while perpendicular to the axis the modulus is approximately 11.7GPa (Callister 2000). However, the bone is not homogeneous and the structure of bone is divided into two types, cortical and cancellous. Cortical bone is a compact bone that makes up the majority of the diaphysis and an outer shell on the epiphysis. Cancellous bone is a lower density spongy bone that makes up the majority of the bone in the epiphyses. The sponge-like structure of cancellous bone is made up of individual struts of bone known as trabeculae which are in close contact with the bone's internal blood supply.

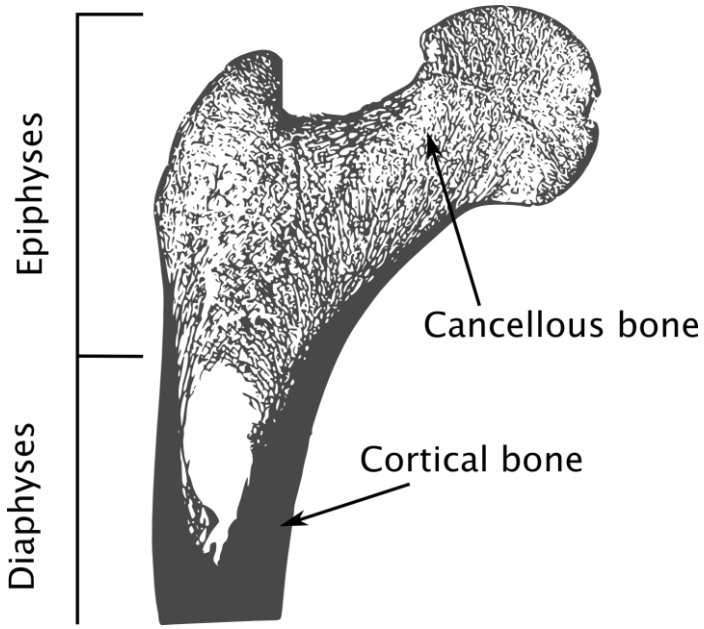

Figure 3: The structure of bone in the femur. Adapted from Gray (1918).

2.2.1.Bone properties

Cortical bone has a density of approximately 1700-2100 kg/m^{-3} (An and Draughn 2000) but due to the high porosity of cancellous bone and its highly variable nature, the density can fall as low as 50 kg/m^{-3} (Gibson 2005). Although studies have attempted to define the density of cortical and cancellous bone, it has been noted that at low densities of cortical bone and high densities of cancellous it is difficult to differentiate between the two bone types (Carter and Hayes 1977). The density of the individual trabecula in cancellous bone has been found to be similar to that of cortical bone (An and Draughn 2000) although other studies disagreed (Zioupos et al. 2008). The overall density and strength of the bone increases with age until bone maturity, at about 35 years old, and then declines (An and Draughn 2000). This is a general trend and on a local scale bone is an adaptive material which can alter its properties based on the applied loading. The density of bone (ρ, g/cm^{-3}) is proportional to its modulus (E, GPa) with the general relationship described in Equation 1(Cowin 2001).

$$E \propto \rho^{p} \qquad \text{Equation 1}$$

Carter and Hayes (1977) found a cubic relationship between the modulus and the density, while Rice *et al.* (Rice et al. 1988) found a slightly better correlation with a squared relationship and other studies have found the power, p, to be slightly less than 2 (Hodgskinson and Currey 1992; Morgan et al. 2003). Carter and Hayes also found that the modulus-density relationship was affected by the strain rate ($\dot{\epsilon}$) according to Equation 2.

$$E = 3790\dot{\epsilon}^{0.06}\rho^{3} \qquad \text{Equation 2}$$

However this is one of many relationships which have been found between the modulus and density. A review of the potential modulus-density relationships for bone was conducted by Helgason *et al.* (2008) in which they found a large degree of variation between studies.

The tensile strength and yield strength of bone (Figure 4) has been shown to be dependent on the bone density (Carter and Hayes 1977; Kopperdahl and Keaveny 1998; Cowin 2001). Although bone strength is dependent on its density, the yield strain can be considered independent of elastic modulus, yield stress and density (Cowin 2001; Morgan and Keaveny 2001), however there is variation in the reported values for yield strain. The yield strain in compression for cancellous bone was found to be 8400με by Kopperdahl *et al.* (1998) and between 7000με (±500 s.d.) and 8500με (±1000 s.d.) by Morgan *et al.* (2001) across several anatomical sites. In tension Kopperdahl *et al.* found the yield strain of cancellous bone to be 7800με and Morgan *et al.* found it varied between 6100με (±500 s.d.) and 7000με (±500 s.d.). Ebacher *et al.* (2007) found cortical bone to be less ductile than cancellous with an ultimate strain of approximately 10000-15000με. In tension cortical bone has a yield strain of approximately 4000με in tension and in compression cortical bone was found to have a higher and more variable yield strain than in tension, between 6500 and 10000με.

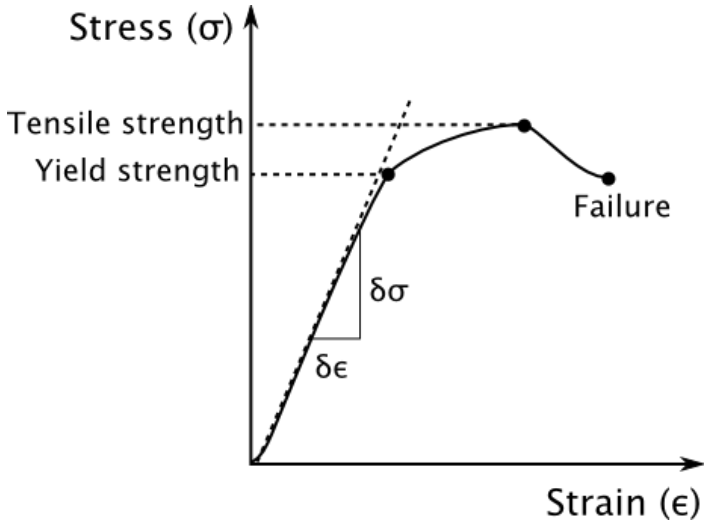

Figure 4: Example of a stress-strain curve for tensile loading to failure of bone.

Using strain gauges attached to a human tibia Lanyon *et al.* (1975) measured the surface strain during normal walking. They found that the surface strain varied through the gait cycle from 640με (±70) to 2370με (±180) in tension and the peak in strain was recorded as the foot left the floor. The compressive strain increased as the load carried by the subject was increased and the highest strains were recorded with the subject running on a treadmill (8470με ±590). The bone on the surface of the tibia is cortical bone and during normal walking the measured strain was significantly lower than the yield strain. The peak strain measured during running was a compressive strain and lower than the upper limit found experimentally for the yield of cortical bone under compressive strain.

Keyak and Rossi (2000) investigated which failure criteria could most accurately predict the failure of bone using finite element models. Experimental results were compared to a finite element model using different failure criteria including maximum normal strain, stress and shear strain. All of the failure criteria predicted the load which caused femoral fracture *in vitro* although the shear strain and the Hoffmann criterion which is based on principal stresses were found to be the most robust when using different loading scenarios. Schileo *et al.* (2008) also compared failure criteria; the von Mises stress, maximum principal stress and maximum principal strain. All three

criteria predicted failure of bone at the location of the fracture found in the experimental study. However, using a compressive principle strain limit of 10400με and a tensile limit of 7300με, the maximum principal strain criterion predicted a more localised failure, in the neck region of the femur, which corresponded to the experimental tests.

Wolff's Law states that bone density and orientation of trabeculae can change in response to mechanical stimulus. Bone adaptive remodelling is based on Wolff's Law and is used to predict where bone will be deposited due to a stress stimulus. Deposition of bone increases the density in that area and in an area of low stress the bone is resorbed by the body and the density lowered (Figure 5). Between the threshold values of low and high stress stimulus there is a lazy or dead zone in which the bone is not affected by changes to its stress state. Beaupré *et al.* (1990) found that the daily stress stimulus (DSS) was approximately 50MPa/day which generated a cyclic normal strain of approximately 400με assuming 10,000 walking cycles per day. They calculated the change in bone density based on the adaptive model in Figure 5 using 20% of the stress stimulus as the width of the lazy zone (w) and predicted a bone density distribution consistent with that found *in vivo.*

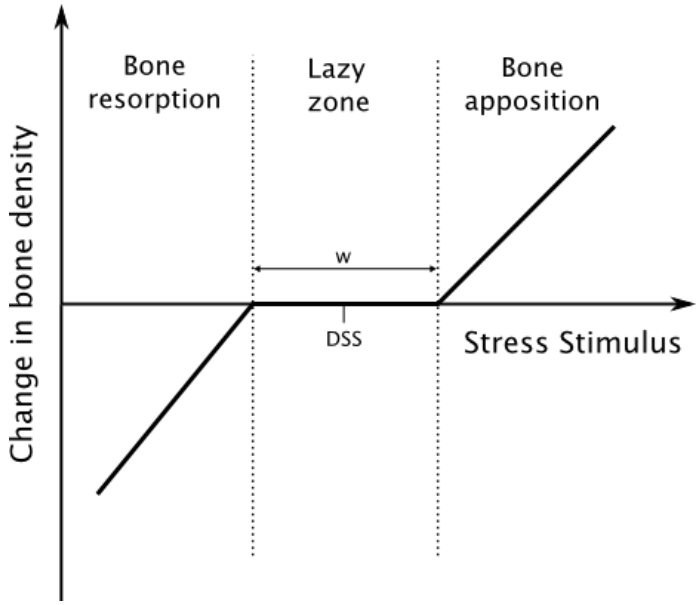

Figure 5: Bone adaptive remodelling including the width of the lazy zone (w) and the daily stress stimulus (DSS). Adapted from Beaupré *et al.* (1990)

2.3. Myology

2.3.1.Structure

Any movement within the body is produced and controlled by muscles and additionally restricted by ligaments (Van Wynsberghe et al. 1995) which are a fibrous tissue that connect bones together. The hip joint has several ligaments and the main capsular ligament covers the whole of the joint. The strength of it and the shape of the articulating surfaces determine the overall stability of the hip.

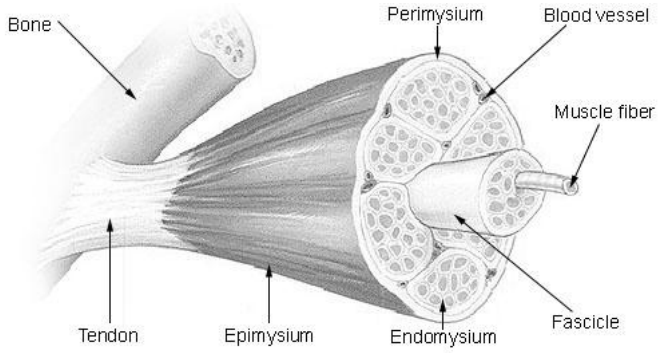

Figure 6: Structure of a skeletal muscle (Young et al. 2000).

Skeletal muscle is the muscle type that creates movement of the skeleton. The area referred to as the muscle belly comprises many fibres bundled together and collectively wrapped in a sheath called the perimysium (Figure 6). Tendons provide a connection between the muscle belly and the bones upon which they act. Muscles are activated by neurons in the spinal cord which then fire electrical impulses down pathways called axons to the muscle fibres. These motor units can either activate all or none of the muscle fibres attached to them. Tension is increased in the muscle by activating additional motor units (Whiting and Zernicke 1998).

2.3.2.Movement

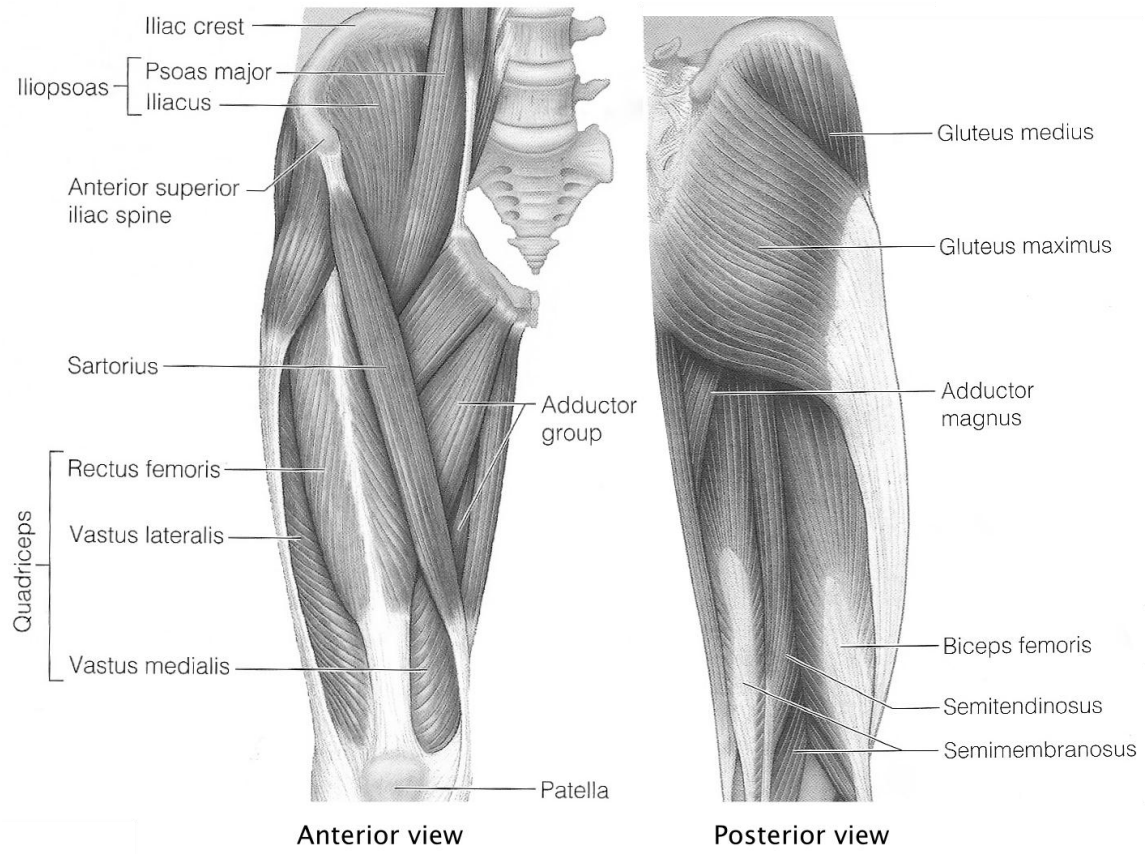

Figure 7: Major muscles in the thigh from a posterior and anterior view (Marieb 2006).

There are approximately twenty-two muscles that cross the hip joint (Figure 7). They all have different attachment points on the skeleton which creates different lines of action and allows different functions to be performed, see Table 1. A skeletal muscle is normally attached to bones in the body by its tendons at a minimum of two points, often referred to as the origin and insertion points or collectively as attachment points. The origin point is the end attached to the part of the body which remains stationary relative to the movement produced by the muscle. The insertion point is the area on the body part that is moved by contraction of the muscle. However a muscle does not always have two specific points that it attaches to and several muscles have a large area on the bone to which the tendon attaches, such as the gluteus maximus (Figure 7).

Muscles	Flexion	Extension	Abduction	Adduction	Medial/ Internal Rotation	Lateral/ External Rotation
Adductor Brevis	✓			✓	✓	
Adductor Longus	✓			✓	✓	
Adductor Magnus		✓		✓	✓	
Biceps Femoris		✓				
Gemellus Inferior						✓
Gemellus Superior						✓
Gluteus Maximus (upper)			✓			✓
Gluteus Maximus (lower)		✓		✓		✓
Gluteus Medius			✓		✓	
Gluteus Minimus			✓		✓	
Gracilis				✓	✓	
Iliacus	✓					
Obturator Externus						✓
Obturator Internus						✓
Pectineus	✓			✓		
Piriformis			✓			✓
Psoas Major	✓					
Quadratus Femoris						✓
Rectus Femoris	✓					
Sartorius	✓		✓			✓
Semimembranosus		✓				
Semitendinosus		✓				
Tensor Fasciae Latae	✓		✓		✓	

Table 1: The muscles which contribute to hip movement.

2.3.3.Muscle force generation

Isometric contraction of a muscle describes a muscle developing tension but not shortening (Huard et al. 2002) and the maximum potential force or muscle strength is developed during isometric contraction. The muscle strength can increase and decrease with activity levels and deteriorates with age (Morse et al. 2005; Haddad and Adams 2006). At any instant of muscle length or velocity there is a maximum tension available in the muscle and Hill (1926; 1938; 1950; 1953) theorised a method for

finding the muscle strength given the instantaneous properties of the muscle and many studies use modified versions of his work. The basic mathematical model theorised by Hill is a three element system containing contractile and spring elements (Figure 8). The contractile element (CE) models the contracting effort of the muscle and the passive element (PE) models the passive spring constant of the muscles fibres. The strength of the musculotendon is related to its current length (l_{MT}) which is the sum of the tendon length (l_T) and muscle length (l_M) taking into account the pennation angle (α) which is the angle of the muscle fibres in relation to the muscle's line of action.

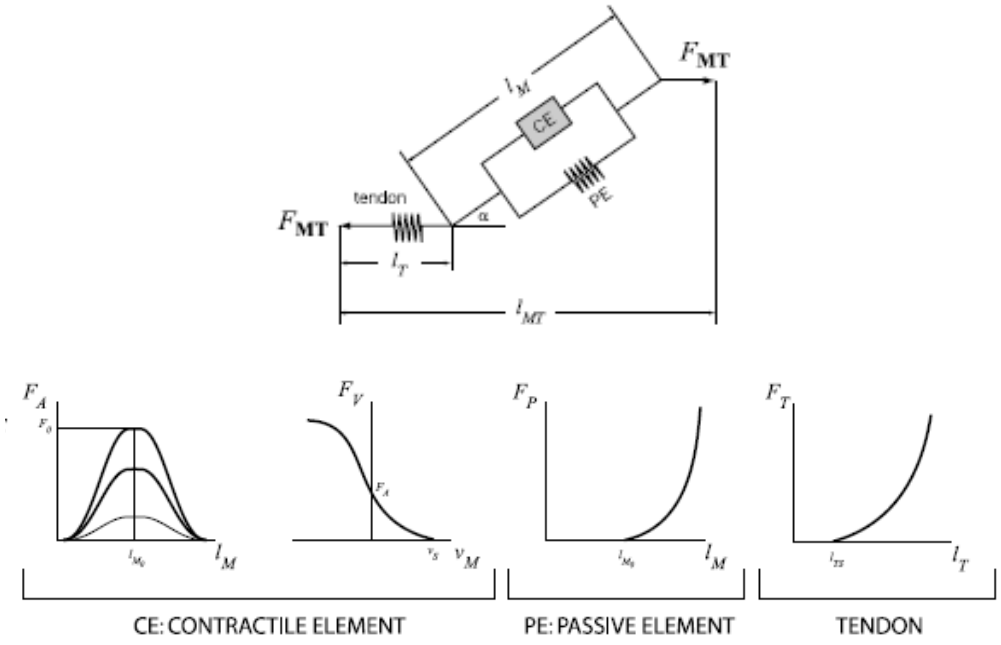

Figure 8: A musculotendon model based on Hill's model (Erdemir et al. 2007). The force in the musculotendon unit (F_{MT}) is affected by the length of the tendon (l_T), length of the muscle (l_M), spring constant in the muscle passive element (PE) and the tendon, the muscle contraction in the contractile element (CE) and the muscle pennation angle (α).

The strength of a muscle is proportional to the physiologic cross-sectional area (PCSA) of the muscle (Mow and Huiskes 2005) and the orientation of the muscle fibres (Garrett and Duncan 1988). The PCSA is the muscle cross-sectional area perpendicular to the muscle fibre direction. There are two components of muscle tension, the active

tension generated by activity in the muscle fibres and the passive tension created by the physical lengthening of the muscle and tendon. As the muscle lengthens the tension increases to the muscle strength and then decreases with further muscle extension until the passive tension increases (Figure 9). The force in the muscle is also proportional to the velocity of the contraction and Hill's muscle model relating velocity and force was experimentally shown by Bressler and Clinch (1974) using the sartorii muscle from a toad.

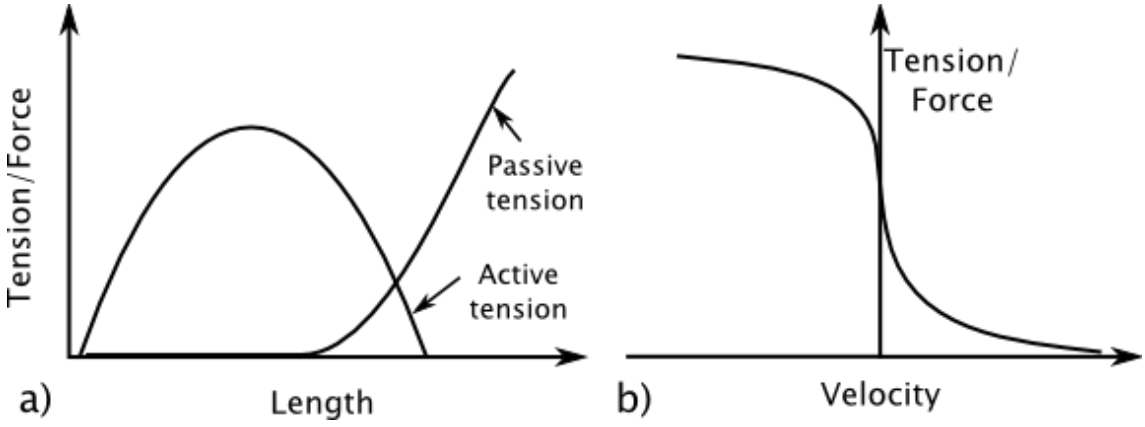

Figure 9: Maximum available muscle tension relationship with muscle length (a) and muscle velocity (b). Adapted from Low and Reed (1996).

The resultant force vector for a muscle can be described as the line of action and this is affected by the alignment of the fibres within the muscles as well as the route the muscle takes through the body. The muscle path is not always a direct route between the attachment points, as this can be obstructed by parts of bone or other soft tissue. When the skeleton moves it is possible for the position of the obstructing parts to change relative to the muscle, resulting in an alteration in the muscle's path. Pennate muscles contain fibres that do not run straight along the line of action of the muscle and change the strength of the muscle. The angle between the overall line of action for the fibres and the muscle's line of action is the pennation angle. This angle is used to relate the muscle's overall length to the fibres' length which can then be used in a Hill type muscle model to calculate the strength of the muscle.

2.3.4.Muscle injury and repair

Injury in muscles reduces the ability to generate force and during hip arthroplasty muscles can be divided or dissected (Meneghini et al. 2006). Lacerations to the muscle generally heal but can be rebuilt with a dense connective scar tissue instead of muscle tissue, reducing the function of the muscle. Lacerations that transect the muscle fibres are the most detrimental type of laceration for muscle recovery, particularly if they cut off the blood supply to areas of the muscle (Garrett and Duncan 1988). After injury a muscle goes through three stages of recovery; degeneration and inflammation, regeneration and fibrosis (Huard et al. 2002). The fibrosis stage is where scar tissue is formed which causes a reduction in strength of the healed muscle. The fibrosis stage starts approximately two to three weeks after it is damaged and it can take more than 6 weeks for normal function to be achieved (Malik and Dorr 2007).

The biological and the mechanical properties of a muscle can be measured to investigate how affected a muscle is following laceration and healing. Tests to find a muscle's mechanical strength and strain properties have been conducted to find the point of the muscle that is weakest and to compare repair methods. Kääriäinen *et al.* (Kääriäinen et al. 1998) conducted a study in rats to investigate the recovery of muscles after laceration. The elongation of the healed muscles was measured as load was applied to failure of the muscle. They found a reduction in both the length of the muscles at the point of failure and the load required for failure of the muscles compared to the undamaged muscle in the non-operated leg, known as the contralateral leg. The failure load was measured as recovering only to approximately 50% of the contralateral muscle however this was attributed to the atrophy of the muscle rather than damage caused by the laceration. The reduction in elongation was attributed to the scar tissue that formed at the laceration site as the scar had a higher elastic modulus.

In addition to the change in mechanical properties, the biological response of a muscle can also be affected by muscle damage (Crow et al. 2007). The quantity of force that a

muscle can produce can be reduced as a result of damage and repair and the method used for measuring the strength in the muscles is explained in the review paper by Huard *et al.* (2002). A study by Garrett and Duncan (1988) used the extensor digitorum muscle of the New Zealand white rabbit to investigate the effects of partial and full laceration on strength and shortening ability. The partial lacerations, of between 50% and 75%, and the full lacerations were made along the width of the widest section of the muscle belly and then the muscles were allowed to heal for twelve weeks before the muscles ability to provide tension and shorten were examined. Garrett and Duncan found that fully lacerated muscles only regained 54% tension strength and partially lacerated muscles regained approximately 62% compared to the controls. The ability to shorten was also affected by the laceration although to a lesser extent than the reduction in tension. The partially lacerated muscle was able to shorten as much as the control and the totally lacerated muscle achieved 80% of the shortening of the control. However it was discovered that the proximal section, between the origin point and the laceration, performed all the shortening in the healed muscle. Due to the limited *in vivo* data on shortening ability of the sections of fully lacerated muscle it has not yet been incorporated into models predicting muscle strength.

Crow *et al.* (2007) conducted a study in rabbits to investigate different repair methods following a complete dissection of the muscle belly in the extensor digitorum longus. They compared several methods of repairing a lacerated muscle by testing the force it could produce with the application of an electric stimulus and by performing a tensile test on the extracted muscle. The two electrical stimuli chosen were twice and ten times the threshold voltage needed to cause involuntary contraction. They found that using ten times the threshold, 10T, after 12 weeks of healing the sutured muscles had approximately 75% of the strength compared to the control muscles. However using only twice the threshold, 2T, gave only 40% of the strength of the control muscules. This suggests that the strength reduction caused by lacerating is not uniform over the force range of a muscle and that a muscle does not recover to its full strength after

laceration. The muscles that were left with no repair fared less well after 12 weeks and at 10T they only achieved 61% of the control muscle's strength. However at 2T the unrepaired muscle had a greater strength, 56% of the control, than the repaired muscle.

Therefore, muscles that have been lacerated do not recover their full strength when healed. The healed muscle strength depends on several factors including the manner of repair and the level of damage. A partially dissected muscle retains more strength than a completely dissected muscle and it is possible that the quantity of partial laceration might also affect the final strength. However, no literature studies have been found that compare different levels of laceration and therefore the variation in muscle strength caused by different quantities of laceration cannot yet be determined. During hip arthroplasty surgery many of the muscles are divided along the line of the muscle fibres rather than lacerated. This will affect the muscles differently to laceration across the body of the muscle and even the position of laceration can affect the healed muscle strength. Lacerated muscles have been shown not to reach their original strength after healing and therefore cannot be assumed to be the same as those of a normal subject.

2.4. Movement at the hip

The hip can rotate in three directions; flexion-extension, abduction-adduction and internal and external rotation (Figure 10). Flexion of the hip decreases the angle between the leg and the trunk by raising the leg in front of the body. The range of motion is approximately 90° but this can be increased if the knee is in flexion and even further, to approximately 150°, if the knee is drawn to the chest (Kingston 1996). Extension of the hip increases the angle between the anterior surface of the thigh and the trunk from the anatomical position. The range of motion is increased from approximately 40° if the knee is in flexion, to a maximum extension angle of approximately 60° if the knee is drawn towards the back (Kingston 1996). Abduction of the hip increases the angle between the midline of the body and the thigh and has a

range of approximately 30° (Kingston 1996). Adduction of the hip is the opposite of abduction and has a similar range of motion. Medial or internal rotation of the hip brings the anterior thigh and knee closer to the midline of the body and has an approximate range of motion of 30° whereas lateral or external rotation is the opposite movement but has a larger range of motion, approximately 60° (Kingston 1996).

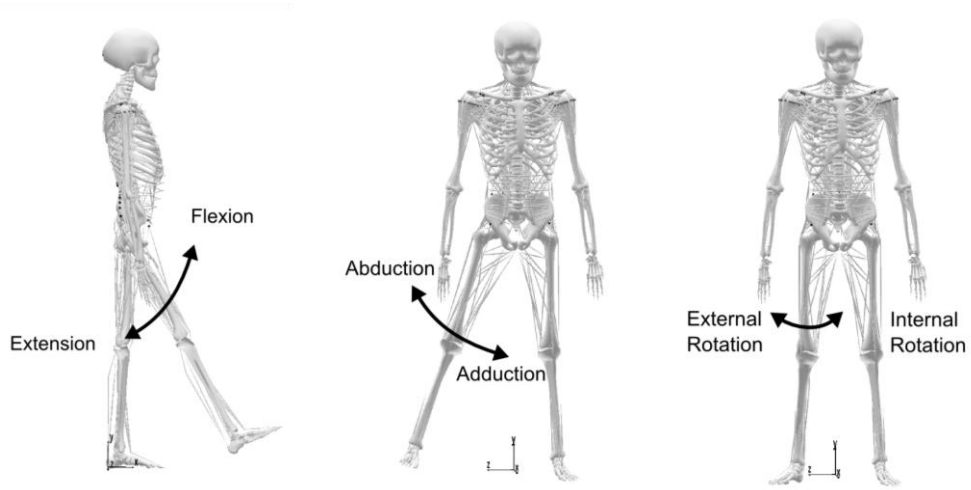

Figure 10: Definitions of the hip rotations.

2.4.1.Gait

Gait is the description for any movement on foot such as walking or running. Normal walking speeds are often used when analysing gait, however other activities such as stair climbing are also investigated to study the range of motion produced by the joints and the change in angle of the applied force through the joint. Normal walking is particularly easy to study since it is an activity that all ambulating patients perform on a regular basis (Morlock et al. 2001). The gait cycle is defined by convention as starting at heel strike, the point at which the heel first touches the ground. At heel strike the body weight is supported by both legs, called double leg stance, and as the gait cycle progresses the body weight is transferred over to the opposite leg, called single leg stance. The original leg lifts off from the ground and then toe off occurs at the point just before the foot leaves the ground. The section of the gait cycle while the foot is in contact with the ground is referred to as the stance phase and then the

section as the leg swings through to start the cycle again is known as the swing phase (Figure 11).

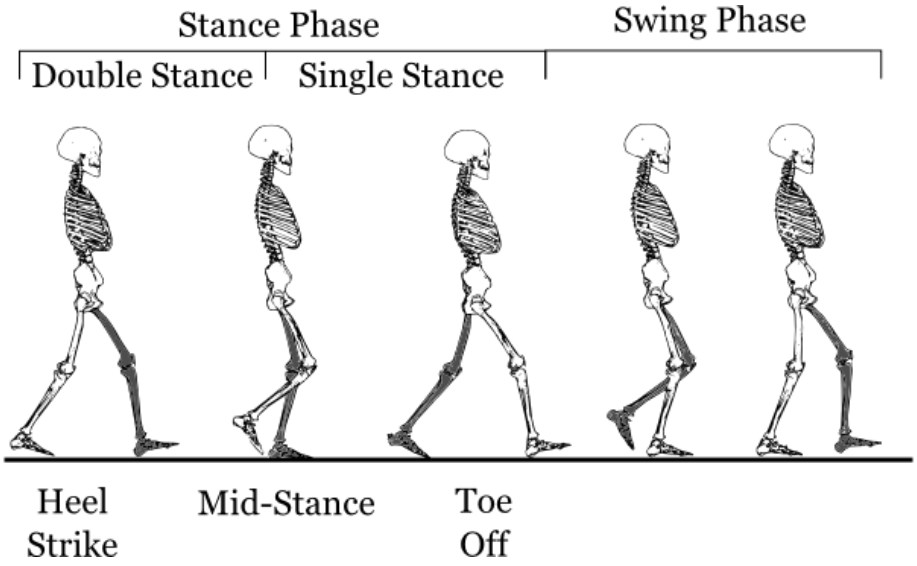

Figure 11: The main stages in the gait cycle shown with the left leg.

The way a person walks can be used to investigate a disease or the success of a treatment related to the lower limbs (Crowinshield et al. 1978), for example during an individual's lifetime their gait pattern can change and the range of flexion-extension angle has been measured to increase with walking speed and decrease with age (Crowinshield et al. 1978). This 'gait analysis' can be used to compare stride length, walking velocity, joint angles and moments to identify specific problems. A subject's gait can be measured using cameras monitoring markers on the person's skin. The markers can either be retro-reflective or light emitting to help the cameras that record their movement as the subject walks in a predefined area (Vaughan et al. 1992) (Figure 12). However, monitoring gait in this manner is not without error and during the movement some markers can become occluded. The software which is used to collate and output marker positions then must calculate the concealed marker position using the previous frames and information on the blind spots of the system or, alternatively the user can manually input the position (Cerveri et al. 2003). Gait analysis can measure an individual's gait pattern by investigating the position of the lower limbs and pelvis through the gait cycle (Figure 11). These positions (and their first and

second derivatives with time, together with knowledge of the inertial properties of the limb segments) can then be used to calculate the torque in the leg during the gait cycle and can be analysed in conjunction with data regarding the ground reaction force to predict the net forces in the leg.

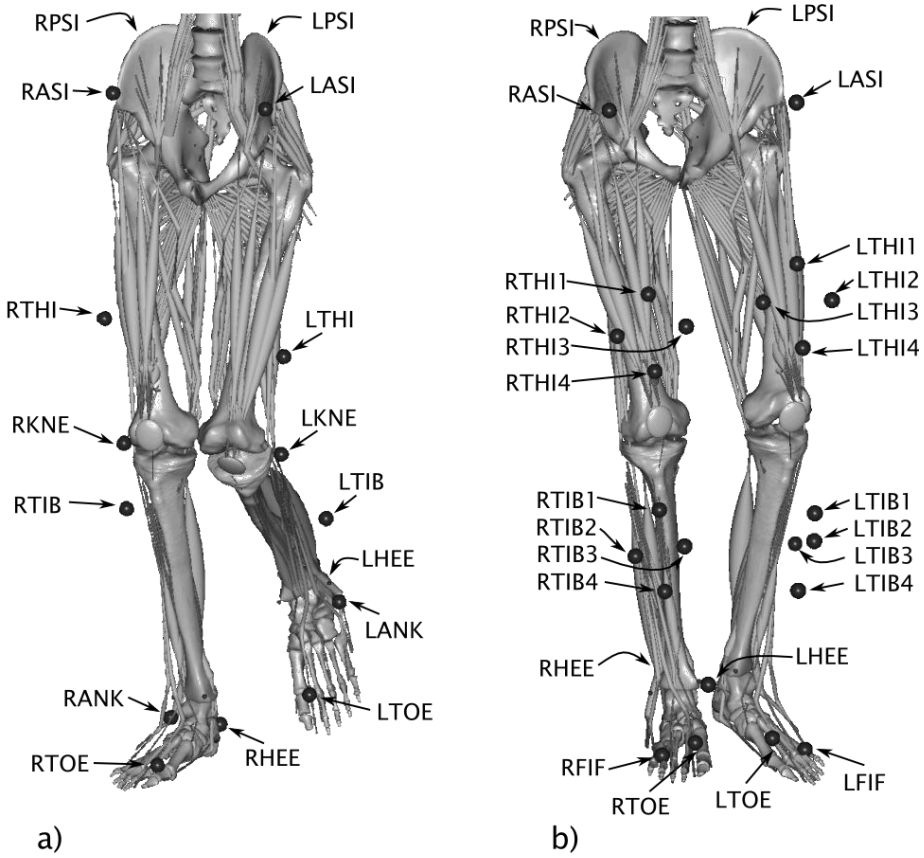

Figure 12: Example of two skin marker setups. a) modified Helen Hayes and b) alternative modified Helen Hayes.

The major source of error associated with gait analysis is the relative position of a marker on the skin compared to the underlying point on the attached limb which the marker is assumed to represent (Cappozzo et al. 1996). The markers are used to monitor the movement of the limb as a whole, however the skin moves with respect to the limb and so there is an error associated with the use of skin markers. The magnitude of the error depends on the position of the marker on the limb, the limb position, quantity of fat and muscle contraction. Bony landmarks can be used to reduce the errors from skin and soft tissue movement for example placing markers close to the knee instead of over the calf muscle. Some studies have been conducted

with markers on pins that have been drilled into the bone to provide a more stable and reliable output (Fuller et al. 1997; Benoit et al. 2006) and although these studies can help identify and quantify the errors, they are both invasive and not without their own sources of error. Bone markers can cause pain which can restrict normal gait, the pin can also restrict skin and soft tissue movement (Lundberg 1996) and the patient is at risk of infection. However a comparison of pin markers and skin markers by Fuller *et al.* (1997) showed that skin mounted marker positions were up to 20mm from the underlying bone position they were attempting to record. Unfortunately the marker errors are not constant and therefore cannot be accounted for systematically although it was found that faster motion increases the error (Fuller et al. 1997). The flexion angle at the knee calculated with the skin markers was offset by up to 30° and increased with increasing flexion angle. Ground reaction forces are sometimes measured at the same time as recording the marker trajectories.

Once the patient's movements are recorded, using gait analysis software, the pattern of the subject's gait can be studied or more detailed analysis can take place. The torque at each of the joints in the system can be calculated and the range of angles that each of the joints obtain. However the muscle forces cannot be directly calculated. They can only be predicted using optimisation equations and additional information concerning the positions and strength of the muscles and the mass and inertia properties of the subject (Chapter 3.1).

2.5. Measured forces in the body

Patient specific studies have investigated the forces at the hip after arthroplasty surgery. Joint contact forces have been measured *in vivo* using artificial joints but muscle forces have not been measured directly in the body. Several studies have measured the force across the hip using an instrumented hip implant and have given an insight into the forces at the hip of the studied patients at the time that they were examined (Rydell 1966; Davy et al. 1988; Bergmann et al. 1993; Brand et al. 1994; Taylor et al. 1997; Bergmann et al. 2001; Taylor and Walker 2001). Unfortunately

these studies only consider a limited number of patients due to their invasive nature. However they do provide forces which can be used within computational models to compare implant designs.

2.5.1.Hip contact forces

Typically an instrumented hip prosthesis has a number of strain gauges mounted on it. The first published measurement of the contact force in a hip replacement was in 1966 when Rydell (1966) used wires to carry the signal from the strain gauges on the prosthesis through the skin. This limited the time over which the experiment could be conducted as the wires were removed once the trial was complete, which was six months after implantation. Subsequent researchers have used internal batteries (Davy et al. 1988) or external induction coils (Bergmann et al. 1993; Taylor et al. 1997; Bergmann et al. 2001) to power wireless transmitters in the implant allowing a greater scope for monitoring the forces through the hip. The force at the hip is usually measured throughout the whole gait cycle but often the data presented in the literature are only the peak forces. Since all patients are different, an attempt to normalise the force data has been made and forces are usually presented as a percentage of the patients body weight (BW) or a multiple of the body weight.

Rydell (1966) recorded forces with a variety of different activities and found that walking speeds of approximately 1m/s produced peak forces of 1.59BW and 3BW in the two patients tested. As predicted, faster walking speeds increased the forces across the hip for both patients. The peak forces obtained during stance phase and swing phase are shown in Table 2.

Reference	Year	Patient	Walking speed	Max force (BW)	Heel strike (BW)	Toe off (BW)	Time post-op (months)
Rydell (1966)	1966	Patient 1	0.9m/s	1.59	1.51±0.13	1.59±0.11	6
			1.3m/s	1.8	1.80±0.29	1.76±0.18	6
		Patient 2	1.1m/s	2.95	2.95±0.16	2.23±0.12	6
			1.4m/s	3.27	3.27±0.32	2.55±0.19	6
Davy *et al.* (1988)	1988		Walking with aid	1			3 days
				1.5			6 days
				2.6			16 days
				2.8			31 days
Brand *et al.* (1994)	1994		Normal	2.4 – 3.25	2.0–3.0	1.9–3.25	90 days
			Slow	2.25 – 2.5	2.2–2.5	2.2–2.5	90 days
Taylor *et al.* (1997; 2001)	1997	IM	Normal	2.5			6
				2.9	2.9	2.8	12
				3.4	3.4	3	18
	2001	GF	Normal	2.32 – 3.3	1.32–1.47		11
				1.87 – 2.35	0.92–1.12		12
				2.26 – 3.01	0.55–0.58		24
		VN	Normal	0.9 – 1.9			12
Bergmann *et al.* (1993; 2001)	1993	EB left	1 kph	2.93			30
			3 kph	3.03			30
			5 kph	3.94			30
		EB right	1 kph	2.93			30
			3 kph	3.52			30
			5 kph	4.71			30
		JB	3 kph	4.64			8
	2001	HSR	Slow	2.39	2.39	1.88	11–31
			Normal	2.37 – 2.6	2.49±0.11	1.88±0.09	11–31
			Fast	2.58 – 3.14	2.12±0.15	2.81±0.28	11–31
		KWR	Slow	2.18 – 2.8	2.44±0.36	2.32±0.14	11–31
			Normal	2.28 – 2.68	2.46±0.2	2.31±0.1	11–31
			Fast	2.48 – 2.89	2.69±0.21	2.35±0.13	11–31
		IBL	Normal	2.74 – 3.1			11–31
		PFL	Slow	2.42 – 2.81			11–31
			Normal	2.1 – 2.34			11–31
			Fast	2.15 – 2.22			11–31

Table 2: Peak measured hip contact forces during gait.

Several other studies have subsequently obtained hip contact forces from instrumented hip prostheses. However different instrumented prosthesis designs and methods of transferring the strain gauge data have been used to those in Rydell's study. Davy *et al.* (1988) used an implant that could transmit a signal out of the body to be picked up by an external antenna. Davy *et al.* measured the forces in the hip at several intervals up to 31 days post operatively. The first trial was conducted just 3 days after implantation and the patient was walking with the aid of a walker, forces of 1BW were recorded. The forces measured increased at 6 days and again at 16 where they remained constant to the end of the trial at 31 days. The data they obtained gives peak forces in gait of 2.6–2.8BW after 31 days post-operatively however the patient was allowed to use a walker or crutches to help them walk. The results are similar to patient 2 from the study by Rydell (1966) despite the fact that the patient in the Davy *et al.* study was using walking aids. Taylor *et al.* (1997) considered the shaft forces in the femur instead of the hip contact forces, however the results confirm that the internal forces increase with time post-operation.

Bergmann *et al.* (1993; 2001) have also measured the forces across the hip. The implant used was instrumented with strain gauges in the femoral neck and powered with induction coils, one externally and one internal to the implant. This allows the freedom to conduct a study over a longer period than in previous work. The peak forces in these studies for normal gait vary between 2.1BW (Patient PFL, Bergmann et al. 2001) and 3BW (Patient KWR, Bergmann et al. 2001). Differences in walking speed have been found to alter the hip contact forces and in general, the forces through the hip increase with an increase in walking speed (Rydell 1966; Bergmann et al. 1993; Bergmann et al. 2001). The walking speed has been predetermined by the researcher in some studies (Bergmann et al. 1993), however in the later studies the walking speed was the patient's normal walking speed (Bergmann et al. 2001) and this could have affected their hip contact force.

Bergmann *et al.* (1993) also investigated a patient with a bilateral hip replacement. The force magnitude and direction were different for the two hips when compared during a gait cycle. The differences between the hips could be due to muscle strength differences caused by surgery, different placement position of the implant or physiological differences between the right and left sides of the patient. This is a clear indication that investigations into the mechanisms behind this phenomenon are important. Some differences between the right and left sides of normal subjects, who can be assumed to have both hips in the normal centre of rotation, have been predicted using gait analysis and musculoskeletal models and therefore some of the disparity found in the bilateral hip replacement patient could be due to natural variation.

Some studies have also measured the forces obtained during other activities (Rydell 1966; Davy et al. 1988; Bergmann et al. 1993; Bergmann et al. 2001). The activities that generate the largest forces include walking at normal and fast speeds, 2-1-2 stance, stair descending and stair climbing. In these activities the hip contact forces range between approximately 2.5BW and 3BW. The most extreme forces recorded were while patients stumbled. Two patients (Patient EB left hip and Patient JB, Bergmann et al. 1993) were recorded stumbling and producing 7.2BW and 8.7BW across their hips, however patients have been unable or unwilling to subsequently generate these forces voluntarily.

Commonly the literature illustrates that, during gait, the peak force at heel strike is greater than at toe off (Davy et al. 1988; Lu et al. 1998; Bergmann et al. 2001). However, it has been shown by Brand *et al.* (1994) that the toe off to heel strike ratio is not always constant within the same patient. There are also studies that confirm that some patients have a greater peak at toe off than heel strike (Davy et al. 1988; Bergmann et al. 2001). Davy *et al.* (1988) investigated three partial load bearing patients who were using crutches where only one of three had a toe off force greater than heel strike. The patient KWR in Bergmann *et al*'s study had eight normal speed

gait cycles published of which two showed a larger or similar magnitude toe off compared to the heel strike force. The limited number of studies and the differing conditions under which the studies were conducted does not allow definitive conclusions to be drawn, however the range of results presented in the literature does illustrate the range of variability within one patient and the inter-patient variability.

Measured forces recorded using instrumented hip replacements have found an average peak hip contact force at normal walking speed without aids to be 2.69BW using the studies by Rydell *et al.* (1966), Brand *et al.* (1994), Taylor *et al.* (1997; 2001) and Bergmann *et al.* (1993; 2001) (Table 2). However there is a large spread of data with the minimum value of peak force during a gait cycle found in the study by Taylor *et al.* of 0.9BW (patient VN) and the largest peak force measured by Bergmann *et al.* at 4BW (patient JB) in two separate gait cycles. It is difficult from the limited data to obtain realistic average values or capture the variability likely in the general population, particularly since all these patients had received hip replacements. Yet the measured data gives an indication of the forces that can be expected across the hip.

There is variability between studies on the forces in the posterior – anterior direction throughout the gait cycle as illustrated by Brand *et al.* (1994) and Bergmann *et al.* (2001) who obtained significantly different forces in the posterior direction. Brand *et al.* measured forces of approximately 0.75BW in an anterior direction at approximately HS and the force remained in an anterior direction throughout the gait cycle. However the patients in study by Bergmann *et al.* had a measured peak posterior force between 0.2BW and 0.6BW at HS.

The reported literature suggests that the peak forces across an implanted hip are approximately 3.5BW excluding extreme events such as stumbling. The range of data published covers different patients and a variety of instrumentation design. These peak forces increase postoperatively reaching a relatively constant level in the force magnitude after approximately 16 days (Davy et al. 1988). Although the range of peak

forces in the literature for normal gait is 2.11-3.5BW the majority of results are in a smaller range of 2.5-3BW. It must be acknowledged that such a small number of patients do not allow firm conclusions to be drawn for the general population. It is important to understand and quantify the forces experienced at the hip as this allows any replacement joints to be modelled and tested under reasonable conditions.

2.5.2.Muscle forces

There are currently no techniques for measuring the muscle forces directly and therefore indirect methods of investigating the muscle force and activity have been investigated. Musculoskeletal models can predict muscle forces and are discussed in chapter 3.1. Electromyography (EMG) allows the electrical signals from muscles to be recorded. The technique uses pairs of electrodes, which are identical to eliminate galvanic potential, to record the voltage potential across the muscle. The potential is directly related to the electrical impulses causing movement in the muscle. There are two main types of electrode, surface and indwelling. Surface electrodes can be used to investigate only the surface muscles. To study underlying muscles indwelling electrodes, such as wire electrodes, can be inserted through the skin using a needle into the muscle below (Vaughan et al. 1992).

EMG can be used to investigate which muscles are active during the gait cycle and then those readings can be compared to the activity levels from musculoskeletal models (Crowninshield and Brand 1981) (Chapter 3.1). Vaughan *et al.* (1992) measured the EMG of 28 major muscles in the lower extremity of a normal man during a gait cycle (Figure 13). Several studies have been published that use EMG data as a validation method (Crowninshield and Brand 1981; Glitsch and Baumann 1997; Hoek van Dijke et al. 1999). The onset and offset points of activity from EMG readings can be used to ascertain if a computational model is modelling a realistic body response to a movement. Some studies have calibrated the readings from the EMG to predict the forces generated by the muscles (Milner-Brown and Stein 1975; Cholewicki and Mcgill

1994; Lloyd and Besier 2003) but this is difficult since currently the methods for calibrating the force are not always considered reliable (Erdemir et al. 2007).

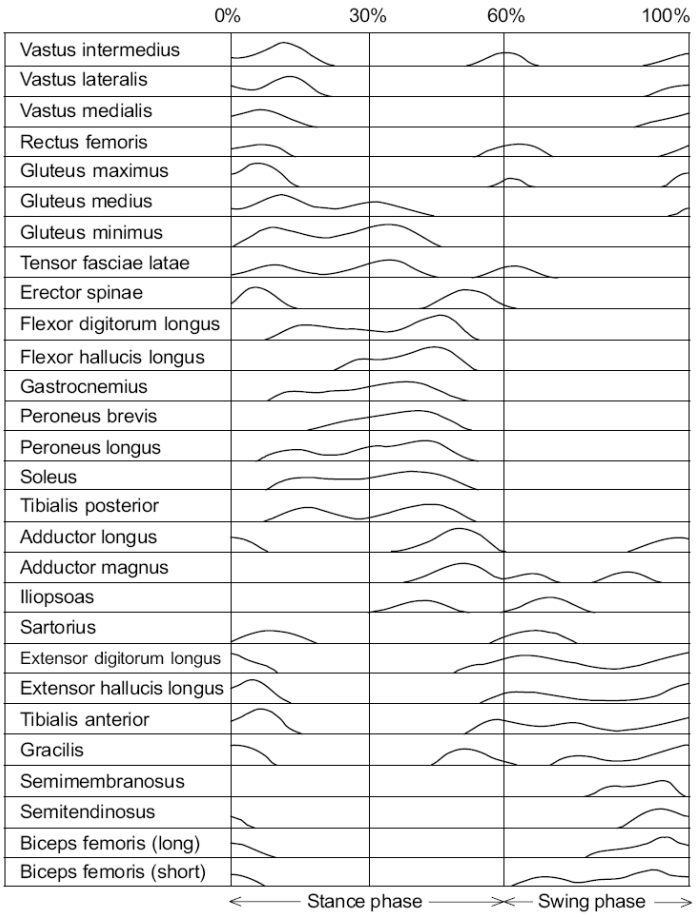

Figure 13: The EMG of 28 major muscles in the lower extremity (Vaughan et al. 1992).

2.6. Diseases affecting the movement of the hip

The hip joint can become damaged either through injury or disease and this can lead to pain or lack of function in the hip. Damage to the femoral head or femoral neck due to injury requires surgical intervention either in the form of surgical pins, plates or even an artificial replacement joint. The bearing surfaces in both the femoral head and the acetabular are protected by cartilage. However damaged cartilage has little reported ability to heal (Suh et al. 1995) and therefore diseases which affect the cartilage such as arthritis, osteoarthritis and rheumatoid arthritis can be problematic. The breakdown of cartilage can lead to the bones of the joint rubbing against each other, leading to pain and loss of function. There are drugs used to treat arthritis,

however in cases with severe problems the joint can be replaced with an artificial prosthesis. Although arthritis can affect all age groups it mainly affects elderly people and osteoarthritis is the main reason for hip arthroplasty (National Joint Registry 2005).

Traditionally a hip replacement was only conducted in elderly patients usually to eliminate the pain associated with disease or osteoarthritis. These patients are typically not active and the replacement joint usually outlived the patient. However the demand for hip implants is growing for several different reasons. First, the population is living longer therefore the elderly population require a longer life from a hip prosthesis. Second, there is a growing number of younger patients, currently approximately 12% of patients having hip replacement in England and Wales are under 55 years old (National Joint Registry 2005) and a replacement hip is expected to allow them to resume an active lifestyle. The success of the standard cemented hip replacement procedure, 95% after 10 years (Malchau et al. 2002), makes total hip arthroplasty a popular alternative to the pain caused by disease in the joint. However the age of patients at the time of surgery and current increases in life expectancy mean hip replacements will be required to last for longer and allow as active and functional a lifestyle as possible.

2.7. Joint replacements and failure modes

In 2005 approximately 62,000 hip arthroplasty surgeries were carried out in England and Wales (National Joint Registry 2005) and the majority of these surgeries used a total hip arthroplasty (THA). A standard hip replacement surgery removes the head of the femur and replaces it with an artificial head. The acetabular cup is also replaced with a plastic cup to give the prosthetic head an artificial bearing surface (Figure 14).

Figure 14: Example of the component parts of a cementless total hip replacement Adapted from DePuy Orthopaedics (2010).

2.7.1.Types of joint replacement and fixation methods

During the arthroplasty surgery the femoral head is removed and a hole is reamed in the femur. A stem, usually metal (CoCr, titanium or stainless steel), is implanted down the shaft of the femur and if it does not come with a head attached one is fitted during surgery. The femoral head is usually made of either ceramic or CoCr and rotates in the acetabular cup. The cup replaces the acetabular socket in the pelvis and is usually made of Ultra High Molecular Weight Polyethylene (UHMWPE).

The main alternative to a traditional total hip arthroplasty is a resurfacing. This is normally a metal hemisphere which covers the femoral head negating the reason to remove it. However, a resurfacement can only be used if the femur is deemed to be in sufficiently good condition by the surgeon. A resurfacing hip joint has the advantage over total hip replacement because it is bone conserving on the femoral side however the cup revision is similar to that of a conventional arthroplasty. Resurfacings cannot be used in all situations as they require that the bone of the femoral head is undamaged and in a relatively natural shape to allow the implant to fit into position. They have a large head size, closer to anatomical size which has the theoretical advantage of a greater range of motion and lower stress concentrations in the liner of the acetabular cup (Siopack and Jergesen 1995; Kluess et al. 2007). However, the

Charnley prosthesis, which is a total hip replacement and normally considered the 'gold standard' to which other replacement joints are compared (Wroblewski and Siney 1993), has a smaller-than-anatomical femoral head and has performed well clinically for more than 30 years (Charnley 1972). Most resurfacings are a metal on metal bearing surface which reduces the level of wear particles, unfortunately there are concerns over the health implications of accumulation of metal particles in the body as they are feared to be carcinogenic (Witzleb et al. 2006).

There are two main methods of fixing an implanted joint replacement to the bone, either it can be cemented or uncemented. A third hybrid option is also used where one component is cemented and the other is fixed with an uncemented method. Once mixed, bone cement sets quite rapidly with an exothermic reaction, therefore it is mixed during surgery and must be used within a limited amount of time. The cement forms a grout between the bone and the implant and is the traditional method of fixing implants in place. In England and Wales in 2005 the total hip arthroplasty was fixed using cement in approximately 57% of total hip replacements.

An uncemented hip stem can be either smooth, porous coated or a combination of the two. A smooth stem is fixed to the femur using a press-fit between the bone and implant. Studies have shown that the stress in the bone surrounding a press-fit stem are higher than with a porous-coated stem (Huiskes 1990) and therefore many stems have some porous coating. A porous coated stem has a roughened surface to allow for bone in-growth. The surface often contains several layers of cobalt-chromium beads which are separated by 50-400μm to encourage the in-growth of bone onto the implant surface (Bauer and Schils 1999). Some stems only have a proximal porous coating to transfer the hip load through more of the proximal femur. Fully coated stems have been reported to transfer load more distally through the stem which can lead to bone resorption in the proximal femur (Tensi et al. 1989) (Chapter 3.2.1).

The surface of a porous coated stem is often sprayed with a coating of hydroxylapatite (HA) as it was found that the coating improved the success rate of the implant fixation (Bauer and Schils 1999). HA has a similar composition as the mineral component of bone and is said to be osteoconductive, allowing a strong bond to be created between the bone and the implant. An HA coating can encourage a shell of bone around the implant within approximately two weeks of implantation and therefore the initial mechanical stability of a cementless implant regardless of coating relies on the press-fit provided by the surgeon (Bauer and Schils 1999).

Movement of the implant surface relative to the surrounding bone also affects the likelihood of bone in-growth (Pilliar et al. 1986; Jasty et al. 1991; Szmukler-Moncler et al. 1998) (Section 2.7.3) and with excessive relative movement only fibrous tissue will grow in the region around the bone which gives poorer clinical results (Engh et al. 1987). Many computational analyses have modelled cementless stems to calculate the relative motion between the implant and bone (Section 3.2.1). These studies have found that the area of stem covered in porous coating (2009) and implant geometry (2010) affect the micromotion and predict that this would affect the bone growth onto the stem.

The temperature reached in the exothermic reaction of the bone cement setting is high enough that it kills the surrounding bone (Mjöberg et al. 1986; Little et al. 2008). Cement also deteriorates over time and small pieces of cement can both cause a reaction in the body to remove them and reduce the effectiveness of the cement to transfer load from the implant to the surrounding bone, however cemented implants have a history of successful procedures (Malchau et al. 2002). They allow the patient to bear weight on their operated leg within days of the operation which the cementless technique does not. An uncemented hip must be given time for the bone to grow to form the bond between the implant and the femur and this lack of mobility is detrimental to the patient's muscles particularly in the elderly who lose muscle strength rapidly and only slowly regain it.

2.7.2.Surgical methods for hip arthroplasty

The surgical procedure for a total hip replacement involves cutting both the skin and soft tissue. Where the incision is made and which soft tissues will be divided or dissected depends on the specific approach used by the surgeon. There are several different approaches employed, each with different advantages and disadvantages. The most frequently used techniques are the posterior and anterior approaches (Kärrholm et al. 2008). When they are compared the main difference is that the anterior or anterolateral approach divides the abductor muscles, whereas the posterior approach allows a quicker surgery and potentially better postoperative function and gait pattern. The main disadvantage of the posterior or posterolateral approach is that it appears to increase the risk of post operative dislocation (Robinson et al. 1980; Vicar and Coleman 1984; Hedlundh et al. 1995; Parks and Macaulay 2000; Masonis and Bourne 2002).

The surgeons have started to reduce the length of the incision and in some cases make two incisions in an attempt to reduce the impact to all soft tissue. In addition, these minimally invasive surgeries (MIS) are designed to reduce blood loss, hospital stay and length of scar. An alternative approach advocated by Charnley, the transtrochanteric approach which involves a trochanteric osteotomy, cutting the greater trochanter, instead of dissecting the surround muscles. This method was suggested because bone can heal completely seamlessly whereas muscles will always heal to leave scar tissue. The trochanteric osteotomy has declined in popularity (Kennon et al. 2003) however it has been used successfully when there are additional problems such as femoral deformity (Della Valle et al. 2003). Several studies have shown disadvantages to the trochanteric approach citing dislocation, longer hospital stays and greater blood loss (Robinson et al. 1980; Vicar and Coleman 1984) or found no significant advantage to using that approach (Menon et al. 1998). Vicar and Colman (1984) compared the posterior, anterolateral and transtrochanteric surgical approaches and found that trochanteric bursitis was twice as common and there was a fivefold increase in the

incidence of haemotomas when using the transtrochanteric approach. The increase in haemotomas raises concerns about the approach since 58% of the haemotomas were associated with morbidity (Vicar and Coleman 1984).

Vicar and Colman (1984) found that dislocation was four times more likely with a posterior approach than either the anterolateral or transtrochanteric approaches. Hedlundh *et al.* (1995) also compared the dislocation rates of patients with either a posterior or anterolateral transtrochanteric approach and found an increased risk of dislocation in posterior approach patients within the first 14 days after surgery. Robinson *et al.* (1980) and Masonis and Bourne (2002) found that patients with the posterior approach are at greater risk of dislocation compared to lateral approach patients but found that the risk could be reduced by repairing the soft tissue.

Although the posterior approach has an increased risk of dislocation it continues to be one of the most commonly used surgical approaches. The range of motion at the hip has been found to be larger with the posterior approach compared to the lateral approach (Whatling et al. 2008) and in the posterolateral approach compared to the anterolateral (Madsen et al. 2004). The trunk inclination is an indication of abductor weakness and Madsen *et al.* (2004) found greater inclination with anterolateral approach than posterolateral approach. Gore *et al.* (1982) also found the abductor strength in posterior approach patients was closer to healthy patients than in anterolateral approach patients. Despite these studies finding that the surgical approach can affect the functionality at the hip not all studies agree. Downing *et al.* (2001) found that there were no significant differences in the abductor strength between the posterior and lateral approach patients. Pospischill *et al.* (2010) found no significant differences in the range of motion or gait kinematics between the anterior and lateral approach patients. Mayr *et al.* (2009) found that although the surgical approaches may result in very similar functionality at the hip, recovery may not occur at the same speed. They found that the gait of anterior approach patients returned to

nearly normal after approximately one year compared to the two years it took for the anterolateral patients.

Normally the hip function affected by the damage of muscles with a posterior approach is extension (gluteus maximus), abduction (gluteus minimus, gluteus medius and tensor fasciae latae) and lateral rotation (piriformis and the quadratus femoris), but in the anterior approach abduction (gluteus medius, gluteus minimus, tensor fasciae latae) and knee extension (vastus lateralis) are affected (Meneghini et al. 2006). However the muscles are not all affected equally and Meneghini *et al.* (2006) attempted to quantify the level of damage done to the muscles, using the dimensions of the damaged area, depending on the surgical approach. The anterior Smith-Peterson approach was shown to have been sparing of the gluteus minimus, which is a major abductor, compared to the posterior approach but caused damage to the tensor fasciae latae which might cancel out the positive effect on abduction of the hip. Madsen *et al.* (2004) found that the posterolateral approach gave a greater range flexion/extension and lower abduction weakness than the anterolateral approach. Whatling *et al.* (2006) investigated the difference in gait between the lateral and posterior surgical approaches and found that the posterior approach tends to lead to a more normal gait pattern.

Minimally invasive surgery (MIS) is conducted as it reduces the impact on the muscles and tendons. This has been shown to increase the speed of recovery and the functionality of the joint post operatively, suggesting that standard surgical approaches which divide muscles reduce the success of the surgery (Berger 2006). This is not found in all studies, Bennett *et al.* (2006) found no difference between the gait of patients regarding the difference between a posterior minimally invasive surgery and standard incision length procedure. However this surgery was a simple reduction in the length of the incision whereas MIS is designed to reduce the impact to all soft tissue. Kennon *et al.* (2003) describes the minimally invasive anterior approach in which the abductor mechanism is left untouched, and which has a lower blood loss

and reduced complication rates than standard arthroplasty surgery. This leads to a reduction in the quantity of soft tissue trauma and faster postoperative mobilisation suggesting that the muscle damage in standard surgery is significant. Gait analysis did not show statistically significant differences between the different surgical approaches although studies have shown an abductor weakness in a group with a lateral approach (Whatling et al. 2006).

2.7.3.Failure modes of joint replacements

Failure of a hip arthroplasty is usually defined as the point when either the femoral or acetabular components require replacement. Revision surgery removes the defective components and replaces them with new ones however these operations are longer, more expensive and more difficult than primary operations as the bone quality is normally worse than in the original operation and the old implant can be difficult to remove. Arthroplasty registers have been set up in many countries to monitor the details of hip arthroplasty surgery and the reasons for failure, with the normal failure criteria taken to be revision surgery. Comparisons are made between a variety of factors such as implant designs, hospital and reasons for primary hip replacement. The longest running hip arthroplasty register is the Swedish Hip Arthroplasty Register (Malchau et al. 2002) which has been recording hip arthroplasty surgery since 1979 in contrast to the register in England and Wales (National Joint Registry 2005) which has yet to reach enough data for long term analysis.

The main causes of revision with cementless hip replacements are dislocation (33%), loosening (23%), deep infection (12%) and fracture of the femur (17%) (Kärrholm et al. 2008). The causes of cemented hip replacement are similar although there is a higher rate of dislocation and infection but a lower percentage of fracture. Surgical error, pain and implant fracture also cause the arthroplasty to be revised but in total only accounted for approximately 13% of cementless revision surgeries. The major reason for long term failure is aseptic loosening, but short term failure is more often caused by dislocation or by infection (Ulrich et al. 2008).

The risk of dislocation is affected by surgical approach, implant design, orientation of components and the restoration of the muscle tension (McCollum and Gray 1990). As described in Section 2.7.2 a posterior approach to the hip increases the risk of dislocation. The posterior approach can also increase the likelihood of a retroverted cup, one which is rotated backwards, due to the angle of the patient's pelvis (McCollum and Gray 1990; Archbold et al. 2006) and this increases the likelihood of a posterior dislocation of the hip. Inadequate restoration of the tension in the abductor muscles during surgery can lead to a limp and also increases the risk of dislocation (McCollum and Gray 1990).

Excessive movement of the component is termed loosening and requires a revision surgery. Aseptic loosening of an arthroplasty component can be caused by several factors:

- high stress at the bone-implant (cementless), bone-cement or cement-implant interface (cemented)
- wear particles
- lack of bone in-growth onto the implant surface (cementless) or
- stress shielding

If the stress at the interface is higher than the material's strength then the interface bond can fail and this can lead to movement of the component with respect to the bone (Huiskes 1993).

Bone is adaptive and can become more or less dense depending on the loads applied to it and therefore alter its modulus (Section 2.2). Too little stress in the bone can result in resorption of bone in that area. In the natural hip this situation is unlikely to occur since the body weight is transferred through the bone. However the modulus of a hip prosthesis is much higher than that of bone, for example a typical prosthesis made of cobalt chromium has a modulus of approximately 220GPa but the modulus of bone is only approximately 17.4GPa (Callister 2000). This can lead to bone

remodelling and potentially the loosening of the implant (Huiskes et al. 1987). Bone resorption due to the stiffness of the implant is known as stress-shielding and can be seen as radiolucent areas on patient's post-operative x-rays. The stiffness of the stem (1990) and the surface area of fixation (1995) have also been shown to affect the load transfer through the femur and hence the remodelling of the bone (Section 3.2.1).

Wear particles can also result in gross loosening of the implant by eliciting an inflammatory response from the bone which attempts to remove them (Ingham and Fisher 2000). Unfortunately the cells in the body used to remove the particles of wear, macrophages, can also locally remove healthy bone at the same time. Fluid flow around the implant distributes the wear particles and excessive wear can lead to gross loosening of the stem or cup and potentially revision. Although this phenomenon was known as cement disease it also occurs in cementless hip arthroplasties and is mainly due to the wear from the bearing surface. To reduce the wear in the joint, ceramic on ceramic, ceramic on polyethylene and metal on metal bearing surfaces have been used as these materials have been found to produce less wear (Dumbleton and Manley 2005; Essner et al. 2005). However these materials have different problems associated with their use. There is concern that metal particles could increase the risk of cancer (Dumbleton and Manley 2005). The tough surface of ceramics means they produce low wear however due to their brittle nature they are prone to fracture (Anwar et al. 2009).

In cementless implants initial stability is usually created with a push fit between the implant and bone. The bone is then encouraged to grow up to the surface of the implant to create a strong fixation (Section 2.7.1). A gap between the bone and implant can slow or prevent the growth of bone on to the stem surface. A gap of less than 2mm can be filled by cancellous bone and denser bone can be generated if the implant surface is in contact with the bone (Bobyn et al. 1981). Attachment of the implant is stronger the smaller the gap and with an HA coating the gap should be less than 1mm for a strong fixation (Dalton et al. 1995). Relative movement between the

bone and implant can also reduce or prevent the growth of bone onto the implant surface. Micromotion less than 20μm (Jasty et al. 1991) or 28μm (Pilliar et al. 1986) has been found to allow bone growth and micromotion greater than 40μm (Jasty et al. 1991; Engh et al. 1992), 50μm (Szmukler-Moncler et al. 1998) or 150μm (Pilliar et al. 1986) has been found to result in the growth of fibrous tissue and reduce the growth of bone onto an implant. Fibrous tissue can provide a weak, temporary fixation for the implant however both a gap at the interface or fibrous tissue allows micromotion and perpetuate the production of fibrous tissue (Viceconti et al. 2001). As the layer of fibrous tissue is increased, the fixation of the implant weakens and the micromotion between bone and implant increases (2001). Immobilisation can reduce the fibrous tissue layer and allow a stronger fixation to be generated with a Ti coated implant, however with an HA coating the fixation was stronger than the Ti implant and was not as effected by immobilisation (Søballe et al. 1993).

The reasons for hip replacement failure can usually be attributed to one of three areas, implant related, surgical related and patient related. The Swedish Hip Arthroplasty Register records a large difference in survivorship depending on the clinic type that the patient was treated at, suggesting that the surgeon is a large source of variation in the lifetime of a hip replacement (Malchau et al. 2002). The orientation and placement of the prostheses is not always the same as the preoperative plan and this can be for a variety of reasons from surgeon error to actual conditions *in vivo* differing from expected conditions. There are guidance systems to give surgeons a better knowledge during surgery of the position of the implant. It is also possible prior to surgery to use CT scans to get a three dimensional view of the patient rather than the standard two dimensional view from a traditional x-ray. Guidance systems and CT scanners are expensive and there are concerns with the health risks associated with CT scans so these options are not always used.

As discussed earlier, there are several surgical approaches that can be used to implant the prosthesis and these different techniques require surgeons to divide different

muscles and ligaments (Section 2.7.2). Minimally invasive techniques reduce the impact on the hip tissue, reduce the blood loss and the size of the resulting scar but can impair the surgeons' vision of the hip. The registers do not monitor the range of motion a patient has after surgery or the post-surgery pain levels. Although pain levels are difficult to monitor, techniques such as the Harris hip score (Mahomed et al. 2001) are commonly used post surgery to allow surgeons to discover if there has been a reduction in pain. The range of motion that a patient has post surgery is traditionally only of secondary consideration as the objective of the surgery is the elimination or reduction of pain. However patient expectations are increasing particularly in the younger, more active patients.

The design of the implant and the associated instrumentation required during surgery also affects the lifetime of the hip prosthesis. There are different types of hip replacement in shape and design, fixation method and material. The majority of the femoral heads implanted in England and Wales (National Joint Registry 2005) are metal and only 25% of the femoral heads are ceramic. Approximately 33% of the nearly 65,000 total hip replacements conducted in England and Wales in 2007 were cementless, compared to 38% cemented. In England and Wales there are approximately 110 brands of hip stems on the market of which more than sixty are cementless hip stems, however there are only five that have more than a 5% share of the market (National Joint Registry 2005). The two most popular cementless stems are the Corail (Depuy) and Furlong HAC (Joint Replacement Instrumentation Ltd) with 27% and 24% of the market respectively. They have a similar revision rate after three years, 2.6% in the Corail and 2.7% in the Furlong in England and Wales (National Joint Registry 2009).

The patients themselves are also extremely important in the lifetime of the prosthesis. The age of a patient, their post-surgery activity levels and original reason for arthroplasty can all affect the time until failure of the implant (National Joint Registry 2005). Hip surgery is commonly postponed for as long as possible since it is not

advisable to enter into any surgery unless necessary and the survivorship likelihood of the implant is increased with increasing age of the patient (Malchau et al. 2002). Patients often assume that a hip replacement will allow them the same level of activity that they enjoyed pre-operation or expect that the replacement will allow them normal levels of activity. This is not the primary reason for replacing a hip and high activity levels reduce the lifetime of the implant, leading surgeons and postoperative care workers to try and encourage low activity levels (Siopack and Jergesen 1995).

3. Review of musculoskeletal and finite element analysis of the proximal femur

Total hip arthroplasty is an extremely successful surgical procedure for relieving hip pain, restoring function to the joint and improving quality of life (Bachmeier et al. 2001; Kärrholm et al. 2008). However, with an increasing population, even a small percentage of failed hip arthroplasty surgeries represents an increasingly large number of patients. In 2008 there were approximately 6,600 revision surgeries out of approximately 71,400 total hip replacements in England and Wales (National Joint Registry 2009). This was an increase from 5,800 revisions out of a total of approximately 62,000 total hip replacement surgeries recorded for 2005 (National Joint Registry 2005) and the number of people needing total hip arthroplasty surgery is expected to rise (Birrell et al. 1999). Patient demographics are changing and patients are increasing in weight (National Joint Registry 2009) and becoming younger (Kärrholm et al. 2008) and potentially more active.

Analyses of hip implants can be categorised into three broad areas, clinical trials in patients, *in vitro* lab tests and computational modelling. Non-invasive clinical studies, such as gait analysis or reviews assessing the arthroplasty lifetime in a patient group, can be used to compare different implant types, surgical procedures, fixation methods and even patient related factors such as activity levels. Patients and their implants can also be assessed using more invasive procedures such as radiostereometric analysis (RSA), which involves implanting tantalum beads around the replacement joint as internal markers. RSA can provide detailed information about the displacement of the implant components however these studies only involve a limited number of patients due to the invasive and expensive nature of the investigation. Clinical studies provide dependable results since they study patients *in vivo*, however due to the large number of potentially confounding variables the flexibility of the studies is limited and normally only one variable per study is investigated. Additionally clinical studies require a large number of patients to provide statistically significant research. Revision

surgery is used as a measure of how well a particular prosthesis, hospital or procedure is performing, however this is a crude method of ascertaining the overall performance of the replaced hip. Clinical studies are starting to measure pain levels and quality of life (Kärrholm et al. 2008) however these can be difficult to assess.

Gait analysis measures the position of the legs as a person walks and records their foot reaction on the ground using a force plate (Section 3.2). These data can be used to calculate the joint angles and moments during the gait cycle and, using a musculoskeletal model, muscle and joint contact forces can be predicted (Section 3.3). Muscle and joint forces can be used to compare the functional outcome of a range of total hip replacements, although this is still limited to the specific individuals monitored in the study. However, since it is not an invasive study, a larger number of patients can be investigated than by using instrumented hip replacements. Ideally the range of forces predicted by musculoskeletal modelling of clinical studies would be used to inform computational and experimental analyses of hip replacements.

Laboratory experiments are used to investigate the stability of an implant and the wear on the bearing surface. This type of analysis provides a greater flexibility than the clinical studies since a wider range of implants and loading conditions can be used and comparisons can be made to other implants. However the loading conditions used in the tests must be obtained from other studies and the testing procedure is slow and relatively expensive compared to computational modelling. *In silico* analyses are both quick and very flexible and allow a wide range of designs, loading criteria and scenarios to be modelled (Section 3.2). However they are limited by the data used to create them and so the models are only as reliable as the input geometry and loads. This makes the modelling technique good for examining trends by investigating a large number of scenarios and comparing the models to investigate the best situation. They can then be compared to clinical or experimental studies to evaluate the robustness of the modelling procedure.

3.1. Musculoskeletal analysis

Instrumented hip prostheses have been used to measure the actual forces across the hip (Section 2.5). However, the studies contain only a small number of patients who have undergone total hip arthroplasty. The angle and moment at the joints during gait can also be measured using gait analysis (Section 2.4.1) and inverse dynamic musculoskeletal analysis can use gait analysis to predict the joint moments. Forward dynamic musculoskeletal analysis is used to predict gait using predicted internal forces or torques and can be compared to gait analysis to validate the assumptions made to generate the movement. However, finding accurate force data or methods of describing the force production in the muscles is difficult and so adds error into the analysis. Inverse dynamic musculoskeletal models use the kinematics and kinetics measured during gait analysis in the equations of motion to determine the net forces and torques acting at the joints (Erdemir et al. 2007). Optimisation is required to predict muscle and joint contact forces from the results of an inverse dynamic analysis.

3.1.1. Inverse dynamics

Inverse dynamics calculates the joint forces and moments using anthropometric data about each modelled limb segment, kinematic data and external forces (Robertson et al. 2004). The anthropometric data for each limb consists of its mass, length, inertia properties and centre of mass. These are usually scaled from cadaver measurements to the data collected from the gait analysis subject using the subject's body weight and height. Gait analysis is used to collect the kinematic data usually with skin mounted markers to measure the position, velocity and acceleration of the individual limbs (Section 2.4.1). Ground reaction forces are also measured for inverse dynamic analysis of the lower limbs. The equations of motion are then used to calculate the net joint forces and torque.

Typically each limb segment has a minimum of three markers attached to it to enable its position and orientation to be captured. However each modelled segment has only six degrees of freedom (DOF) and with constraints at the joints this is reduced further.

To reduce this over-determinant system, standard kinematic analysis in inverse dynamics neglects some of the measured marker coordinates. Andersen *et al.* (2009) used an optimisation based approach to calculate the movement in the joints from all the measured marker data when applied to a musculoskeletal model with joint constraints. They found that the optimised marker followed the trajectories of the measured markers more closely than the modelled markers using the standard approach. They also found root-mean-square (RMS) error associated with the acceleration of the markers was reduced by 60% using the optimisation based approach.

3.1.2. Predicted muscle and joint contact forces

The muscle forces and joint contact forces are calculated by balancing the external forces acting on each limb segment. However, there are more muscles than equations of dynamic equilibrium and therefore the system of equations which relates the muscle forces to the limb segment accelerations is indeterminate. Individual muscle forces can be predicted either by reducing the number of muscles in the models (Paul 1966) or by using optimisation techniques (Seireg and Arvikar 1975; Johnston et al. 1979; Brand et al. 1986; Brand et al. 1994; Glitsch and Baumann 1997; Stansfield et al. 2003; Lenaerts et al. 2008). The optimisation provides assumptions about the manner in which the body recruits muscles to enable the muscle forces to be calculated. Several different optimisation criteria have been suggested in the literature. The main criterion for minimisation used in the literature is either muscle force (Seireg and Arvikar 1973; Seireg and Arvikar 1975; Crowninshield et al. 1978; Patriarco et al. 1981; Glitsch and Baumann 1997; Rasmussen et al. 2001) or muscle stress (Johnston et al. 1979; Brand et al. 1986; Brand et al. 1994; Glitsch and Baumann 1997; Stansfield et al. 2003; Lewis et al. 2007) which is the muscle force normalised by its PCSA. The optimisation in the majority of these studies minimises the sum of their individually defined criteria (Crowinshield et al. 1978; Johnston et al. 1979; Patriarco et al. 1981; Lenaerts et al. 2008), however several studies increased the order to the power of two

or three, for example to the sum of the squared or cubed muscle forces (Brand et al. 1986; Glitsch and Baumann 1997; Hoek van Dijke et al. 1999).

The review paper by van Bolhuis and Gielen (van Bolhuis and Gielen 1999) compared different optimisation techniques. They investigated several different optimisation models by comparing the modelled results to electromyography (EMG) patterns from an isometric experimental investigation of the arm. They concluded that none of the models they investigated fitted the activation patterns found from EMG data however the worst fit were the minimisation of either the sum of forces or metabolic energy consumption. The best fit for the experimental data were of the second order, the minimisation of the sum of the squared forces, stress, metabolic rate or muscle activation.

Brand *et al.* (1994), Stansfield *et al.* (2003) and Heller *et al.* (2001) used measured hip contact forces to validate their musculoskeletal model. Brand *et al.* compared the hip contact force measured using an instrumented hip to separately recorded gait analysis from the same patient and reported a good correlation. They used a muscle recruitment which minimised the sum of the muscle stresses cubed and predicted hip contact forces approximately 0.5BW higher than the measured forces at the heel strike and toe off peaks. However since the motion capture and the hip force measurement were not simultaneous and they found variation between the gait cycles of this patient it is difficult to assess the validity of their comparison. Stansfield *et al.* and Heller *et al.* used gait analysis data captured simultaneously with the measurement of hip contact forces using an instrumented hip implant (Bergmann et al. 1993; 2001) and both studies found good comparisons between the measured and predicted hip contact forces. Heller *et al.* used a muscle recruitment based on minimising the sum of the muscle forces whereas Stansfield *et al.* minimised the maximum muscle stress before minimising the sum of the muscle and joint forces. Heller *et al.* predicted the hip contact force better during stance than swing phase and the predicted force tended to be a slight overestimate. The largest deviation from the measured force was 33%

although the average difference was between 2-23% during normal walking. Stansfield *et al.* also found a difference of between 14-18% during several different activities including different walking speeds and stand to sit. During normal walking the difference between the peak in measured and predicted forces varied between 6-21% and the difference was lower at heel strike compared to toe off. They found that the measured forces were higher than those predicted by the musculoskeletal model during late stance and early swing phase and that the predicted force pattern was smoother than the measured force. Although there are differences between the measured and predicted forces these studies have shown that the musculoskeletal models can reasonable predict the hip contact forces. However the different recruitment criterion used to activate the muscles can produce variation in the muscle activity which may not substantially affect the resultant hip contact force.

EMG has also been used to validate several musculoskeletal models. Hoek van Dijke *et al.* (1999) who used first order muscle contraction intensity, Patriarco *et al.* (1981), who used first order muscle force and Seireg and Arvikar (1975), who used a combination of joint moments and force, all found a good correlation between EMG readings and the output from their models. However they all used a different criterion which suggests that the models are not sensitive to the optimisation criteria when comparing the activity of the muscles. This was also found by Brand *et al.* (1986) who found that their output forces were more sensitive to the PCSA of the individual muscles than the analysis criteria.

Calculating the muscle activity using an optimisation technique is not always an accurate description of the real muscle activations. In particular it has been shown using EMG that some of the active muscles produce a force that is counter to the overall joint movement (Glitsch and Baumann 1997) and these muscles are described as antagonistic muscles. Hoek *et al.* (1999) imposed antagonistic muscle activity in their model though it was found to only have a minor effect on the activity of the non antagonistic muscles.

3.1.3.Muscle modelling

The prediction of muscle force using the recruitment criterion for minimising the muscle force is relatively straightforward but it does not account for the differing sizes of the muscles. The recruitment criterion using the muscle stress normalises the muscle using their physical size measured by their PCSA (Section 2.3). An alternative method of normalising the muscle force is to use the muscle's current force generating capacity and calculate the activity of the muscle. Several groups have investigated muscle models to calculate the potential force of a muscle in a specific situation and have compared how well they relate to observed behaviour (Hill 1926; Hill 1938; Hill 1950; Hill 1953; Lloyd and Besier 2003; Thaller and Wagner 2004; Scovil and Ronsky 2006). Hill (1926; 1938; 1950; 1953) conducted a series of experiments on frog and toad muscles to create a model capable of predicting the force in a single muscle. He discovered that there is a relationship between the velocity of the contraction within the muscle and the maximum force available (Section 2.3.3).

Delp *et al.* (1995) defined a musculoskeletal model which was subsequently used to predict the effects of the change in location of the hip centre of rotation by altering the joint angles (Delp and Maloney 1993). They used a Hill-type muscle model and the activation patterns recorded by EMG to calculate the force in the muscles of their musculoskeletal model. Their musculoskeletal model calculated the length and velocity of muscle-tendon unit and then predicted the force in the muscle by calibrating the force-velocity and force-length curves to the EMG activity. However this type of model requires muscle activation patterns for all the muscles in the model for each modelled scenario and therefore is mainly useful for comparing the muscle generating capacity in different scenarios (Delp and Maloney 1993).

Hybrid models have been created using both EMG data and an optimisation strategy to calculate the force in the remaining muscles (Cholewicki and Mcgill 1994). Lloyd *et al.* (2003) created a hybrid musculoskeletal model for gait using the EMG data from

surface electrodes and then calculated the activity and strength of the deeper muscles using inverse dynamics. These studies reported successful results however it is not always possible to obtain all the required data from the same study and hybrid models require all the relevant data from the same patient.

The peak force a muscle can generate is during isometric contraction and at the peak isometric contraction the muscle has its optimal muscle fibre length. Wickiewicz *et al.* (1983) have measured the optimal muscle length and other parameters for the muscles in the lower extremity to allow the calculation of the tendon length (Hoy et al. 1990). Muscles vary in size and this has been shown to influence the strength of a muscle. Hill muscle models are commonly used in musculoskeletal models to predict muscle strengths (Zajac et al. 2002). The majority of muscle models are derived from Hill's original equations and use the physiological cross-sectional area of muscles, many of which have been published in studies (Brand et al. 1986; Klein Horsman et al. 2007). However currently there is no accurate method of determining the PCSA of all the muscles in a living subject (Brand et al. 1986) and so some element of scaling must take place to fit the parameters reported in the literature to individual patients.

3.1.4.Anatomical modelling

Musculoskeletal models mathematically define a muscle's line of action by two discrete points. The moment arm of a muscle, with respect to a joint axis, is directly related to the origin-insertion length and the joint angle. Therefore it is important that the accuracy of the body model containing the muscles with their individual attachment points and the body segments' anthropometric data is considered (An et al. 1984). Physiologically a muscle has an area of attachment and this has led many studies to split some of the larger muscles into several sub units to allow the different lines of action and different muscle activities to be modelled. Van der Helm and Veenbaas (1991) investigated the need for these separate units and the quantity required to give a reasonable representation of human anatomy. They modelled muscles at the shoulder with up to 200 units and found that the number of sub units needed

depended on the number of degrees of freedom the muscle influenced. Due to the relatively small attachment sites and muscles with fibres that run parallel to the line of action of the muscle, the need to separate the muscles into sub units is less in the lower extremity than the shoulder. Several studies have published muscle attachment points from cadavers and they have divided the muscles into sub-units appropriate to the attachment size and line of action of the muscles (Dostal and Andrews 1981; Klein Horsman et al. 2007).

3.1.5.Predicted forces

Musculoskeletal models have predicted a wide range of peak forces for normal gait from approximately 3-7BW (Table 3) and in general the predicted forces tend to be higher than those measured *in vivo* (Chapter 2.5.1). Some musculoskeletal models have used healthy subjects (Paul 1966; Crowinshield et al. 1978; Johnston et al. 1979; Glitsch and Baumann 1997) who could have higher forces than hip replacement patients and in general these models have higher forces than the models with gait from THA patients. However the musculoskeletal models often neglect antagonistic muscles which could potentially increase the joint contact forces. Several studies have compared their predicted forces to experimentally measured forces in an attempt to validate their musculoskeletal models. As discussed in chapter 3.1.2, Brand *et al.* (1994), Stansfield *et al.* (2003) and Heller *et al.* (2001) all found a good comparison between the measured and predicted hip contact forces.

Reference	Year	Peak hip force during gait (BW)	Subject description	Recruitment criterion	Muscle units per leg	Additional model details
Paul (1966)	1966	4.46 (3.39 average)	Healthy	-	6	
Seireg *et al.* (1975)	1975	5.4	-	Total muscle forces + 4x total joint moments	31	
Crowninshield *et al.* (1978)	1978	3.3-5 (4.3 average)	Healthy	Total muscle stress	27	Hip, knee and ankle – 3DOF
Johnston *et al.* (1979)	1979	~5.5	Healthy	Total muscle stress	30	Hip, knee and ankle – 3DOF
Brand *et al.* (1986)	1986	4.7-5.2	-	Total cubed muscle stresses	47	
Brand *et al.* (1994)	1994	~3.4	Post THA	Total cubed muscle stresses	47	
Glitsch and Baumann (1997)	1997	6.9	Healthy	Total squared muscle stresses	47	Hip – 3DOF, knee and ankle – 1DOF
Heller *et al.* (2001)	2001	2.5	Post THA	Total muscle force	47	Hip, ankle and femoro-tibial – 3DOF, patello-femoral – 1rot. DOF, 2 trans. DOF
Stansfield *et al.* (2003)	2003	~3	Post THA	Max muscle stress and additionally total muscle and joint forces	48	Hip – 3DOF, ankle – 1 DOF, knee – physiological constraints
Lenaerts *et al.* (2008)	2008	1.2-4.4	Pre THA	Total muscle activity	44	Hip – 3 DOF, knee and ankle – 1 DOF
Frasse *et al.* (2009)	2009	~4	Healthy	Squared muscle stresses	30	

Table 3: The predicted peak hip contact forces from several musculoskeletal models including details about the models.

3.2. Finite element analysis

Hip prostheses have been analysed using a range of different computational models. Traditionally static tests were used to compare different implant types often representing just the peak loading on the hip during gait (Rohlmann et al. 1983; Huiskes 1990). The models have become more sophisticated and patient-specific

models are now generated from CT scans (Schileo et al. 2008). Different implant coatings have also been modelled and adaptive models are used to investigate the effect of these, and altered bone loading, on the biological response (Bitsakos et al. 2005). These models only represent one individual but hip arthroplasty is performed on a wide range of the population and the type of person likely to receive a hip replacement is expanding. Recently probabilistic models have attempted to quantify the differences that occur in patients, such as differing bone geometry or the range of likely positions for the implant (Kayabasi and Ekici 2008).

Although finite element models have become more complex in their geometry there are still major differences in the forces applied to the models, the boundary conditions used and the output parameters employed. Computational studies of hip implants use a range of loading conditions from only a hip force to more complex loading scenarios involving several muscle forces in addition to the hip contact force. The magnitude of the forces applied is also variable between studies, however most investigations only represent an average patient during the peak in hip loading in normal gait. The limitations of simplified loading conditions are discussed later in this chapter. The boundary conditions are also variable between computational analyses, although many finite element studies are comparative studies with an experimental set up and are constrained by the potential scenarios available *in vitro*. There are also a range of output parameters used in the finite element analyses including stress, strain, shear strain, bone density, deflection and micromotion. Due to the large volume of data that a model usually produces these output parameters are usually reduced to a single system response such as the maximum, minimum or mean value. However the range of output parameters can make comparisons difficult both between studies and with clinical results. It can also be difficult to find which parameter is the most useful as a predictor of a clinically relevant outcome.

3.2.1. Computational studies of cementless hip implants

Although cementless implant designs are also analysed in the same manner as cemented implants there are additional challenges such as investigating the ingrowth of bone into the implant surface. Many studies have modelled cementless implants to investigate their effect on the surrounding bone and to predict the outcome of different situations. However unlike cemented hip arthroplasties the desired fixation of the implant to the bone does not occur straight away and therefore the primary stability of cementless implant can be analysed by modelling the implant and bone immediately after surgery before bony ingrowth. Alternatively the secondary stability of the implant can be analysed by assuming a full osseointegration of the femur and implant. In the primary stability cases the implant is assumed to have a frictional coefficient between the bone and implant to represent either the rough coated surface or a smooth surface finish whereas a fully bonded model represents the ideal osseointegrated case which would not occur for several weeks post operatively and is dependant on the primary stability. Some of these finite element studies have been identified in Table 4 with a summary of the implant type, loading conditions, the boundary conditions and the output parameters reported in their study along with the major findings of the study.

Reference	Implant Type	Forces applied	Boundary conditions	Major findings
Tensi *et al.* (1989)	Generic straight stem	Hip and abductor.	Fixed distal end. Coated area – fully bonded.	Principle shear stresses between 1-1.5MPa with level walking loads. Increase in lateral stress with a proximal coating compared to fully coated stem.
Huiskes (1990)	Omnifit (Osteonics)	Hip force only.	Fixed mid-shaft. Coated area – fully bonded.	Interface stress greater than 10MPa at distal end of fully coated stem. Lower proximal interface stresses and higher distal stresses in fully coated compared to partially coated stem.
Cheal *et al.* (1992)	AML (DePuy)	Hip and various muscle forces.	Fixed mid-shaft. Fully bonded.	At toe off the max. interface shear stress, at the distal end, was approx. 10MPa in the CoCr stem and was lower in the titanium and composite stems.
Keaveny and Bartel (1993)	AML (DePuy)	Hip and abductor.	Fixed mid-shaft. Coated area μ=1.73.	Relative motion of the stem was reduced with an increase in coated area, in particular in implants without collar support.
Rotem (1994)	Generic stem	Hip and abductor.	Fixed mid-shaft. Frictional contact.	Normal and shear stresses found to be higher in stainless steel stem compared to a composite stem.
Keaveny and Bartel (1995)	AML (DePuy)	Hip and abductor.	Fixed mid-shaft. Ingrowth areas – bonded, non ingrown areas μ=1.73	Max. relative motion between the implant and bone was reduced from approx. 700µm with typical ingrowth to approx. 150µm with ideal ingrowth.
Taylor *et al.* (1995)	Freeman (Corin Medial Ltd)	Hip force only. Hip force with abductor, iliotibial tract and Iliopsoas.	Fixed distal end. Coated area – bonded, smooth area – μ=0 or 0.25	Lower peak principal stress in bone of approx. -4MPa in cemented or coated models compared to approx. -13MPa in press fit stem model. Similar differences found in peak principal strain.
Biegler *et al.* (1995)	Mallory-Head (Biomet) and Harris-Galante (Zimmer)	Hip, abductor and ground reaction.	Ground reaction force. Coated area – μ=0.61, smooth area μ=0.42.	Greater micromotion with stairclimbing loads than with one legged stance.
Ando *et al.* (1999)	FMS-anatomic, FMS, Omniflex, Omnifit and IDS (Osteonics)	Hip and abductor.	Fixed distal end. Coated area – μ=0.61, smooth area μ=0.42.	Relative motion and von Mises stresses on the femur were generally lower with an anatomically shaped stem than conventionally shaped stems due to the stem-bone fit.
Viceconti *et al.* (2000)	AncaFit (Cremascoli-Wright)	Internal rotational torque.	Fixed mid-shaft. Contact area – μ=0-0.5.	FEA can predict micromotion reasonably accurately compared to *in vitro* tests.
Viceconti *et al.* (2001)	AncaFit (Cremascoli-Wright)	Internal rotational torque.	Fixed mid-shaft. Contact area – μ=0.2.	A soft tissue layer greater than 500µm could cause micromotion greater than 200µm and prevent osseointegration.

Pancanti *et al.* (2003)	AncaFit (Cremascoli-Wright)	Hip only. Hip, abductor and vasti muscles.	Distal constraint. Contact area – μ=0.3.	Peak micromotion during normal gait ranged from 56-75μm and was higher during stair walking. 18-49% of the stem surface had a micromotion greater than 40μm during normal walking.
Wong *et al.* (2005)	IPS (DePuy)	Hip, abductor and vastus lateralis.	Coated area – μ=0.6, smooth area μ=0.4.	Peak micromotion between 50-60μm was calculated in the normal bone modulus model. Both equivalent strain at the interface and peak micromotion increased with a reduction in bone modulus.
Viceconti *et al.* (2006)	AncaFit (Cremascoli-Wright)	Hip, abductor, vastus lateralis and medialis.	Fixed distal end. Frictional contact.	The micromotion and peak shear stress were strongly affected by body weight, model size and the area of bone in contact with the stem.
Speirs *et al.* (2007)	Nanos (Endoplant)	Hip and various muscle forces.	Joint scenario – constrained nodes at distal condyles and hip. Coated area – bonded, smooth area – μ=0.01	Anteverted and medialised stems generate higher strain along the length of the femur than properly positioned stems. Highest proximal cortical strain in medialised stem model and were up to 500μm larger than the reference position model.
Abdul-Kadir *et al.* (2008)	Alloclassic (Zimmer)	Hip force only.	Fixed distal end. Frictional contact – μ=0.4	An increase in the depth of the implant interference fit reduced micromotion at the interface.
Jonkers *et al.* (2008)	Custom-made prosthesis	Hip and various muscle forces.	Fixed mid-shaft. Fully bonded	Patient specific forces affected the von Mises stress in the femur more than changes to the bone geometry.
Reggiani *et al.* (2008)	AncaFit (Cremascoli-Wright)	Internal rotational torque.	Fixed distal end. Contact areas – μ=0.3.	Planned stem position can reasonably predict the micromotion and von Mises stress of the achieved position.
Park *et al.* (2008)	AncaFit (Cremascoli-Wright)	Hip force only.	Complex fixed distal end. Contact areas only – Coated: μ=0.5, polished: μ=0.3.	Reduction in gaps at the bone-implant interface improved primary stability by reducing micromotion.
Behrens *et al.* (2008)	Bicontact (Aesculap AG) and Spiron (Arge Medizintechnik)	Hip, abductors, tensor fasciae latae and vastus lateralis.	Fixed distal end. Coated region – bonded contact.	Stem shape affects the bone loading and remodelling stimulus.
Andreaus and Colloca (2009)	F2L Multineck (Lima)	Hip, abductor, TFL, vastus lateralis and medialis.	Physiological constraints. Fully bonded	Peak shear strain up to 200% larger under stair climbing conditions compared to normal walking.
Folgado *et al.* (2009)	Trilock (DePuy), AML (DePuy)	Hip and abductor.	Fixed mid-shaft. Frictional and bonded contact based on relative displacement.	Bone mass greater with titanium stem than Co-Cr and for coated stems greater bone mass with taper compared to cylindrical shape.

Park *et al.* (2009)	Versys Fiber Metal Taper (Zimmer)	Hip force only.	Fixed distal end. Rough area – μ=0.5, polished area – μ=0.3.	Micromotion is not significantly affected by gaps in the bone-implant interface provided the contact ratio is greater than 40%.
Pettersen *et al.* (2009)	Summit (DePuy)	Hip and abductor	Fixed mid shaft. Contact area – μ=0.4.	Peak micromotion approx. 40μm in both proximal and distal areas in general agreement with in vitro experiment.
Hu *et al.* (2009)	Alloclassical SL Plus (Zweymüller), Ribbed Anatomical (Waldemar Link), VerSys Fiber Metal Taper (Zimmer) and Secur-Fit (Stryker)	–	Fixed distal end. Interference fit with frictional contact μ=0.4.	Von Mises stress at the bone-implant interface higher with ribbed or sharp edged stems compared to rounded stems.
Sakai *et al.* (2010)	AI-Hip (Aimedic)	Hip, abductor and rotational torque.	Fixed distal end. Frictional contact μ=0.1.	Favourable comparison of AI-Hip stem with micromotion and von mises stress reported in the literature for other cementless stems.
Dopico-González *et al.* (2010)	Proxima (DePuy) and IPS (DePuy)	Hip, gluteus minimus and medius, iliopsoas and vastus medialis	Fixed mid-shaft. Fully bonded and frictional contact models.	Peak micromotion strongly affected by bone and implant geometry.
Gracia *et al.* (2010)	ABG-I and ABG-II (Stryker)	Hip and abductor	Fixed mid-shaft. Frictional contact – μ=0.5.	Higher stress in the proximal region of slightly smaller stem and predicted increase in bone mass.

Table 4: Studies performed using finite element analysis to explore the performance of cementless hip implants.

Studies have been conducted to compare fixation type, both to examine the differences between cemented and cementless implants and to investigate the effects of partial, full or no coating on cementless stems (Tensi et al. 1989; Huiskes 1990; Taylor et al. 1995). Tensi *et al.* (1989) calculated compressive stresses in the distal-lateral region of approximately 1MPa in a fully coated stem during one-legged stance and higher stresses with level walking loads although they only used hip and abductor forces. They also found an increase in the lateral stress with a proximally coated stem compared to the fully coated stem. Huiskes *et al.* (1990) found that the stress pattern at the bone interface was similar between the cemented and cementless cases

although the stress was reduced on the proximal side of the implant and increased on the distal side in the cementless case. Therefore more of the hip load was transferred through the distal portion of the implant compared to the cemented model. They found interface stresses, calculated as the resultant of the interface normal stress and the shear stress, of more than 10MPa at the distal end of a fully coated cementless stem.

Huiskes *et al.* (1990) considered the effect of a titanium stem compared to the CoCrMo alloy and found that the less rigid titanium transferred more hip load to the proximal femur and therefore reduced the interface stresses at the distal interface. There was significantly less stress calculated with a partially coated stem compared to a fully coated stem at the distal interface and this was also found in the study by Tensi *et al.* (1989) where there was a greater stress in the proximal regions with a partially coated stem. Huiskes *et al.* (1990) also modelled a press-fit stem and found that the interface stresses were substantially higher than those found in either the cemented or HA coated stem models. Taylor *et al.* (1995) also found the fixation of the implant using only a press fit either with a smooth implant surface or a ridged surface generated considerably higher peak principal stresses and strains in the cancellous bone than either the cemented or HA coated fixation models. The peak principal stress in the cancellous bone was found to be approximately -4MPa in both the cemented and HA coated models however in the press fit models both the smooth and the ridged stems the peak principal stress was approximately -13MPa compared to only -2MPa in the intact femur model. They found a similar pattern in the peak principal strains where they calculated a peak tensile strain of approximately 3000με in the cemented and HA coated models and approximately 10,000με in the smooth press fit model although the ridged model had a peak tensile strain of approximately 5000με.

Keaveny *et al.* (1995) considered the effects of bone ingrowth which was modelled similarly to the studies comparing stem coating quantity in which the models had assumed full bone ingrowth in the coated scenarios. Keaveny *et al.* found that with

ideal bone ingrowth the proximal loading was reduced compared to no bone ingrowth and the relative motion between the implant and bone was reduced in the bone ingrowth cases compared to no ingrowth. However Biegler *et al.* (1995) found only slight differences between the relative motion of smooth and porous coated stems.

Comparisons have also been made between different cementless implant designs (Ando et al. 1999; Folgado et al. 2009; Hu et al. 2009) and several studies have investigated new material types irrespective of implant design (Huiskes 1990; Cheal et al. 1992; Rotem 1994). Ando *et al.* (1999) found lower von Mises stress and relative motion at the bone-implant interface in an anatomically based implant compared to conventionally designed stems. They found that the anatomically based stem produced a large area of contact between the bone cortex and the implant and they attributed this to the reduction in interface stress compared to the other implant models as it allowed a transfer of load from the stem to the femur in both proximal and distal areas. Hu *et al.* (2009) found that the stresses in the bone surrounding implant designs with sharp corners or ribs were higher than those with a more rounded stem and predicted that the higher stresses would increase the likelihood of fractures in the bone. However, Viceconti *et al.* (2006) found that a finned implant had a greater primary stability, calculated by a lower micromotion of the stem, than a smooth stem due to the larger area of contact between the bone and implant.

The stiffness of the stem material is thought to affect the interface stresses as a more rigid stem transfers the load to the distal regions unlike a more flexible stem which transfers more load to the proximal regions and reduces the stress in the distal regions (Huiskes 1990). Huiskes *et al.* (1990) calculated that with a change in the stem material from CoCrMo to titanium the interface stress would be reduced by more than 20% at the medial-distal interface. Cheal *et al.* (1992) and Rotem *et al.* (1994) also found that a reduction in the prosthesis stiffness resulted in lower interface stresses and Folgado *et al.* (2009) predicted a lower bone mass in the proximal femur, mainly on the medial side, with CoCr stems compared to titanium stems.

Two scenarios are typically modelled in finite element analyses, primary stability, in which the stem has recently been implanted, and the fully bonded scenarios, assuming that osseointegration has reached equilibrium (Table 4). The HA coated models in the study by Taylor *et al.* (1995) and Tensi *et al.* (1989) were assumed to be perfectly bonded to the bone to simulate an ingrown situation. However more recent studies have used a friction coefficient at the bone-implant interface to model the stem before bone ingrowth has occurred (Park et al. 2009; Pettersen et al. 2009; Sakai et al. 2010). The micromotion is often calculated at the interface as it can affect the bone growth onto the surface and hence the stability of the implant (Jasty et al. 1991). Studies have reported that the larger the surface of the stem in frictional contact representing the coated area or ingrown area, the lower the micromotion (Keaveny and Bartel 1993; Keaveny and Bartel 1995). Viceconti *et al.* also reported that the thickness of a soft tissue layer, which was modelled with a low frictional coefficient, affected the micromotion and a layer greater than 500μm could prevent osseointegration onto the surface of the implant. The contact area between the stem and the bone has also been found to affect the micromotion at the interface (1999; 2006; 2008). Ando *et al.* (1999) reported lower relative motion with an anatomically shaped stem due to increased stem-bone fit compared to conventionally shaped stems. Viceconti *et al.* (2006) reported that the peak micromotion was strongly affected by the contact region between the stem and bone and Park *et al.* (2008) also found that a reduction in the gaps at the bone-implant interface, and therefore an increase in the contact region reduced micromotion. However Park *et al.* (2009) reported that, although the bone-implant contact ratio affects the micromotion at low ratios, with contact greater than 40% the micromotion is not significantly affected.

Some studies have taken the research into bone growth and tissue differentiation beyond independent static analyses and used adaptive models to consider the change in tissue type based on the loading of individual elements. Folgado *et al.* (2009) used bone strain in an adaptive model to assess the differences between the amount of

coating on a stem and the material type. A frictional coefficient of 0.6 was used to represent coated surfaces on hip stems and they found that uncoated stems produced the least amount of bone resorption compared to partially and fully coated stem models. Previous studies had found that the uncoated stem was likely to have a shorter lifetime due to high stresses at the interface (Huiskes 1990; Taylor et al. 1995) and Folgado *et al.* also found higher strain at the interface in uncoated stems, however the algorithm used to calculate bone resorption used the higher strain to remodel the bone density. They found that the effect of the coating was less when the stem was tapered rather than cylindrical and the final bone mass was similar in all the coating types with a tapered stem.

The position of the stem can affect the interfacial strain and Speirs *et al.* (2007) showed that an anteverted or medialised stem would generate higher strain along the length of the femur than a properly positioned stem. In particular, they found that during stair climbing the medialised stem generated a higher strain energy density than the reference stem position. However these differences were found to be small compared to the change in strain from an intact femur to an implanted situation. Reggiani *et al.* (2008) also investigated the effects of implant position by comparing a planned stem position with the surgically achieved position. They found only slight differences between the two models although, at peak, found an increase of 12% in the von Mises stresses with the achieved position.

Probabilistic studies allow a wide range of scenarios to be modelled (Viceconti et al. 2006; Park et al. 2009; Dopico-González et al. 2010). Viceconti *et al.* (2006) compared 1000 models of an implanted cementless stem by varying the bone density, patient's body weight, bone size and the quantity of bone-implant contact area. They found the peak micromotion was affected by the total variation applied to the model and the average micromotion was 206±159μm under stair climbing loads. The bone size, body weight and region of implant contact were found to significantly affect the peak shear stress and peak micromotion and the variation in cortical bone density

significantly affected the peak shear stress. However, although the study varied the body weight and used that to vary the loads on the femur, other studies have shown that body weight alone does not account for inter-patient variation (Bergmann et al. 2001; Taylor and Walker 2001). Dopico-González *et al.* (2010) also used a probabilistic model and found peak micromotion at the bone-implant interface was strongly affected by bone and implant geometry. The implant geometry affected the bone-implant interface area and as a consequence has been found to alter the micromotion (Park et al. 2009). Park *et al.* (2009) found that the bone-implant micromotion reduced with an increase in contact ratio between the implant and bone using a statistical model.

3.2.2.Limitations of the applied forces in finite element studies

Despite the improvement in modelling techniques, the consideration of the loads acting across the hip joint has changed little since the earliest finite element studies were reported. Most models use a hip contact force, taken as a multiple of body weight, from either measured *in vivo* data or calculated from a musculoskeletal model. Some models only include an 'abductor' muscle force in addition to the hip contact force (Verdonschot et al. 1993; Keaveny and Bartel 1995; Kayabasi and Erzincanli 2006), although a few models are starting to include a wider range of muscle forces (Stolk et al. 2001; Bitsakos et al. 2005; Jonkers et al. 2008; Afsharpoya et al. 2009). However, there are only a small number of papers that are used to provide these forces and the potential range of joint and muscle force has not been investigated.

Most of the loading conditions used in finite element models are either scaled from measured data or from calculated forces. Several *in vivo* studies have been used to measure the hip contact force in the body using an instrumented hip replacement (Chapter 2.5) and the studies conducted by Bergmann *et al.* (1993; 2001) are the most commonly used of the measured forces. Muscle forces have not been measured in the body and therefore if the computational model has included muscle forces they are taken from either an analytical model such as Paul (1966; 1966) or a musculoskeletal

model, the most commonly used of which are by Brand *et al.* (1982; 1986; 1994), Crowninshield *et al.* (1978; 1980), Duda *et al.* (1996) Heller *et al.* (2001) or Patriarco *et al.* (1981) (Table 4). In recent analyses of cementless implants many studies (Wong et al. 2005; Speirs et al. 2007; Behrens et al. 2008; Hu et al. 2009; Park et al. 2009) have used the musculoskeletal forces predicted by Heller *et al.* (2001; 2005).

Peak joint contact forces for walking are often used in static finite element models and the applied hip contact forces range from 2.3BW (Stolk et al. 2001) to 4.64BW (Cheal et al. 1992). Stumbling loads are also used or the model is loaded to induce fracture in the femur (Lotz et al. 1991; El'Sheikh et al. 2003) and some loads are used in the computational models to allow them to be compared to experimental analysis (Pedersen et al. 1997; Abdul-Kadir et al. 2008; Afsharpoya et al. 2009). There are also some studies using static models which include several instances in the gait cycle such as heel strike, toe off and mid-stance (Bitsakos et al. 2005) although heel strike is generally used as the peak in hip contact force during the gait cycle.

Many FE models include an abductor force and this can range from approximately 1BW (Wong et al. 2005) to approximately 3.5BW (Keaveny and Bartel 1995) for models of gait at the peak hip contact force. The abductor muscle force can also be divided into the glutei muscles (Watanabe et al. 2000; El'Sheikh et al. 2003). Additional muscle forces are added to some models and the most common forces include the iliotibial tract, iliopsoas and vastus muscles (Cheal et al. 1992; Taylor et al. 1996; Simões et al. 2000; Stolk et al. 2001; Bitsakos et al. 2005; Shih et al. 2008; Afsharpoya et al. 2009). These muscle forces have been included in FE studies either to investigate the effect of adding muscle forces to FE models (Duda et al. 1998; Stolk et al. 2001; Bitsakos et al. 2005; Speirs et al. 2007) or to provide a more detailed strain pattern in the femur.

Several studies have found the deformation of the femur to be more physiological in FE models with the inclusion of a more physiological selection of muscle forces (Cheal et al. 1992; Polgár et al. 2003; Speirs et al. 2007) compared to only applying a hip

contact force or hip and abductor forces. Speirs *et al.* (2007) compared the effects of muscle forces on FE models of the femur. They considered three muscle configurations with the forces taken from a musculoskeletal model including 95 muscle units published by Heller *et al.* (2001). All the models had a hip contact force and in addition to that the first model contained only an abductor muscle, the second had the abductor, adductor and vasti muscles and the third had all muscles forces attached to the femur as well as the knee and patella forces from the musculoskeletal model. In the simplified scenarios, the muscle forces included have the same magnitude as in the complex loading scenario, although the abductor force was a combination of the glutei muscles. This does not necessarily reflect the simplified load cases used in other studies, particularly those which have used forces predicted with only a limited number of muscle groups. Speirs *et al.* found that with the inclusion of the complex muscle loading, the deformation of the femur and by inference the strain in the femur was more physiological. Polgár *et al.* (2003) also found the inclusion of complex muscle loading reduced the strain and displacement measured in an intact femur from unrealistic values calculated with simplified loading. They used muscle and hip contact forces from Duda *et al.* (1998) and considered the loads at 10% of the gait cycle, chosen because it was the peak in abductor and adductor muscle force and the hip contact force was less than 1BW. Only considering a single time step in the gait cycle, particularly one with a small hip contact force relative to the muscle forces may over represent the effect of the muscle forces on the femur models at the peak in hip contact force. However, when investigating the whole gait cycle it is important to include a more complex loading regime. Polgár *et al.* (2003) also found that the distribution of muscle force affects the femoral strain. They modelled the muscle forces applied as concentrated forces at the muscles' attachment centroids and compared this to a model with the muscle forces distributed uniformly over the insertion area. The peak tensile principal strain was reduced from approximately 9000με to approximately 1000με and the internal compressive and tensile principal strains were also reduced with the distributed model. Taylor *et al.* (1995) found the addition of an abductor, iliotibial tract and iliopsoas forces to a hip contact force only

reduced the peak minimum principal stress slightly in the cancellous bone in an HA coated implant model although it reduced the peak minimum principal stress in the intact femur model to -0.75MPa which was less than a half the stress calculated with a hip contact force alone.

Bitsakos *et al.* (2005) also investigated the influence of loading conditions and used an adaptive model to calculate bone loss in the femur after a hip arthroplasty. Their study also used a set of muscle forces taken from a musculoskeletal model (Brand et al. 1994; Duda et al. 1996) and reduced the number of muscles included in the FE study without altering the magnitude of the remaining forces. They found that the models with the more realistic set of muscles calculated a smaller quantity of bone loss surrounding the femur and this compared well to clinical data although they commented that the algorithm used to calculate the bone remodelling over-estimates bone loss.

The effect on the strain pattern in an intact femur was also investigated with respect to the inclusion of muscle forces in a finite element model by Duda *et al.* (1998). They used muscle forces predicted from a musculoskeletal model published by Duda *et al.* (1996) using data from Brand *et al.* (1982; 1986). They found that including all the muscle forces attached to the femur from the musculoskeletal model resulted in a maximum principal strain in the femur below 2000με compared to the simplified load cases where the principal strain reached 3000με. The strain pattern along the length of the femur was less variable with the more complex muscle loading. The study stated that the principal strain calculated in their model compared well with *in vivo* measurements of up to 850με on the anteromedial side of a tibia midshaft (Lanyon et al. 1975).

Stolk *et al.* (2001) found that the inclusion of the abductor force had a major effect on the stress and strain in their FE model of a cemented hip implant. However, the addition of iliotibial tract, adductors and vasti muscles had only a minor effect on the

deflection of the femoral head, stress in the implant and the cement mantle, surface strain and strain energy density. Although at 10% of the gait cycle, inclusion of the additional muscle forces reduced the surface strain in the region close to the tip of the implant. Their muscle loading scenario was similar to Duda *et al.* (1998) as it consisted of 19 muscles and the hip contact force calculated from Brand *et al.* (1982; 1986; 1994) and Duda *et al.* (1996). Due to only minor changes caused by the addition of the more complex loading they concluded that only the hip contact and an abductor force are required to "adequately reproduce *in vivo* loading of a cemented THA reconstruction". This study showed that although the additional muscle had a smaller effect, the muscles did affect the strain in the femur, in particular the strain energy density at the stem tip.

Pancanti *et al.* (2003) and Biegler *et al.* (1995) found variation in the micromotion at the bone-implant interface when comparing different loads from different activities. Both studies found higher micromotion with stair climbing compared to normal walking and Biegler *et al.* suggested that patients should avoid high torque activities such as stair climbing until bone ingrowth had occurred. Andreaus and Colloca (2009) also found that stair climbing generated higher strain in the bone in both implanted and intact femurs.

The patient that the muscle forces are calculated for may also be important to the resulting FE model. Jonkers *et al.* (2008) predicted the muscle and joint contact forces using a musculoskeletal model from Lenaerts *et al.* (2008) for two subjects. The hip contact force and 19 muscle forces including the glutei adductors and the iliotibial tract were applied to a subject specific FE model of their implanted femur. The forces were then normalised to the patient's body weight and subsequently applied to the other FE model. The equivalent stress in the femur was affected more strongly by altering the patient's forces than the bone geometry. Although the bone geometry was found to be less important than the forces applied in the model, changes in the bone material properties have been found to affect the bone strain and micromotion (Wong

et al. 2005). Pancanti *et al.* (2003) found high inter-patient variability when considering the micromotion at the bone-implant interface which may contribute to the loading affect on the femoral stresses. They found the variation between patients in the peak micromotion ranged from 75-107μm during the walking upstairs scenarios. However the variation was lower when the patients were modelled walking normally, with peak micromotion calculated to be between 56-75μm. The forces across the hip are also thought to vary with different implant and hip centre positions (Bartel and Johnston 1969; Johnston et al. 1979; Iglic et al. 1993; Bicanic et al. 2009; Erceg 2009). However parametric and probabilistic studies assume that the forces remain the same despite modelling geometric changes (Dopico-González et al. 2010). In order to fully utilise parametric analyses of hip arthroplasty the effects on the hip forces of the geometric changes should be incorporated into studies but this requires detailed understanding of the effects of changing hip centre or implant position and the range of forces that the hip may be subjected to.

3.2.3.Boundary conditions

Many studies constrain a plane of nodes or fix the distal end of the femur to provide equilibrium in the FE models model (Table 4). Polgár *et al.* (2003) showed that fixing the distal end of the femur caused a greater displacement of the femoral head than with the femur fixed at midshaft. They also found no change in the peak tensile principal strain and a reduction in the peak compressive principal strain. However, Speirs *et al.* (2007) showed that a more physiological boundary condition produced a model with a more physiological deflection of the bone and strain pattern. They compared three different boundary conditions, the first fixed the femur at mid shaft, the second fixed nodes on the distal condyles and the third provided a 'joint' constraint. In the joint constraint the knee centre node was fixed in all DOF, the hip node was fixed in two DOF and the lateral condyle node was fixed in one DOF. A deflection of the femoral head of 19mm was found in the model with the distal condyles constrained and in particular there was a large deflection in the anterior-posterior direction. The model with the joint constraint had a femoral head deflection

of only 2mm and a lower surface strain along the length of the femur than either of the other models. The deflection was higher in the fixed mid-shaft model compared to the joint model however the surface strain was similar, although slightly higher, in the medial and lateral mid-shaft. The deflection calculated at the modelled femoral head with the joint constraint was similar to the deflection measured in an *in vivo* study of single legged stance (Taylor et al. 1996). They found a maximum deflection of approximately 4mm medially and 3mm inferiorly.

Phillips *et al.* (2009) produced a more complex model of a femur's loading and boundary constraints. They modelled all the ligaments and muscles as spring elements and modelled an acetabular to which spring elements applied a static load of ⅝BW. The force in each muscle unit was calculated using a force-displacement relationship and the model converged on a minimum deformation scenario for the system. Two models were created and used either a linear or cubic force-displacement relationship for all of the muscles which establish an upper and lower boundary for muscle activation in the system. Principal strains on the surface of the femur show compressive strain on the medial side and tensile strain on the lateral side, at peak between approximately 2000-2500με. The strain on the anterior and posterior surfaces was substantially lower and in general below 500με. Overall deflection of the femoral head was less than 2mm and only 1.6mm in the non-linear model.

4. Objectives

Computational models have the potential to encompass a large design space due to their flexibility. Finite element models are expanding their scope by using probabilistic approaches to investigate both surgical and patient variability rather than the traditional individual patient-specific models. However, neither the patient-specific models nor the broader probabilistic models account for the effects of muscle forces which could potentially be altered due to surgical or patient variation.

The aim of this study is to improve the loading and boundary conditions applied to finite element models of total hip arthroplasty using musculoskeletal models. Existing finite element models do not account for the potential variation in the position of the hip centre or the effect of the surgical technique on the forces in the proximal femur (Section 3.2). However, these scenarios can affect the forces and hence the lifetime of a hip arthroplasty (Section 2.7). Therefore there is a need to merge the knowledge available from musculoskeletal models into finite element analysis to provide a better understanding of the hip arthroplasty under variable conditions. It is hypothesised that using musculoskeletal modelling in combination with finite element models will provide useful and detailed computational analysis of hip arthroplasty.

This study has created a finite element model which applies force data from an adaptable musculoskeletal model (Chapter 5). The resulting hip contact forces from the musculoskeletal model are compared to measured forces from the literature[1]. The extent to which this process improves finite element modelling is then investigated in three areas: patient to patient variation (Chapter 6), hip geometry changes by considering displacements of the hip joint centre (Chapter 7) and muscular changes by simulating alternative surgical techniques (Chapter8). Current finite element models lack a range of hip and muscle forces to apply and Chapter 6 uses several recorded

[1] Manders, C. J., New, A. M. and Rasmussen, J. (2008) *Validation Of Musculoskeletal Gait Simulation For Use In Investigation Of Total Hip Replacement*. Journal of Biomechanics **41**(Supplement 1): S488.

gait patterns to generate musculoskeletal models. The loads across the hip were then normalised to the subject's body weight, as is commonly used in finite element studies (Section 3.2), and applied to the same finite element model of an implanted femur model.

Changes in hip geometry have been investigated using probabilistic techniques and these studies often look at the change in the position of the implant or the shape of the bone and its material properties (Section 3.2.1). During hip surgery the centre of rotation of the hip can be altered and the potential effects on the surrounding musculature have been considered by clinical studies as the cause of altered gait patterns and increased risk of hip replacement revision surgery (Section 2.7.2). Chapter 7 uses a musculoskeletal model to predict the changes in muscle and joint forces as a result of a change in the hip centre[2] and the consequences on the resulting strain and micromotion distribution within the implanted femur.

Hip arthroplasty surgery damages some of the leg muscles to allow the surgeon access to the hip. There are different surgical approaches used and clinical studies have shown that they can affect the patient's range of motion, the strength of some muscles and the risk of revision surgery (Section 2.7.2). Chapter 8 investigates the effect of different surgical approaches using two methods. The first method alters the strength of the relevant muscles in the musculoskeletal model using one non-pathological gait pattern and the resulting forces are applied to the finite element model[3]. The second method uses several gait patterns from patients with different surgical approaches and investigates the resulting range of strain in the finite element model for the surgical approach. Comparisons are then drawn between the synthetically generated force data and real patient data from literature studies. Predictions of the primary stability of a

---

[2] Manders, C., New, A.M. and Taylor. M. *The Influence Of Medialisation And Lateralisation Of The Femoral Head On The Forces Acting On The Hip After Total Hip Replacement*. in *22nd Annual Congress of International Society for Technology in Arthroplasty* 2009. Big Island, Hawaii.

[3] Manders, C.J. and New. A.M. *Effect Of Surgical Approach On Femoral Strain Distribution After Total Hip Replacement*. in *55th Annual Meeting of the Orthopaedic Research Society*. 2009. Las Vegas, NV.

cementless hip stem are performed based on finite element models of the strain and micromotion around the stem and these are compared to clinical data reported in the literature.

5. Methodology

5.1. Musculoskeletal model

A musculoskeletal model was used with patient-specific gait analysis data and the model also to allowed muscle strengths and hip geometry to be changed. The AnyBody modelling programme (AnyBody Technology, v4.1) was used with a generic model from the repository created by the AnyBody research group (AMMR v1.1, http://forge.anyscript.org). The generic model was freely available in the programming language Anyscript, which is specific to the programme AnyBody. The code was changed to reduce the strength of specific muscles in particular models (Chapter 8) and a series of models was created with a modified centre of rotation of the hip (Chapter 7). A general background to musculoskeletal modelling has been covered in Section 3.1. The AnyBody modelling programme is based on the inverse dynamics, where gait analysis data are used as input data and using the equilibrium equations the joint torque can be calculated. The force required to produce the joint torque is then distributed between the muscles crossing that joint and the distribution is calculated via an optimisation process.

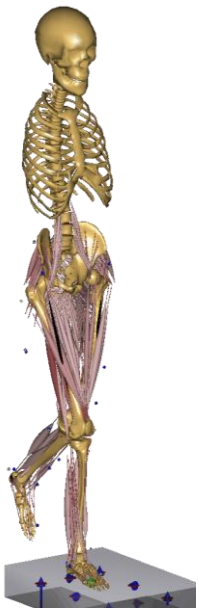

Figure 15: The generic musculoskeletal model including lower limb muscles in the AnyBody programme.

5.1.1.Generic musculoskeletal model

The generic lower limb model comprised two legs, a pelvis, basic spine for lower limb muscle attachment and 163 muscles (Figure 15). Each leg consisted of a thigh, shank and foot segments which were constrained by a spherical joint at the hip and a hinge joint at the knee, ankle and subtalar joint. Each muscle unit had a line of action defined by at least two points of attachment (Table 5). To provide a more physiological representation of a muscle with a large attachment site the individual muscle was modelled as several muscle units. In the body, muscles consist of a number of motor units which can be activated independently producing a force in a specific bundle of fibres (Section 2.3.1). Therefore it is assumed that the model can represent large muscles as independent muscle units to allow the potential lines of action to be modelled. Figure 16 shows the three gluteus minimus muscle units which all have the same attachment site on the thigh segment as the gluteus minimus has a small femoral attachment. However, anatomically the muscle has a large attachment area on the pelvis which is represented by the three attachment points for the modelled muscle units. The positions of the muscle attachment points were taken from a cadaver study (Klein Horsman et al. 2007).

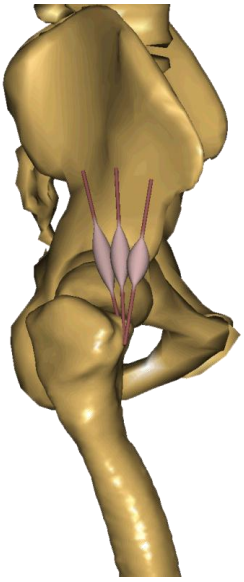

Figure 16: The three gluteus minimus muscle units in the generic musculoskeletal model.

Several muscles have fixed locations which they must pass through called via points and these points, in addition to the muscles' points of attachment, alter the muscle's line of action to represent the path the muscle would take in the body. The via points were based on the local coordinate system of the specified segment and so remain in the same relative position as the model moves. The iliacus and psoas muscles pass over the pelvis and hip capsule, however the musculoskeletal model does not automatically wrap muscles over bony segments. A wrapping surface was defined in the model as a cylinder along the iliac spine and the iliacus and psoas were required to pass over this surface.

Muscle	Attachment Points		Via points	No. of muscle units
Adductor Longus	Pelvis	Thigh		6
Adductor Magnus	Pelvis	Thigh		13
Adductor Brevis	Pelvis	Thigh		6
Biceps Femoris Caput Breve	Thigh	Shank	Shank	2
Biceps Femoris Caput Longum	Pelvis	Shank	Shank	1
Extensor Digitorum Longus	Shank	Foot	Foot	3
Extensor Hallucis Longus	Thigh	Shank	Foot	3
Flexor Digitorum Longus	Shank	Foot	Foot	3
Flexor Hallucis Longus	Shank	Foot	Foot	3
Gastrocnemius	Thigh	Foot	Shank	2
Gemellus	Pelvis	Thigh		2
Gluteus Maximus	Pelvis	Shank	Thigh	12
Gluteus Medius	Pelvis	Thigh		12
Gluteus Minimus	Pelvis	Thigh		3
Gracilis	Pelvis	Shank	Shank	2
Iliacus	Pelvis	Thigh	*	9
Obturator Externus	Pelvis	Thigh		5
Obturator Internus	Pelvis	Thigh	Pelvis	3
Pectineus	Pelvis	Thigh		4
Peroneus Brevis	Shank	Foot	Foot	3
Peroneus Longus	Shank	Foot	Shank, Foot	3
Peroneus Tertius	Shank	Foot	Shank	3
Piriformis	Pelvis	Thigh	Pelvis	1
Plantaris	Thigh	Foot		1
Poplitues	Thigh	Shank	Shank	2
Psoas	Pelvis	Thigh	*	4
Quadratus Femoris	Pelvis	Thigh		4
Rectus Femoris	Pelvis	Shank	Thigh	2
Sartorius	Pelvis	Shank	Thigh, Shank	2
Semimembranosus	Pelvis	Shank	Shank	1
Semitendinosus	Pelvis	Shank	Shank	1
Soleus	Shank	Foot		6
Tensor Fasciae Latae	Pelvis	Shank	Thigh	2
Tibialis Anterior	Shank	Foot	Foot	3
Tibialis Posterior	Shank	Foot	Foot	6
Vastus Intermedius	Thigh	Shank	Thigh	6
Vastus Lateralis	Thigh	Shank	Thigh	8
Vastus Medialis	Thigh	Shank	Thigh	10

Table 5: The muscle units in each leg of the generic musculoskeletal model and the body segments they are attached to. * The iliacus and psoas muscle units have a wrapping surface on the pelvis.

The musculoskeletal modelling proceeded through several stages before the inverse dynamic analysis was performed. A static model of the subject was first created using the measurements taken at the same time as the gait analysis data collection but with the subject simply standing. The modelled markers were positioned on the model in the correct location and the model was scaled to fit the measured markers. The static model was then used as the basic starting point for the dynamic analysis. The scaled model was manipulated at each of the joints to create the same posture as the subject in the initial frame of the dynamic analysis. The positions, velocities and accelerations of the markers through the gait cycle were then used in the optimisation created by Andersen *et al.* (2009) to calculate the joint angles at each time step of the gait cycle. Andersen *et al.* created an optimisation procedure which works within the framework of the AnyBody software and has been shown to substantially reduce errors associated with poor marker position due to skin artefacts (see Section 3.1.1).

Inverse dynamic analysis used the optimised joint angles, generated using the optimisation routine, and the ground reaction forces to calculate the net torque about each axis for each joint in the model for each time step. The force required to create the joint torque was then calculated and divided between muscles. It is not known how the body shares the force between the muscles but there are several theories which have been shown to predict a similar muscle activity to that observed in the body (Section 3.1.2). Several recruitment criteria have been found to predict the muscle activation well (van Bolhuis and Gielen 1999) and the AnyBody programme had recruitment criteria built into the programme allowing the minimisation of the sum of the muscle activity raised to any power or the minimisation of the maximum muscle activity. This study used the recruitment criterion which minimised the sum of the squared muscle activities since it is established in the literature as predicting reasonable muscle activation patterns (Glitsch and Baumann 1997; van Bolhuis and Gielen 1999).

In vivo the muscle activity is based on the electrical signals picked up by an EMG (Section 2.5.2). However in the musculoskeletal model the muscle activity which is used to recruit the muscles' force is calculated as the ratio of the muscles' force to the muscles' potential force. The potential force a muscle can produce changes depending on several muscle parameters such as the length of the muscle-tendon unit and the maximum force the muscle can provide. The relationship between the potential muscle force and the muscle's parameters was investigated by Hill (Erdemir et al. 2007) and the muscle model used in this study is based on his theories. The muscle parameters needed to calculate the potential muscle force were measured by Delp (1990) including the maximum muscle force which is proportional to the physiological cross-sectional area of the muscle. The length of the muscle when its potential muscle force is equal to the maximum muscle force, the optimum muscle-tendon length, is scaled in AnyBody for each musculoskeletal model. The joint angles for the limbs at which the muscle has an optimum muscle-tendon length was calculated by the AnyBody research group (AnyBody Research Group 2009). A series of 'calibration' studies were provided in the AnyBody repository (AnyBody Research Group 2009) specifically created by the AnyBody research group for the muscles in the generic musculoskeletal model. The calibration studies calculate each muscle's tendon length based on the scaled musculoskeletal model and are performed before the inverse dynamic analysis for each separate model.

5.1.2.Patient data

Subject-specific motion capture data were applied to the generic model to create a model specific to the recorded gait trial. The height, weight and gender of the patient were used to scale the muscle parameters in the generic model. The kinematic data collected from the recorded markers were used to scale the geometry of the generic model and calculate the joint angles, velocities and accelerations. The joint positions were defined in the generic model and then the optimisation procedure altered the limb lengths to find the optimum lengths to fit the recorded markers to the marker positions defined in the model. The optimum limb lengths were then fixed through

the inverse dynamic analysis and hence defined the joint positions. Recorded foot reaction forces were applied to the lower limb model through modelled force plates and therefore the kinetics of the system could be calculated. Healthy data have been obtained from either the University of Southampton (Worsley 2009) or the University of Cardiff (Holt and Whatling 2009) and several data sets from total hip replacement patients have also been obtained from University of Cardiff (Table 6).

Description	Height (m)	Weight (N)	Gender	Age	Walking speed (m/s)	Notes
Southampton S1 (L)	1.63	667	Male	64	1.13	Healthy
Southampton S2 (R)	1.66	922	Female	56	1.33	Healthy
Southampton S3 (R)	1.65	853	Female	59	1.10	Healthy
Southampton S4 (R)	1.78	942	Male	55	1.37	Healthy
Southampton S5 (R)	1.63	623	Female	67	1.15	Healthy
Southampton S6 (R)	1.70	657	Female	56	1.49	Healthy
Southampton S7 (R)	1.78	883	Male	67	1.18	Healthy
Cardiff C01 (L)	1.84	775	Male	54	1.15	Healthy
Cardiff C02 (L)	1.57	579	Female	43	1.25	Healthy
Cardiff L01(L)	1.70	912	Male	70	1.09	Left THA (Lateral Approach)
Cardiff L02 (R)	1.65	746	Male	51	1.17	Right THA (Lateral Approach)
Cardiff L03 (R)	1.64	657	Female	65	0.94	Right THA (Lateral Approach)
Cardiff P01 (R)	1.62	559	Male	78	0.83	Right THA (Posterior Approach)
Cardiff P02 (R)	1.62	647	Female	64	0.85	Right THA (Posterior approach), waiting for left THA
Cardiff P03 (R)	1.73	1050	Male	58	1.12	Right THA (Posterior approach)

Table 6: Patient specific data for each musculoskeletal model. (L) and (R) denotes whether the musculoskeletal data from left or right leg was used.

The recorded marker positions were assigned to the model as independent markers and linked to nodes created in the model. The modelled nodes are manually positioned relative to the joints using a single frame then an optimisation procedure

created by Andersen *et al.* (2009) altered their position to fit the measured data through the recorded gait cycle. A second optimisation process calculated the joint angles at each time step and these were used to drive the model (Andersen et al. 2009). This optimisation technique has been shown to reduce the effects of skin artefact errors compared to the standard kinematic analysis approach. Andersen *et al.* compared the acceleration of the measured markers to the acceleration of the nodes on models using both his optimisation technique and the standard kinematic analysis. They found a reduction in the root-mean-squared acceleration error by approximately 60%. The technique also reduces the over-determinacy in the model created by the large number of degrees of freedom associated with the marker data with respect to the available degrees of freedom in the model. Foot reaction forces and moments recorded by force plates are applied to the foot through a modelled force plate. Once the inverse dynamics was performed the gait cycle was normalised to allow comparison between models. The gait cycle was normalised by identifying heel strike for the leg under investigation in two places during the recorded analysis and scaling the time between them to 100%. There are errors associated with this process as it is performed by an observer of the recorded marker analysis and in several of the models the contralateral leg gait cycle was used to normalise the gait cycle because two heel strikes were not recorded for the observed leg.

5.1.3.Musculoskeletal model verification

The musculoskeletal modelling process in AnyBody was compared to literature data in order to investigate the realistic nature of the output forces. The musculoskeletal model, using the data set S1 (Table 6), was compared to the range of measured forces and joint moments from the published study by Bergmann *et al.* (2001). The hip contact force was measured in Bergmann *et al.*'s study using an instrumented hip prosthesis in four patients and gait analysis was simultaneously collected to provide ground reaction forces and hip joint torque. The output for each patient is publicly available from the Hip98 CD (Bergmann et al. 2001) and through the Orthoload

website (Bergmann 2008). This study used the data from all the normal walking speed trials for all four patients (HSR, KWR, IBL and PFL).

The components of the ground reaction force, hip joint torque and hip contact force from the study by Bergmann *et al.* were normalised with respect to the body weight of the patient and then the range of force or torque was calculated. The forces and torque from the S1 data set were also normalised to the subject's body weight. The ground reaction forces have been presented in a global coordinate system and the hip joint torque and hip contact force have been presented in a coordinate system based at the left hip (Figure 17).

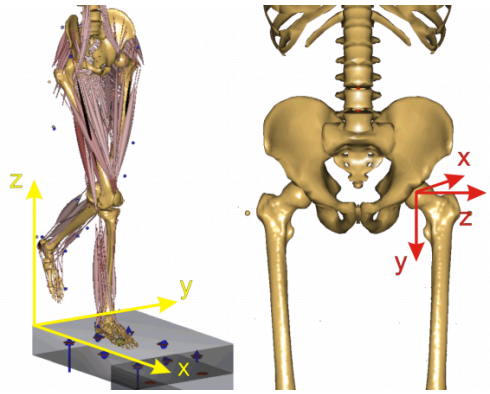

Figure 17: Global and left hip coordinate systems.

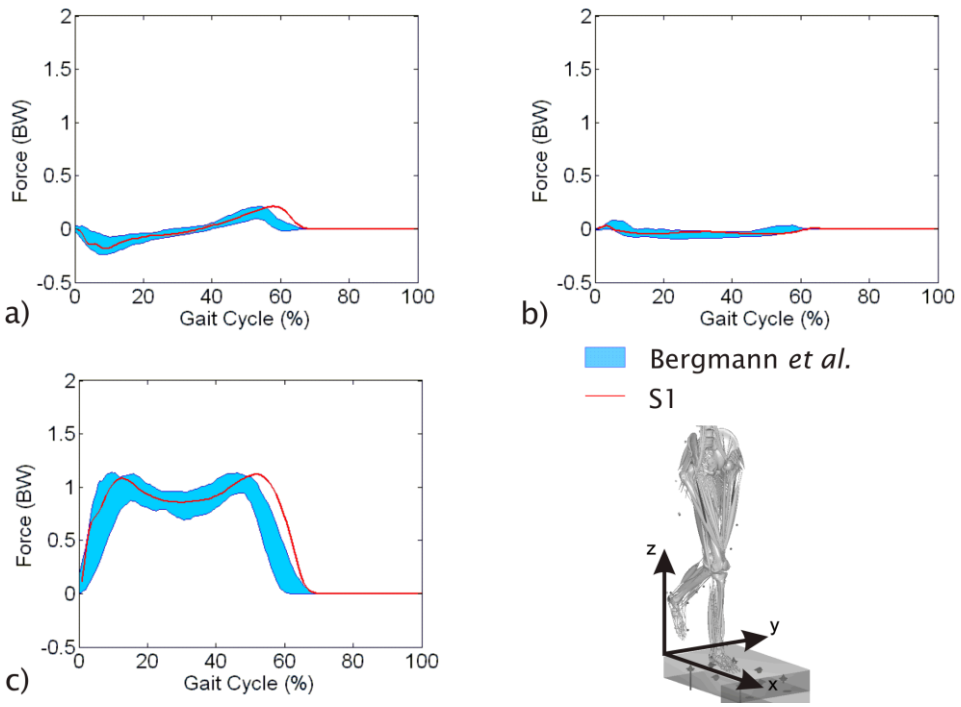

Figure 18: Range of ground reaction forces measured by Bergmann *et al.* (2008) and the ground reaction forces measured for the S1 subject. Foot reaction force components a) Fx, b) Fy and c) Fz.

The ground reaction forces for S1 were similar in magnitude and pattern to the range of force calculated for the Bergmann patients (Figure 18). However the stance phase was longer for subject S1 than with the range measured in the THA patients from the study by Bergmann *et al.* Although this could be due to inaccurate normalisation of the gait cycle, it has been found that single legged support has a smaller percentage of the gait cycle on the affect side of THA patients than in healthy patients (Perron et al. 2000). In terms of lower limb kinematics, the hip joint angles of S1 (Figure 19) fall within or close to the range measured in Bergmann's patients except for a larger flexion angle at toe off. Again, the measured data obtained from total hip replacement patients may have altered gait patterns due to the cause of the arthroplasty or due to the replacement joints.

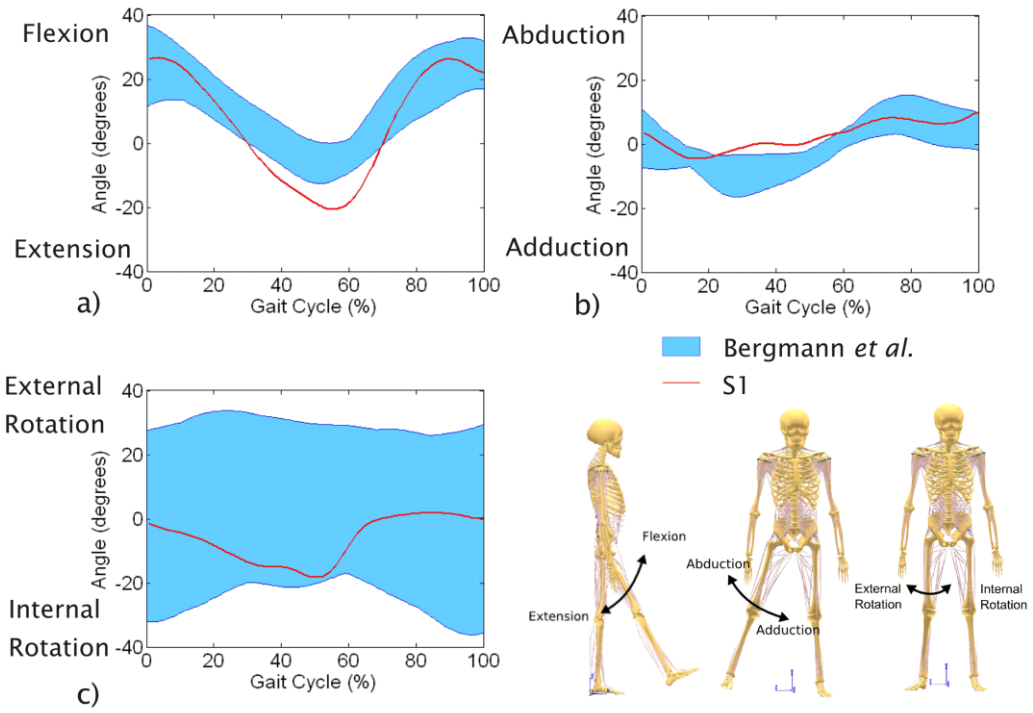

Figure 19: Range of hip angles measured by Bergmann *et al.* (2008) and the hip angle measured for the S1 subject.

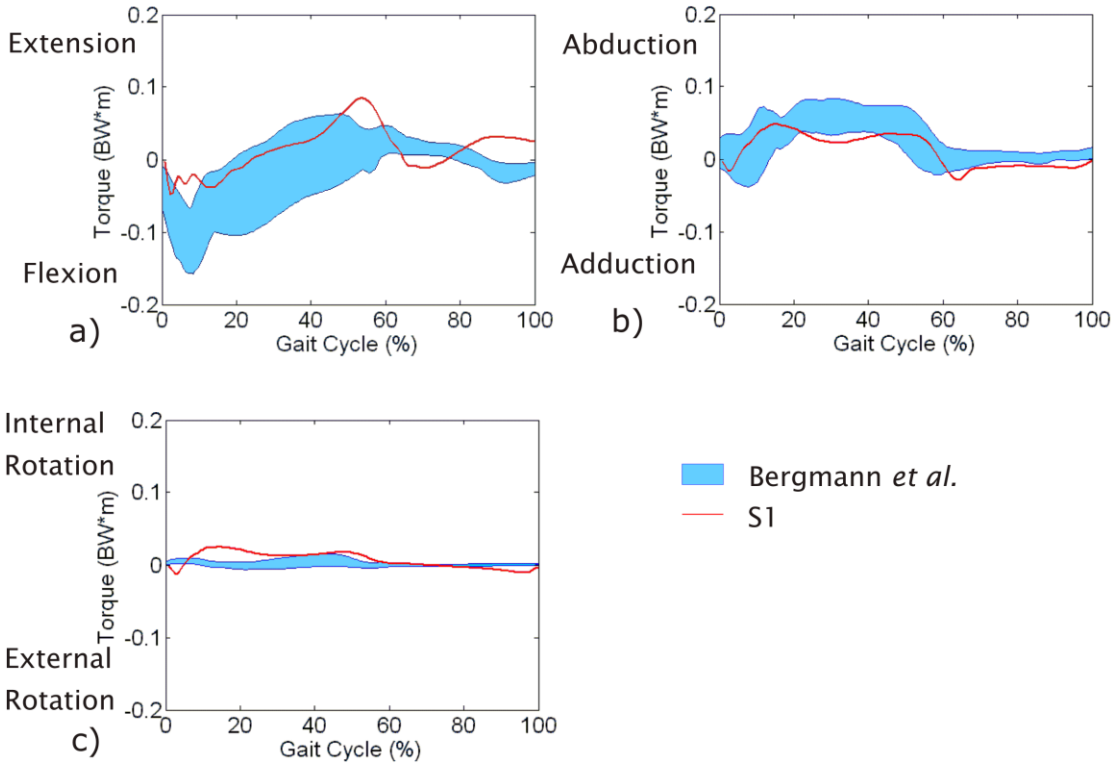

Figure 20: Range of hip joint torque calculated by Bergmann *et al.* (2008) and the hip joint torque calculated in the S1 AnyBody model.

All the torque components calculated for S1 were of a similar magnitude and pattern to those reported by Bergmann *et al.* (Figure 20). S1 had a slightly larger extension torque and external rotational torque than the measured range reported *in vivo*. The internal-external rotational torque was quite small in both the S1 model and the published results from the study by Bergmann *et al.*, however the rotation angle at the hip was quite variable. Although the angle was quite variable between the patients there was limited variability during the gait cycle in each patient. The torque is also affected by the out of plane forces and the externally measured forces were quite small compared to the axial force (Figure 18). In general the hip contact force predicted for S1 (Figure 21) has a similar magnitude to the range of measured hip contact force from Bergmann *et al.*'s study. However, at toe off there are peaks in Fy and Fx which are larger than the measured range.

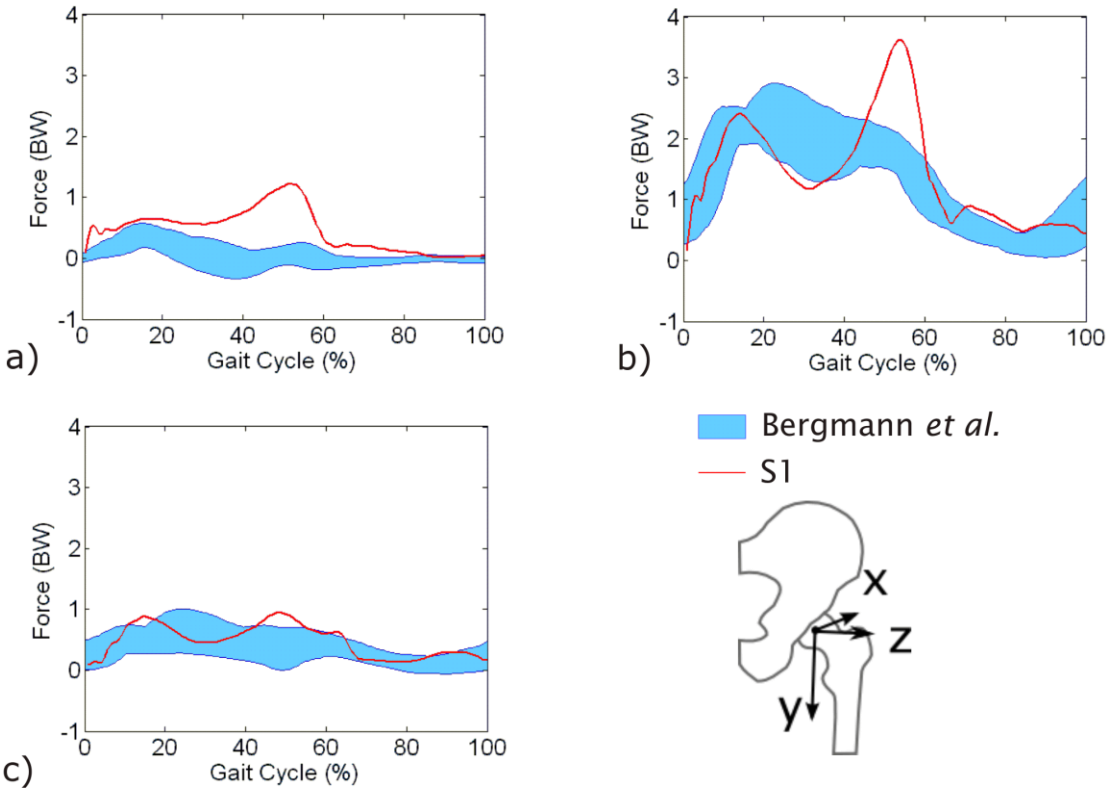

Figure 21: Range of hip joint force calculated by Bergmann *et al.* (2008) and the hip joint force calculated in the S1 AnyBody model. Hip force components a) Fx, b) Fy and c) Fz.

The range of data measured for the four patients in Bergmann *et al.*'s study highlights the potential differences between hip arthroplasty patients. In general, the predicted data from the S1 model compared well with the range of data measured by Bergmann *et al.*'s study. However there were some exceptions, in particular the larger hip contact force at toe off. The reasons for discrepancy between the measured patient data and the modelled individual fit into two broad categories, patient differences or modelling limitations.

S1 was a healthy individual and as such would have a different gait to the THA patients measured in the study by Bergmann *et al*. The THA patients had a shorter stance phase, the portion of the gait cycle from the start of heel strike to the end of toe off, than S1 which could be due to the effects of the arthroplasty or their underlying reasons for surgery. A shorter single legged stance, the portion of the gait cycle with only one foot on the floor between heel strike and toe off, was also found in THA patients compared to healthy patients in a study by Perron *et al.* (2000). A longer stance phase would require the muscles in the leg to be active for longer and produce force for longer, altering the timing of the hip contact force. The hip extension angle measured in the S1 subject was larger than the range measured in the THA patients in the study by Bergmann *et al.* and the reduction in extension angle has been found in a study comparing THA patients and healthy individuals (Perron et al. 2000). Perron *et al.* (2000) found that the extension angle at the hip measured in female THA patients has been found to be lower than healthy individuals during gait. A larger extension angle would require a greater force from muscles crossing the hip to provide the motion and from the flexion muscles to return the hip. The greater the extension angle the smaller the moment arm of the flexor muscles, therefore the flexors would need to produce a greater force to swing the leg from toe off through the swing phase than if the hip had been at a shallower extension angle. At toe off there was a greater extension moment in the healthy model of S1 than in the THA patients which was also found in the study by Perron *et al.* (2000). However there was a lower flexion angle in

the S1 model at 15% of the gait cycle but the hip contact forces were not significantly lower.

The discrepancies between the measured and predicted forces could be caused by the musculoskeletal model over-predicting the forces. Historically musculoskeletal models have over-predicted measured forces and this could be due to the assumptions used to create the models (Section 3.1.5). The AnyBody model assumes that the knee movement can be defined with only a one degree of freedom joint and the foot is modelled as a single segment. Restricting the degrees of freedom in the model reduces the complexity of the calculations to predict the muscle and joint contact forces. However it may reduce the accuracy of the joint angles to allow the model to optimise the position of the limbs to produce a best fit for a position the model cannot reproduce. Therefore the forces across the joints could be incorrectly predicted based on the restricted movement at the joints. In addition to errors at individual joints there could be an accumulation of errors from the ankle to the hip as the ground reaction forces are the only external forces applied to the model. The ground reaction forces and the associated motion capture data was used to first calculate the forces at the ankle, then the knee and finally the hip and simplifications in the modelling of the ankle and knee would therefore affect the force predictions at the hip. The anthropometrics of the model may not precisely represent the modelled individual although scaling was used to produce a more accurate model. However, inaccurate scaling of the generic model and variation in the particular muscle strengths of the individual may result in alterations to the predicted forces. Considering that S1 had a healthy gait and the range of data from Bergmann *et al.*'s study was taken from patients who had undergone total hip arthroplasty the resulting forces are quite similar. Therefore this study concluded that based on the limited *in vivo* data the musculoskeletal model produced acceptable resulting hip contact forces during gait.

5.1.4.Model outputs

The musculoskeletal model produced data for direct comparison between the modelled scenarios and for use in the finite element model. Joint torque and joint contact forces have been reported in the literature and therefore are useful when comparing the output from these investigations to published studies. However a subject's body weight has been linked to the magnitude of the joint contact forces and therefore they are often reported as a percentage or multiple of body weight (Bergmann et al. 2001). Joint torque has also been normalised with body weight to allow comparison between subjects in a similar manner to many studies which report the torque as a multiple of body weight in metres (Heller et al. 2005) or centimetres (Taylor and Walker 2001). Muscle forces have also been reported in the literature; in particular the abductor muscle forces are published as they provide a substantial force across the hip. However, musculoskeletal models vary and may not have calculated the force in the same manner due to the inclusion of different muscle units and differences in the attachment positions of the muscles. All muscle forces have been reported in this study as a multiple of the subject's body weight to provide consistency across all reported forces and allow comparison with forces published in the literature.

The muscle forces were generally reported as part of a group (Table 7) and along with the hip joint torque and contact forces were reported at each time step in the gait cycle. Hip contact forces and the muscle forces attached to the proximal femur were used as the input forces for the finite element model. The locations of the muscle forces' attachment to the femur were recorded and additional data were collected to allow the forces to be applied in an alternative coordinate system.

Muscles	Muscle Groups			
	Abductors	Adductors	Flexors	Extensors
Adductor Brevis		✓	✓	
Adductor Longus		✓	✓	
Adductor Magnus		✓		✓
Biceps Femoris Caput Breve				✓
Gluteus Maximus (inferior)		✓		✓
Gluteus Maximus (superior)	✓			
Gluteus Medius	✓			
Gluteus Minimus	✓			
Gracilis		✓		
Iliacus Longus			✓	
Iliacus Medius			✓	
Iliacus Mid.			✓	
Pectineus		✓	✓	
Piriformis	✓			
Rectus Femoris			✓	
Sartorius	✓		✓	
Semimembranosus				✓
Semitendinosus				✓
Tensor Fasciae Latae	✓		✓	

Table 7: The muscles included in the abductor, adductor, extensor and flexor muscle group definitions.

5.2. Finite element model

5.2.1. Finite element model

The femur surface geometry and material properties were taken from a computer tomography scan of a femur from a 43 year old male with an estimated height of 1.73m, derived from the length of the femur. The weight of 84.7kg was estimated from an average body mass index (BMI) for hip replacement patients of 28.3 (National Joint Registry 2009).

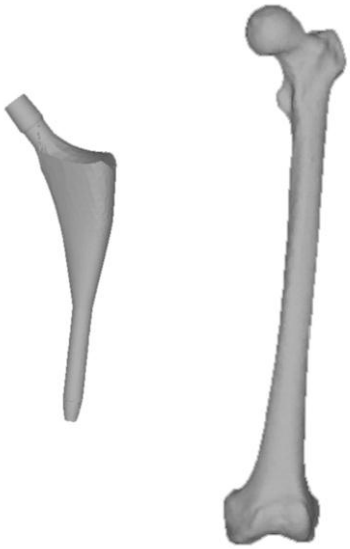

Figure 22: Surface geometries of IPS implant and intact femur, not scaled relative to each other.

The appropriately sized IPS component to fit the bone geometry was chosen and in-house code (New 2008), which employed the design software Rhinoceros (v4, Robert McNeel & Associates, Barcelona, Spain), was used to position the implant in the appropriate location for implantation of the prosthesis surface model into the femur geometry. The prosthesis was first moved to align the shaft midline with the femur midline. The prosthesis was translated along the axis of the femur midline to level the centre of the prosthesis head with the femoral head centre and rotated about the axis to align the femoral neck with the prosthesis neck.

Boolean operations were then performed in Rhinoceros with the implant and femur surface models to generate a surface model of the implanted. The surface of the prosthesis was removed from the femur geometry and the femoral head and neck were also removed at an angle of 20° from the femur midline. Additionally two other sections of bone were removed. Bone was removed from above the implant to allow the implantation of the prosthesis. A second smaller section of bone was removed from the intermediary canal below the distal tip of the implant, to represent over-reaming as performed during surgery.

The resulting surface geometry was meshed as a volume using ANSYS ICEM (v11, Ansys Inc, Canonsburg, PA, USA) and the subsequent finite element analysis was conducted in ANSYS (v12, Ansys Inc, Canonsburg, PA, USA). The femur and implant finite element models were meshed simultaneously to provide coincident nodes at the interface between the two parts. The coincident nodes allow micromotion along the interface between the femur and implant to be measured easily by measuring the resultant distance between each set of coincident nodes.

Once the volume mesh had been generated the bone material properties were applied to the femur volume from the CT data using BoneMat (Zannoni et al. 1998) which applies a linear relationship between the Hounsfield units (HU) and bone density (ρ, g/cm^3) (Equation 3).

$$\rho = 0.0009HU + 0.47 \quad \text{Equation 3}$$

A nonlinear relationship is used to calculate the Young's Modulus (E, MPa) from the calculated density (Carter and Hayes 1977) (Equation 4).

$$E = 2875\rho^3 \quad \text{Equation 4}$$

The Poisson's ratio was set at 0.3 for all bone elements. The density varied between 0.377 and 2.057 and therefore the Young's modulus in the bone elements ranged from 154MPa to 25GPa. The implant is made of cobalt chromium alloy and the Young's modulus and Poisson's ratio were assumed to be 220GPa and 0.3 respectively.

5.2.2.Force application

The forces from the musculoskeletal models were translated to the same coordinate system as the finite element model and then normalised relative to the subject's body weight before being applied as a multiple of the patient's body weight. This was achieved using three, manually defined, points on both the AnyBody and ANSYS models (Figure 23). The rotation and translation needed to convert the attachment points from the local AnyBody coordinate system to the ANSYS coordinate system was then calculated in a series of steps. The three points were the centre of the femoral

head (1), top of the greater trochanter (2) and bottom of the condyles (3) and they were manually found in the ANSYS model and correspond to points available in the AnyBody model, the hip centre, the piriformis femoral attachment and the plantaris femoral attachment point. A scale factor was calculated based on the relative distance between the points 2 and 3 on both models and this was used to scale the coordinates along the length of the femur. However the other planes were not scaled due to the small dimensions and the lack of easily defined points to calculate a scaling factor.

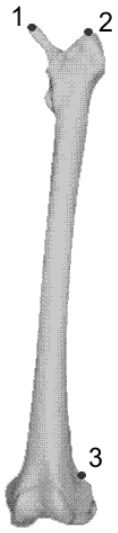

Figure 23: The location of the rotational points on the femur used to align the musculoskeletal and finite element models. 1) Centre of femoral head, 2) top of greater trochanter, midway between anterior and posterior bone surfaces and 3) bottom of the condyles.

Lines between these points were mathematically constructed and the angles between them calculated. All three points in each set were temporarily translated to position point three at the global origin and therefore allow the angle between the lines for the shafts to be calculated using trigonometry. The angle in each plane was calculated and then the AnyBody points were rotated to match the ANSYS points before the next plane was calculated. After the angle was calculated, rotational matrices were used to rotate all of the AnyBody points simultaneously about the global origin. Once all three planes

were matched, both of the lines representing the femoral shaft were aligned to the global z axis and then the difference between the femoral neck angles was calculated and a rotational matrix was used to align the AnyBody points with the ANSYS points. The rotation aligning the shaft line with the z axis was then undone and the points were translated to align the AnyBody and ANSYS greater trochanter points. The resulting transformation was then used to align all the AnyBody attachment points to the ANSYS global coordinate system.

It should be noted that the skeletal geometry used to create the generic model in AnyBody was not the same as the femur geometry used in the finite element model. Therefore the attachment points from the AnyBody model did not always sit on the surface of the mesh. To resolve this, the coordinates of the attachment points were used to create keypoints in the finite element model and from these keypoints surface nodes were selected to allow the forces to be applied. However before the forces can be applied to the model they also need to be converted to the ANSYS coordinate system. The forces were output from AnyBody as a force along each plane. Since these planes are not the same in the finite element model the forces' vectors needed to be transformed. Using the same transformation procedure as the attachment points the forces were treated as coordinates and then converted back to force before being normalised to the body weight of the AnyBody modelled subject. To apply the forces to the ANSYS model the normalised forces were multiplied by the assumed body weight of the finite element model.

Anatomically muscles are attached to an area of the femur surface. However the musculoskeletal model has reduced this area to an attachment point or several points. Applying the muscle force to a point on the finite element model would produce peak element strains. To reduce the effects of point loads the muscle force was divided equally and applied to several surface nodes. The keypoint was used to select the closest node on the surface of the mesh. Then all the surface elements within the defined radius were selected and the force was equally split between all of the nodes.

To select these nodes the straight line distance between each node and the prime node calculated. If this distance was less than or equal to the defined attachment radius then the node was retained, if not it was deselected. Only surface nodes were considered and only the nodes in a small area centred around the prime node were considered to reduce the computational expense of calculating the distance to every node in the model.

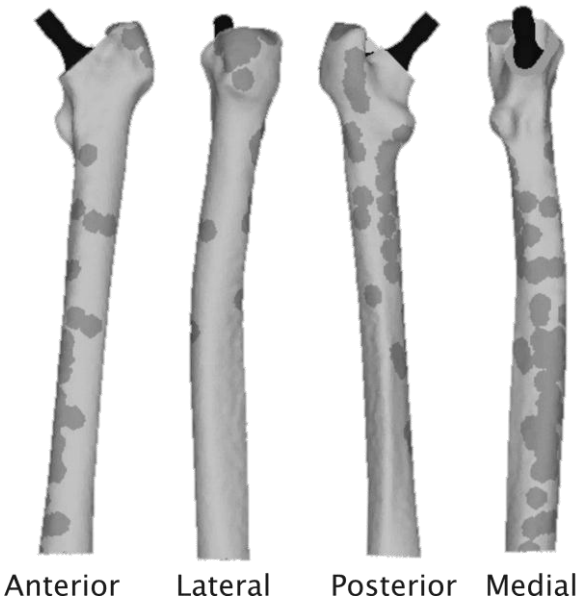

Figure 24: Attachment sites for the muscle forces applied to the finite element model of the implanted femur.

A series of finite element models was generated with the forces from discrete points along the gait cycle. Starting at 5% of the gait cycle and continuing every 5% up to 65%, thirteen models in total were created for each scenario to investigate the stance phase of gait.

5.2.3.Boundary conditions

An uncemented implant is not perfectly bonded to the bone and therefore a finite element model should consider frictional contact between the implant and bone. The finite element model contains contact elements on the bone surfaces that touch the implant and target elements on the implant surface. When a target element comes

within the "pinball" region of a contact element the model assumed that the surfaces had come into contact. In this model the pinball region was defined by a radius automatically calculated by ANSYS. All models in this study assumed a coefficient of friction of 0.3 (Viceconti et al. 2000). There is no gap between the implant and bone elements in this model at the contact region as it is assumed that in vivo on a macro scale a cementless implant initially has a push fit in the bone (Bauer and Schils 1999).

Many studies have been conducted using models of only the proximal femur (Crowninshield et al. 1980; Taylor et al. 1996; Duda et al. 1998; Hung et al. 2004; Kayabasi and Erzincanli 2006). A range of boundary conditions has been used on partial femur models, applying either fixed degrees of freedom on selected nodes at the distal end of the femur (Taylor et al. 1996; Duda et al. 1998; Kayabasi and Erzincanli 2006) or on the whole of the cutting plane (Crowninshield et al. 1980; Hung et al. 2004). Speirs *et al.* (2007) investigated the differences in the displacement and strain distribution within the femur as a function of boundary conditions. The most physiological deflection of the bone was found using 95 muscle forces and their joint constraint model. The boundary conditions for the joint constraint model were a knee node constrained in 3 translational DOF, a hip node constrained in two DOF and a node on the distal lateral epicondyle constrained with one DOF. The hip node constraint allowed only deflection of the leg along the y axis and the distal-lateral epicondyle node prevented the femur from moving along the x axis. Phillips *et al.* (2009) also investigated a physiological boundary condition for their finite element model producing an equilibrium condition by modelling all the muscle and joints on the femur and found it generated very low deflection of the femoral head (Chapter 5.2.3).

Ideally a whole femur would be constrained by the muscle forces and joint contact forces and moments at both the hip and knee and the resulting system would be in equilibrium. However this proved to be a complex problem in this study, particularly due to the scaling from the musculoskeletal model to the finite element model. To

simplify the boundary conditions a plane of nodes approximately perpendicular to the femur shaft was constrained in all six DOF. This type of boundary condition has been used in literature studies but the location of the boundary plane appears to be variable (Jonkers et al. 2008; Shih et al. 2008; Sakai et al. 2010). The location of the boundary plane of constrained nodes for this study was chosen following an investigation into the effect of the position on the strain and micromotion in the proximal femur. Seven models were created starting with a fixed plane of nodes 12mm from the distal end of the femur and each subsequent model had the plane of nodes moved proximally by 40mm (Figure 25). The hip contact and proximal muscle forces from the S1 musculoskeletal model at the first peak in hip contact force, 15% of the gait cycle, were applied to each model.

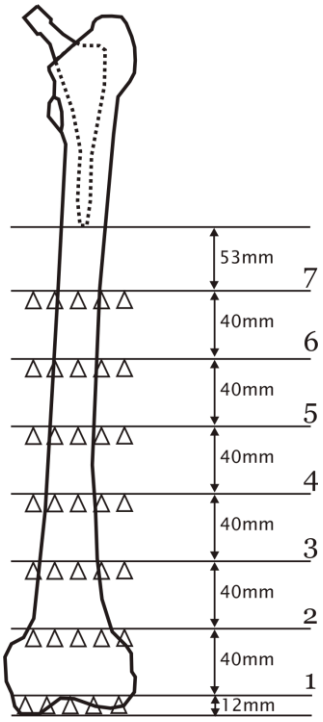

Figure 25: The positions for the fixed plane of nodes used in the boundary constraint study (not to scale).

The strain at the bone-implant interface did not change significantly with the position of the boundary plane (Figure 26). The mean and median equivalent strains at the bone-implant interface were similar in the different boundary condition models. The

strain at the 99th percentile altered slightly by an initial reduction as the boundary constraint was moved proximally and then a slight increase from position 3 to position 7. There were greater differences found in the micromotion calculated in the seven boundary constraint models (Figure 27). The mean and 75th percentile micromotion increased with a more proximal boundary constraint although boundary model 4 had similar micromotion to that calculated in models 1 and 2. There was less than 1% increase in the median and mean micromotion in model 4 compared to model 1, however there was a 14% increase in the mean micromotion in model 7 compared to model 1.

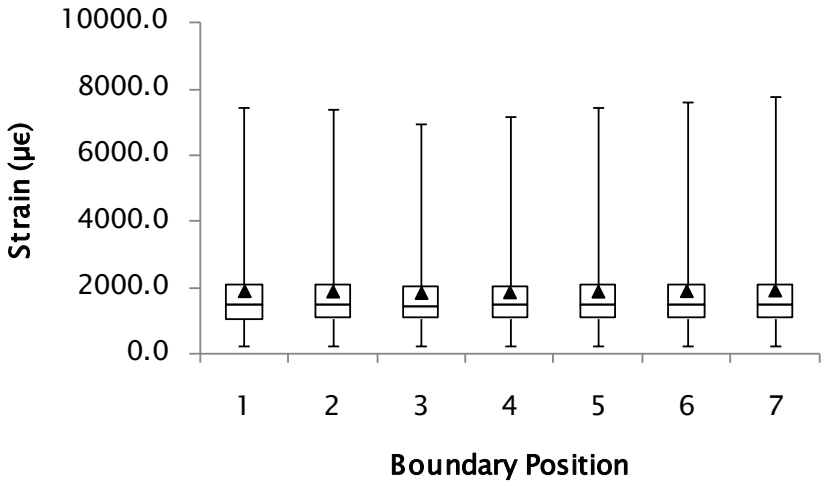

Figure 26: The equivalent bone strain at the bone-implant interface in the boundary constraint models. The median strain, 25th and 75th percentiles are displayed in the box plot with the 99th and 1st percentiles shown as the error bars. ▲ denotes the mean strain.

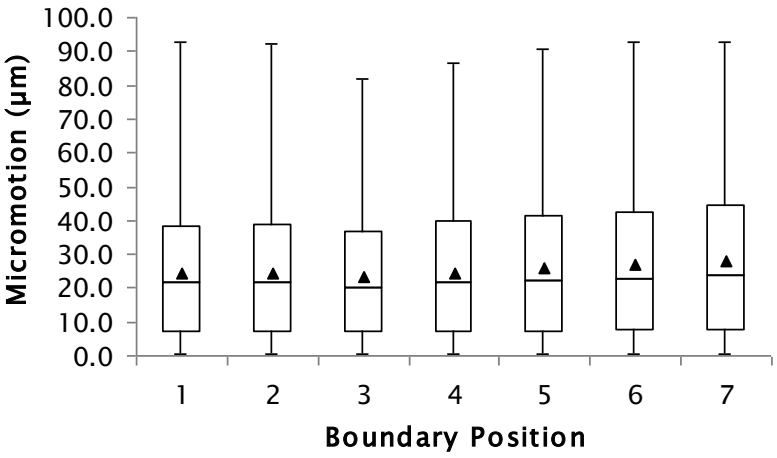

Figure 27: The micromotion at the bone-implant interface in the boundary constraint models. The median strain, 25th and 75th percentiles are displayed in the box plot with the 99th and 1st percentiles shown as the error bars. ▲ denotes the mean micromotion.

The strain pattern in the proximal femur is shown in Figure 28. The areas of high strain remained in the same location and there were only minor changes in the strain pattern which reflects the small changes in the interface strain. In the anterior cross-sectional view there is a slight change in strain on the posterior surface of the bone-implant interface. There is also a minor change in the strain on the lateral surface of the bone-implant interface shown in the medial cross-section and both of the changes in strain increase as the boundary position is moved closer to the proximal femur.

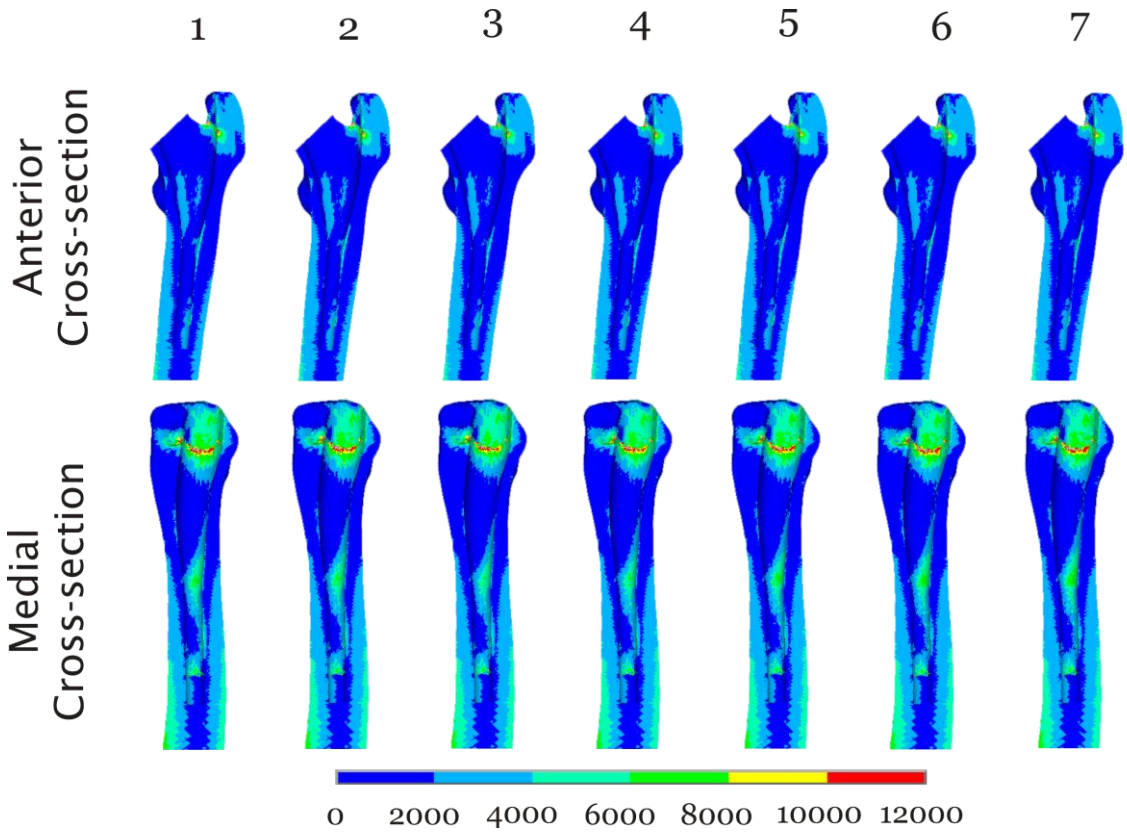

Figure 28: Medial and anterior cross-sectional views of the equivalent strain (με) in the proximal femur for the seven boundary constraint models. Model 1 had the most posterior boundary constraint and model 7 had the most anterior boundary constraint. Anterior cross-sectional views were taken in the y-z plane at the centre of the femoral head. Medial cross-sectional views were taken in the x-z plane at the centre of the implant femoral shaft.

The strain did not substantially alter with different locations of the boundary plane. The micromotion at the interface between the bone and implant was also considered and the percentage of elements with a micromotion greater than 40μm was found to change only slightly with the different boundary positions. Only the proximal femur was under investigation and therefore calculating the strain distribution in the distal femur increased the computational time of each modelled scenario without enhancing the results. Boundary position four, with the fixed nodes 173mm from the base of the implant, had similar results to the models with the boundary positions at one and two but removed some of the distal femur elements. However with positions five to seven,

with a more proximal constraint, the strain and micromotion increases more sharply and therefore position four was used in subsequent models.

5.2.4.Finite element mesh

A mesh convergence study was conducted to generate a mesh that produced reliable strain and micromotion results. Five models were created in ANSYS ICEM with a range of element sizes and subsequent numbers of solid elements (Table 8). The median strain at the bone-implant interface remained similar as the number of elements in the models was increased with less than a 5% variation between the models (Figure 29). There was a difference of 13% in the mean strain in model 2 compared to model 5. The strain calculated in model 4 appeared to converge with the strain calculated in model 5 and there was a 1% or less difference between the 25th and 75th percentile strain in the two models. The difference in the median strain was also less than 1%. The mean micromotion calculated for the five models was calculated to be within 14%, however model 4 only had a 4% increase in mean micromotion as compared to model 5 (Figure 30). Model 4 appeared to converge with the model 5 with respect to the micromotion where 5% or less difference was calculated between the mean, median, average and quartile micromotion.

Model no.	No. of elements in mesh	Maximum element size/ refined element size (mm)
1	125,000	2/0.1 (prosthesis), 4/0.5 (femur)
2	245,110	1.5 (all)
3	291,646	2/0.1 (prosthesis), 3/0.5 (bone)
4	574,887	1 (prosthesis), 2 (bone)
5	1,185,265	1 (prosthesis), 1.5 (bone)

Table 8: The number of elements and maximum element size in the five mesh convergence models. Refined element size is the minimum element size allowed at complex geometry locations.

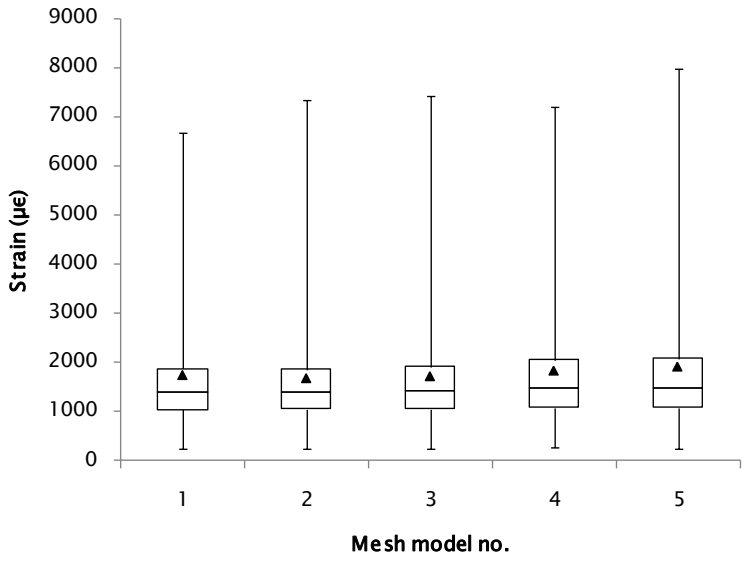

Figure 29: The equivalent bone strain at the bone-implant interface in the different mesh models. The median strain, 25th and 75th percentiles are displayed in the box plot with the 99th and 1st percentiles shown as the error bars. ▲ denotes the mean strain. Loading remains constant with all models.

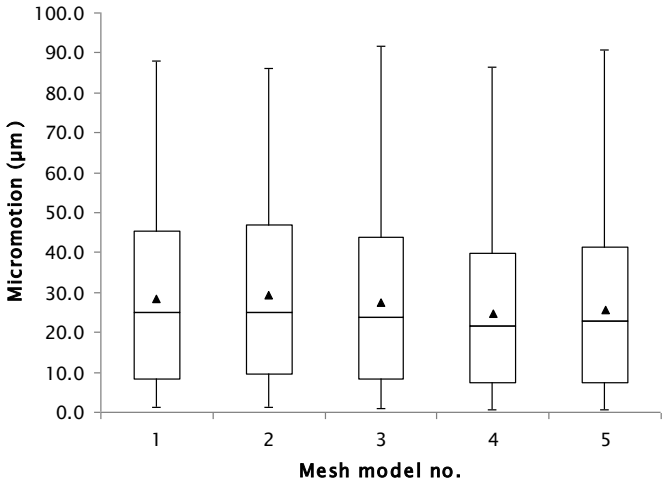

Figure 30: The equivalent micromotion at the bone-implant interface in the different mesh models. The median micromotion, 25th and 75th percentiles are displayed in the box plot with the 99th and 1st percentiles shown as the error bars. ▲ denotes the mean micromotion. Loading remains constant with all models.

Figure 31 shows the equivalent strain in a cross-section of the models from both an anterior and medial view. In particular the strain on the lateral surface of the bone-implant interface and around the distal end of the implant is similar in models 4 and 5 but is reduced in the other three models. The strain in the greater trochanter also varies in the first three models but is similar between the fourth and fifth models. The fifth model contains approximately 1.1million elements and was considerably more computationally expensive to run than model 4 which only has approximately half the number of elements. The convergence study showed that model 4 produced similar results to model 5 and suggested that the mesh converged at model 4. Therefore the mesh density associated with model 4 was used in subsequent studies.

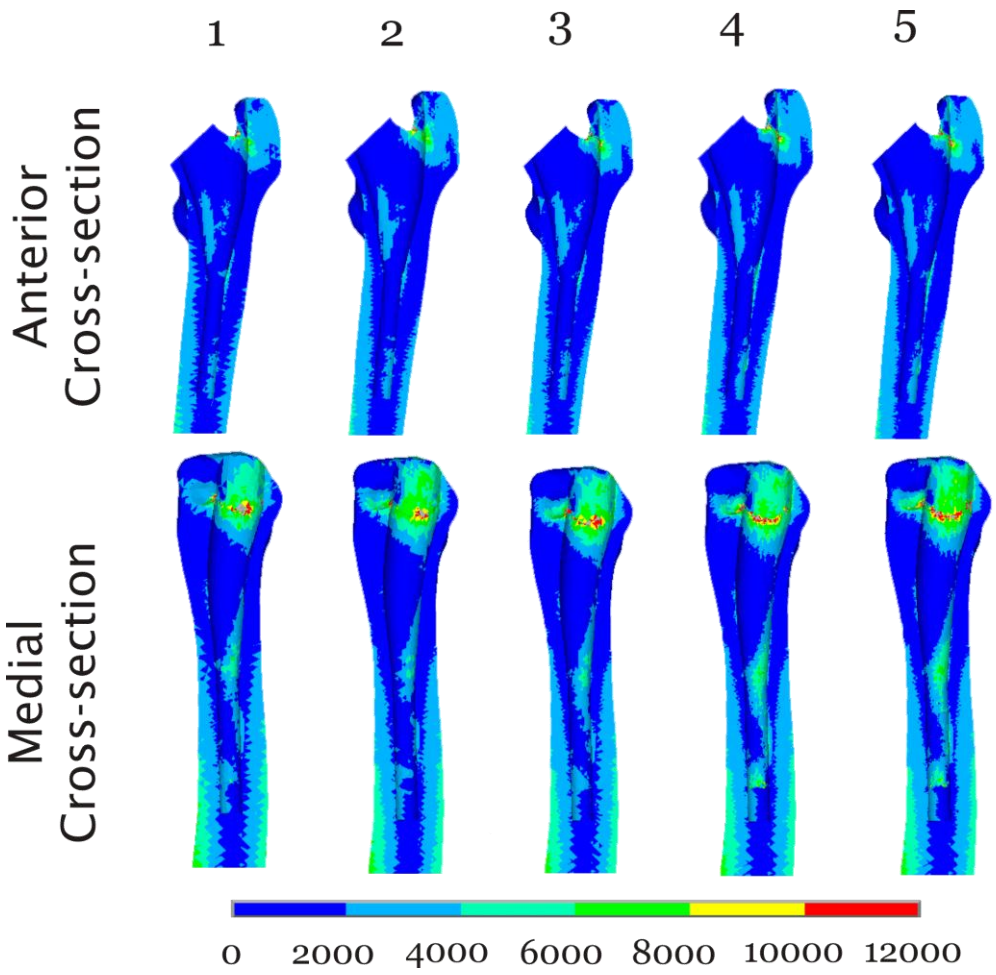

Figure 31: Medial and anterior cross-sectional views of the equivalent strain (με) in the proximal femur for the five convergence study models. Loading remains constant with all models. Anterior cross-sectional views were taken in the y-z plane at the centre of the femoral head. Medial cross-sectional views were taken in the x-z plane at the centre of the implant femoral shaft.

5.2.5.Output requirements

Finite element analysis is widely used to calculate the stresses and strains in the bone-implant interface and in the surrounding bone to predict fixation stability and the potential for stress shielding and bone resorption. However a wide range of metrics have been reported to compare different models including the peak, mean and percentage volume over a threshold in principal, equivalent and intensity of stress and strain (Simões et al. 2000; Watanabe et al. 2000; Stolk et al. 2001; Speirs et al. 2007;

Reggiani et al. 2008; Park et al. 2009). The reported regions under investigation have included the contact interfaces and zones of the proximal head.

Bone is constantly remodelling due to the loads applied through it. Instability can occur at the bone-implant interface if there is too much or too little force through the bone. Too high a force can cause the bone to fail and too low a force can cause the bone to resorb (Section 2.2). Although femoral stress is commonly reported in the literature (Watanabe et al. 2000; Reggiani et al. 2008) it was not used in this study because the failure stress of bone is affected by the location of the bone and its modulus. However, failure strain of bone, in general, is not affected by its location in the body (Morgan et al. 2003). The bone mesh incorporates the range of bone density and material properties within the cortical and cancellous bone which makes strain an important failure indicator. Equivalent strain (ϵ_e) is calculated from the principal strains and allows both tensile and compressive strains to be considered within a single parameter (Equation 5). As discussed in section 2.2.1 the yield point of strain has been found to be independent of apparent bone density whereas yield stress varies with density and location in the bone (Cowin 2001).

$$\epsilon_e = \frac{1}{1+\upsilon}\left(\frac{1}{2}[(\epsilon_1-\epsilon_2)^2+(\epsilon_2-\epsilon_3)^2+(\epsilon_3-\epsilon_1)^2]\right)^{\frac{1}{2}} \qquad \text{Equation 5}$$

ϵ_e = equivalent strain
ϵ_1, ϵ_2, ϵ_3 = principal strains
ν = Poisson's ratio

High strain along the interface between the bone and implant has been found to indicate an increased risk of loosening (Taylor et al. 1995) and the peak strains in the bone or at the bone-implant interface are often used to compare models. However, the effect of the modelled scenario in the study by Taylor *et al.* on the majority of the bone is not reported. Peak strains calculated in finite element models are also subject to modelling errors and due to an error in one element unrealistically high values can be produced. Comparing the mean strain reduces the risk of single elements causing

inconsistent results, however the pattern of strain in the bone is not reported. Several studies have reported mean values of stress or strain (Wong et al. 2005; Jonkers et al. 2008; Gracia et al. 2010), but mean values can be influenced by a few unfeasibly large values or moderated by a large number of low strain elements which are unaffected by the modelled changes.

Using the mean strain as an output parameter also does not show what percentage of the bone is at risk of failure due to the scenario. The equivalent strain at which bone yields is approximately 7800με in tension and 8400με in compression (Kopperdahl and Keaveny 1998). In this study to compare the risk of the failure of bone due to yield the percentage of elements with an equivalent strain greater than 7000με is calculated. Only normal gait was considered in this study, which does not produce the harshest loading conditions that a hip arthroplasty may encounter during its lifetime. Therefore the use of box plots showing the change in distribution of strain were also used to highlight which scenario may be more detrimental to the lifetime of the hip prosthesis despite small only changes to the predicted increase in strain greater than the threshold, as gait is not expected to cause bone failure. In order to examine the load transfer within the entire femur the proximal femur was divided into 20 regions based on the concept of Gruen zones (Gruen et al. 1979). The proximal femur was divided into five longitudinal sections shown in Figure 32 and each section was further divided into four zones by a plane at 45° and -45° to the x-y plane based at the femoral shaft midline to create anterior, lateral, posterior and medial zones.

Bone growth around the implant is crucial to forming a strong fixation in cementless hip prostheses and the amount of micromotion between the implant and the bone has been reported to affect osseointegration. High levels of micromotion at the bone-implant interface correlate to poor biological fixation of the implant and studies have found micromotion greater than 40μm (Jasty et al. 1991; Engh et al. 1992), 50μm (Szmukler-Moncler et al. 1998) or 150μm (Pilliar et al. 1986) reduce the formation of bone and therefore increase the risk of implant loosening. Micromotion in this model

is defined as the distance between initially coincident contact nodes. An experimental study by Engh *et al.* (1992) found that micromotion of 40μm or greater produced some micro cracks in the bone interface. This study has looked at both the mean micromotion and the percentage of elements at the interface with a micromotion of 40μm or greater as a method of comparing the potential stability of the interface with each scenario.

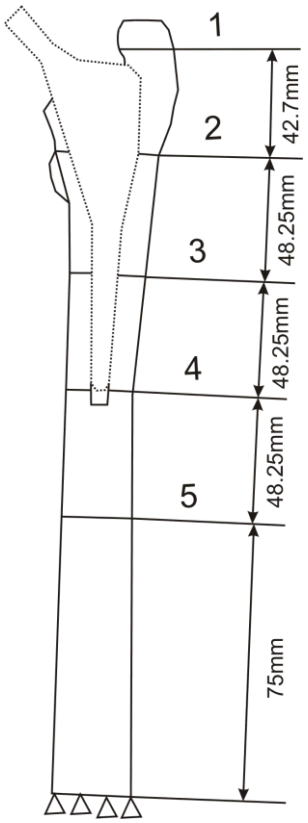

Figure 32: The division of the femur into five regions which were additionally divided into four sections; anterior, posterior, lateral and medial.

5.2.6.Model verification

The muscle and hip joint forces were applied to a finite element model of an intact femur to investigate the internal strain pattern (Figure 33). The predicted forces from the S1 model at 15% and 50% of the gait cycle were applied to the femur. At 15% of gait the cross-sectional view shows strains of approximately 4000-6000με at the femoral neck on the superior side which are low in comparison to the yield strains of bone, which is approximately 7800με in tension and 8400με in compression (Kopperdahl and Keaveny 1998). Hence, the study predicted that the risk of failure

during normal gait would be low which is as expected. The peak strains in the implanted femur model are due to a modelling defect. The interface between the bone, implant and proximally reamed section of bone provided a challenging region to mesh accurately. Unfortunately a very small number of elements were either an unacceptable shape or bridged the interface. As a result these small elements have been calculated to have unlikely levels of strain and should be ignored in the resulting models. As peak strains can be caused by small errors in the model they are not useful for comparing models with *in vitro* or *in vivo* studies. Due to the potential for small errors to cause an unlikely strain in an element, peak strain values have not been used in this study.

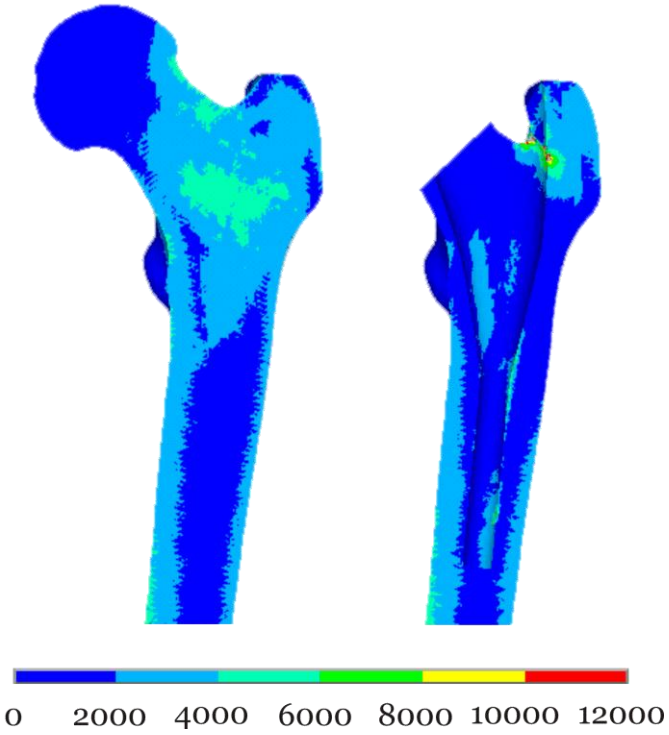

Figure 33: Distribution of equivalent strain (με) in cross-section of a whole and implanted femur at the first peak in hip contact force.

Figure 34 shows the strain distribution in each zone of the bone for both the whole and implanted femur models. The zones are labelled 1 for the most proximal through to 5 for the most distal (Figure 32). The zones with the largest variation between the models the proximal zones in the anterior, posterior and medial sides and in all cases

the implanted femur has a lower mean strain. Hip prostheses have extremely high modulus values compared to the surrounding bone and the load is transferred through the prosthesis (Huiskes 1990). This reduces the load through the proximal bone and hence the strain is lowered. The percentage of elements at the bone-implant interface with a micromotion at over a threshold value of 40μm was approximately 8% at the first peak in hip contact force, 15% of gait, and 13% at the second peak in hip contact force, 53% of gait. This is similar to the findings from a recent finite element study by Kadir and Kamsah (2009) They used three different implant types and found that at toe off the percentage of the implant surface with a micromotion above 40μm was between 8-10%.

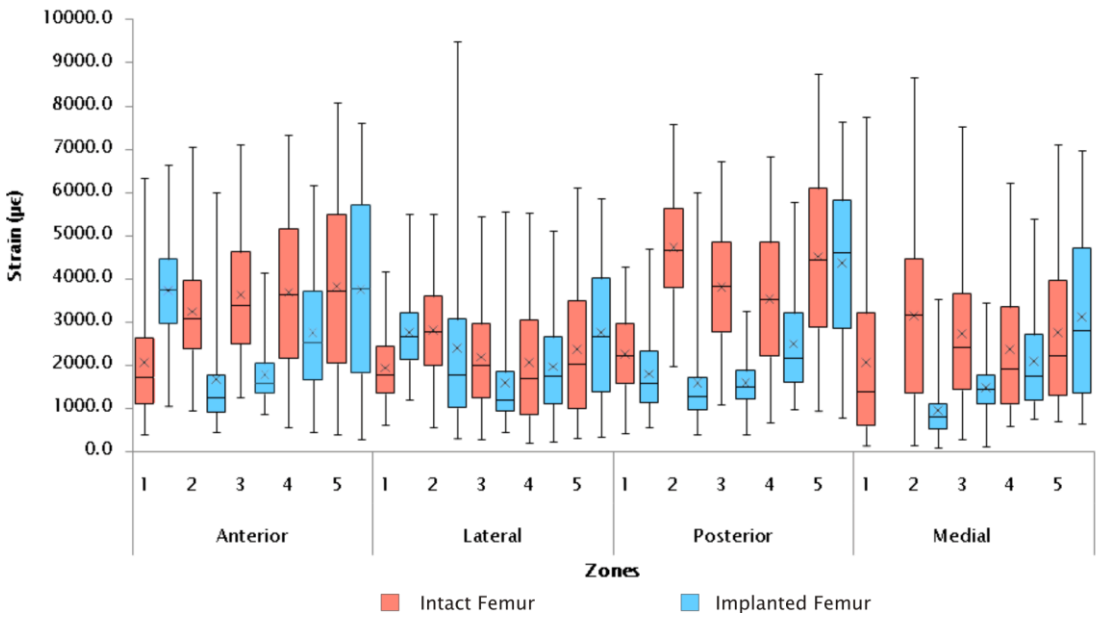

Figure 34: The mean equivalent strain (με) in each zone of the implanted and whole femur models at 15% of gait. The median strain, 25th and 75th percentiles are displayed in the box plot with the 99th and 1st percentiles shown as the error bars. x denotes the mean strain.

5.3. Summary

A finite element model can be used to complement clinical studies by providing internal strains and the micromotion between the implant and bone. However, to

provide realistic results or trends between models, realistic input forces need to be used and a comparison needs to be made between measured results. Musculoskeletal models can provide a prediction of the internal forces in the body but muscle forces cannot be measured directly and joint contact forces can only be measured by including an artificial component into the body which could alter the forces. Therefore the joint contact forces, moments and angles from the musculoskeletal model were compared to several measured patients' data to establish that the model was reasonable. These forces were then applied to a finite element model and that was found to compare favourably to a literature study. The finite element model provides an insight into the likely comparative results between the studies conducted rather than a physiologically accurate outcome. However computational modelling reduces the time and cost of investigating variables in an *in vitro* or clinical setting and can highlight the parameters which should be focused on in more depth.

6. Influence of patient variability on predicted musculoskeletal forces and subsequent primary stability of a cementless hip stem

In vivo studies have shown that there is variability between the kinematics and joint contact forces of different people (Bergmann et al. 1993; Taylor et al. 1997; Bergmann et al. 2001; Taylor and Walker 2001). However, despite detailed geometry and material properties applied to finite element models, many are at best subject specific and often use a generic loading regime scaled to the subject specific model (Behrens et al. 2008; Andreaus and Colloca 2009). Although forces are varied by patient weight, *in vivo* studies have found a range of hip contact forces despite normalising to the body weight of the patient (Chapter 2.5.1) and it is reasonable to predict that the same inter-patient variation may occur in muscle force generation. By neglecting the potential for patient variation, computational studies can only investigate the effect of arthroplasty on one individual and since hip arthroplasty has been found to perform well in the majority of patients (Malchau et al. 2002) this approach may overlook patient groups that could be adversely affected by the implant design or surgery. Probabilistic models are beginning to investigate the effects of implant position and geometry changes but there is only a limited range of loading data used (Pancanti et al. 2003; Viceconti et al. 2006). The variation in forces across the hip due to different subjects may have a greater effect on the primary stability and associated stress distribution than the patient specific geometry (Jonkers et al. 2008). This study investigates the differences in predicted joint contact and muscle forces and the subsequent differences in strain and micromotion generated by a finite element model of an implanted femur.

6.1. Musculoskeletal and finite element modelling

Nine musculoskeletal models were created from the generic model using the kinematic and kinetic data from the healthy individuals S1-7 and C01-02 (Table 6, Section 5.1.2).

The subject group consisted of four males and five females with an age range of 43-67 years (Table 6). The generic model, described in section 5.1.1, was scaled to fit the marker data collected for each subject. The angles and moments through the gait cycle were calculated for each joint by the AnyBody programme using marker data collected for each subject during a gait cycle at a freely selected normal walking speed. The walking speed for the healthy individuals ranged between 1.13-1.49m/s with a mean of 1.24m/s.

The musculoskeletal forces from each subject-specific model were then applied to a finite element model of the implanted femur (Chapter 5.2). The musculoskeletal forces were normalised relative to the subject's body weight and applied as a multiple of the assumed body weight of the finite element model, 84.7kg, and kept the same for each subject. A series of static analyses were conducted at intervals of 5% of the gait cycle from 0-95%. The equivalent strain and micromotion was calculated for the whole of the bone-implant interface in each subject specific model. Mean strain and micromotion were then calculated for the interface. To investigate the primary stability of the implant, the percentage of elements with a strain greater than the threshold of 7000με and the percentage of elements with a micromotion greater than 40μm were also calculated (Section 5.2).

6.2. Results

6.2.1. Variation in the hip range of motion and musculoskeletal forces

In general, the hip joint begins the gait cycle in flexion and abduction and moves into extension and adduction through the stance phase of gait reaching peak extension at approximately toe off (Figure 35). The hip then flexes through the swing phase to bring it back to the same relative position as at the start of the gait cycle (Figure 35). The mean flexion angle over the whole group varied from 27° in flexion to 13° in extension during toe off with a peak flexion angle of 34° and a peak extension angle of 21° (Figure 35a). The range of motion in flexion-extension varied between 34° and 48° for the nine patients.

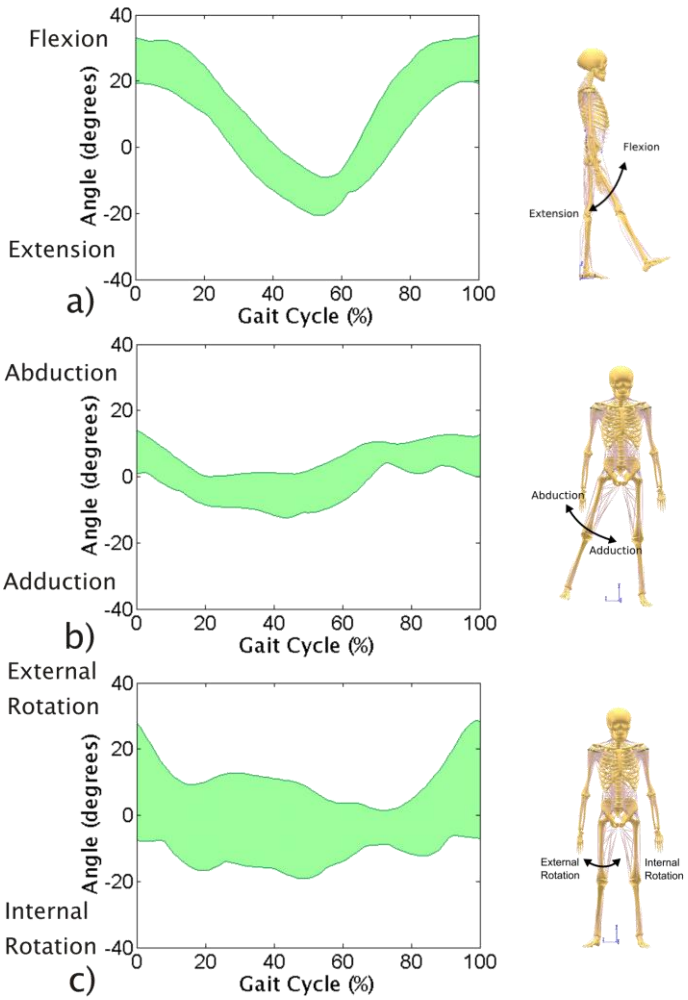

Figure 35: Range of hip joint angle through the gait cycle in the healthy individuals. a) flexion-extension angle, b) abduction-adduction angle and c) external-internal rotation angle.

The difference between the healthy subjects in angle of flexion-extension and adduction-abduction angle remained relatively constant through the gait cycle with a mean difference of 11° in flexion-extension and 15° in adduction-abduction (Figure 35a and b). The range of flexion-extension during the gait cycle varied from 34° in subject S3 to 47° in subject S4 and the range of abduction-adduction motion ranged from only 8° in subject S2 to 24° in subject C01 (Table 9). There was a larger variation between the subjects' internal-external rotation angle and a mean difference between the patients was 24° over the gait cycle (Figure 35c). The range of internal-external rotational motion over the gait cycle ranged from 13° in subject S2 and 31° in subject

S4 (Table 9) although only S6 also had a range greater than 21°. However the measurement of the internal-external rotation of the hip is prone to error as it measured by closely spaced markers and therefore the resulting differences may be partly due to error rather than solely variation between the patients.

	Range of motion (°)		
	Flexion-Extension	**Abduction-Adduction**	**Internal-External Rotation**
Minimum	34	8	13
Maximum	47	24	31
Mean	41	16	19
Median	42	15	15

Table 9: The range of motion measured in the nine healthy subjects during a gait cycle.

The torque at the hip was normalised relative to the subject's body weight by dividing the joint torque by the subject's body weight. The normalised torque was reported as a multiple of body weight times metres in a similar manner to Heller *et al.* (2005) and this allowed the joint torque to be compared between the individual models and with published results. The mean flexion-extension torque across all the healthy subjects ranged from 0.11BW*m in flexion to 0.22BW*m in extension (Figure 36a). The abduction torque measured at the hip for the healthy individuals ranged from a maximum of 0.10BW*m to a maximum adduction torque of 0.07BW*m (Figure 36b). There was only a small internal-external rotational torque through the gait cycle and a narrow range between the healthy individuals (Figure 36c). The peak ground reaction force in the superior direction ranged between 1.0BW and 1.4BW, however in the lateral and anterior directions were significantly smaller with peak forces of approximately 0.3BW in lateral direction and 0.1BW in an anterior direction. Therefore, despite the angular change, the forces acting on the hip in the anterior-lateral plane were relatively small, which produced a small joint torque.

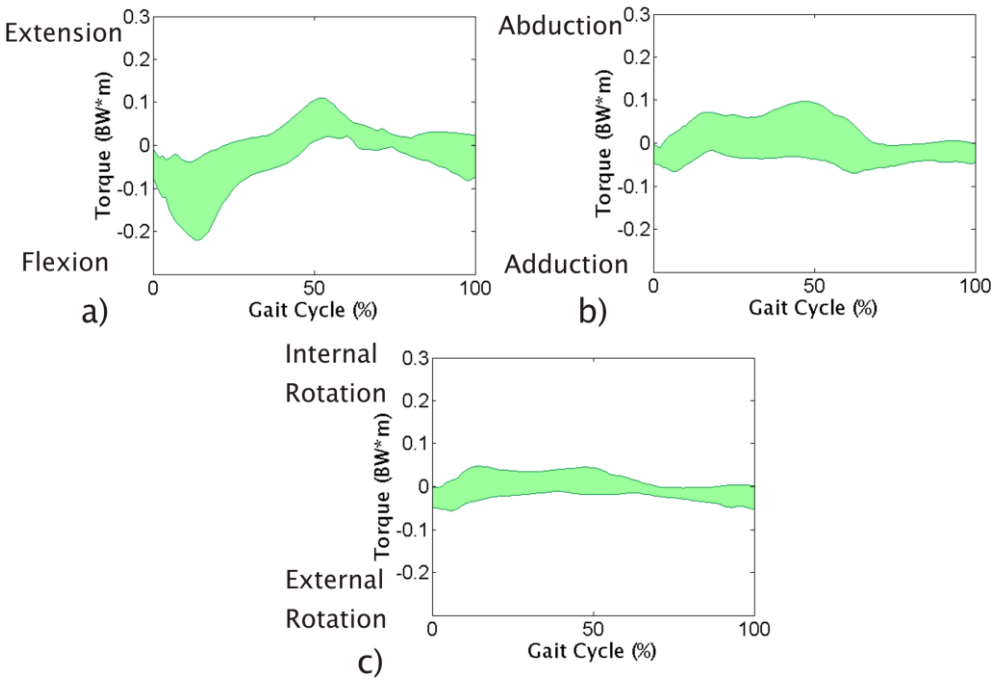

Figure 36: Range of hip joint torque through the gait cycle for the healthy individuals

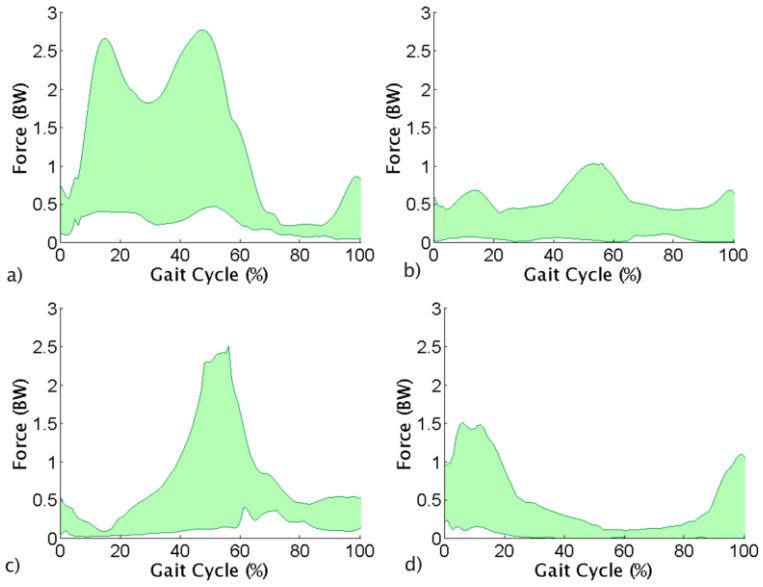

Figure 37: Range of combined muscle forces through the gait cycle for the healthy individuals. a) abductor force, b) adductor force, c) flexor force and d) extensor force.

The muscle and joint contact forces were calculated using a recruitment criterion based on distributing the load across the muscles by minimising the sum of the squared muscle activities (Chapter 5.1). The individual muscle forces were combined

into groups depending on the actions they provided at the hip (Table 7). The largest range in the abductor muscle group was at toe off where there was a variation of 2.5BW between the different healthy patient models (Figure 37a). However, the range was dominated throughout the gait cycle by a large force in subject C02 and a particularly small force at approximately 15% of the gait cycle in S3, whereas the remainder of the group covered a smaller range (Figure 38).

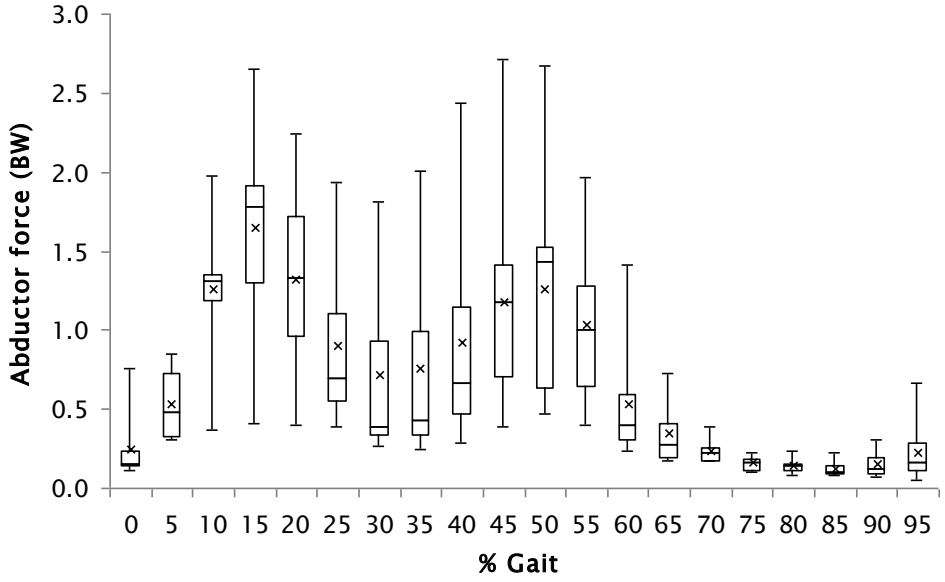

Figure 38: The resultant abductor muscle force in the healthy subject models at each time step in the gait cycle. The median percentage of elements, 25th and 75th percentiles are displayed in the box plot with the minimum and maximum shown as the error bars. x denotes the mean percentage of elements.

The adductor and flexor muscle groups are most active at toe off and this coincides with the largest range across the subject specific models (Figure 37b and c). Literature studies investigating flexor and adductor muscle activity using EMG have also found those groups to be active at toe off (Vaughan et al. 1992). There is a range of approximately 1BW in the adductor muscle group from almost no predicted force in subject C01 to a peak force of 1BW in S3. There was a variation in the combined muscle force for the flexor group of approximately 2.2BW at toe off (Figure 37c). Model C01 and C02 were predicted to have a small flexor force at toe off and had a

peak in force slightly later than toe off during the start of the swing phase. The range in the extensor muscle group is approximately 1.3BW across the nine models.

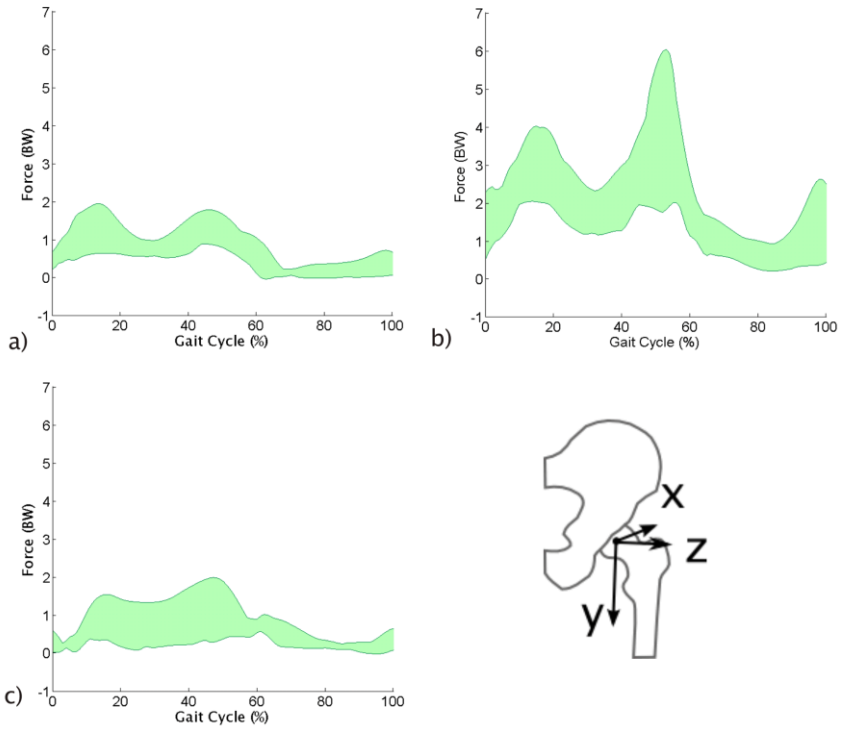

Figure 39: The range of force in each component of the hip contact force through the gait cycle for the healthy individuals. Hip force components a) Fx, b) Fy and c) Fz.

Subject model	Body Weight (N)	Walking speed (m/s)	Peak hip contact force (BW)	
			First peak	Second peak
S1	667	1.13	2.63	3.88
S2	922	1.33	3.72	3.26
S3	853	1.10	2.25	4.73
S4	942	1.37	4.54	2.74
S5	623	1.15	4.23	6.17
S6	657	1.49	3.36	4.51
S7	883	1.18	3.16	2.19
C01	775	1.15	3.70	2.63
C02	579	1.25	4.10	4.14

Table 10: Patient details and peak hip contact forces for the healthy patients.

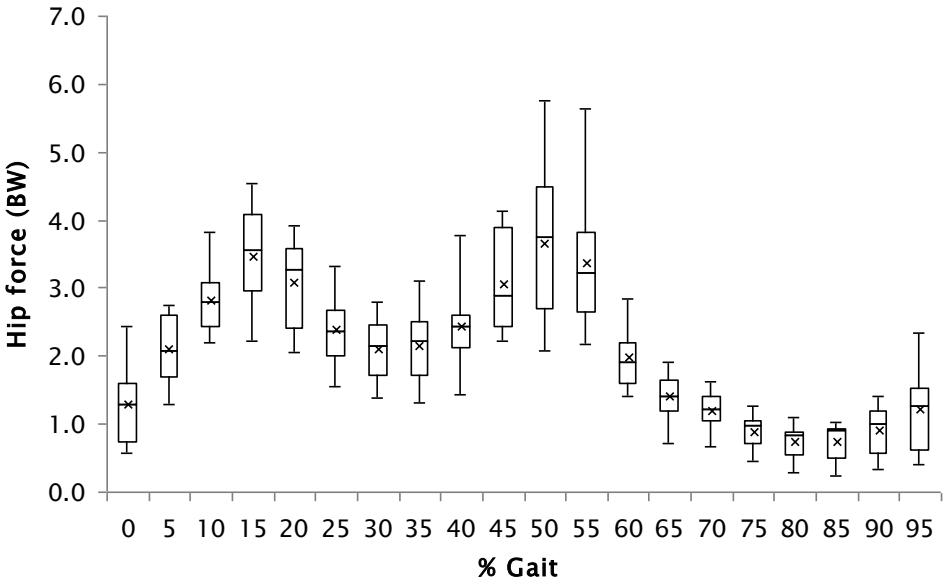

Figure 40: The resultant hip force in the healthy subject models at each time step in the gait cycle. The median percentage of elements, 25th and 75th percentiles are displayed in the box plot with the minimum and maximum shown as the error bars. x denotes the mean percentage of elements.

The hip contact force in the superior-inferior direction had a range of approximately 2BW at 15% of gait and 4BW at 50% of gait (Figure 39a). There was a smaller variation in the medial-lateral component of hip force although the largest range, approximately 2BW occurred at toe off (Figure 39b). The anterior-posterior component of force had the smallest range across the healthy patients, with a maximum variability of approximately 1.5BW at 15% of gait (Figure 39c). The resultant hip contact force at the first peak, 15% of gait, varied between 2.2BW to 4.5BW and varied between 2.0BW and 6.1BW at the second peak, 50% of gait (Table 10).

6.2.2.Variation at bone-implant interface

The mean strain at the bone-implant interface peaked at approximately toe off and ranged from 1100με to 4080με (Figure 41a). The percentage of elements with a strain greater than 7000με also peaked at toe off and ranged from 0.1% to 11% (Figure 41b). The peaks in strain occurred at the peaks in muscle and hip joint contact forces (Figure 37 and Figure 39). The strain distribution at the bone-implant interface for all of the

healthy subjects at each time step was plotted in Figure 42. The 75th percentile of the interface strain was less than 2500με throughout the gait cycle and was only greater than 2000με at 15% and 50% of the gait cycle. The distribution of strain was also skewed towards the low end of the strain range.

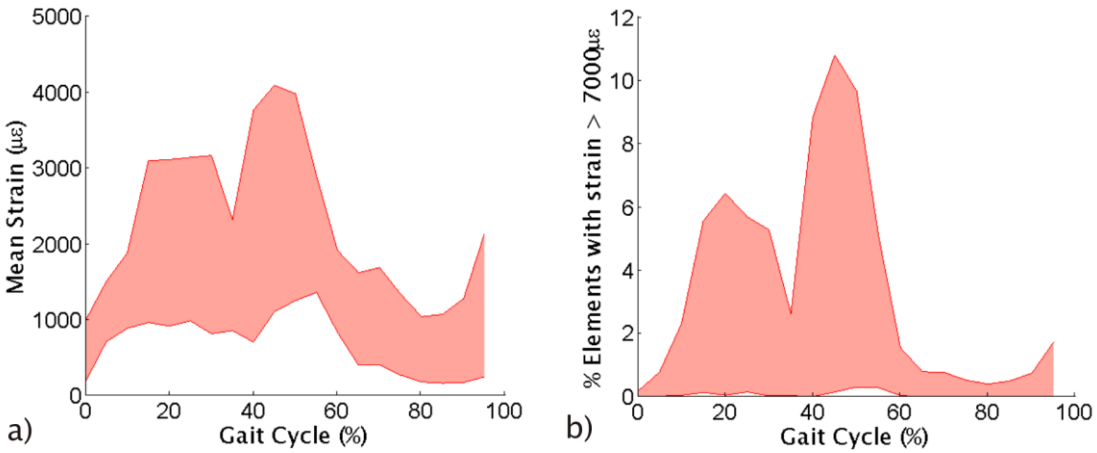

Figure 41: Range equivalent strain at the bone-implant interface across the nine healthy patients. a) mean strain, b) percentage of elements at the interface with a strain greater than 7000με.

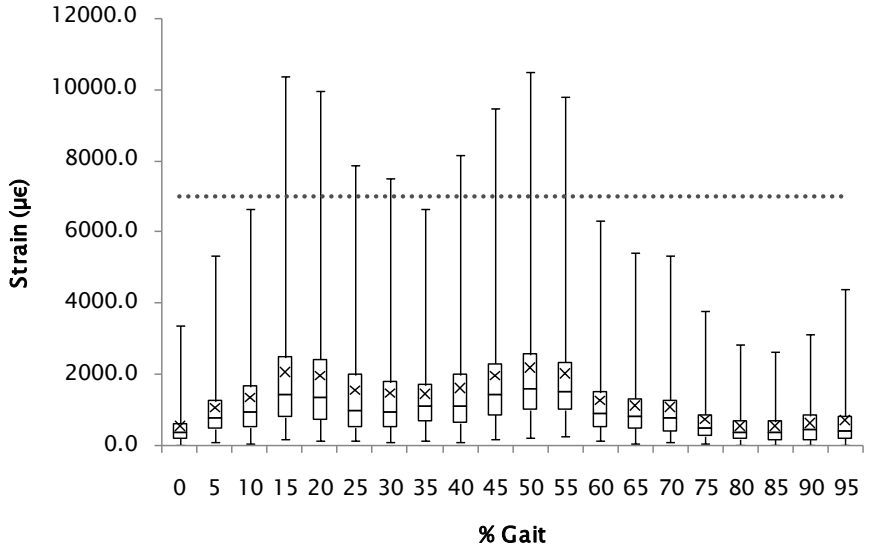

Figure 42: The strain at the bone-implant interface for all of the healthy subject models at each time step in the gait cycle. The median percentage of elements, 25th and 75th percentiles are displayed in the box plot with the 1st and 99th quartiles shown as the error bars. × denotes the mean strain.

High micromotion between the implant and bone has been reported to reduce the ability of the bone to grow onto the stem (Jasty et al. 1991) and a threshold of micromotion greater than 40μm was used in this study to assess the affect of the loading on the potential for bone growth onto the stem. Loading associated with subject S5 was found to have the largest micromotion at toe off with a mean micromotion of 58μm and a percentage of elements greater than the threshold of 67% (Figure 43). The variability between the subjects was relatively low at toe off, particularly in the percentage of elements with a micromotion greater than the threshold compared to the remainder of the gait cycle, although the peak in micromotion was at toe off in all of the subject models. A more detailed investigation of the distribution of micromotion at the bone-implant interface found that despite the large percentage of elements with a strain greater than the threshold of 40μm none of the models had greater than 1% of the elements with micromotion larger than 150μm. The maximum micromotion measured at the interface ranged from 136μm-230μm. The 99th percentile for all the models combined only reached greater than 100μm at toe off and the 75th percentile remained below 40μm in all but five time steps at 15% and 50% of gait (Figure 44).

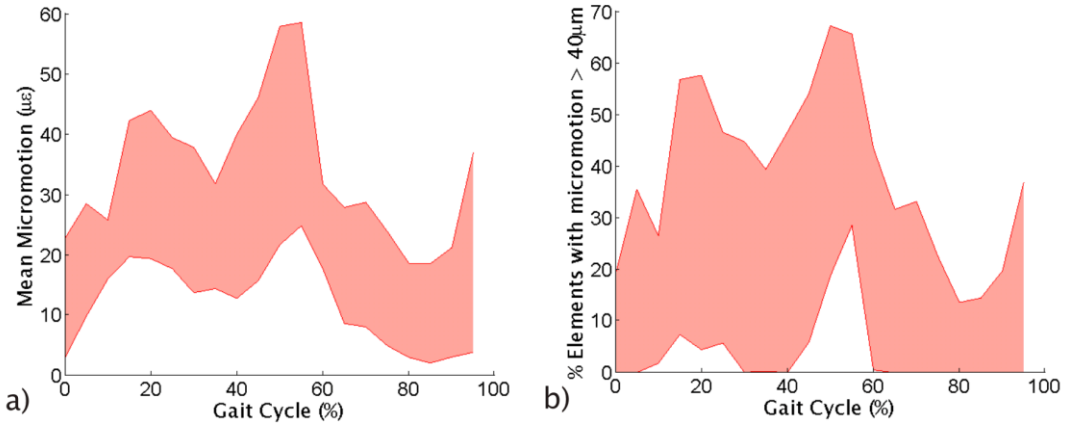

Figure 43: Range micromotion at the bone-implant interface across the nine healthy patients. a) mean micromotion, b) percentage of elements at the interface with a micromotion greater than 40μm.

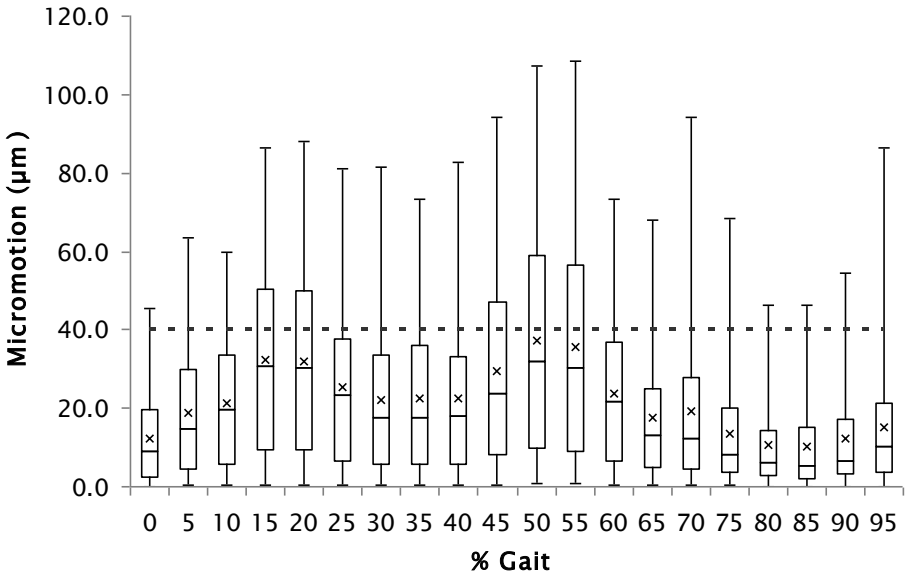

Figure 44: The micromotion at the bone-implant interface in the healthy subject models at each time step in the gait cycle. The median percentage of elements, 25th and 75th percentiles are displayed in the box plot with the 1st and 99th quartiles shown as the error bars. x denotes the mean micromotion.

The mean strain at the interface, for each time step in the gait cycle, for each subject was plotted against the resultant hip contact force in that time step to calculate the relationship between the applied forces and the primary stability (Figure 45a). For low values of resultant hip contact force the mean strain correlated well, but as the hip contact force increased, the correlation with the mean interfacial strain decreased and overall there was an R^2 value of 0.63. The hip contact force was also compared to the percentage of elements with a strain greater than the threshold and the correlation was slightly weaker with an R^2 value of 0.57 (Figure 45b). The mean strain (*MSTR*) and the percentage of elements with a strain greater than the threshold (*PSTR*) both increased proportionally with the normalised hip contact force (*NHF*) (Equation 6 and Equation 7)

$$MSTR = -47.41NHF^2 + 76.45NHF \quad \text{Equation 6}$$

$$PSTR = 0.27NHF^2 - 0.14NHF \quad \text{Equation 7}$$

The percentage of elements with strain greater than threshold can only provide a limited investigation of the strain distribution as many of the scenarios with a low hip contact force had a very low number of elements with strain greater than the threshold. The low correlation between the strain and the hip contact force indicates that muscles forces should be included in the finite element model to enable better prediction of the strain.

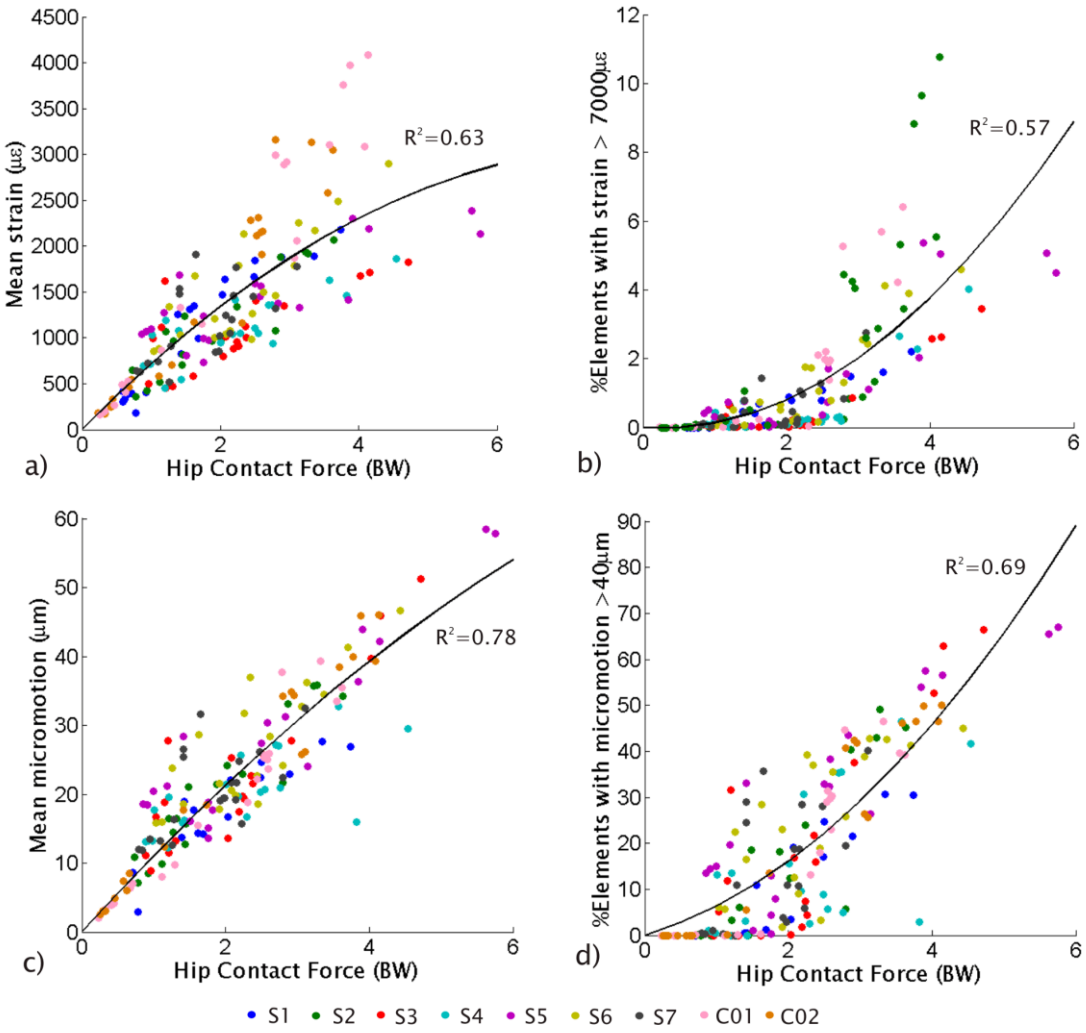

Figure 45: Correlation between resultant hip contact force and a) mean strain b) percentage of elements with a strain greater than the threshold c) mean micromotion and d) percentage of elements with a micromotion greater than the threshold at the bone-implant interface for each hip displacement scenario at each modelled time step for each healthy individual.

The mean micromotion at the bone-implant interface was also plotted against the hip contact force and there was a stronger correlation with an R^2 value of 0.78 (Figure 45c). The percentage of elements with a micromotion greater than the threshold was also compared to the hip contact force applied in the modelled scenarios and a slightly weaker correlation was found with an R^2 value of 0.69 (Figure 45d). However the lower correlation may have been caused by little or no micromotion greater than the threshold in several of the scenarios, as was found with the percentage of elements with a strain greater than the threshold. The mean micromotion (*MMICRO*) and the percentage of elements with a micromotion greater than the threshold (*PMICRO*) both increased with the normalised hip contact force (*NHF*) (Equation 8 and Equation 9)

$$MMICRO = -0.41NHF^2 + 11.46NHF \quad \text{Equation 8}$$

$$PMICRO = 1.73NHF^2 - 4.51NHF \quad \text{Equation 9}$$

The hip contact force has a good correlation with the micromotion and mean strain however there was still some unexplained variability. The lateral and posterior components of the hip contact force and the abductor force were also compared to the micromotion and strain. Both the mean strain and the percentage of elements with a strain greater than the threshold correlated well with the abductor force and the lateral component of the hip contact force (Table 11) and had a higher correlation coefficient than the resultant hip contact force. However the greatest influence on the micromotion was from the resultant hip contact force.

	Mean strain (με) (MS)	% elements > 7000με (PS)	Mean micromotion (μm) (MM)	% elements > 40μm (PM)
Resultant hip contact force (RH)	$MS = -47.41RH^2 + 765.45RH$ $R^2 = 0.63$	$PS = 0.27RH^2 - 0.14RH$ $R^2 = 0.57$	$MM = -0.41RH^2 + 11.46RH$ $R^2 = 0.78$	$PM = 1.7RH^2 + 4.61RH$ $R^2 = 0.69$
Hip contact force (posterior component) (PH)	$PH = -541.52PH^2 + 2417.36PH$ $R^2 = 0.40$	$PS = 1.99PH^2$ $R^2 = 0.45$	$MM = -17.17PH^2 + 47.25PH$ $R^2 = 0.25$	$PM = -5.13PH^2 + 33.24PH$ $R^2 = 0.3$
Hip contact force (lateral component) (LH)	$LH = -368LH^2 + 2417.36LH$ $R^2 = 0.69$	$PS = 2.69LH^2 + 0.04LH$ $R^2 = 0.75$	$MM = -16.85LH^2 + 51.49LH$ $R^2 = 0.41$	$PM = -5.84LH^2 + 39.82LH$ $R^2 = 0.44$
Abductor force (A)	$MS = -403.34A^2 + 2192.16A$ $R^2 = 0.61$	$PS = 1.04A^2 + 0.32A$ $R^2 = 0.79$	$MM = 12.19A^2 + 42.93A$ $R^2 = 0.21$	$PM = -6.97A^2 + 35.09A$ $R^2 = 0.48$

Table 11: Variables potentially affecting strain and micromotion at the implant-bone interface. Equation of line of best fit and correlation coefficient.

6.3. Discussion

This study has found variability in the kinematics of healthy patients and using a musculoskeletal model predicted differences in the muscle and hip joint contact forces between individuals. In general the musculoskeletal forces fitted well with results reported in the literature (Johnston and Smidt 1969; Crowinshield et al. 1978; Johnston et al. 1979; Bergmann et al. 2001). The predicted musculoskeletal forces were then applied to a finite element model of an implanted femur and the resulting strain and micromotion also showed a wide variation. However only nine subjects were used in this study and therefore this investigation can only highlight the potential differences between healthy subjects.

6.3.1. Joint kinematics and kinetics

The range of motion at the hip during gait in healthy subjects was found to be similar but slightly higher than that measured in a study by Dujardin *et al.* (1997) which compared 55 healthy individuals. They found a range of motion in flexion-extension to be 20-42° however this was lower than the range of 34-47° found in this study. However Crowinshield *et al.* (1978) calculated a similar range of flexion-extension

motion, approximately 25°-50° for healthy subjects at a walking speed of 1.2m/s and Bergmann *et al.* (2001) found a peak hip flexion angle of 36.7°. Bergmann *et al.* also found a peak extension angle of 12.7° and the range of motion was smaller than that measured in this study and varied between 27° and 41°. However the patients measured in the study by Bergmann *et al.* had all undergone total hip arthroplasty which can reduce range of motion (Madsen et al. 2004).

In abduction-adduction Dujardin *et al.* found a range of 2-20° compared to the 8-24° measured in this study. In the study by Bergmann *et al.* (2001) reported abduction-adduction angles between 8-31° which is higher than that found in either of the healthy studies. Although Dujardin *et al.* found smaller ranges of abduction-adduction and flexion-extension they recorded a larger range of internal-external rotation 3-40° compared to only 13-31° measured in this study. The largest range of internal-external rotation found in the study by Bergmann *et al.* was 23°. However the internal/external rotation of the leg is prone to higher error during the gait analysis data collection procedure due to the small distance between the markers in the transverse plane and the potential for skin artefact errors to overwhelm the movement. In this study the joint angles were defined by scaling the generic musculoskeletal model to fit the marker positions and this can introduce error into the joint angles due to inaccuracy in defining the modelled markers. Errors in the joint centre positions have been found to affect the joint angles (Stagni et al. 2000) and therefore could affect the variation found between the individuals.

The maximum abduction torque of 0.10BW*m was only slightly larger that measured by Bergmann *et al.*, 0.08BW*m. However the torque at the hip joint measured in the study by Bergmann *et al.* (2001) showed a smaller range of flexion-extension torque between 0.06BW*m in flexion and 0.16BW*m in extension across their four THA patients compared to 0.11BW*m in flexion to 0.22BW*m in extension calculated for the healthy individuals in this study. In this study there was only a small internal-external rotational torque calculated through the gait cycle from 0.05BW*m in internal

rotational torque to 0.06BW*m in external rotational torque. The calculated results in this study were slightly larger than that measured by Bergmann *et al.* where a maximum of 0.02BW*m was found. In general the torque calculated in the healthy individuals in this study was higher than that measured for the THA patients by Bergmann *et al.* although of a similar magnitude and this could be due to disability caused by the joint replacement.

6.3.2.Musculoskeletal forces

Vaughan *et al.* (1992) measured the electrical activity of the major leg muscles and found the abductor muscles were active during the stance phase of gait which corresponds to the activity predicted in this study. Johnston *et al.* (1979) predicted a peak abductor force of almost 2BW during gait and Heller *et al.* (2001) predicted a peak abductor muscle force of approximately 1BW. The peak combined abductor force predicted in this study ranged from 1.3-2.8BW. However Johnston *et al.* and Heller *et al.* based their musculoskeletal model on different descriptions from the literature to the muscle attachment descriptions used in this study and in addition to potential differences in the attachment points the muscles were divided into greater numbers of sub units in this study. The muscle units included in their abductor group may also have differed slightly. The large range of abductor force predicted in this study had a high upper limit due to subject C02 who had the largest lateral component of hip contact force and the largest abduction-adduction and internal-external rotational torque at 15 and 50% of the gait cycle. At 15% of gait subject S3 had a particularly low abductor group force compared to the group which considerable extended the range of abductor force. Vaughan *et al.* (1992) measured EMG activity in the gluteus maximus and biceps femoris muscles during the initial stance phase of gait and in this study the extensor muscles, which includes the gluteus maximus and the biceps femoris, were also predicted to be active and provide a force at the start of the gait cycle.

The range of resultant hip contact force measured by Bergmann *et al.* (2001) was lower than that predicted for the healthy patients in this study. However, the measured range overlaps with the lower forces predicted by the musculoskeletal models (Figure 46). Although the measured forces tend to be lower than the predicted forces they are from patients who have undergone total hip arthroplasty surgery and have altered kinematics. Musculoskeletal modelling has predicted peak resultant hip contact forces between 1.2BW (Lenaerts et al. 2008) and 5.5BW (Johnston et al. 1979) and peak hip contact forces measured from patients with a total hip replacement have been reported to range from 1.6BW (Rydell 1966) to 3.4BW (Taylor et al. 1997) with the patient walking at normal speed.

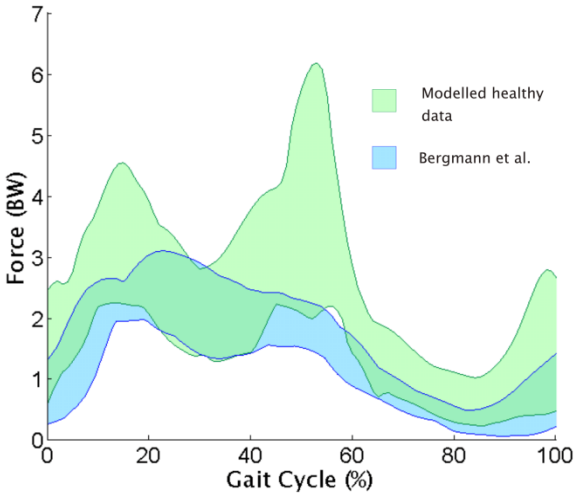

Figure 46: Range of resultant hip force through the gait cycle in the healthy individuals compared to the range measured by Bergmann *et al.* (Bergmann 2008).

The high toe off force predicted in this study of up to 6.1BW is significantly higher than that measured in *in vivo* studies. It may be caused by the limitations of the musculoskeletal model, in particular the one degree of freedom knee and solid foot model which increase the forces in the gastrocnemius and soleus muscles. These muscles affect the forces at all the joints predominantly at toe off. However only two subjects (S3 and S5) out of the nine modelled were predicted to have hip contact forces at toe off greater than 4.5BW which could indicate that these subjects were major

outliers in terms of the general population or that the errors associated with measurement of their data collection were larger. Both subject models were collected at Southampton with marker set containing fewer markers than the Cardiff subjects. A smaller number of markers provides less redundancy for the optimisation in AnyBody to calculate the kinematics of the system and potentially reduces the reliability of the predicted musculoskeletal forces. The subject with the highest hip contact force also had the lowest weight and a no correlation was found between an increase in the body weight of the subject and a decrease in the peak normalised hip force (R^2=0.14). There was also no correlation found between an increase in height and a decrease in the peak normalised hip force (R^2=0.14). The correlation between an increase in hip contact force prior to normalisation was found to be a stronger correlation with an increase in the subject's body weight (R^2=0.28) and no correlation to an increase in the subject's height (R^2=0.02). However the two subjects with the largest resultant hip contact force at toe off did not have the largest joint angles during the gait cycle and subject S3 had the smallest range of flexion-extension. Subject S5 did have the largest flexion group muscle force at toe off, the largest medial component of hip force and also had the largest flexion-extension torque at toe off which all would have contributed to the large hip contact force.

6.3.3.Finite element model

Micromotion at the bone-implant interface has been investigated extensively in the literature with regard to cementless implants (Viceconti et al. 2006; Abdul-Kadir et al. 2008; Hu et al. 2009; Park et al. 2009; Pettersen et al. 2009; Sakai et al. 2010) due to the potential for excessive micromotion to reduce bone formation (Pilliar et al. 1986; Szmukler-Moncler et al. 1998). Micromotion greater than 40μm at the bone-implant boundary can indicate early loosening due to poor growth of the bone onto the prosthesis surface (Engh et al. 1992). In a finite element study using the hip contact forces measured in Bergmann *et al.*'s (2001) study, and the muscle forces calculated for those patients, the percentage of the stem surface in which micromotion was above 40μm ranged from 18% to 49% (Pancanti et al. 2003). In this study the percentage of

elements with a micromotion greater than 40μm varied between 30-67%. However, the percentage of elements is not directly comparable to the percentage of the surface area and so a direct comparison of these studies cannot be made. Park *et al.* (2009) predicted micromotion in a variety of regions at the bone-implant interface in a model without gaps between the femur and implant. They found the mean micromotion varied between 35-55μm across these regions. In this study the micromotion was calculated for the whole of the interface rather than regions of bone however the mean micromotion was between 28-58μm during toe off in the subject-specific models. Pettersen *et al.* (2009) reported peak micromotion in a finite element model of an implant cementless hip to be approximately 40μm however in a similar experimental set up found maximum micromotion 76μm. This study found throughout the gait cycle the 75th percentile of micromotion was below 40μm although at the peaks in hip contact force, 15% and 50% of gait, the micromotion increased at the interface. The maximum micromotion predicted in this study was larger than that measured by the study by Pettersen *et al.* although of a similar magnitude.

Finite element studies investigating cementless hip arthroplasty have more commonly considered stress than strain (Chapter 3.2.1). However, some studies have investigated strain as it has been shown to be a better predictor of bone fracture (Schileo et al. 2008). Wong *et al.* (2005) found the mean interface equivalent strain was between 1400-1900με at the peak joint contact force during normal walking. The range of mean strain calculated in this study at the toe off peak in the gait cycle was between 1100-4080με which although it encompasses the mean predicted by Wong *et al.* has a substantially higher upper limit. However the resultant hip contact force used in the study by Wong *et al.* was approximately 2.4BW based on the forces from Bergmann *et al.*'s study. Using the correlation found in this study between the mean strain and the hip contact force a mean strain of approximately 1500με would be predicted which is within the range calculated by Wong *et al.*

6.3.4.Limitations

Motion capture is prone to error mainly due to skin artefact errors which reduce the accuracy of the recorded position of markers. These errors can be reduced by placing the markers on bony landmarks and this study also improved the accuracy of the calculated joint angles by resolving the over-determinate system of marker coordinates with an optimisation procedure. However the internal-external rotational angle of the hip can easily be affected by errors in data collection and the angle is further affected by the limited knee model which therefore restricts all leg rotation to be about the hip. The recruitment criterion used to predict the muscle forces is based on the assumption that the body recruits muscles to reduce overall muscle activity and studies have shown that it provides a reasonable representation of the *in vivo* situation for gait (Glitsch and Baumann 1997; van Bolhuis and Gielen 1999).

The musculoskeletal models are not from the same patients as the finite element models and linear scaling has been used to apply the loads to the finite element model. Ideally the models would have a continuity of the patient however this is unlikely to be possible in all but a small number of models and was not possible in this study. The femur was constrained by a cut plane of nodes at mid shaft which is not a physiological constraint but an investigation of the boundary conditions in this model showed that the strain and micromotion were unaffected by the constraint compared to fixed distal condyles.

6.3.5.Conclusions

This study has shown that differences between healthy subjects can be captured using this combined musculoskeletal and finite element method. It has also been found that there is large variation between healthy patients in both the predicted musculoskeletal forces and the calculated strain and micromotion around the implant. It has been previously commented that finite element studies do not incorporate a wide range of input forces into their models and therefore investigations into the range of forces which affect the hip could be useful in preclinical testing of hip replacements. The variability found in this study indicated that more work should be conducted into the

effect of patient variation on the implanted femur and that variability between patients should be considered when conducting preclinical analysis of hip prostheses. However this study has only investigated one implant design and other designs could be more or less sensitive to patient variation. The extent to which a prosthesis design could be affected by patient variation would be useful when conducting preclinical testing. Most implants currently in use are considered successful in the vast majority of patients (Kärrholm et al. 2008), however there is a small proportion of patients who require revision surgery. Therefore it is the extremes of the population rather than the average or ideal patients who should also be considered when conducting preclinical testing of implants. However the population under investigation should be carefully considered as pre-operative THR patients are unlikely to have similar kinematics to the healthy population and therefore pre-operative patients should be compared to healthy subjects to assess the differences in their applied forces. A hip arthroplasty may alter the kinematics of a pre-operative patient back towards a healthy subject, although this would not occur immediately, so a hip replacement would be required to perform well with both immediately post-operative kinematics and kinetics and longer term post-operative gait. It would seem prudent to investigate the range of forces and subsequent implant primary stability from each population for comparison as well as providing a database of forces for preclinical testing. In addition to preclinical testing the correlations found between the hip contact force and the resulting strain and micromotion at the bone-implant interface could be used as a first step in predicting potential outcomes for specific patients and this could be useful in a surgical decision support process.

7. Influence of hip centre displacement on predicted hip forces and the corresponding effect on the primary stability of a cementless hip stem

7.1. Introduction

During hip replacement surgery the geometry of the hip can be altered, either by a change in the position of the centre of rotation of the hip, defined by the vertical distance from the interteardrop line (VHC) and the horizontal distance from the teardrop (HHC), or by a change in the femoral offset (FO) (Figure 47). Bone graft can be used to attempt to restore the anatomical centre of the hip but cups can loosen following the use of bone graft (Mulroy and Harris 1990; Atilla et al. 2007) so it is not always used (Dearborn and Harris 1999). Alternatively large acetabular cups are used to fill the space in the pelvis (Agarwal 2004) or if there is an absence of bone above the anatomical acetabular position then the surgeon may deliberately choose to place the acetabular cup in a superior position (Agarwal 2004). The acetabular cup position affects the centre of rotation of the hip replacement and the use of a press fit cup often requires that the pelvis be reamed more medially and superiorly than a cemented cup (Wan et al. 2008). The patient's position on the table can also affect the position of the centre of rotation of the hip replacement if the surgeon has not taken into account the rotation of the pelvis (McCollum and Gray 1990; Archbold et al. 2006). Modular femoral necks, which allow the length and angle of the femoral neck of the implant to be altered, can change the position of the hip centre and the femoral offset and the inappropriate use of these modular implants can be detrimental (Lecerf et al. 2009).

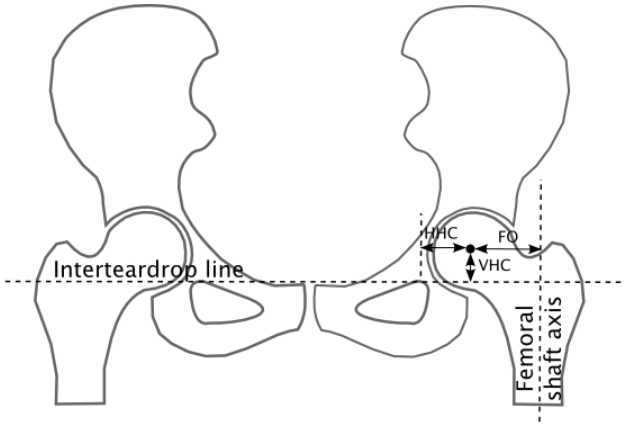

Figure 47: Definitions for the femoral offset (FO), vertical hip centre (VHC) and horizontal hip centre (HHC).

In vivo studies have found that the range of displacement of the hip centre relative to the hip centre on the contralateral limb can be between 4.4mm laterally to 19.1mm medially and 8.6mm inferior to 15.8mm superior (Table 12). Russotti *et al.* (1991) found a range of 18- 29mm in the VHC and 28-41mm in the HHC in thirty-four total hip replacement patients. The mean displacement from the measured normal hip centres was 5mm medially and 4mm (s.d. 8mm) proximally.

The modular hip prosthesis Profemur (Wright Medical Technology, Arlington, Tennessee) allows the hip centre to be offset by up to 10mm in an anterior-posterior direction by allowing up to a 15° anteversion or retroversion angle in the femoral prosthesis (Wright Medical Technology 2010) and the S-ROM (DePuy Orthopaedics, Warsaw, Indiana) allows an offset of up to 20mm in an anterior-posterior direction by allowing a 30° anteversion or retroversion angle (DePuy Orthopaedics 2010). However, *in vivo* the range of anterior-posterior hip centre displacement may encompass a wider area due to the surgical placement of the acetabular cup.

Reference	Displacement (mm)			
	Medial	Lateral	Superior	Inferior
Wan et al. (2008)	19.1	4.4	15.8	8.6
Girard et al. (2006)	7.1	3.8	11.2	6.2
Bicanic et al. (2009)*	10	30	30	10

Table 12: Range of hip centre displacement measured in total hip arthroplasty patients. * Displacement of hip centre for the majority of patients in this study fell within specified range.

Clinical, experimental and analytical studies have been used to investigate the effects of displacing the hip centre, and poor positioning of the hip centre is correlated with loosening of either the femoral prosthesis or acetabular cup (Callaghan et al. 1985; Karachalios et al. 1993). Pagnano *et al.* (1996) looked at patients with a superior displacement of the hip centre of more than 15mm and found they had a higher likelihood of revision compared to those with no displacement, however Russotti and Harris (1991) found acceptable results with proximally displaced hips. Hirikawa *et al.* (2001) also found that hips displaced medially and superiorly had good clinical results and found poor results with a lateralised hip centre.

Mathematical analysis of the hip has shown that a medial displacement reduces the load across the hip and that a lateral displacement increases the joint contact forces (Bartel and Johnston 1969; Johnston et al. 1979; Iglic et al. 1993; Bicanic et al. 2009; Erceg 2009). Delp and Maloney (1993) looked at the effect on the moment and force generating capacity of the muscles and found that with a medial displacement there was a reduction in the muscle generating capacity of the abductor and adductor muscle groups but an increase with a lateral displacement. Johnston *et al.* (1979) and Lengsfeld *et al.* (2000) also predicted a reduction in resultant hip contact force with a 10mm medialisation of approximately 1BW. In general a superior displacement is considered to increase the load across the hip (Bartel and Johnston 1969; Johnston et al. 1979; Lengsfeld et al. 2000; Bicanic et al. 2009; Erceg 2009), however lateralisation

has been found to affect the forces more significantly than a superior displacement (Iglic et al. 1993; Bicanic et al. 2009). A posterior displacement has also been found to increase the hip contact force (Johnston et al. 1979; Lengsfeld et al. 2000), although Lengsfeld *et al.* (2000) found that with a straight leg the hip force was increased with anterior displacement. The analytical studies have investigated an area as large as a 60x60x60mm grid based around the natural hip centre (Johnston et al. 1979).

This study aims to compare the modelling process involving the musculoskeletal model and the finite element model with clinical and analytical studies of a displaced hip centre. The study then aims to establish a range of potential hip contact and muscle forces which could result from the displacement of the hip centre during hip arthroplasty. The strain and micromotion at the bone-implant interface are important indicators of the potential performance of the joint replacement (Huiskes 1993). A high strain at the interface between the bone and implant could indicate localised bone fracture or compromised primary stability and potentially loosening of the implant. The micromotion between the femoral component and the femur affects the ability of the bone to grow at the interface and provide a stable fixation.

7.2. Model

The musculoskeletal model described in section 5.1 was used with the kinematic and kinetic data collected from the Southampton healthy subject S1 (Table 6). As discussed above, the hip centre can be affected by the arthroplasty surgery by the placement of the acetabular cup, implant position or implant neck length. *In vivo* these factors can affect both the femoral offset and hip centre at the same time (Traina et al. 2009), however to separate the potentially compounding factors only the position of the hip centre was altered in the musculoskeletal model. The position of the hip centre node on the pelvis was moved to represent a displacement of the acetabular cup and the femoral neck length was maintained. The length and orientation of the femur were not altered and hence the whole leg was affected by the hip centre displacement (Figure 48). To maintain the relative position of the ground reaction force the position

of the force place was moved simultaneously to the hip centre. This produced the correct location of the centre of pressure relative to the hip (Figure 48). The muscle attachment points were not altered because the aim of the model was to allow surgically displaced hip centres to be modelled, and the muscle tension was maintained in each hip position by recalculating every muscle tendon length (Section 5.1.1).

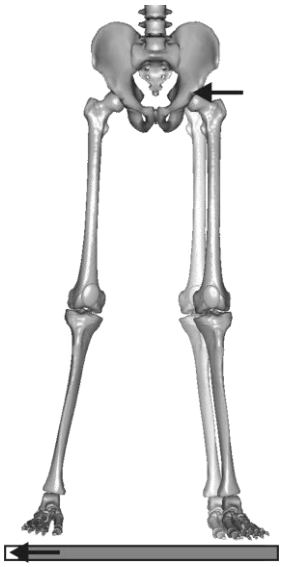

Figure 48: Example of a medially displaced hip and force plate in the AnyBody model without muscles.

This study has investigated a 10mm grid in a 40x40x40mm cube based around the original centre of rotation (Figure 49) derived from the positions found in clinical studies (Russotti and Harris 1991; Wan et al. 2008), the potential positions allowable in the modular prostheses (DePuy Orthopaedics 2010; Wright Medical Technology) and the ranges used in analytical studies (Lengsfeld et al. 2000; Bicanic et al. 2009). However some of the positions were discarded as they produced unfeasible solutions. In the unfeasible models some of the muscle activities were greater than one which shows a predicted muscle force larger than the muscle strength calculated in the model. The recruitment criterion minimises the activity of the muscles and a muscle force greater than its strength would only be predicted if the model calculated that more force was needed than the muscle's strengths would allow. Therefore these

models were discarded due to the model's inability to calculate a feasible solution. This removed region comprises an area with an anterior displacement of 20mm and an inferior displacement of 10mm or more and some of the surrounding positions (Figure 50).

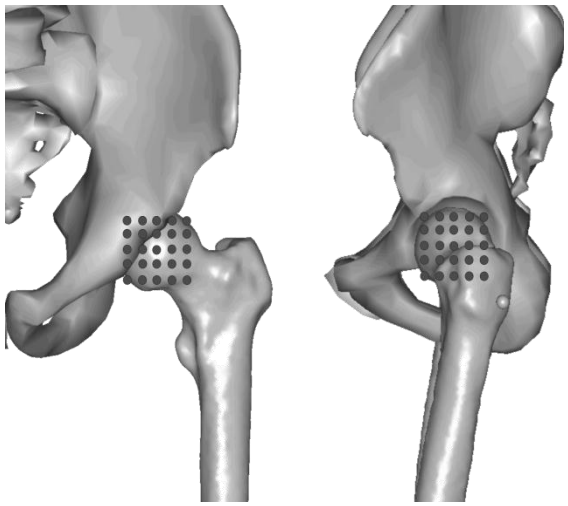

Figure 49: Approximate positions of hip centre in the displacement scenarios displayed in the coronal and sagittal planes

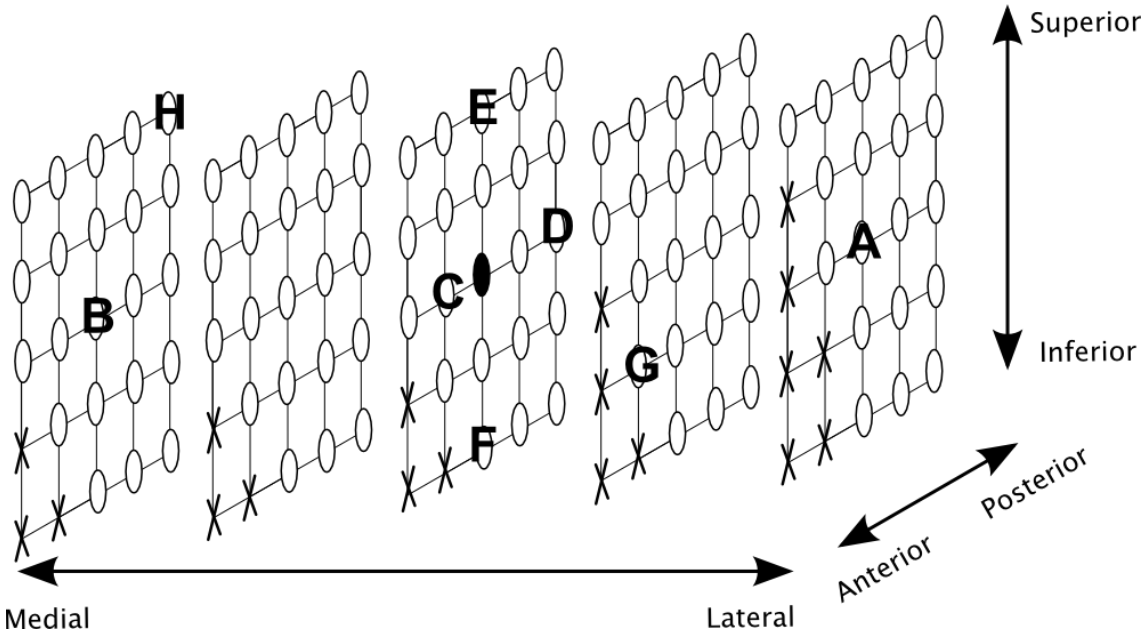

Figure 50: The modelled positions of hip displacement (○) and the discarded positions (X) and the baseline position (●) is at the centre. Six scenarios modelled in finite element analysis labled A-H.

Following the musculoskeletal investigation into the effect of the changing hip position a series of finite element analyses were performed on nine hip position scenarios. The scenarios chosen were the extreme displacement positions; six scenarios (Labled A-H, Table 13) with a maximum and minimum displacement in each plane, the scenario with the largest peak resultant hip contact force and the smallest and the baseline positions. The hip contact force and the relevant muscle forces were normalised relative to the body weight (BW) from the musculoskeletal model. The force vectors were then transformed to the coordinate system of the finite element model and applied as a function of the assumed body weight for the implanted model (Chapter 5.2.2). The swing phase was modelled in the musculoskeletal analysis and the forces at the hip were substantially lower in the swing phase compared to the stance phase. The comparison of healthy patients in chapter 6 found a larger variation in the micromotion during stance than swing phase and therefore a static analysis of each scenario was generated at 5% increments of the gait cycle through only the stance phase of gait from 5% to 65%. The strain and micromotion at the bone-implant interface were compared between the scenarios to investigate the effect on the lifetime of a cementless hip arthroplasty.

7.3. Results

7.3.1. Musculoskeletal analysis

Large resultant hip contact forces were found with the hip displaced by 20mm anteriorly despite removing the models with unfeasible solutions. The largest force was 6.0BW at 53% of gait cycle (just before toe off), with the hip displaced just 20mm in an anterior direction. The range of available displacement in the anterior direction was defined from less reliable sources compared to the displacement ranges for the lateral-medial and superior-inferior directions since it was not taken from *in vivo* studies. In addition, Delp and Maloney (1993) found in their study that a displacement of 20mm anteriorly did not fit within the anatomy of the pelvis. Therefore the hip displacement range of 10mm anterior to 20mm posterior displacement was considered for the remainder of this study. The range of resultant hip contact force was reduced

at toe off by approximately 1BW in the revised displacement area compared to the original region (Figure 51).

There was a larger range in force at the second peak in force, 52% of the gait cycle than the first peak, 11% of the gait cycle. The largest resultant hip contact force was with a displacement of 10mm anteriorly, 10mm inferiorly and 10mm laterally (4.9BW) and was 29% larger than that generated by the baseline model (3.8BW). The lowest resultant hip force at the second peak in the gait cycle was found when the hip was displaced by 20mm posteriorly, 20mm superiorly and 20mm medially (2.5BW) and was 34% lower than the reference model.

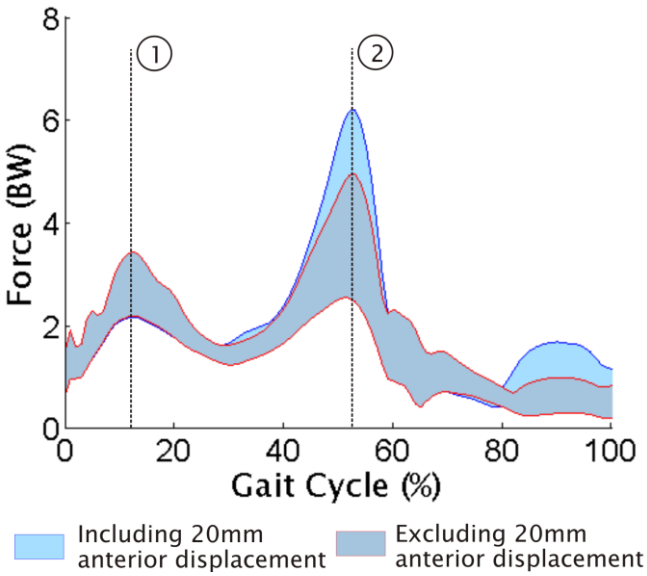

Figure 51: Range of resultant hip contact force as a result of hip centre displacement. First peak in force occurs at approximately 11% of the gait cycle (1) and second peak in force occurs at approximately 52% of the gait cycle (2).

In general the resultant hip force increased with lateral, inferior and posterior displacement at the first peak however at the second peak the resultant force increases with anterior displacement. Figure 52 shows the peak resultant hip contact force as the hip centre was displaced along two axes and held constant in the third, at both peaks in hip contact force. Hip centre displacement had a smaller effect on the hip force at the first peak compared to the second peak and the change was caused by a

combination of posterior and inferior displacement (Figure 52c). At toe off anterior displacement caused the largest change in hip force (Figure 52f). The effect of a posterior-anterior displacement on the hip contact force was dependant on the position in the gait cycle. At 11% of gait there was a small increase of approximately 0.1BW in the hip force with 20mm posterior displacement but at 52% of gait there was a larger increase in the hip force with a 10mm anterior displacement of approximately 0.5BW.

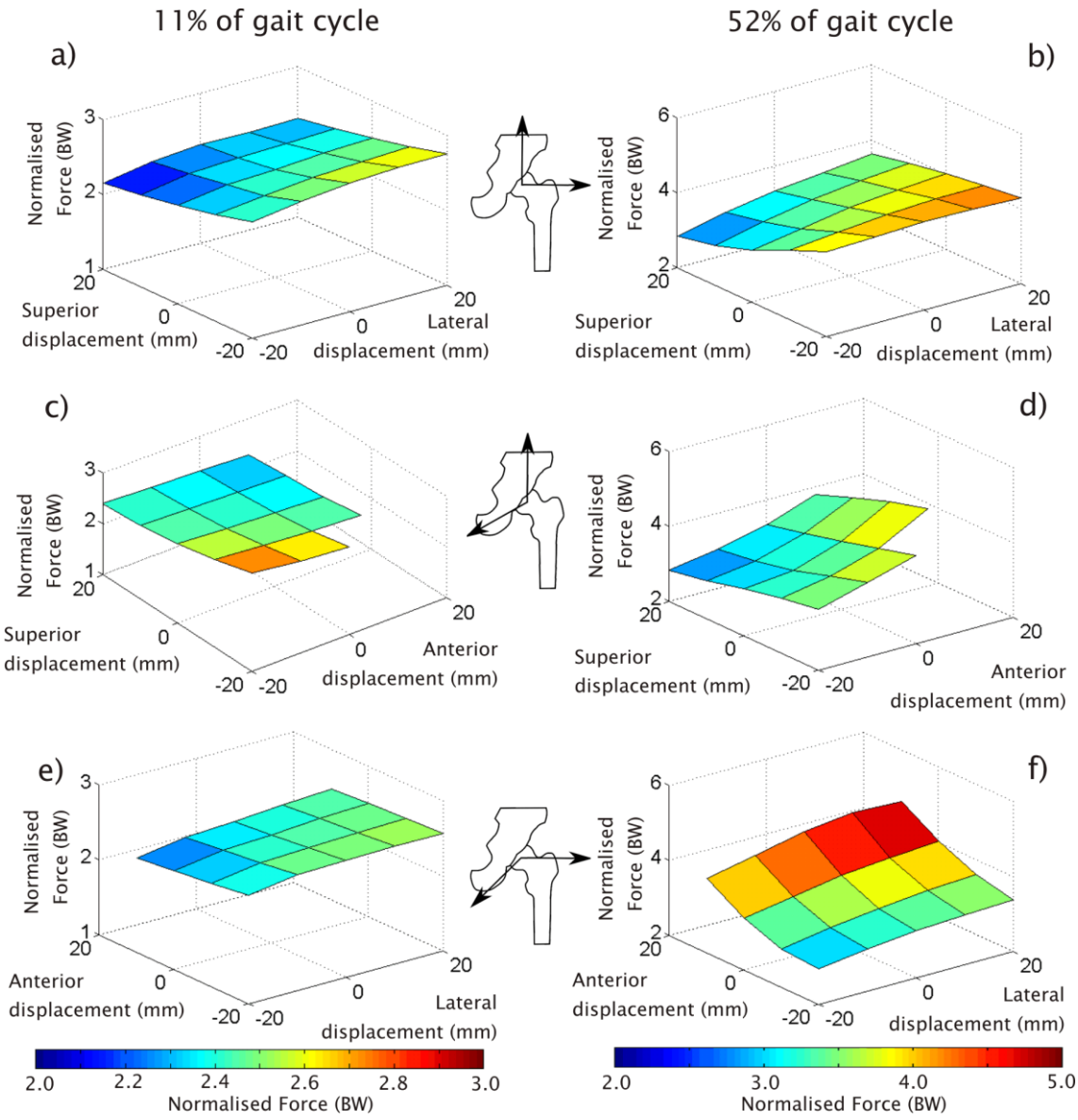

Figure 52: Resultant hip contact force at 11% (a, c and e) and at 52% of the gait cycle (b, d and f) due to displacement in superior and lateral directions a) and b), displacement in anterior and superior directions c) and d) and displacement in anterior and lateral directions e) and f).

Hip displacement did not affect the components of hip contact force equally and this resulted in changes to the angle between the resultant hip force and the y-axis through the femoral shaft. In the baseline model the hip force angle in the frontal plane was approximately 20° at the first peak in resultant hip contact force and 12° at the second peak in hip contact force in a medial direction. In the sagittal plane the

angle was affected by the relative magnitudes of the inferior-superior and the posterior-anterior hip force components. In the baseline model the sagittal plane angle was approximately 15° at the first peak in hip contact force, 15% of the gait cycle and 18° at the second peak in hip contact force, 50% of the gait cycle in a posterior direction. Lateralisation of the hip increased the lateral and inferior components of the hip force, however there was a much larger increase in force in the lateral component compared to the inferior component. Therefore there was an increase in the angle between the resultant force and the axis through the femur shaft in the frontal plane at both 15% and 50% of the gait cycle (Figure 53a and b). There was only a small increase in the anterior component of hip force with lateralisation and the hip force angle in the sagittal plane increased slightly at 15% of gait and reduced slightly at 50% of gait. Medialisation of the hip produced an opposite trend in the hip force angle although with a slightly larger magnitude. The maximum change in the sagittal plane was an increase of 3° due to a 20mm medial displacement at 50% of gait (Figure 53b) compared to a reduction of 10° in the frontal plane with a 20mm medial displacement at 15% of gait (Figure 53a).

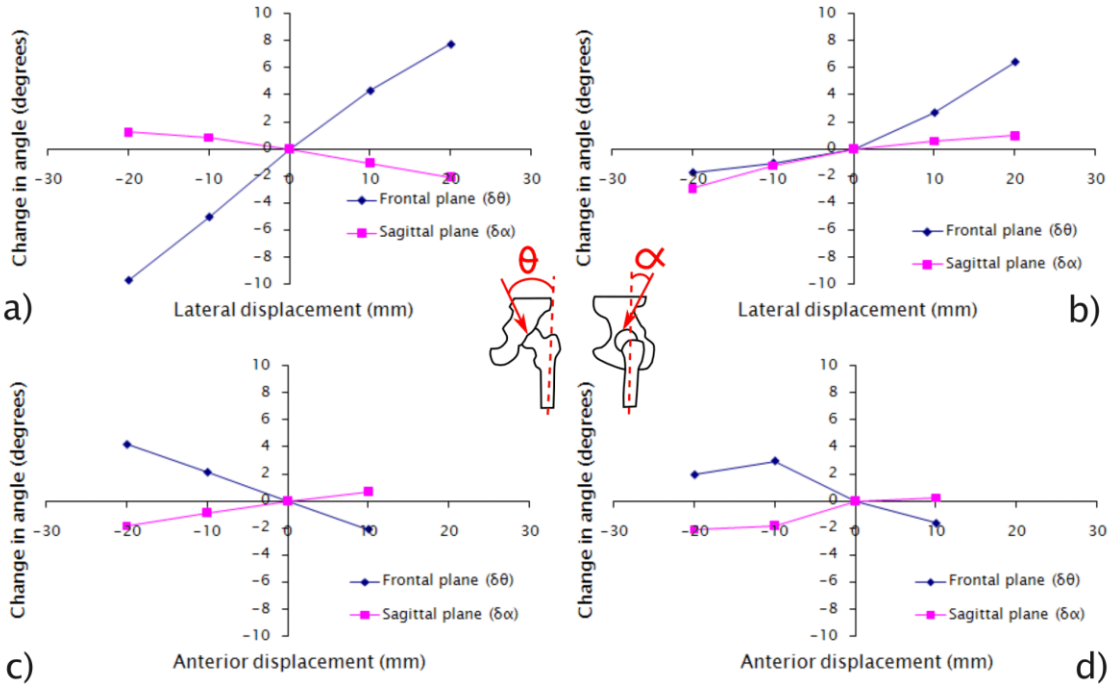

Figure 53: The change in hip force angle in the frontal (δθ) and sagittal plane (δα). a) lateral displacement at 15% of gait, b) lateral displacement at 50% of gait, c) anterior displacement at 15% of gait and d) anterior displacement at 50% of gait.

There was a smaller effect on the hip force angle in the frontal or sagittal planes with an anterior-posterior displacement. The lateral and inferior components of the hip force increased with a posterior displacement at 15% of gait although there was a larger increase in the lateral component and therefore the frontal plane angle increased (Figure 53c). At 50% of gait there was an 18% increase in the inferior component with a 10mm anterior displacement and negligible difference in the lateral component which resulted in a decrease in the frontal plane angle with anterior displacement (Figure 53d). The anterior component of hip force increased with anterior displacement in particular at toe off, however there was also an increase in inferior force due to anterior displacement. The reduction in sagittal angle due to a 10mm anterior displacement was less than a degree and there was only an increase of 2° with a 20mm posterior displacement at 50% of gait and a similar increase at 15% of gait.

The individual muscle forces calculated in the musculoskeletal model were combined into groups (Table 7). The combined force of the abductor muscles was also affected by the displacement of the hip centre and there was a range of more than 1BW at 15% and 50% of gait (Figure 54). The abductor force was reduced by medial, anterior and superior displacement. The lowest abductor force was with the hip centre displaced by 10mm anteriorly, 20mm superiorly and 20mm medially. At 15% of gait the peak force in this scenario was 0.94BW, which is 37% lower than the naturally positioned hip at toe off (1.5BW). The largest abductor force at toe off was with the hip displaced by 20mm inferiorly and 20mm laterally (2.28BW). There was also a large range in the combined muscle force from the flexor group at toe off of approximately 1BW (Figure 55).

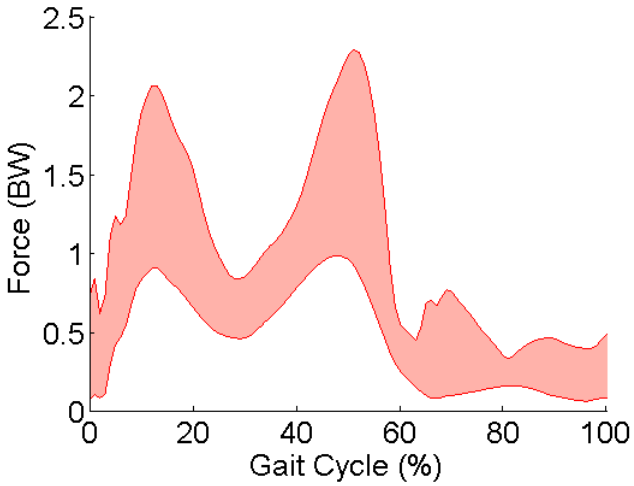

Figure 54: Range of abductor force as a result of hip displacement excluding the models with a hip displacement of 20mm anteriorly.

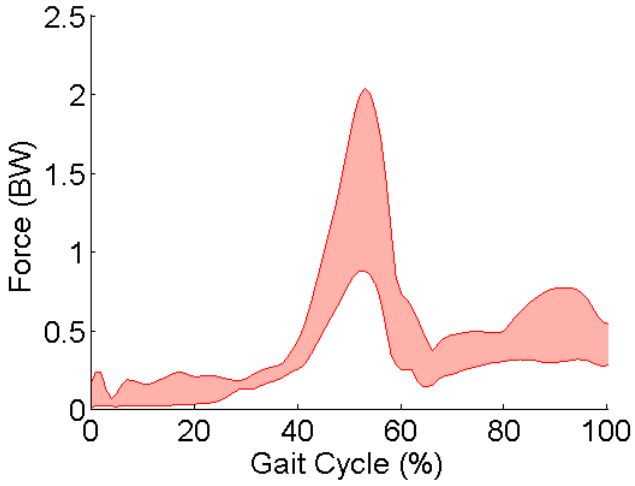

Figure 55: Range of flexor force as a result of hip displacements excluding the models with a hip displacement of 20mm anteriorly.

7.3.2.Finite element analysis

The hip contact and muscle forces from nine scenarios were applied to the finite element model (Table 13). The scenarios were chosen to represent the extremes of displacement applied to the musculoskeletal model. Scenarios A-F had the maximum displacement in only one direction whilst maintaining the baseline position for the other directions. Scenarios G and H were created using the musculoskeletal forces from the hip positions with, respectively, the largest and smallest resultant hip contact forces at the second peak in hip contact force, 50% of gait.

Scenario	Lateral displacement (mm)	Anterior displacement (mm)	Superior displacement (mm)	Resultant hip contact force (BW)	
				First peak	Second peak
Baseline	0	0	0	2.17	3.58
A	-20	0	0	1.96	3.20
B	20	0	0	2.26	3.90
C	0	10	0	2.10	4.10
D	0	-20	0	2.31	3.15
E	0	0	20	2.11	3.19
F	0	0	-20	2.30	3.97
G	10	10	-10	2.18	4.92
H	-20	-20	20	1.98	2.44

Table 13: The position of the hip in the finite element scenarios

The femoral implant is vulnerable to failure due to loosening at the bone-implant interface which can be caused by the bone exceeding its yield strength (Huiskes 1993). Bone can yield in tension with strains greater than 7800με (Kopperdahl and Keaveny 1998) and the percentage of elements with a strain greater than 7000με was used to compare the scenarios. The strain at the bone-implant interface was measured in all scenarios through the stance phase, 5-65% of gait. The range of mean interfacial strain over all the scenarios was larger at approximately 15% and 50% of gait (Figure 56a). The percentage of elements with a strain greater than the yield strength increased from just less than 1% in scenario H to more than 4% at toe off due the hip displacement in scenario G (Figure 56b). Micromotion at the implant-bone interface greater than 40μm reduces the likelihood of bone growth (Kadir and Kamsah 2009). At toe off, the percentage of bone elements at the interface with a micromotion greater 40μm peaked at 42%, in scenario G, compared to only 5% in scenario H (Figure 57b). The mean micromotion also peaked at 15% and 50% of gait and there was a larger range across the scenarios at 50% of gait compared to the rest of the stance phase (Figure 57a).

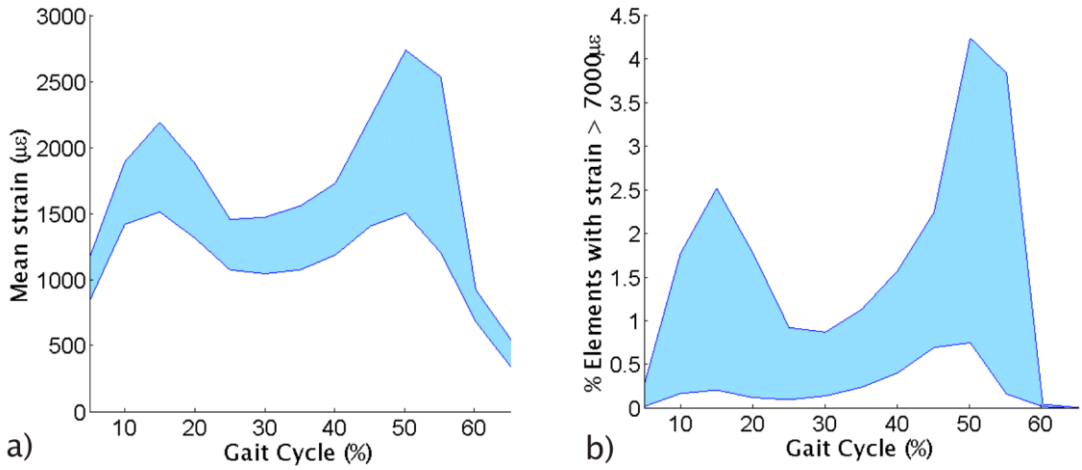

Figure 56: The range of strain at the bone-implant interface in the eight scenarios and the baseline model - a) mean strain b) percentage of elements with a strain greater than 7000με.

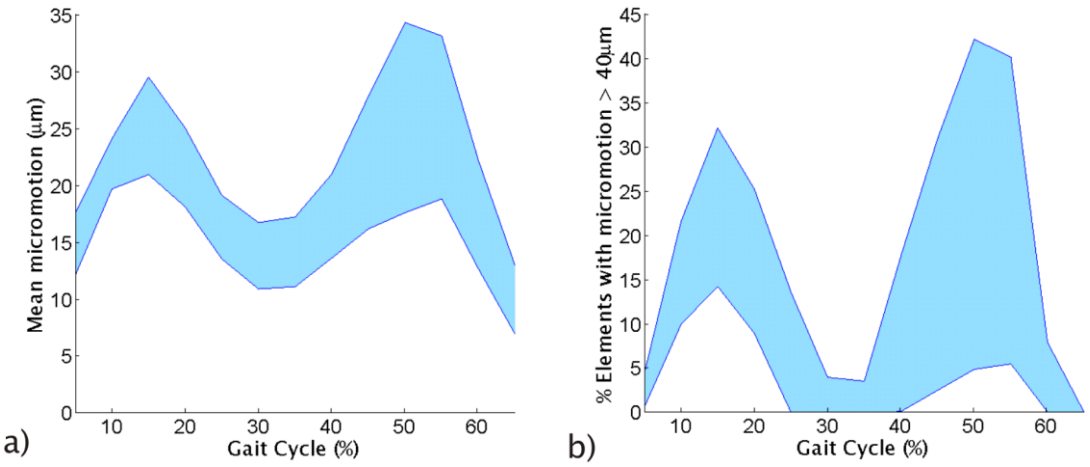

Figure 57: The range of micromotion in the eight scenarios and the baseline model – a) mean micromotion b) percentage of elements with a micromotion greater than 40µm.

The scenarios were compared over the stance phase by calculating the maximum strain and micromotion for each element between 5 and 65% of the gait cycle. The percentage of elements with a strain greater than 7000µε during the stance phase of gait was lower with a medially displaced hip than the baseline scenario (Figure 58). The laterally displaced scenario, anteriorly displaced scenario and inferiorly displaced scenarios had larger percentages of elements with a strain greater than yield than the baseline model. The medial-lateral displacement affected the strain in the elements more than displacement in either an anterior-posterior or inferior-superior direction. Displacing the hip by 20mm laterally (scenario B) increased the percentage of elements with a maximum strain over yield from 3% to 4.5%. However displacing the hip 10mm medially, 10mm anteriorly and 10mm inferiorly (scenario G) increased the percentage of elements with a strain over 7000µε to 5.2%. An increased percentage of high strain at the bone-implant interface reduced the strength of the fixation and can increase the likelihood of implant loosening. The micromotion at the interface also showed larger percentage of elements with micromotion over the threshold with lateralisation of the hip. The increased micromotion at the hip due to lateral, inferior and anterior displacement increases the risk of the bone failing to grow onto the surface and the implant loosening which would require revision surgery.

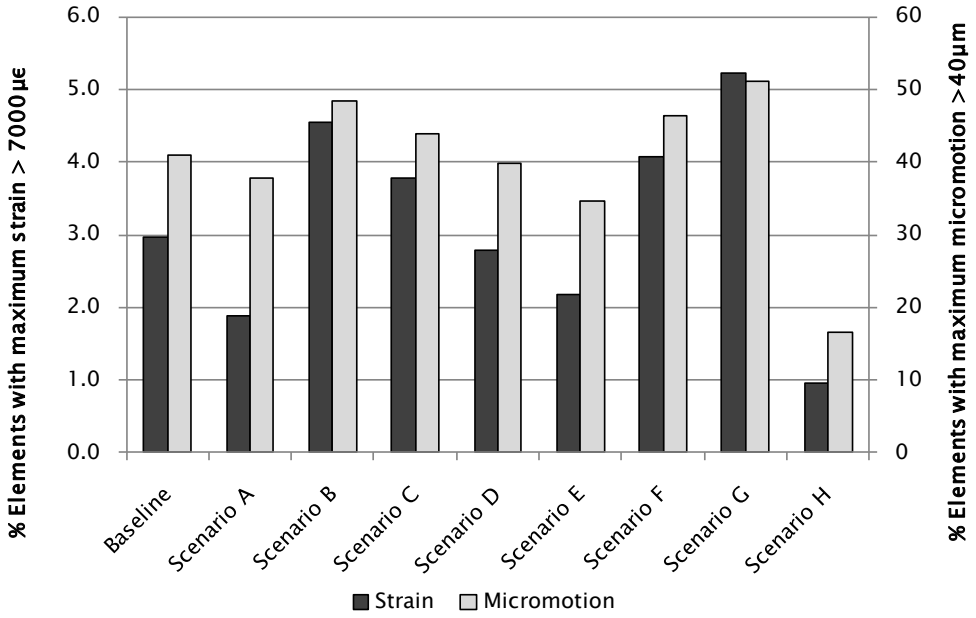

Figure 58: Percentage of elements with a maximum strain greater than 7000με and the percentage of elements a maximum micromotion greater than 40μm at the bone-implant interface during the stance phase of gait.

The strain and micromotion at the bone-implant interface were found to be proportional to the resultant hip contact force. The mean strain, mean micromotion, percentage of elements with a strain greater than 7000με and the percentage of elements with a micromotion greater than 40μm in each scenario at each time step in the stance phase was plotted against the resultant hip contact force (Figure 59).

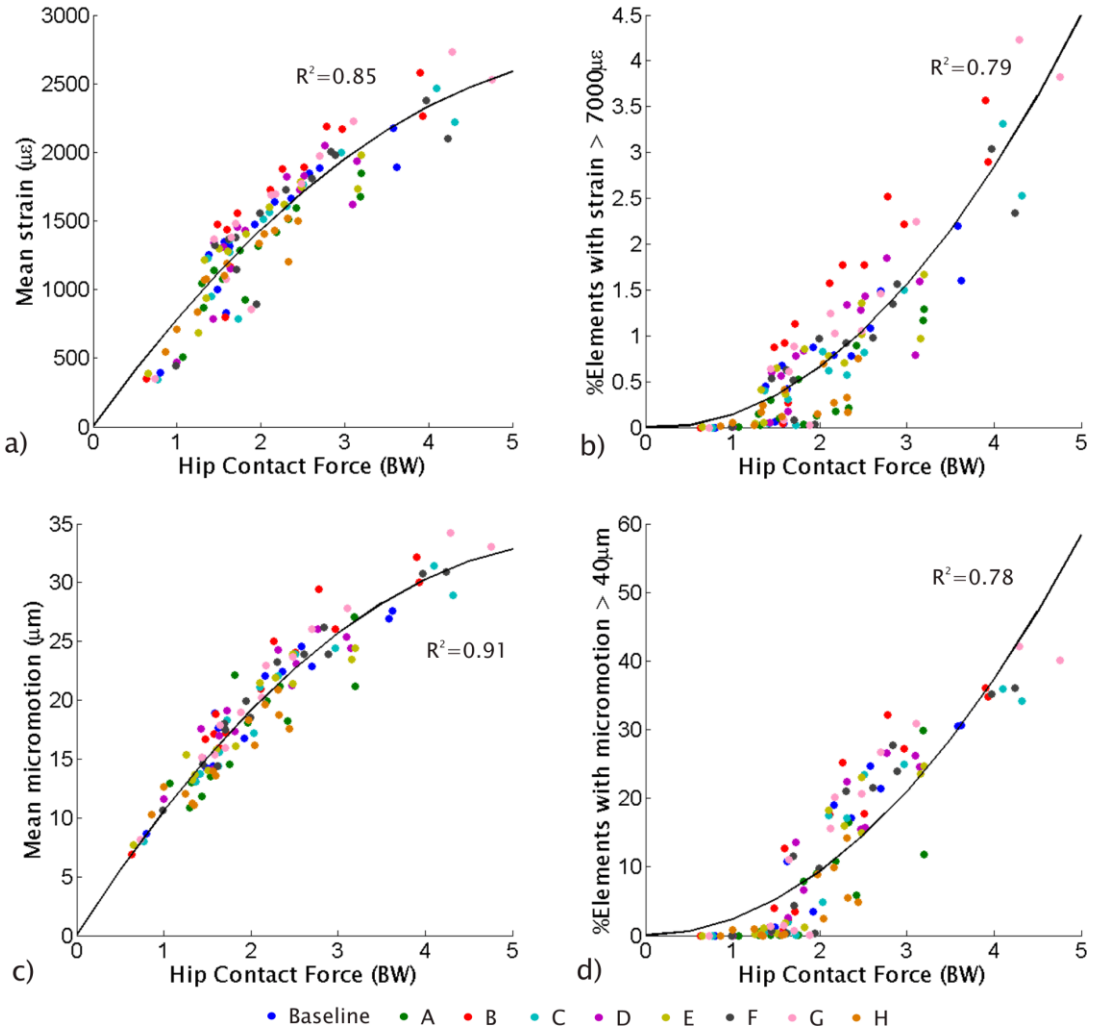

Figure 59: Correlation between hip contact force and a) mean strain at the bone-implant interface, b) percentage of elements with a strain greater than 7000με at the bone-implant interface, c) mean micromotion and d) percentage of elements with a micromotion greater than 40μm for each hip displacement scenario at each modelled time step.

An R-squared value of 0.91 was found for a second order polynomial relationship between the mean micromotion and the hip force. However the correlation between the percentage of elements with a micromotion greater than 40μm and the hip contact force was lower than with the mean micromotion and had an R-squared value of 0.78. The mean micromotion (*MMICRO*) and the percentage of elements with a micromotion greater than the threshold (*PMICRO*) both increased proportionally with the normalised hip contact force (*NHF*) (Equation 10 and Equation 11)

$$MMICRO = -NHF^2 + 11.57NHF \quad \text{Equation 10}$$

$$PMICRO = 2.33NHF^2 - 0.01NHF \quad \text{Equation 11}$$

The correlation between the strain at the bone-implant interface and the hip contact force also had a higher R-squared value with the mean strain (R^2=0.85) compared to the percentage of elements with a strain greater than 7000με (R^2=0.79). The mean strain (*MSTR*) and the percentage of elements with a strain greater than the threshold (*PSTR*) both increased with the normalised hip contact force (*NHF*) (Equation 12 and Equation 13)

$$MSTR = -6.67NHF^2 + 85.1NHF \quad \text{Equation 12}$$

$$PSTR = 0.19NHF^2 - 0.05NHF \quad \text{Equation 13}$$

There was a strong correlation between the resulting strain or micromotion and the hip contact force which indicates that the risk of failure of the interface increases with hip contact force.

7.4. Discussion

Clinical studies have found significant variability in the location of the hip joint centre (Girard et al. 2006; Wan et al. 2008; Bicanic et al. 2009) and several studies have found that this can affect the lifetime of a total hip arthroplasty (Callaghan et al. 1985; Karachalios et al. 1993). Analytical analysis and *in vivo* studies have found that a displacement of the hip centre from the natural position is likely to influence both the hip joint contact force and the surrounding muscle forces (Johnston et al. 1979; Russotti and Harris 1991; Hirakawa et al. 2001). Changes in the loads across the hip may affect the strain surrounding the implant and this could indicate the positions for the hip centre which may have a reduced lifetime.

7.4.1. Medial-lateral displacement

Analytical and musculoskeletal models have predicted that the hip force would reduce with medialisation of the hip and increase with lateralisation (Bartel and Johnston 1969; Johnston et al. 1979; Iglic et al. 1993; Lengsfeld et al. 2000). This model

calculated an increase in resultant hip contact force of approximately 0.3BW with a 20mm lateral displacement and a similar reduction in the hip force with a 20mm medialisation at toe off. However Lengsfeld *et al.* (2000) found approximately 1BW reduction with a 10mm medialisation of the hip with a flexed single leg stance. Johnston *et al.* (1979) found a reduction of approximately 1BW with a 10mm medialisation and approximately 2BW decrease in hip contact force with a 20mm medialisation at the second peak in hip contact. However Iglic *et al.* (1993) only found an increase in hip contact force of approximately 0.5BW with a 20mm lateralisation in one-legged stance. Current *in vivo* data (Bergmann et al. 2001) suggests that the hip contact would not be as large as the approximately 5.5BW predicted at the first peak in force by Johnston *et al.* and that their model may have been over-predicting the hip contact force. The model by Johnston *et al.* may have been more sensitive to small changes in the joint centre position due to the over prediction of the baseline hip contact force.

The change in abductor force due to lateral-medial displacement of the hip had a large effect on the hip contact force. Johnston *et al.* found more than 1BW decrease in the combined abductor force with a 20mm medialisation of the hip but Iglic *et al.* found a decrease in the abductor force of approximately 0.75BW and the combined abductor force in this study reduced by approximately 0.5BW with 20mm medialisation. Johnston *et al.* maintained the position of the femoral condyles and therefore with a medialisation of the hip they reduced the moment due to the ground reaction force and the force requirement for the abductors. In this study the whole leg and the position of the ground reaction force were displaced simultaneously by the same distance and therefore there was no relative change between them which would reduce the moment about the hip. Hence the required abductor force in this study was lower than in Johnston *et al.*'s study and may account for the smaller reduction in hip contact force due to medialisation of the hip.

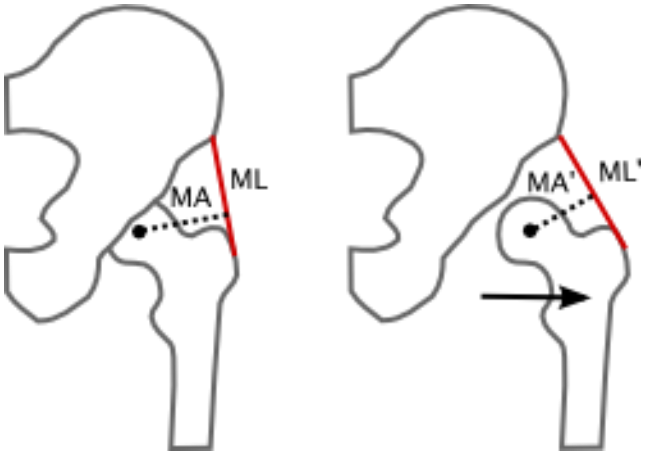

Figure 60: The effect of displacing the hip centre laterally on the muscle length (ML) and the moment arm (MA) of an abductor muscle.

Delp and Maloney (1993) found that the abductor muscles have a reduced moment arm (MA) with a lateralisation of the hip (Figure 60) and found that the adductor muscles had an increased moment arm with lateralisation. Lenaerts *et al.* (2009) also found that a lateral displacement of the hip decreased the abductor moment arms resulting in additional muscles being recruited which produced a larger abductor force and a larger, less vertically orientated, contact force. They found that with a lateral displacement of the hip, both the vertical and lateral components of hip force increased, however there was a larger increase in the vertical component resulting in a reduction in the frontal plane angle. They found the mean frontal plane angle to be 16.3° which is similar to the angle in this study of 20° at 11% of gait. Although both the vertical and lateral components of hip contact force increase with lateralisation as in Lenaerts *et al.*'s study there is a much larger increase in the lateral component of force compared to the vertical component and therefore the frontal plane angle increased with increasing lateralisation compared to their study where they found it reduced. They also found that the sagittal plane angle became more posterior with a lateralisation of the hip due to reduction in the anterior component of the hip contact force. The sagittal plane angle in this study became more posterior during double leg stance as the anterior component of the hip contact force reduced during double leg stance with lateralisation. However the anterior hip force component increased at the

peak in force during single leg stnace and therefore the angle increased with increased lateralisation. Although the trend for the change in sagittal angle is similar during double leg stance, the mean angle found in Lenaerts *et al.*'s study was a considerably smaller 2.7° compared to the 15° posteriorly of the femoral shaft axis predicted in this study at the peak in hip force during double leg stance. This study agreed that the abductor moment arms were reduced and as a consequence there was an increase in the abductor force predicted in the models with a lateralised hip. However the lateral component of force was increased substantially compared to the vertical component due to the abductor forces and therefore it was found that the hip joint angle in the frontal plane became more laterally orientated.

This study found a linear relationship between the hip contact force and the strain at the bone-implant interface. The laterally displaced hip scenarios were predicted to have higher hip contact forces and therefore higher strain along the interface than the medially displaced hip scenarios. High strain at the bone-implant interface increases the risk of revision surgery due to loosening of the implant (Huiskes 1993; Taylor et al. 1995). Micromotion calculated in this study was also found to increase with hip contact force and therefore increase with a laterally displaced hip position compared to a medial placement. Micromotion greater than 40μm has been found to reduce the likelihood of bone growth onto the implant (Kadir and Kamsah 2009) and therefore reduce the stability of the interface increasing the risk of loosening. The high micromotion and strain at the bone-implant interface predicted an increased risk in revision surgery due to loosening or reduction in primary stability with a lateral placement of the hip. Increased loosening has been found by clinical studies in laterally displaced hip replacements (Yoder et al. 1988; Georgiades et al. 2010).

7.4.2.Superior-inferior displacement

Mathematical studies have shown that the hip contact force increases with superior displacement of the hip or that it decreases with inferior displacement (Bartel and Johnston 1969; Johnston et al. 1979; Lengsfeld et al. 2000; Bicanic et al. 2009; Erceg

2009). The abductor muscles' moment arms have been predicted to decrease with superior displacement (Delp and Maloney 1993; Kiyama et al. 2009) and reduce the moment generating capacity (Delp et al. 1994). Superior displacement also reduces the length of the abductors which reduces the functionality of the muscles and increases the risk of dislocation (Jerosch et al. 1997). However this study has found an increase in the hip contact force with inferior displacement and a decrease in the force with superior displacement. The forces of the adductors, abductors and flexors collectively increased by approximately 0.9BW with a inferior displacement of 20mm however the hip contact force only increased by 0.4BW. The leg length was increased in Johnston et al's study, which predicted an increase in hip force with superior displacement, by maintaining the position of the femoral condyles. In this study the whole leg was displaced relative to the pelvis and the leg length was maintained by displacing the foot reaction force. Although superior placement of the hip has also been shown to increase the risk of revision (Pagnano et al. 1996), clinical studies have also found no adverse effects on the abductors (Dearborn and Harris 1999), no difference in the amount of wear generated by a superiorly displaced hip centre (Mackenzie et al. 1996; Wan et al. 2008) and that without a lateral displacement a superiorly displaced hip can have acceptable clinical results (Russotti and Harris 1991). Doehring *et al.* (1996) found that a superolateral displacement produced a significant increase in the hip contact force, however found no significant difference between hip force with a normal hip centre and either a 25mm or 37mm superior displacement using an experimental model. Iglic *et al.* (1993) also found only a slight change in the hip contact force as a result of inferior-superior displacement compared to the effect of medial-lateral displacement.

The high micromotion and strain at the bone-implant interface calculated in this study predict an increased risk in revision surgery due to loosening with an inferior placement of the hip. However it has been reported in some clinical studies that superiorly displaced hip replacements have an increased risk of loosening (Yoder et al. 1988; Georgiades et al.), although some studies have not found a change in the risk of

revision with superiorly displaced hip centres (Russotti and Harris 1991; Hirakawa et al. 2001). The strain and micromotion in the inferiorly displaced hip scenarios was found to be higher than that of the superiorly displaced hip scenarios due to the prediction of higher hip contact forces which have been found to have a positive correlation with the micromotion and strain.

7.4.3.Posterior-anterior displacement

Johnston *et al.* (1979) found a reduction in the hip contact force with anterior displacement at the peak in hip contact force during double leg stance. This study found a reduction in hip force with anterior displacement at 11% of gait but an increase in force with anterior displacement at 52% of gait. Lengsfeld *et al.* (2000) also found that the position of the hip affected the change in force due to anterior-posterior displacement. They considered both flexed and straight leg scenarios and found with a flexed leg there was a 4BW increase in the hip force with posterior displacement and a 0.4BW increase in the hip force with anterior displacement in the straight leg scenario. The straight leg scenario had a similar increase in force to that found in this study with anterior displacement scenario at the peak in hip force during double leg stance. Lengsfeld *et al.* (2000) also found the hip force angle increased in the sagittal plane by 1.5° with a 10mm medial displacement, 7° with a 10mm posterior displacement and increased by 2.5° with superior displacement. In the frontal plane they found an increase of 2° with a 10mm medial displacement, a 4° increase with a 10mm anterior displacement and less than 1° increase with a 10mm superior displacement. However, this study found the frontal plane angle increased by 2.7° with a 10mm lateral and by 2.9° with a 10mm posterior displacement at 52% of gait but there was no significant change with a superior displacement.

The change in hip contact force during single leg stance is largely affected by the flexor muscles, in particular the rectus femoris. The moment arm (MA) of the rectus femoris increases with a posterior displacement of the hip centre (Figure 61). The kinetics of the model were not changed and therefore a larger force was required to

provide the same torque with a smaller moment arm. This did not affect the heel strike portion of the gait cycle since the muscle was only used from toe off to flex the hip for the swing phase. Delp and Maloney (1993) found that the moment arm of the flexor muscles was reduced by anterior displacement.

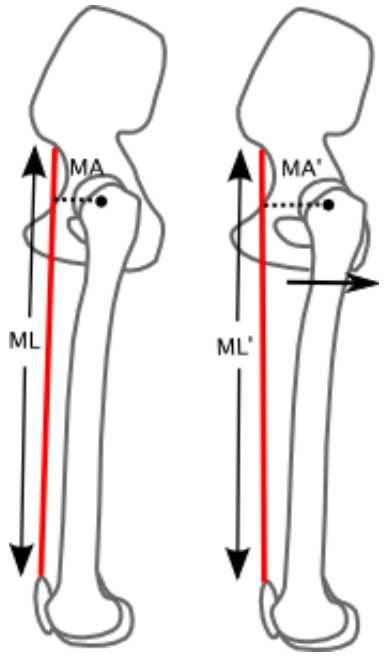

Figure 61: The effect of displacing the hip centre posteriorly on the muscle length (ML) and the moment arm (MA) of the rectus femoris.

One of the most common causes of revision for a cementless arthroplasty is dislocation (Kärrholm et al. 2008) and it often occurs in a posterior direction (McCollum and Gray 1990). An increase in the sagittal angle produces a force in a more anterior direction which reduces the likelihood of a posterior dislocation by increasing the force needed to produce a large posterior force. In this study a posterior displacement of the hip increases the anterior component of the hip contact force with respect to the inferior force which would reduce the likelihood of revision due to dislocation. In addition to a posteriorly orientated force increasing the risk of dislocation, it also increases the rotational force on the hip which can lead to loosening or micromotion which reduces the ability of the bone to form a stable fixation with the implant (Mjöberg et al. 1984; Harris et al. 1991; Nistor et al. 1991).

7.4.4.General discussion

A hip displacement of 10mm laterally, inferiorly and anteriorly from the baseline position was predicted using the musculoskeletal model to produce the highest peak hip contact force (4.92BW). However Johnston *et al.* (1979) found that the largest resultant force was approximately 6.5BW with the hip displaced 20mm laterally, 20mm superiorly and 10 posteriorly and the lowest peak hip contact force was with the hip displaced by 20mm medially, 20mm inferiorly and 10mm anteriorly. Delp and Maloney (1993) agreed with Johnston *et al.* that a inferior-medial positioning for the hip is important as it improves the moment generating capacity of the majority of the muscles. This study agreed that medial displacement the hip force reduced but found that the hip force was lowered with a 20mm posterior and superior displacement. Speirs *et al.* (2007) found that with the hip centre offset by 6mm medially, 2mm posteriorly and 4mm superiorly from the baseline there was no significant change in the peak hip contact force. They did find an anteversion angle of 11° increased the peak hip contact force by approximately 0.1BW. An anteversion of the femoral implant displaced the hip centre in a posterior direction however the femur and its muscle attachments would be moved anteriorly with respect to the centre of rotation. An anteversion of the hip replacement was not investigated in this study however a posterior displacement of the hip centre increased the resultant hip contact force during double leg stance in partial support of the findings reported by Speirs *et al.*

The output parameters for strain and micromotion of mean and percentage of elements over a threshold at the bone-implant interface were all found to have a strong correlation to the hip contact force. The relationship between the interface strain or micromotion and the hip contact force was strongly influenced by the large hip contact force. The relationship between the strain and micromotion and the hip contact force was also investigated in the healthy subject group (Chapter 6.2.2) and the correlations are similar, in particular the mean strain. Although at larger hip contact forces the healthy subject group predicted a higher percentage of strain and a larger mean micromotion (Figure 62).

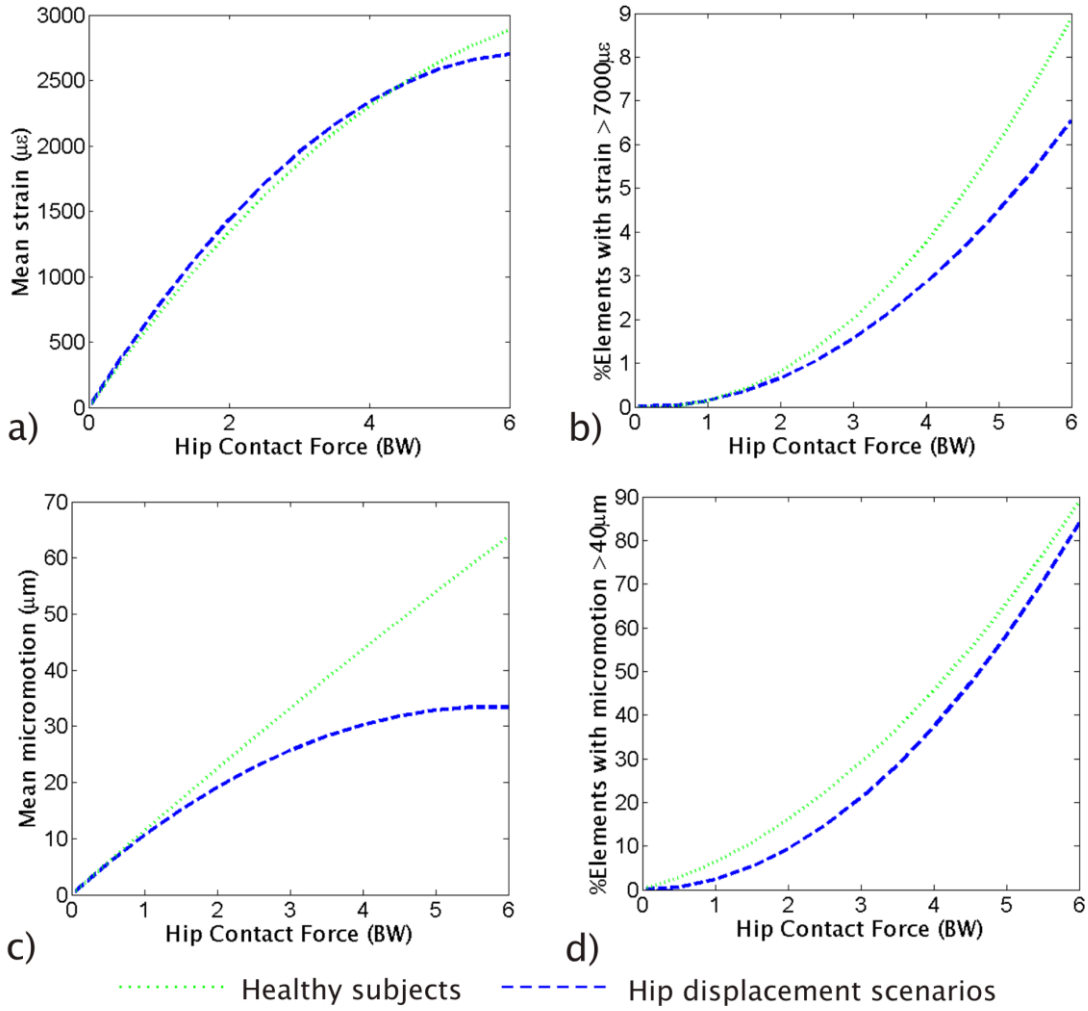

Figure 62: Relationships between hip contact force and the strain and micromotion at the bone-implant interface in the healthy subject group and the hip displacement scenarios.

This study has used the same kinematics and kinetics for each hip position scenario, an assumption made by Johnston *et al.* (1979) which may not reflect the gait pattern from a patient. However the analysis gave an indication of the potential effects of displacing the hip centre and the errors which could be associated with ignoring the variation in forces in a post hip arthroplasty patient. The abductor muscles in particular could have been affected by the alteration of the centre of hip rotation. Weak abductor muscles can cause a limp in the gait of the patient and thus the assumption to maintain the kinematic data may be invalid. The gait pattern affects the moments and forces and some studies have predicted that a displacement of the hip

affects the strength of the hip muscles (Delp and Maloney 1993; Vasavada et al. 1994). This study recalibrates the muscle tension in each muscle for each hip position scenario. However Delp and Maloney (1993) showed that retensioning the abductor muscles affected their strength, in one study they found the abductor muscle strength reduced by 44% with a 20mm superior displacement of the hip. However in a subsequent study by Vasavada *et al.* (1994) using the same model but retensioning the abductor muscles, they found that the abductor muscle strength was only reduced by 18% with a 20mm superior displacement.

There are physiological constraints on the hip centre positions due to the size and shape of the pelvis and some of the modelled hip positions produced over-activity in the muscles. However, it may have been due to the maintained kinematics which caused the over-activity. A THR patient with a displaced hip centre may alter their kinematics to compensate for the change in moment arms of the muscles and hence muscle strength as has been reported in some patients with reduced strength in selected muscles (Madsen et al. 2004). The over-activity predicted by the musculoskeletal model suggested that were these hip positions physiologically possible the kinematics would be required to change to allow the patient to walk.

7.5. Summary

This study agreed with mathematical and clinical studies that medial displacement of the hip centre would reduce the loads across the hip and reduce the risk of hip replacement revision compared to a laterally displaced hip. However this study found a reduction in resultant hip force with both superior and posterior displacements contrary to other studies. The centre of pressure has been maintained relative to the foot and the leg geometry has not been changed which affects the moments and subsequent forces on the hip. This study has also found that during double leg stance the largest peak force was with a posterior displacement and has shown that the point in the gait cycle affects the change in hip contact force by affecting muscle groups which can be active at different times during gait. Most studies have found that the

peak in hip contact force was during double leg stance and have used that peak in force to compare different scenarios. Clinical studies have found mixed results with superior placement of the hip (Russotti and Harris 1991; Mackenzie et al. 1996; Pagnano et al. 1996; Dearborn and Harris 1999; Wan et al. 2008) which indicates that a superior displacement of the hip may not be as straight forward a relationship as that predicted by previous mathematical models. The strains and micromotions predicted by this study were found to be largely dominated by the joint contact force. The study found that provided the hip joint contact force was modelled correctly the modelling procedure can produce a reasonable prediction of the primary stability of the hip stem and the other musculoskeletal forces may be of less importance.

8. Influence of surgical approach on the kinetics and musculoskeletal forces at the hip and the subsequent primary stability of a cementless hip stem

8.1. Introduction

Hip arthroplasty surgery divides and damages some of the soft tissues surrounding the hip to allow access to the joint. Different surgical techniques allow the hip to be approached from a variety of angles which leads to different levels of damage in a range of soft tissues. The most frequently used techniques are the posterior and lateral approaches although a small number of hip arthroplasty surgeries are conducted using an anterolateral or anterior approach (National Joint Registry 2009).

The main criticism of the posterior approach is the increased risk of dislocation (Robinson et al. 1980; Woo and Morrey 1982; Vicar and Coleman 1984; Hedlundh et al. 1995; Parks and Macaulay 2000; Zimmerman et al. 2002) but the abductor function is better (Whatling et al. 2008) and there is a lower likelihood of a postoperative limp (Masonis and Bourne 2002). Robinson *et al.* (1980) found that dissection of the hip external rotators, which occurred during the posterior surgical approach, affected the likelihood of dislocation and that the risk of dislocation was reduced by reattaching them. During a posterior approach the major muscle affected by the surgery is the gluteus maximus and in general the gluteus medius is not compromised (Berry et al. 2003). However, in a study by Meneghini *et al.* (2006) damage to the gluteus medius and minimus was found in both the minimally invasive surgery (MIS) lateral and posterior approaches. The posterior approach has been found to have a larger range of motion than the lateral approach (Whatling et al. 2008) and despite the greater chance of dislocation the posterior approach provides better post-operative hip function (Zimmerman et al. 2002).

There are various lateral approach techniques but regardless of the modification to the original technique they all affect the gluteus medius and minimus and increase the likelihood of a postoperative limp (Masonis and Bourne 2002). However, some studies have found no difference in abductor function between the posterior and lateral approaches (Downing et al. 2001). There are also studies which have found no functional differences between anterior and lateral approach patients once they are fully healed (Pospischill et al. 2010; Restrepo et al.), although the speed of recovery maybe different between the approaches (Mayr et al. 2009; Restrepo et al.). The lateral approach has also been found to have the lowest risk of dislocation compared to the other approaches (Masonis and Bourne 2002).

The incision for the anterior approach is made through the anterior tensor fascia latae and can result in additional damage to the rectus femoris, gluteus minimus and minimal damage to the gluteus medius and in some cases the piriformis is transected (Meneghini et al. 2006). The anterolateral approach has been found to have a smaller range of motion than the posterolateral approach which resulted in an abnormal gait pattern (Madsen et al. 2004).

Muscle laceration can result in a reduction in the maximum force the muscle can produce, defined as the muscle strength, even after the muscle has been allowed to heal (Section 2.3.4). Muscles regain approximately 60% of their original strength after partial laceration (Garrett et al. 1984) but, due to the difficulty in isolating the force produced in a single muscle, there is a lack of data to quantify a relationship between the amount of muscle damage and resulting healed muscle strength. The muscles damaged during total hip arthroplasty are not all lacerated but in some cases divided along the lines of muscle fibres. However, the surgical approach can reduced the strength of some of the muscles, in particular, the abductors can be affected by the lateral approach (Baker and Bitounis 1989). The Trendelenburg test is used to assess the abductor muscle weakness at the hip and a positive test indicates muscle weakness. Lateral approach patients have been reported to have a greater chance of a

positive Trendelenburg test than posterior approach patients (Baker and Bitounis 1989) and of a limp due to abductor weakness (Masonis and Bourne 2002). However, Downing *et al.* (2001) found no significant differences in abductor strength between the lateral and posterior approaches. Currently only a study by Heller *et al.* (2003) has used a musculoskeletal model to investigate the influence of surgery on the magnitude of the muscle and joint contact forces across the hip and their study modelled separate patients which added patient variation to the comparison between the models.

The type of surgical approach used has also been associated with variation in the level of bone loss around hip prostheses (Perka et al. 2005) and bone loss can be affected by the strain level since bone remodelling is affected by the loads through the bone. Finite element models have been used to examine the effect a hip arthroplasty procedure has on the implanted femur (Hung et al. 2004; Speirs et al. 2007). Muscle forces are altered during arthroplasty surgery and using gait analysis, studies have compared the gait patterns in post-operative patients. However it is not clear whether the gait is affected by the surgical approach (Madsen et al. 2004; Whatling et al. 2008).

This study has conducted two investigations comparing the differences between the surgical approaches. The first investigation altered a musculoskeletal model to simulate the potential loss of strength in specific muscles due to different total hip arthroplasty surgical approaches. Three different approaches were modelled; posterior, anterior (Smith-Petersen) and lateral. The approaches were modelled by simulating damage in the muscles and the specific muscles which were damaged in the models were based on the recorded muscles damaged during minimally invasive surgery and traditional surgery (Hardinge 1982; Meneghini et al. 2006). However, the level of damage modelled was the same proportion in each muscle regardless of the level of damage which may occur during minimally invasive or traditional surgery. The second investigation compared musculoskeletal models generated for THA patients who underwent either a posterior or lateral surgical approach. The musculoskeletal forces from all the models in both studies were subsequently applied to the finite element

model to compare the strain distribution and micromotion at the bone-implant interface. The first study was used to investigate the potential for the modelling technique, combining altered musculoskeletal models using generic kinematic and kinetic data and finite element models, to predict an influence on the outcome of hip arthroplasty due to surgical approach. The second study was then conducted to provide some verification for whether there are appreciable differences between the surgical approaches and whether the modelling process had correctly identified any trends.

8.2. Musculoskeletal simulation of three total hip arthroplasty surgical approaches

A baseline musculoskeletal model was generated using the healthy gait analysis data set S1 (Chapter 5.1.2). Three surgical approach scenarios were then created by modifying the baseline model to simulate the potential reduction in strength in specific muscles due to a total hip arthroplasty. Literature studies have found that lacerated muscles do not recover their original strength after they have healed (Garrett et al. 1984). However, muscles damaged during surgery are often divided along the muscle fibres rather than cut across their muscle belly and the effect of this type of damage to the muscle strength is unknown. Therefore, this study assumed that all surgically affected muscles in the simulated arthroplasties had an equal percentage reduction in their muscle strength. This study aimed to investigate the maximum potential damage at the hip and hence largest potential change in the forces across the hip. Altering the muscle strength provided an indirect method of affecting the force the muscle was able to produce in the musculoskeletal model. The model used a muscle recruitment criterion based on minimising the sum of the squared muscle activities (Chapter 5.2.1). The muscle activity was calculated in the model as the muscle's force normalised by the muscle's strength and therefore the muscle force is reduced by the modelling process during the muscle recruitment procedure.

Each surgical approach was modelled in one leg of the model by reducing the muscle strength of the muscles which were reported in the literature as damaged during surgery (Hardinge 1982; Meneghini et al. 2006). The ultimate strength of the damaged muscles was reduced to 60% based on the strength of muscles after healing measured in the literature (Garrett and Duncan 1988; Crow et al. 2007) (Chapter 2.3.4). Table 14 lists the muscle units which were modelled as damaged in the three scenarios and the original strength of the muscle units in the baseline model.

Muscle name (no. of muscle units)	Baseline Strength (N)	Smith-Petersen	Posterior	Lateral
Gluteus medius (anterior) (6)	260.9	60%	60%	60%
Gluteus medius (posterior) (6)	418.6	60%	60%	60%
Gluteus minimus (anterior) (1)	413.1	60%	60%	100%
Gluteus minimus (middle) (1)	334.6	60%	60%	100%
Gluteus minimus (posterior) (1)	305.7	60%	60%	100%
Gluteus maximus (superior) (6)	342.2	100%	60%	100%
Gluteus maximus (inferior) (6)	154.9	100%	60%	100%
Piriformis (1)	334.6	100%	60%	100%
Tensor fasciae latae (2)	181.8	60%	100%	60%
Rectus femoris (2)	596.9	60%	100%	100%
Vastus lateralis (inferior) (6)	73.7	100%	100%	60%
Vastus lateralis (superior) (2)	1218.6	100%	100%	60%

Table 14: The muscle units altered in the musculoskeletal surgical approach scenarios and their individual strengths. In the surgical approach scenarios the strength is given in percentage of control strength.

Fourteen finite element analyses were performed for each surgical scenario at intervals of 5% over the stance phase of gait from 0% to 65%. The forces predicted by the musculoskeletal model for the muscles attached to the proximal femur and the hip contact forces were calculated for the specific time step using linear interpolation. The forces from each of the three scenarios were normalised to the assumed body weight (BW) of 84.7kg.

8.2.1.Results

The resultant hip contact force shows little difference in the magnitude of force across the hip due to the different surgical scenarios except for the lateral approach which resulted in an increase of 12% at 11% of the gait cycle. Over the whole gait cycle the root-mean-square (RMS) of the resultant hip contact force was increased by 5% in the lateral approach scenario compared to the baseline model. The lateral approach had increased anterior-posterior and inferior-superior hip force components during double leg stance compared to the other scenarios and the baseline (Figure 63). All the scenarios had a slightly increased hip contact force during single leg stance compared to the baseline model.

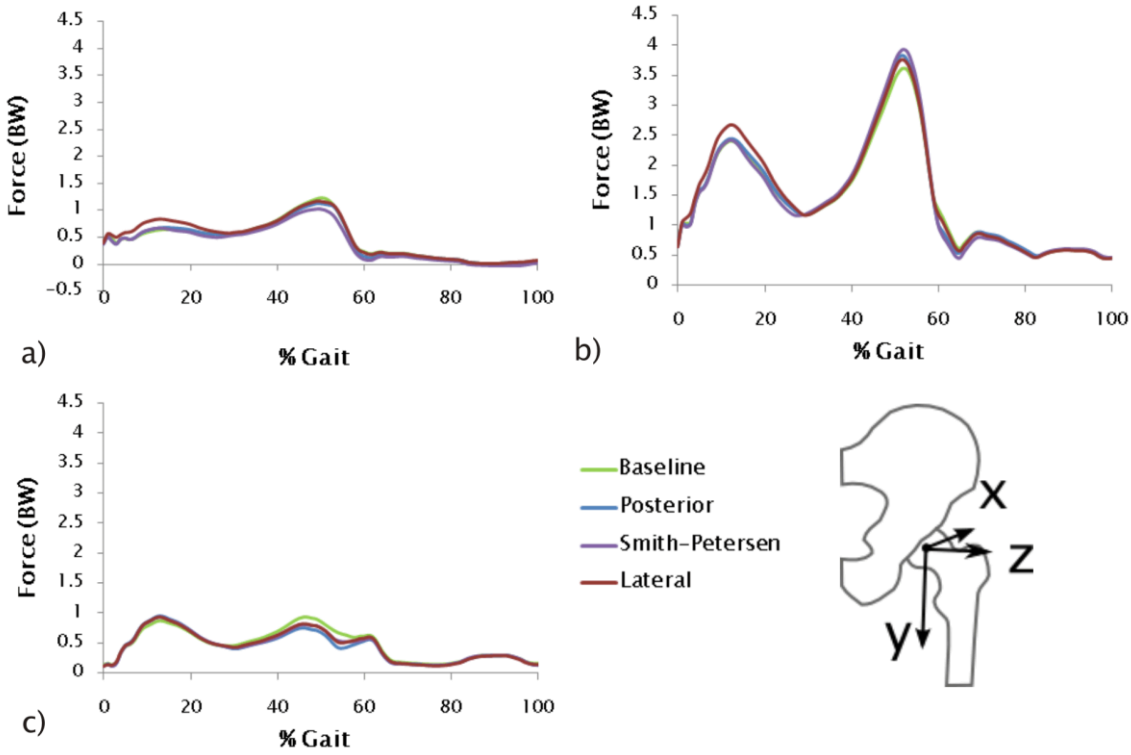

Figure 63: The force components of the hip contact force for the three surgical approach scenarios and the baseline model. a) Fx, b) Fy and c) Fz.

To compare the effect of the modelled scenarios on the muscles, individual muscle forces were combined into groups. The largest differences between the scenarios were found in the abductor group and in the flexor group at toe off (Figure 64). During single leg stance all of the surgical approach scenarios had a lower abductor force than

the baseline model, however, during double leg stance both the lateral and the Smith-Petersen scenarios had a larger abductor force than the baseline model by 10% and 5% respectively. The posterior scenario had a lower abductor force throughout the stance phase resulting in a reduction of 11% in the RMS over the whole gait cycle. Due to the lower force during single leg stance there is also an overall reduction in the abductor force with the Smith-Petersen scenario. This was caused by a reduction in the strength of the gluteus medius, minimus and in the case of the posterior approach, the gluteus maximus superior. There was an increase in the combined flexor force for all the scenarios compared to the baseline, with the largest increase, of 14%, in the posterior approach.

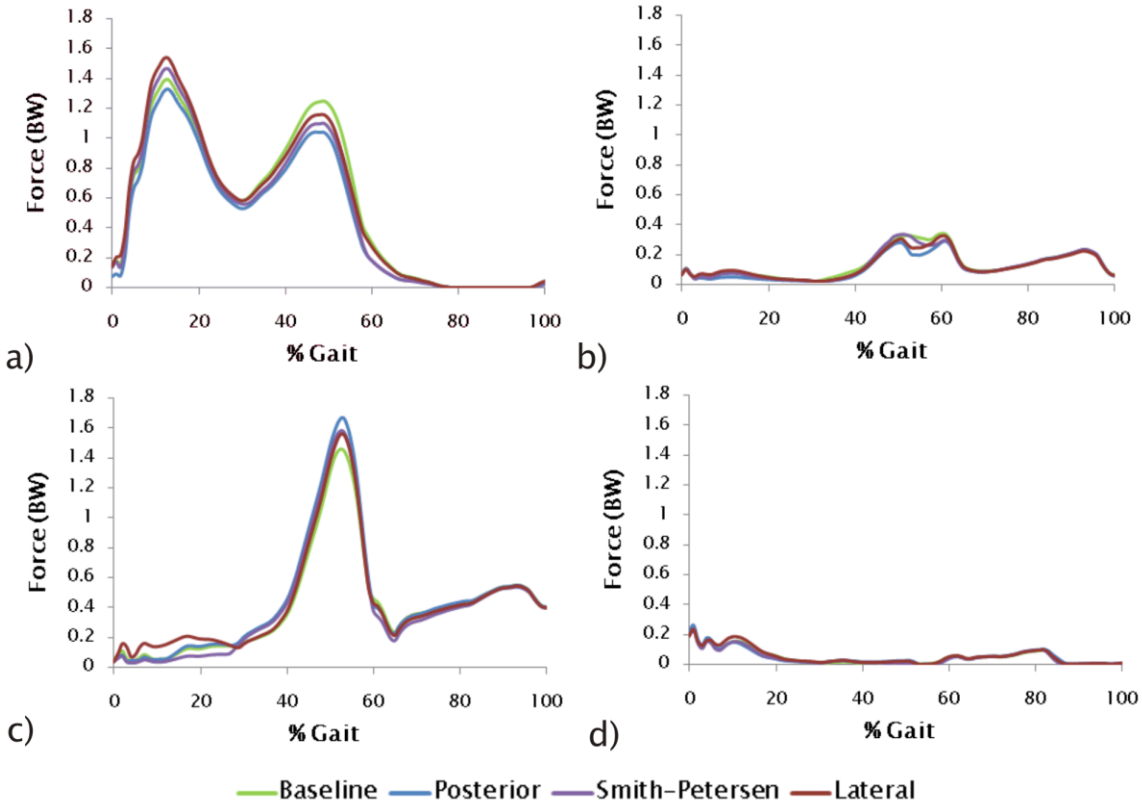

Figure 64: The combined force from each muscle group for the three scenarios and the baseline model. a) abductors, b) adductors, c) flexors and d) extensors.

There was an increase of 9% in the mean strain at the bone-implant interface in the lateral scenario, although the differences between the surgical approach scenarios and the baseline model were only slight (Figure 65a). However the percentage of elements

with a strain greater than 7000με was increased by 31% in the posterior model at 15% of gait (Figure 65b). The Smith-Petersen scenario had a larger percentage of elements which had a strain greater than 7000με during the gait cycle with a total of 3.2% compared to only 3% in the baseline model.

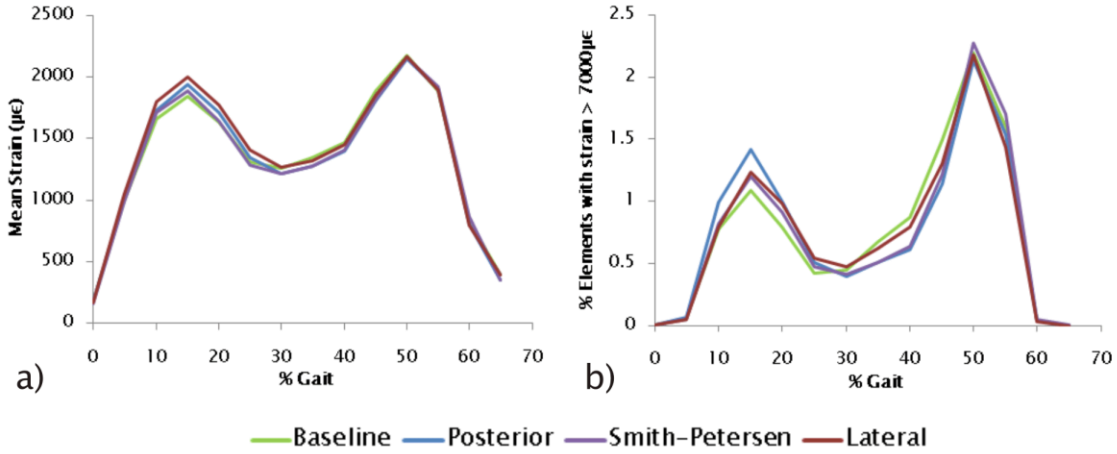

Figure 65: Strain at the bone-implant interface during the stance phase of gait for all three surgical approach scenarios and the baseline model. a) mean strain and b) the percentage of elements with a strain greater than 7000με.

There were only slight differences in the mean micromotion, similar to the differences between the scenarios' mean strain (Figure 66a). The lateral scenario had an increase in the percentage of elements with a micromotion greater than 40μm of 22% compared to the baseline model (Figure 66b). Both the Smith-Petersen and the lateral approach scenarios had a larger percentage of elements with a micromotion greater than 40μm during the gait cycle.

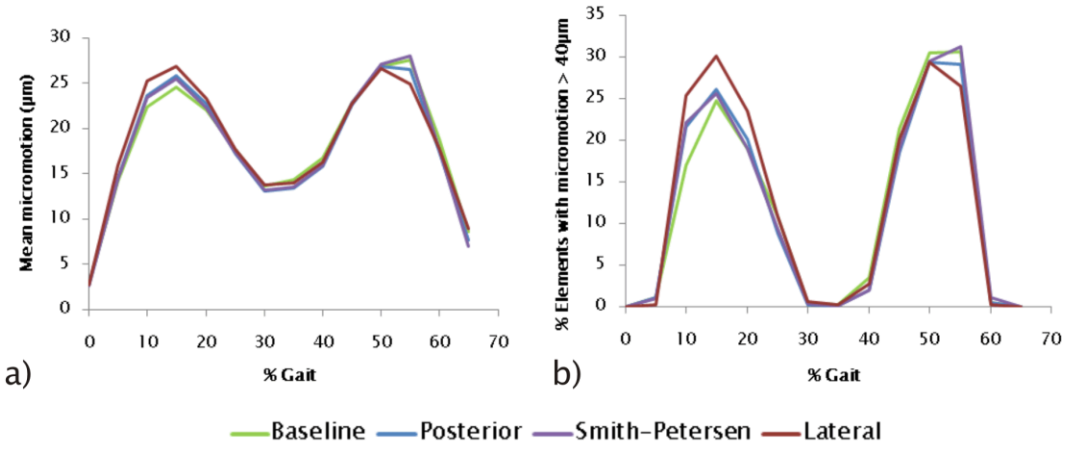

Figure 66: Micromotion at the bone-implant interface during the stance phase of gait for all three surgical approach scenarios and the baseline model. a) mean micromotion and b) the percentage of elements with a micromotion greater than 40µm.

8.3. Patient specific surgical approach models

In the second investigation six gait analyses from THA patients were used to create musculoskeletal models (Holt and Whatling 2009). Three of the patients had undergone a lateral approach (L01-03) and the other three had gone through a posterior approach (P01-03), however only one of the posterior approach patients had a full gait cycle recorded and the other two were missing the final 20% of their gait cycles. Six patient-specific finite element analyses were performed at intervals of 5% over the stance phase of gait from 0% to 65%. The musculoskeletal forces were normalised to the patient's body weight and then transformed to the finite element model which had an assumed body weight of 84.7kg (Chapter 5). Five of the patients had undergone THA on their right hip and their forces were transformed to the left joint so they could be applied to the finite element model of a left femur. The range of force, strain and micromotion was calculated for each surgical approach and compared to the results from the healthy gait subjects presented in Chapter 6.

8.3.1.Results

Joint angles and torque were calculated in the musculoskeletal models from the optimised marker positions for each model. The THA patient groups had a smaller range of flexion-extension angle because although they had a similar peak flexion angle they did not have as large an extension angle (Figure 67a). The posterior approach group had a larger range of flexion-extension angle compared to either the lateral group or the healthy group, despite the healthy group containing nine subjects instead of the three in each of the THA patient groups. The posterior group had the largest flexion angle of 43° although the lateral group had a maximum flexion angle of 40°, however the THA patient groups only had very small maximum extension angles of 6° and 4° respectively. The healthy group had a maximum flexion angle of 34° and a maximum extension angle of 21° making the variation in the healthy group larger than either of the THA groups.

The abduction-adduction angle was similar across all three groups (Figure 67c and d). The healthy group had a maximum abduction angle of 14° and the posterior and lateral groups had similar maximum abduction angles of 10° and 14° respectively. The THA groups had slightly lower maximum adduction angles, of 9° and 8° for the posterior and lateral groups respectively, compared to 12° for the healthy group. The healthy group had a large variation in external-internal rotation angle as discussed in Chapter 6, however the range measured for the two THA patient groups extended into more internal rotation than the healthy group, in particular the lateral group had a larger internal rotation during toe off and the early part of the swing phase (Figure 67e and f). The maximum external rotation angle in the healthy group was 29° compared to the maximum of 3° in the posterior group and only internal rotation of the hip in the lateral group. However the lateral group had the largest maximum internal rotation angle of 26° compared to 19° in both the healthy and posterior groups.

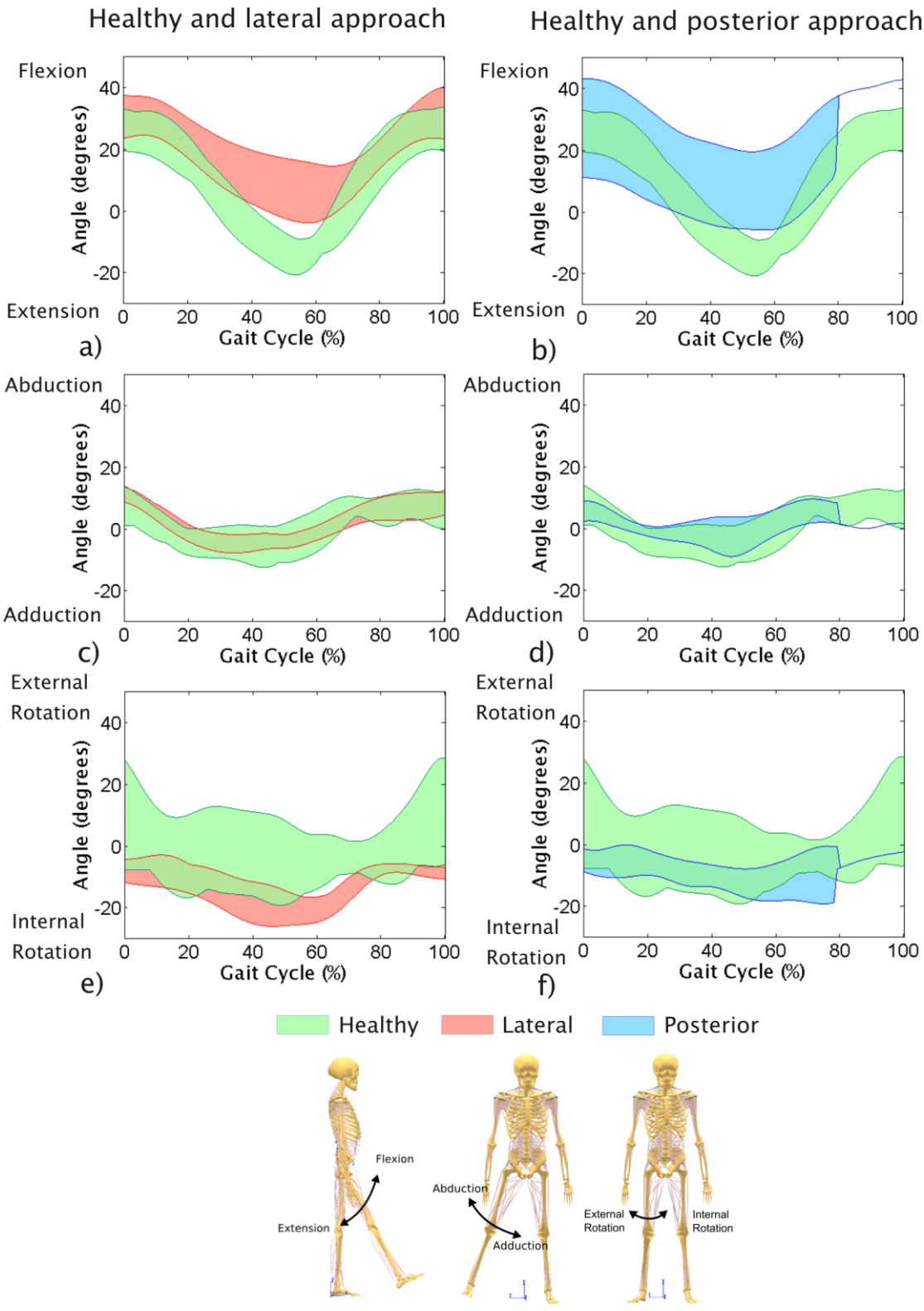

Figure 67: The range of hip joint angles through the gait cycle in the two THA patient groups and the healthy group.

There was a smaller range of torques in the THA patient groups compared to the healthy group however the torque measured in the THA patients fell within the range measured by the healthy group (Figure 68). The abductor and internal rotation torque were at the upper boundary of the range measured by the healthy group and the abduction-adduction torque measured for both the THA patient groups had a smaller range between maximum and minimum flexion-extension torque.

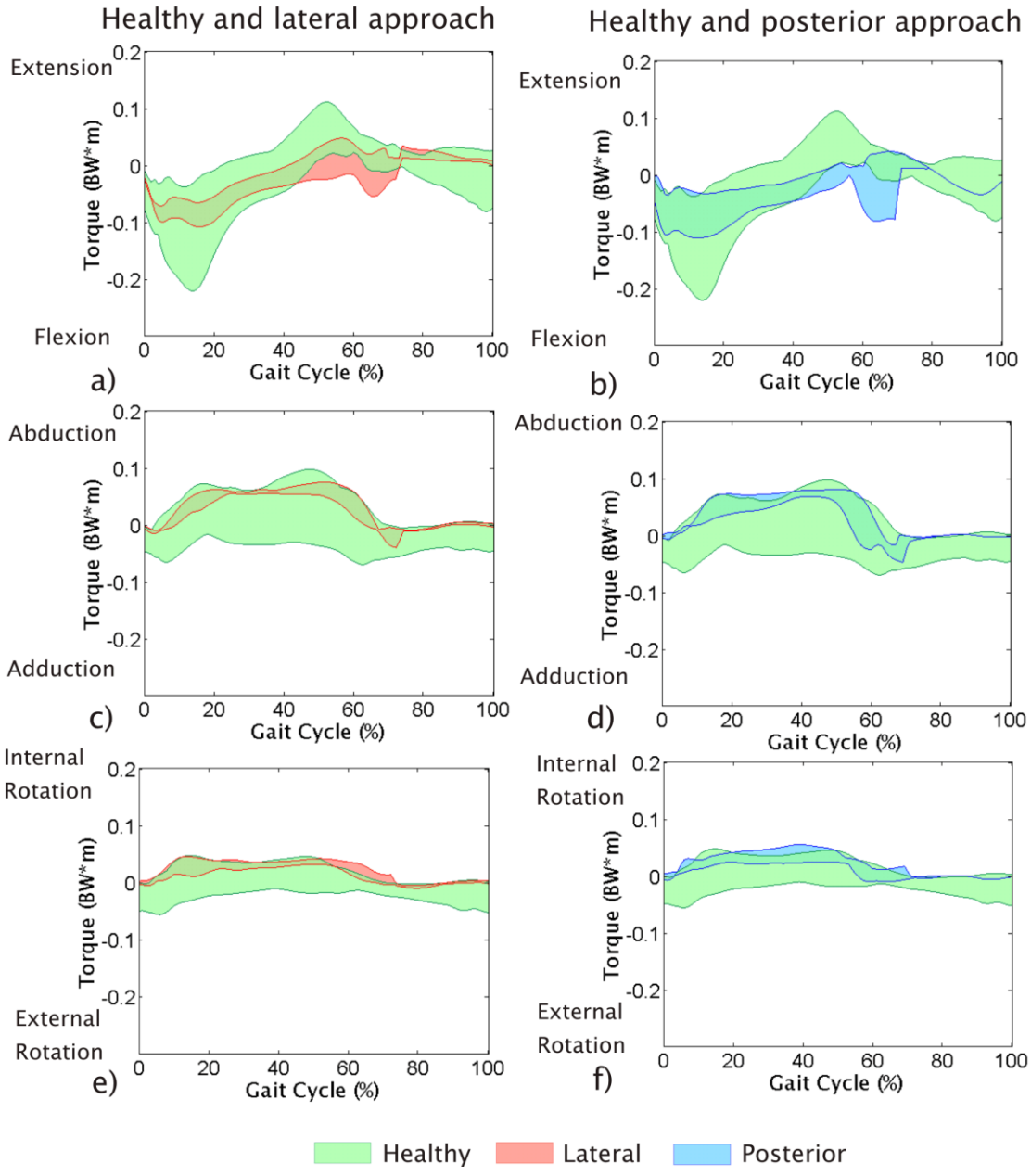

Figure 68: The torque at the hip through the gait cycle for the two THA patient groups and the healthy group.

The resultant hip contact force range predicted for the healthy subjects encompassed the ranges predicted for the two surgical approach patients throughout the gait cycle (Figure 69). During the first peak in force, the hip force in both of the patient groups was at the upper boundary of the range predicted for the healthy group. The range of resultant hip contact force predicted in the groups was generally larger in the healthy group and at the first peak the healthy patient's hip contact force varied from 2.3-4.5BW compared to the posterior approach patient group which varied from 3.4-4.4BW (Table 15). The lateral approach patient group which had a peak resultant hip force during double leg stance between 2.5-4.6BW was very similar to that predicted for the healthy group.

Subject model	Body Weight (N)	Peak hip contact force (BW)	
		First peak	Second peak
S1	667	2.63	3.88
S2	922	3.72	3.26
S3	853	2.25	4.73
S4	942	4.54	2.74
S5	623	4.23	6.17
S6	657	3.36	4.51
S7	883	3.16	2.19
C01	775	3.70	2.63
C02	579	4.10	4.14
P01	559	4.39	3.14
P02	647	3.39	2.76
P03	1050	3.44	2.17
L01	912	2.50	2.40
L02	746	4.59	3.68
L03	657	3.50	2.97

Table 15: Patient details and peak hip contact forces for the healthy and THA patients.

The healthy group had a larger number of individuals in the group (n=9) than either of the patient groups independently (n=3). Therefore the low numbers of individuals in the groups could result in inter-individual variation overwhelming true differences between the groups. At toe off there was an outlier in the healthy group with a peak in resultant hip contact force of 6.2BW which was larger than the remaining peak toe off forces by more than 1BW. However, despite discounting subject S5 as an outlier the peak toe off hip contact forces are generally larger in the healthy group than in the two surgical approach groups at toe off. In general, the healthy group have a greater range of extension at the hip and a larger extension torque at toe off and this would result in a larger force at the hip at toe off.

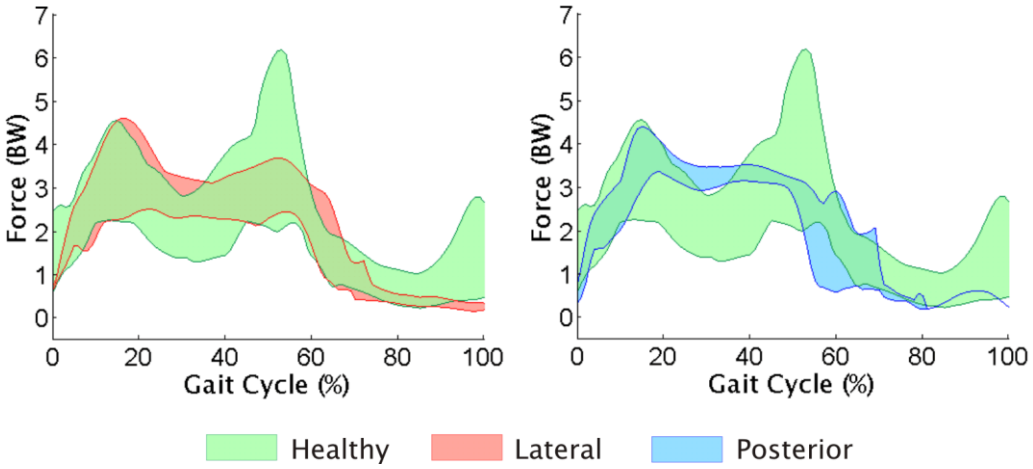

Figure 69: Range of resultant hip contact force predicted for the two THA patient groups and the healthy group.

Walking speed has been shown to affect the hip contact force and the patient groups had a slower walking speed than the healthy subjects (Table 16). Faster walking speeds have been shown to increase the hip contact force (Rydell 1966; Bergmann et al. 1993; Bergmann et al. 2001). The healthy group have a large toe off peak and higher forces during the swing phase, however the hip contact force for the three groups is similar at the first peak in hip contact force.

Subject group	Range of walking speed (m/s) (Average)
Healthy (S1-7 & C01-2)	1.13-1.49 (1.24)
Posterior approach (P01-3)	0.83-1.12 (0.93)
Lateral approach (L01-3)	0.94-1.17 (1.07)
Combined THA patient groups	0.83-1.17 (1.00)

Table 16: The range and average walking speed for the subject groups

The posterior component of the hip contact force in the THA patient groups was at the lower boundary of the range predicted for the healthy subjects (Figure 70a), however the lateral component was at the top of the healthy group range (Figure 70c). The THA patients had a less pronounced reduction in hip force during mid-stance in all components of the hip contact force.

The combined force from the abductor muscles ranged between 1.0-3.0BW in the lateral patient group compared to the range between 0.4-2.7BW in the healthy group at 11% of gait (Figure 71a). The posterior approach patient group also had a range of abductor force at the upper boundary of the healthy subject group at 11% of gait. However, at 52% of gait, the force from the abductor muscles had reduced in the THA patients compared to the healthy group. The muscle forces predicted for the other muscle groups were all found to be small compared to the healthy group but still within the range predicted for the healthy subjects (Figure 71).

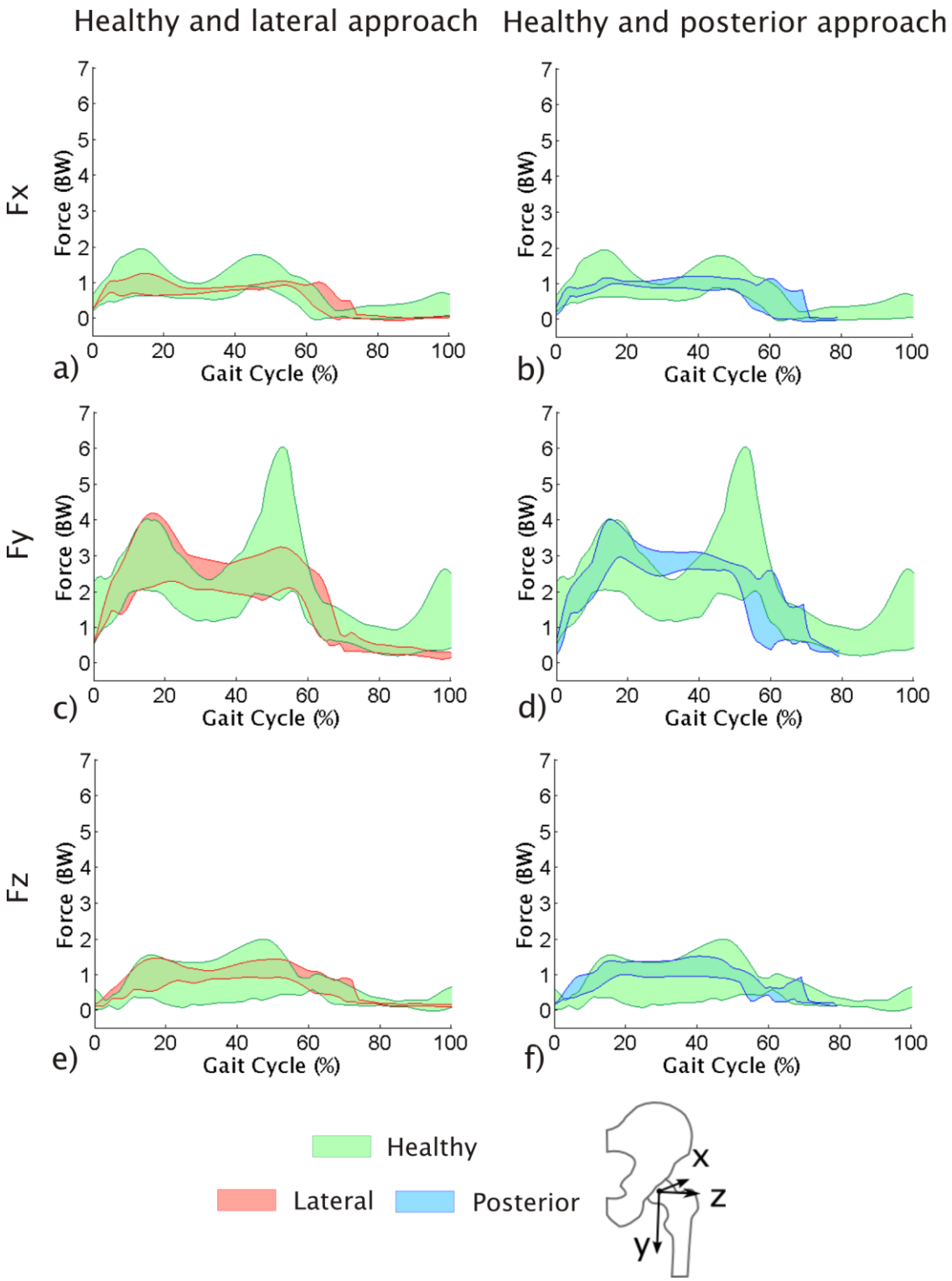

Figure 70: The force components of the hip contact force for the THA patient groups and the healthy group. a) and b) Fx, c) and d) Fy and e) and f) Fz.

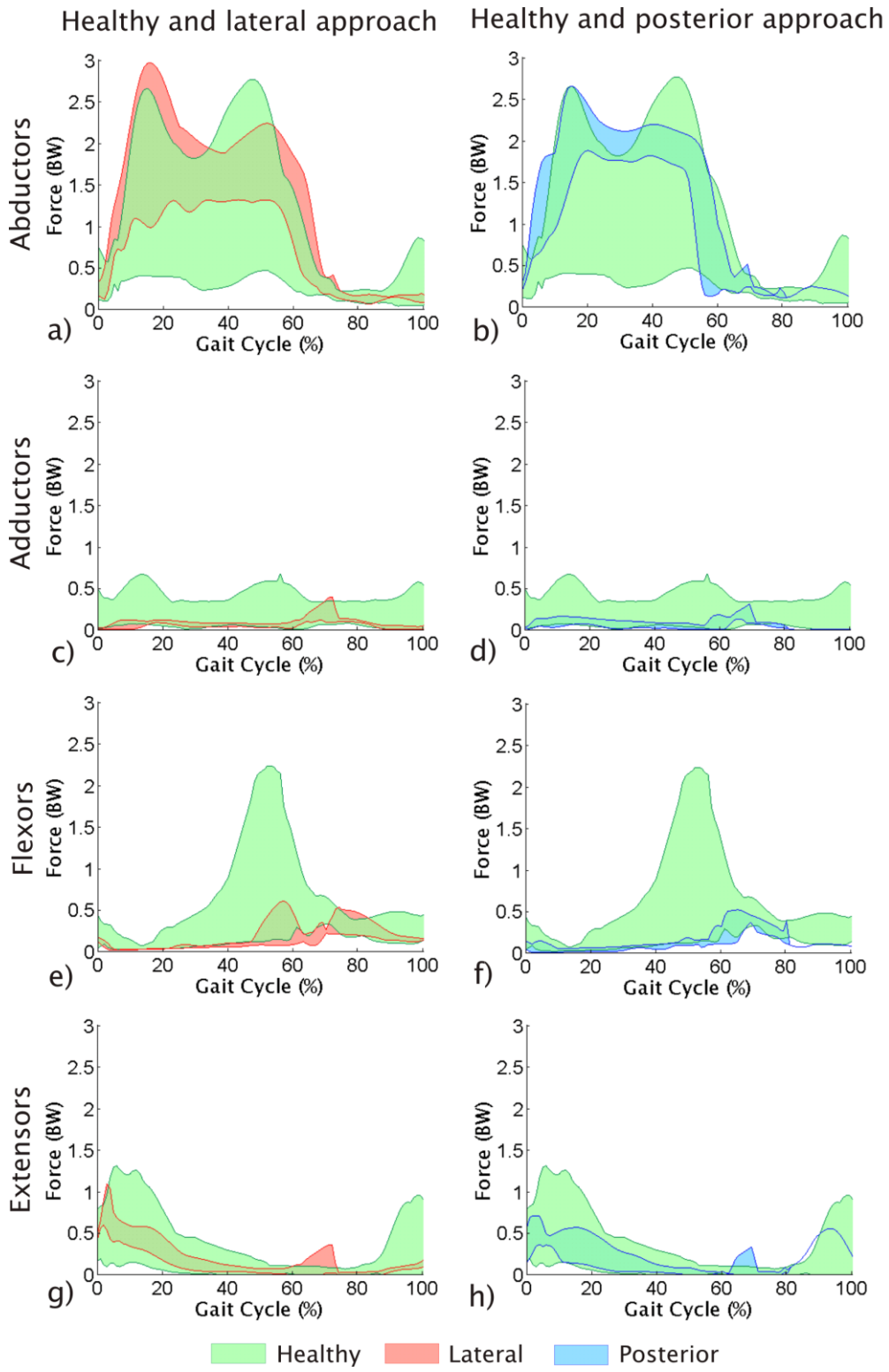

Figure 71: Range of combined muscle forces through the gait cycle for the two THA patient groups and the control group. a) and b) abductor force, c) and d) adductor force, e) and f) flexor force and g) and h) extensor force.

The strain at the bone-implant interface in the finite element model was found to vary dependent on the surgical approach. The mean strain at the interface was similar for all three groups although the lateral approach group had a larger mean strain between approximately 15 and 30% of the gait cycle (Figure 72a) yet with such a low number of subjects within each group this is not likely to be a statistically significant difference. The lateral group also had a large percentage of elements with a strain greater than 7000με compared to the range predicted for the healthy group.

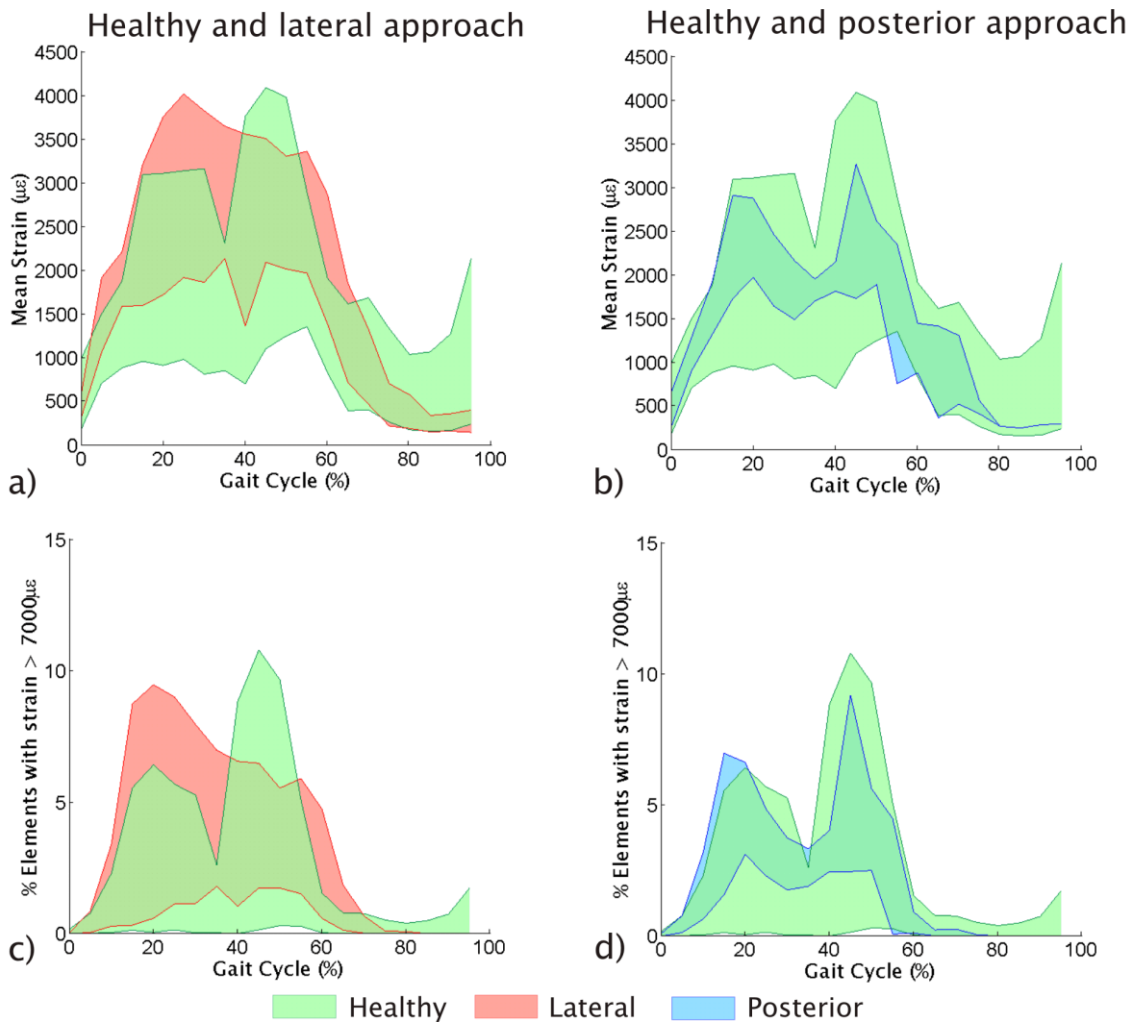

Figure 72: Strain at the bone-implant interface during the gait cycle for the two THA patient groups and the control group.

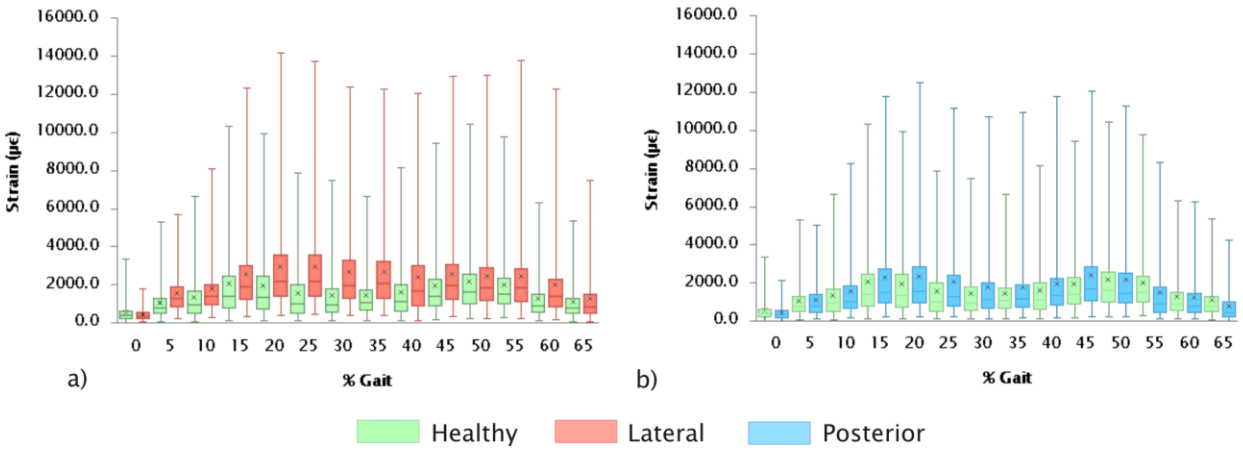

Figure 73: The strain at the bone-implant interface in the healthy subjects, a) lateral THA patients and b) posterior THA patients. The median percentage of elements, 25th and 75th percentiles are displayed in the box plot with the 1st and 99th quartiles shown as the error bars. x denotes the mean strain.

The strain in both the lateral and posterior groups, with the strain from each patient in the group combined, had a substantially higher 75th and 99th percentile strain than the healthy group (Figure 73). Overall, there was a larger percentage of elements with a high strain during the gait cycle in the posterior approach group but the range predicted for the healthy group encompasse the majority of the range predicted for the posterior and lateral approach groups (Figure 74).

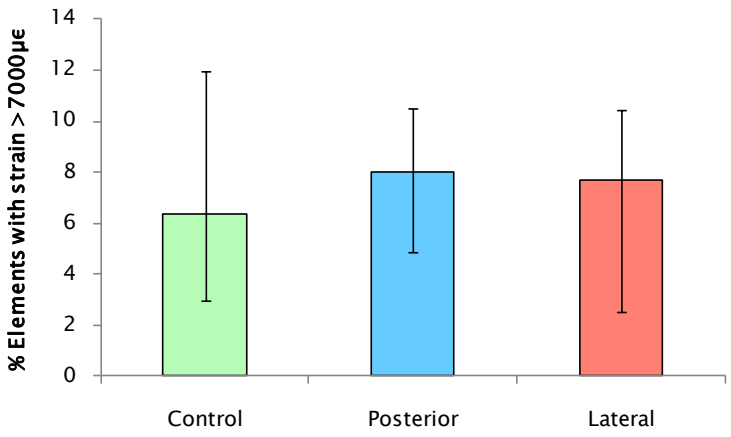

Figure 74: The percentage of elements at the bone-implant interface which had a strain greater than 7000με during the gait cycle. The mean and range predicted for the two THA patient groups and the healthy subject group.

Trends between the three modelled groups found with the micromotion at the bone-implant interface were similar to those found with the interfacial strain. The mean micromotion was similar for all three groups, however, at 15% of gait both the posterior and lateral groups had a larger micromotion than the healthy group (Figure 75a and b). The distinction between the three groups was clearer when investigating the percentage of elements with micromotion greater than 40μm. There was a larger surface area of the interfacial bone with micromotion greater than 40μm in the posterior approach group compared to the lateral group and both patient groups had a larger area of bone with a micromotion greater than 40 μm than the healthy group (Figure 75c and d).

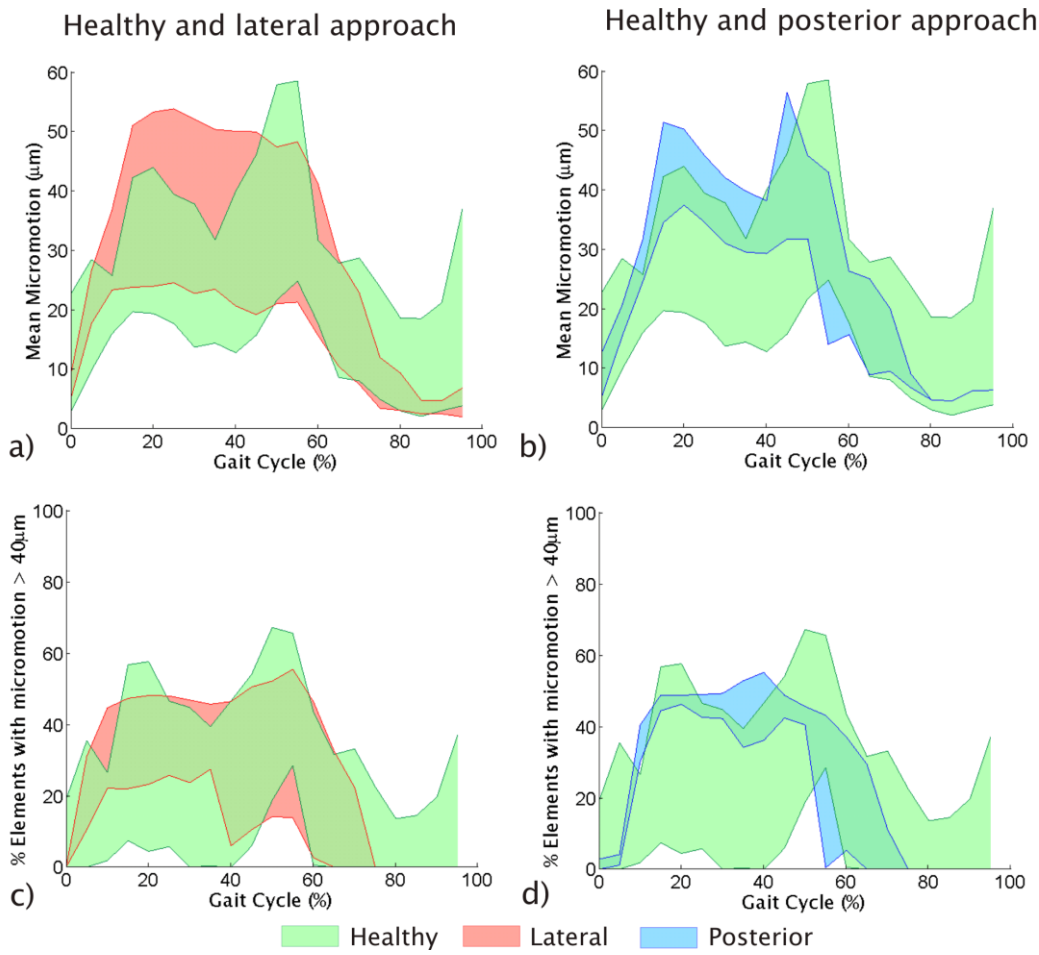

Figure 75: Micromotion at the bone-implant interface during the gait cycle for the two THA patient groups and the control group.

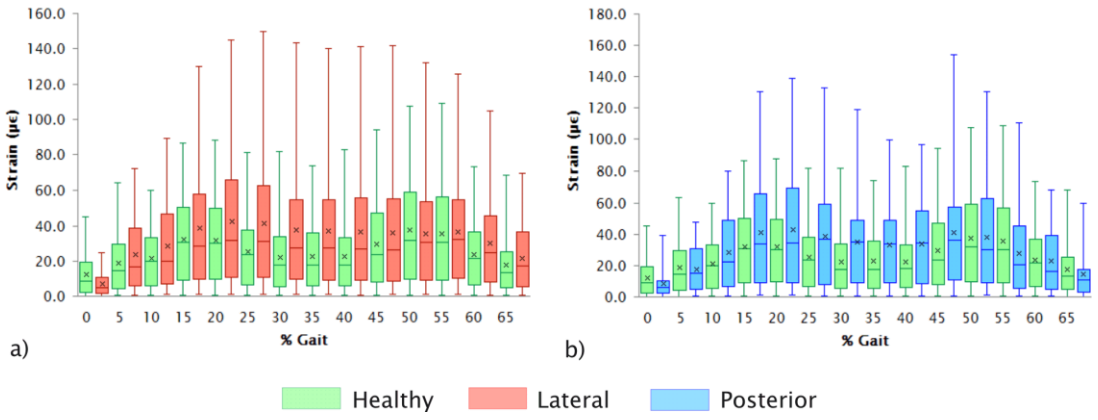

Figure 76: The micromotion in the healthy subjects, a) lateral THA patients and b) posterior THA patients. The median percentage of elements, 25th and 75th percentiles are displayed in the box plot with the 1st and 99th quartiles shown as the error bars. x denotes the mean micromotion.

The micromotion covered a wider range in particular in the lateral approach patients but also in the posterior approach patient groups compared to the healthy patient group (Figure 76). The micromotion was also found to be higher in the THA groups than the healthy group. During the gait cycle there was a greater percentage of elements with a micromotion greater than 40μm in the posterior group compared to the healthy or lateral groups (Figure 77). However the range predicted for the healthy group extended over the ranges predicted for the posterior and lateral groups.

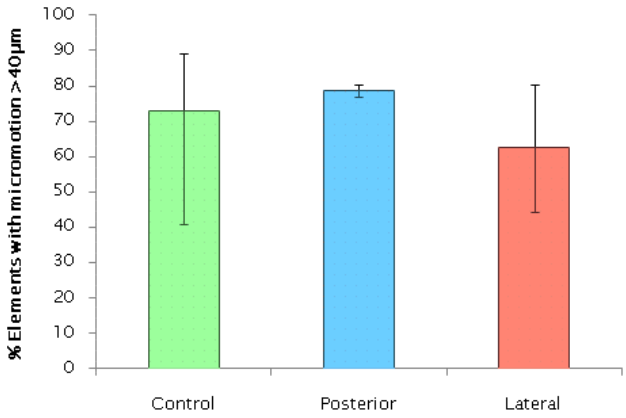

Figure 77: The percentage of elements at the bone-implant interface which had a micromotion greater than 40μm during the gait cycle. The mean and range predicted for the two THA patient groups and the healthy subject group.

8.4. Discussion

Clinical studies have suggested that the risk of revision of a total hip implant can be affected by the surgical approach, in particular the risk of hip dislocation (Robinson et al. 1980; Vicar and Coleman 1984; Hedlundh et al. 1995; Parks and Macaulay 2000; Masonis and Bourne 2002) and there is evidence for a decreased risk of revision due to loosening with a posterior approach (Kärrholm et al. 2007). This study compared the strain and micromotion at the bone implant interface to investigate the increased risk of loosening caused by either high strain leading to breakdown of the interface or high micromotion indicating lack of bone growth onto the implant surface. Using a combination of a musculoskeletal model and a finite element model two methods of

investigation were conducted. The first study altered muscle strengths in a healthy gait pattern and generated surgical approach scenarios. However this study did not find significant differences in the predicted forces and hence in the strain at the bone-implant interface between the lateral, posterior and anterior Smith-Petersen approaches. The second study used motion capture data from THA patients with either a lateral or posterior approach and found strain and micromotion were generally increased in the posterior approach group compared to the lateral approach group and the models based on healthy subjects.

8.4.1. Musculoskeletal simulation of surgical approaches

There were no major differences found between the musculoskeletal simulated surgical approach scenarios modelled in this study and the baseline model in either the musculoskeletal forces or the finite element predicted strain and micromotion. This lack of significant differences between the scenarios may be because a healthy gait pattern was maintained for all the scenarios. It may be that the gait pattern affects the forces, and hence the strain in the femur, more significantly than changes to the muscle forces. Other studies, which have changed musculoskeletal parameters (Johnston et al. 1979), have also maintained the kinematic and kinetic data from the subject for a range of modelled scenarios. However, some clinical studies have shown that the gait pattern can be affected by the surgical approach and therefore the predicted forces may not be directly comparable to clinical scenarios.

Heller *et al.* (2003) created patient-specific musculoskeletal models of THA patients and modelled anterolateral approach by reducing the PCSA of the gluteus medius by 30% to reduce the force produced by the muscle. They found that the force across the hip was redistributed due to the reduction in the PCSA of the gluteus medius. The muscles attached to the proximal femur had a slightly lower force and the muscles which spanned both the hip and knee had an increased force compared to the models without muscle PCSA reduction. They found an overall increase in the hip contact force during the gait cycle and a maximum increase of 12%. This study modelled the

lateral approach with only the gluteus medius, of the abductor muscles, damaged and found a peak increase in the hip contact force of 12%. However the other modelled scenarios with a larger proportion of the abductor muscles reduced in strength did not have significantly increased hip contact forces. The muscle forces in this study were not altered substantially. In the study by Heller *et al.* the muscles' strengths were calculated as a static parameter that was directly proportional to the PCSA which was reduced in the damaged muscles. Consequently the muscles' strengths remained constant throughout the gait cycle. In this study the muscle strength was also reduced by a specified percentage however the strength was based on the Hill muscle model rather than static muscle parameters. The Hill model calculates the muscle strength based on several factors including the length of the muscle tendon unit and therefore the muscle strength varies through the gait cycle as the joint angles change. The proportional reduction in the muscle strength would have been different between these two studies. A reduction to 60% of the original PCSA, in the study by Heller *et al.*, was further reduced by a factor of 0.85 to prevent the muscles from producing maximum force during gait. However in this study a reduction to 60% of the muscle strength produced a smaller reduction in the muscle strength although the resulting change in the muscle strength was variable and so the absolute muscle strength values would also have been different. Lower muscle strengths in the Heller *et al.* study could have produced a stronger response by the muscle recruitment process and therefore a more substantial change in the muscle forces. However when lower muscle strengths were tested in this study over-activity was calculated in some muscles. This study also used a quadratic recruitment criterion whereas Heller *et al.*'s study used a linear criterion which could result in a different allocation of the muscle forces.

The largest increases in muscle force between the surgical approach scenarios and the baseline model was in the flexor muscle group, mainly the rectus femoris and the tensor fasciae latae which span both the hip and the knee joints. A reduction in the strength of these muscles may reduce the strain in the lateral femoral zones. The Smith-Petersen scenario also had a reduced strength in the gluteus medius and in the

gluteus minimus both of which attach to the femur on the lateral zone 2. The rectus femoris was also reduced in strength in the Smith-Petersen scenario but this muscle does not attach to the proximal femur. The rectus femoris is a knee extensor and the vastus muscles also extend the knee. To compensate for a reduction in strength of the rectus femoris the musculoskeletal model produced slightly more force in the vastus muscles and this model predicted an increase in the vastus lateralis muscle units which increased the strain along the lateral side of the femur.

The strain around the femoral implant is indicative of the changes in bone density after a hip replacement. Damborg *et al.* (2008) found that the bone density increases along the lateral side of the femur and reduces on the medial side. This study found lower strain in the medial than the lateral zones. However Perka *et al.* (2005) found a reduction in the bone density in the lateral approach patients compared to anterolateral patients and the strain calculated in this study did not indicated a significantly lower strain at the bone-implant interface for the lateral approach scenario.

8.4.2.Patient specific surgical approach models

Clinical studies have compared the functional outcome of total hip replacement based on the surgical approach (Gore et al. 1982; Downing et al. 2001; Madsen et al. 2004; Whatling et al. 2008; Mayr et al. 2009; Pospischill et al. 2010). However not all studies have found differences between the alternative approaches (Mayr et al. 2009; Pospischill et al. 2010). This could be partly caused by surgical ability since a clinical study has found that the surgeon's experience affected the dislocation rate in posterior approach patients (Hedlundh et al. 1996). However, the range of flexion-extension motion has been found to be greater in posterior approach patients than anterior or anterolateral patients (Madsen et al. 2004). This study found the range of extension at the hip was reduced compared to the healthy subject group and found a wider variation between the posterior patients than within the lateral patient group. However the two THA patient groups had similar flexion-extension angles.

Glaser *et al.* (2008) compared two minimally invasive surgical approaches, the anterolateral and the posterolateral to the traditional surgical approach. They found a similar range of joint angles in the traditional approach to that found in the healthy group in this study. Their range of flexion angle varied through the gait cycle between approximately 35° and -22° which is similar to the 33° to -22° measured in the healthy group in this study. However this study found a reduction in the maximum extension angle in the THA patient groups compared to the healthy group. Glaser *et al.* found a reduced extension angle in both of the minimally invasive studies, the posterolateral group had a maximum extension angle of approximately 3° and the anterolateral group had a maximum extension angle of approximately 10° which is similar to that measured in the THA patient groups in this study. Mayr *et al.* (2009) also found a reduced flexion-extension angle with THA patients compared to healthy subjects. They found that the minimally invasive patients had peak hip contact forces between 2.52-3.54BW which was lower than the peak hip forces predicted in the traditional approach patients which were between 2.91-4.11BW. This study found the hip contact force predicted for all three groups to be in general similar except during toe off. During double leg stance the THA patient groups had slightly higher hip contact forces compared to the healthy subjects and this agreed with the study by Glaser *et al.* (2008) that found greater muscle damage at the hip increased the hip force. A higher incidence of a Trendelenburg limb, which indicates abductor weakness, has been found in anterior approach patient compared to posterior approach patients (Vicar and Coleman 1984). In this study no clear difference was found between the THA patients groups in abductor force predicted in the musculoskeletal models during the gait cycle. The abductor force during double stance in both THA patient groups were above the range found in the healthy group but was lower during single stance than the healthy group. However, overall the ranges predicted for the THA patients fell within the range predicted for the healthy patients.

This study found that the lateral approach group had more internal rotation than the posterior group however Glyn-Jones *et al.* (2006) found the opposite to be true when measuring the gait of THA patients. Gore *et al.* (1982) also found more internal rotation with a posterior approach compared to an anterolateral approach but more normal abductor muscle strength. This study found that both the lateral and posterior approach patients had similar abductor force although this was only measured during normal walking.

Greater bone loss has been found in patients with the lateral approach and Perka *et al.* (2005) found bone loss on both the medial and lateral sides of the proximal femur with the lateral approach. This study found lower strain at the bone-implant interface in the lateral approach compared to the posterior approach however both THA groups had higher strain than the healthy subject group. This study has only considered a very small number of patients in the two THA groups and comparisons between the groups may only be inter-individual differences.

8.4.3.Comparison of modelling processes

Although some individual muscle forces predicted by the musculoskeletal models were affected by a reduction in strength of the muscles altered in the surgical approach scenarios, overall there was little change in the predicted hip joint contact forces or the muscle group forces. Therefore with little change in the applied forces, the finite element models of the implanted femur did not predicted major differences in the micromotion or strain at the bone-implant interface between the modelled surgical approaches. The change in muscle forces marginally affected the strain predicted in the femur particularly in the lateral zones of the femur. The primary stability of the modelled implants can be investigated using the strain and micromotion at the bone-implant interface, however the results from this study would suggest the investigation was not sensitive enough to distinguish any real differences between the surgical approaches. A clinical study comparing THA patients with fracture as their cause of primary surgery found that posterior approach patients were less likely to require

revision due to loosening (Kärrholm et al. 2007). Due to the higher risk of dislocation the effects of loosening on the revision rate of a posterior approach patient would be more difficult to establish conclusively.

In the musculoskeletal modelling simulation of surgical approach the same kinematic and kinetic data were used in all of the models and this meant that there were no errors associated with inter-patient variation. Several studies have found that the ranges of motion at the hip and general gait kinematics were not significantly dissimilar between patients with different surgical approaches (Mayr et al. 2009; Pospischill et al. 2010). However other studies have found that the surgical approach can alter the patient's gait (Gore et al. 1982; Whatling et al. 2008) and differences between surgical approaches due to altered kinematics would be ignored in this modelling process. The second study only modelled three patients with each surgical approach but found differences in the joint angles between the healthy and the THA patients, in particular the extension angle and torque at toe off. However, between the THA patient groups only internal-external rotation of the hip appeared different, although this could be due to gait analysis measurement errors or low patient numbers. The percentage of bone-implant interfacial elements with a high strain and the percentage with a high micromotion were distinctly different over the gait cycle between the two THA patient groups. However the study was conducted with a small number of THA patients in each group. Therefore more patients would be needed to establish whether the differences found were due to patient to patient variation or the muscular damage caused by the surgical approach.

The musculoskeletal models were scaled to the patient height and weight, however the finite element model remained the same for each patient or scenario. The muscle and hip joint contact force was scaled to the assumed body weight of the finite element modelled femur but patient-specific bone geometry was not obtained in this study. Ideally a complete set of patient data, including gait analysis and patient-specific FE model would be used but obtaining CT scans and gait analysis from the same patient

was not possible in this study. However the forces applied to a finite element model have been found to have a greater effect on the bone strains than the bone geometry (Jonkers et al. 2008).

The effects of the potential muscular damage caused during arthroplasty surgery may also alter forces across the knee. These studies have only considered the effects on the hip and proximal femur however some of the muscles affected by the surgery span both the hip and knee such as the rectus femoris and tensor fasciae latae. Heller *et al.* (2003) found that these muscles had an increased force due to a reduction in PCSA in muscles damaged in the lateral approach.

The study modelling the surgical approaches by reducing muscle strengths did not find major differences between the scenarios but the study comparing THA patients did find differences in the strain and micromotion measured at the bone-implant interface. This would suggest that the musculoskeletal modelling to finite element analysis process is more sensitive to alterations in the gait pattern than to changes to muscle strengths. However, to investigate the potential differences between the surgical approaches with confidence larger numbers of patients would be required.

9. Discussion and conclusions

Total hip replacement provides excellent relief from the debilitating pain and loss of motion that can occur with arthritis or hip fracture, the main causes of hip arthroplasty. However, with the expanding and aging population, replacement joints are required to last longer and perform better. To analyse hip replacements, clinical, experimental and computational studies are performed in an attempt to predict how well a replacement may perform in the general population. Computational modelling can provide a flexible framework to investigate the behaviour of hip replacements and the surrounding bone and tissue structures. However, it is crucial that accurate input data are used to build those models or the resulting predictions will be inadequate to provide useful information for patients, surgeons and engineers on the likely lifetime and functionality of the replacement.

9.1. Strengths of combined musculoskeletal and finite element modelling

This study combined inverse dynamic musculoskeletal analysis, which predicted muscle and joint contact forces from motion capture data, with finite element analysis, which calculated strain and micromotion in implanted hip scenarios. The process of predicting musculoskeletal forces, using an inverse dynamic musculoskeletal model, and applying them to a finite element model to calculate the primary stability has been shown to produce reasonable results when compared to *in vivo* measured hip forces and similar strain and micromotion to other computational studies.

A study was conducted into the variability between healthy subjects (Chapter 6). It investigated both the range of musculoskeletal forces and the resulting primary stability of a total hip replacement based on their hip forces. The study found a wide range of predicted musculoskeletal forces and corresponding strain and micromotion with only a small number of subjects. Currently, the vast majority of computational analyses use only a single load case from either Bergmann et al. (2001) or Heller et al. (2001; 2005) and do not account for the variation between patients except for scaling

to patient body weight (2003; 2005; 2007; 2008; 2009; 2009). This study found that after accounting for body weight there are still significant differences between healthy subjects. However, healthy subjects are not the population group who undergo total hip arthroplasty, often the pre-operative patients have mobility problems at the hip. Further investigations should be conducted to study the pre-operative and post-operative patient groups for information on the hip immediately post surgery and for the longer term.

A study investigating post-operative patients was also conducted to investigate potential differences between the effects of different surgical approaches and between THA patients and healthy subjects (Chapter 8). The musculoskeletal forces predicted for patients with a total hip replacement were generally lower than those predicted for the healthy subject group in particular at the toe off peak. The healthy subject group had a pronounced second peak in hip contact force, in many cases larger than the first peak, however both total hip replacement patient groups had a substantially lower force during single leg stance than during double leg stance and in general a less pronounced peak in force. In the subsequent primary stability of the hip stem there was less variation between the THR patients than the healthy subjects and as with the musculoskeletal forces there was generally lower strain and micromotion at approximately 50% of the gait cycle compared to the healthy group. Only a very limited number of subjects were modelled and the resulting differences could be artificially created by the lack of data or could indicate a real variation between the populations. In order to investigate the potential differences between these groups, larger numbers of patients from representative populations are needed. Larger numbers of surgical approach patients may also allow differences to be found between the surgical approaches.

A study was also conducted to investigate the effects of displacing the centre of rotation of the hip on the hip musculoskeletal forces and primary stability of a cementless stem (Chapter 7). The hip contact force and abductor force were calculated

to increase with hip displacement in lateral, inferior and anterior directions. There was a range of more than 1BW in the resultant hip contact force between the hip displacement scenarios with a maximum displacement of 20mm in a lateral, medial, inferior, superior and posterior direction and 10mm displacement in an anterior direction. However the kinematics and kinetics of the musculoskeletal system were maintained for all the hip displacement scenarios. The differences between the hip displacement scenarios were of a similar magnitude to those found in the subject variability study (Chapter 6) and therefore investigating patient variation could produce a reasonable range of forces to apply to preclinical tests. The hip displacement scenarios all maintained the kinematics from the natural position of the hip and the greater the displacement of the hip the more likely this assumption would not hold true. However, as the modelled displacement of the hip increased so did the predicted change in the musculoskeletal force. Therefore it is difficult to distinguish between changes due to hip displacement and changes caused by the model maintaining the kinetics from a gait pattern which could be unsuitable for the hip position. Hip displacement cannot easily be measured accurately *in vivo* as a CT or x-ray of both hips is required for comparison with the contralateral limb. Even with the position of the contralateral hip it may not be possible to calculate the natural hip centre. To conduct a similar hip displacement study to the one conducted in this investigation but with patient-specific data would require a larger patient group with detailed knowledge of their hip displacement, which could prove difficult. Modelling a large enough range of THR patient data could reduce the need to investigate hip centre displacement or surgical approach as it would capture the range of musculoskeletal forces and potential primary stability of the implant. This would allow preclinical testing to incorporate a larger and more representative population when investigating new designs. However it does not help inform surgical decisions on the appropriate surgical approach or hip centre position for individual patients.

9.2. Limitations of combined musculoskeletal and finite element modelling

This study considered altering parameters within the musculoskeletal model whilst maintaining the kinematics and kinetics from the original gait data. As previously discussed, the hip displacement investigation yielded differences between the various scenarios considered although resulted in uncertainty over the likelihood of maintaining the gait with the larger changes in the hip centre which produced the larger differences in musculoskeletal forces. Surgical approaches were also modelled in this study by reducing the strength of relevant muscles. However this did not result in substantial differences in hip forces or subsequent predictions of primary stability. Therefore one of the limitations of this combined musculoskeletal and finite element modelling process was that manipulation of the musculoskeletal model sometimes produced scenarios with overativity in the muscles and therefore could not be considered reasonable results. However motion capture data provided useful scenarios which highlighted differences in musculoskeletal forces and subsequent predictions of primary stability.

Some assumptions have been made in these models either to allow investigations to take place when otherwise it would be impossible or unethical to do so or to simplify the modelling process. The finite element model was not the same as the musculoskeletal modelled subject and therefore scaling was required to adjust the points of force application to fit the finite element modelled implanted femur however it would be impractical to obtain CT scans of all of the musculoskeletal patients and impossible to do so for a large number of patients for preclinical testing. Linear scaling does not account for all the differences between the patients but it allows a straightforward analysis and the musculoskeletal modelling also involves linear scaling to match the motion capture to the model. The forces from the musculoskeletal analysis were normalised to the body weight of the subject before they were subsequently applied to the finite element model although this scaling process may not scale the forces to accurately represent the modelled individual. A fixed cut plane

in the mid shaft of the femur is not a physiological boundary constraint and it has been reported in the literature that the micromotion and displacement in the femur are affected by the boundary constraint. However this study only considered the primary stability of the implant by investigating the strain and micromotion at the bone-implant interface and a study conducted in this report showed that these metrics were unaffected if the boundary constraint of a cut plane was far enough from the tip of the stem.

Patient-specific gait analysis and their associated muculoskeletal models was found to be predict a greater variation in musculoskeletal forces than altered musculoskeletal models based on a single gait analysis. However, each patient walked at a self selected speed and there was a difference between the healthy and post-operative patients' walking speeds, which has been shown to alter hip contact forces (Rydell 1966; Bergmann et al. 1993; Bergmann et al. 2001). To avoid differences in normal walking speeds affecting the hip contact or other musculoskeletal forces and therefore indroducing an additional factor to that studied in the investigation, some research has dictated the walking speed (Bergmann et al. 1993). However, a forced walking speed can change an individual's gait pattern and therefore could affect their musculoskeletal forces at the hip. Therefore, to reduce the affects of walking speed on hip contact forces, large numbers of patients could be used to provide a larger population base for comparison or the results could be normalised between subjects with respect to their walking speed.

Skin artefact errors are a major source of error in the musculoskeletal model as they reduce the accuracy of the recorded markers used to measure the movement of the lower limbs for gait analysis. The effects of skin artefacts were reduced by including more markers to create an over-determinate system and then using optimisation to calculate the position of the limb segments and by placing the markers away from areas which are prone to larger skin artefacts. Skin artefacts errors on the thigh and shank increase the inter-marker rotations, in particular in the transverse plane which

reduces the reliability of the measurement of internal-external rotation at the hip and also the knee (Gao and Zheng 2008). Unfortunately skin artefacts appear to be caused by many factors and therefore cannot be easily removed from the data (Benoit et al. 2006; Gao and Zheng 2008) although the errors have been found to be similar between patients and could be assumed to be a systematic error in the modelled predictions (Cappozzo et al. 1996). However, in general the internal-external rotation range of motion is small compared to the flexion-extension, although similar to the abduction-adduction ranges. Therefore it has a very limited role in affecting the line of force through the hip joint and therefore should not dominate the resulting muscle and joint contact forces.

The recruitment criterion used to predict the muscle activity and hence the muscle and joint contact forces assumes that the body recruits muscles by reducing their normalised force. However, although this has not been proven, studies have suggested that the active muscles tend to correspond to this method during movements such as normal gait (Glitsch and Baumann 1997; van Bolhuis and Gielen 1999). Muscle forces have not been measured *in vivo* and only experiments such as those conducted by Hill (1926; 1938; 1950; 1953) provide insight into the factors affecting the force generated in the muscle. Despite all the potential errors the predictions of musculoskeletal models and in particular the modelling conducted in this study have generally produced similar joint contact forces to those measured with instrumented implants (Bergmann et al. 2001). However it is acknowledged that some muscles act antagonistically which would tend to increase the forces across the joints (Glitsch and Baumann 1997), yet musculoskeletal models tend to over-predict the joint contact forces although this may partly be due to the comparison with measured forces from THA patients.

The modelling process is quasistatic, a series of independent time steps, both in the musculoskeletal model and the subsequent finite element analysis. The musculoskeletal modelling programme, AnyBody does not allow for the previous

muscle state to be considered when calculating the muscle activity and force. Hill's analysis of the available force from a muscle found it was related to the velocity of contraction which is not accounted for in the muscle modelling in this musculoskeletal model and may affect the predicted forces. However since the musculoskeletal analysis used an optimisation technique to calculate the muscle force including additional information about the muscle state at a previous time would complicate the analysis and as yet has not been developed for this software. Incorporating the muscle state from a previous time step has been considered in a study by Davy and Audu (1987) and they found that it did not affect the predicted muscles force significantly but produced a lag in the output forces.

Although the surface strain has been recorded on the tibia *in vivo*, it is extremely difficult to obtain accurate surface strains across the bones whilst they are in the body, and it is not currently feasible to measure the internal stresses and strains. Therefore validating finite element models is a challenging task and one that cannot be established conclusively. Many finite element models investigating hip replacement only conduct one analysis at the peak in hip contact force (Cheal et al. 1992; Stolk et al. 2001; Wong et al. 2005; Gracia et al. 2010) although in some cases heel strike and toe off are considered (Bitsakos et al. 2005). However, although this study considers time steps through the stance phase of gait and in some cases through the whole gait cycle the analysis is only at individual time steps. The time steps investigated in the finite element analysis are not necessarily the same as those predicted in the musculoskeletal model and therefore linear interpolation is used to calculate the forces at the time steps required by the finite element models which may introduce a small element of error into the force application.

In this study the hip contact force was applied directly to the femoral component in a debonded model of the bone and implant. The load across the interface caused stress on the bone and where the load was transferred through cancellous bone, with a low modulus compared to cortical, the strain could be high. In particular, at the bone-

implant interface in the proximal, lateral surface the modulus was lower than along the shaft of the implant. In this study the challenging geometry at the interface between the implant bone and reamed section of bone above the implant generated a small number of irregular elements and the subsequent finite element analysis produced unreasonable high strains in these elements. Therefore the maximum strain was not used in the analyses as it would have been dominated by the irregular elements.

9.3. Practical applications of combined musculoskeletal and finite element modelling

The investigations undertaken by this study highlighted the range of forces which could be applied to the hip either due to patient variation, muscular damage from surgery or hip position. The investigations then considered the effect of these changes in force on the strain and micromotion in the femur. The changes in the hip position influenced the hip contact force considerably as did the patient variation and the difference in surgical approach modelled from the total hip replacement patients but changes to the muscle strength did not significantly affect the hip contact forces. All of these studies had limitations; in particular the models comparing THA patient models only had a small number of patients in each group which was not enough to make statistically relevant comparisons. However, both the patient variation and surgical approach patient studies produced a wider variability in the hip contact force and subsequently in the strain and micromotion than was seen in the study comparing models with reduced muscle strengths.

Preclinical testing of hip implants is often only conducted with an average patient loading conditions and the range of muscle and hip contact forces predicted in this study could improve the applicability of those studies to the general population. More healthy and THA subjects could be modelled using the musculoskeletal model to improve the representation of the general population, however the studies conducted here have found that there is variation between patients even after normalising for their body weight. Since the majority of total hip arthroplasty surgeries are successful

preclinical testing needs to broaden the scenarios under which the implants are tested to find areas in which new replacement joints may improve on existing designs.

The study investigating the variability between models of healthy forces applied to an implanted femur found a strong correlation between the hip contact force and the finite element calculated micromotion and strain at the bone-implant interface. These correlations provide a rough estimation of the likely micromotion or strain a patient may encounter. However the peak hip contact force would need to be calculated and the correlation between the peak hip force and the subjects' body weight was found to have a much lower correlation. An increase in the number of modelled individuals may improve the reliability of the predicted relationships between post-operative patients and predicted outcomes using this combined musculoskeletal and finite element process.

Combined musculoskeletal and finite element modelling of total hip replacement has the potential to account for surgery and patient related variability using motion capture data. The variability calculated using this technique could provide more detailed load cases for preclinical tests on total hip replacement stems and help to improve the success of hip replacement in a wider population.

10.References

Abdul-Kadir, M. R., Hansen, U., Klabunde, R., Lucas, D. and Amis, A. (2008). "Finite Element Modelling of Primary Hip Stem Stability: The Effect of Interference Fit." Journal of Biomechanics **41**(3): 587-594.

Afsharpoya, B., Barton, D. C., Fisher, J., Purbach, B., Wroblewski, M. and Stewart, T. D. (2009). "Cement Mantle Stress under Retroversion Torque at Heel-Strike." Medical Engineering and Physics **31**(10): 1323-1330.

Agarwal, S. (2004). "The Difficult Primary Hip." Current Orthopaedics **18**(6): 451-460.

An, K. N., Tankakashi, K., Harrigan, T. P. and Chao, E. Y. (1984). "Determination of the Muscle Orientation and Moment Arms." Journal of Biomechanical Engineering **106**(3): 280-282.

An, Y. H. and Draughn, R. A. (2000). Mechanical Testing of Bone and the Bone-Implant Interface, CRC Press LLC.

Andersen, M. S., Damsgaard, M. and Rasmussen, J. (2009). "Kinematic Analysis of over-Determinate Biomechanical Systems." Computer Methods in Biomechanics and Biomedical Engineering **12**(4): 371-384.

Ando, M., Imura, S., Omori, H., Okumura, Y., Bo, A. and Baba, H. (1999). "Nonlinear Three-Dimensional Finite Element Analysis of Newly Designed Cementless Total Hip Stems." Artificial Organs **23**(4): 339-346.

Andreaus, U. and Colloca, M. (2009). "Prediction of Micromotion Initiation of an Implanted Femur under Physiological Loads and Constraints Using the Finite Element Method." Proceedings of the Institution of Mechanical Engineers, Part H: Journal of Engineering in Medicine **223**(5): 589-605.

Anwar, I., Bhatnagar, G. and Atrah, S. (2009). "Delayed Catastrophic Failure of a Ceramic Head in Hybrid Total Hip Arthroplasty." The Journal of Arthroplasty **24**(1): 158.e155-158.e158.

AnyBody Research Group (2009). "Anyforge." from http://forge.anyscript.org.

Archbold, H. A. P., Mockford, B., Molloy, D., McConway, J., Ogonda, L. and Beverland, D. (2006). "The Transverse Acetabular Ligament: An Aid to Orientation of the Acetabular Component During Primary Total Hip Replacement: A Preliminary Study of 1000 Cases Investigating Postoperative Stability." Journal of Bone and Joint Surgery (Br.) **88**(7): 883-886.

Atilla, B., Ali, H., Aksoy, M. C., Caglar, O., Tokgozoglu, A. M. and Alpaslan, M. (2007). "Position of the Acetabular Component Determines the Fate of Femoral Head Autografts in Total Hip Replacement for Acetabular Dysplasia." Journal of Bone and Joint Surgery (Br.) **89**(7): 874-878.

Bachmeier, C. J. M., March, L. M., Cross, M. J., Lapsley, H. M., Tribe, K. L., Courtenay, B. G. and Brooks, P. M. (2001). "A Comparison of Outcomes in Osteoarthritis Patients Undergoing Total Hip and Knee Replacement Surgery." Osteoarthritis and Cartilage **9**(2): 137-146.

Baker, A. and Bitounis, V. (1989). "Abductor Function after Total Hip Replacement. An Electromyographic and Clinical Review." Journal of Bone and Joint Surgery (Br.) **71**(1): 47-50.

Bartel, D. and Johnston, R. (1969). "Mechanical Analysis and Optimization of a Cup Arthroplasty." Journal of Biomechanics **2**(1): 97-102.

Bauer, T. W. and Schils, J. (1999). "The Pathology of Total Joint Arthroplasty: 1. Mechanisms of Implant Fixation." Skeletal Radiology **28**(8): 423-432.

Beaupré, G. S., Orr, T. E. and Carter, D. R. (1990). "An Approach for Time-Dependent Bone Modeling and Remodeling - Application: A Preliminary Remodeling Simulation." Journal of Orthopaedic Research **8**(5): 662-670.

Behrens, B. A., Wirth, C. J., Windhagen, H., Nolte, I., Meyer-Lindenberg, A. and Bouguecha, A. (2008). "Numerical Investigations of Stress Shielding in Total Hip Prostheses." Proceedings of the Institution of Mechanical Engineers, Part H: Journal of Engineering in Medicine **222**(5): 593-600.

Bennett, D., Ogonda, L., Elliott, D., Humphreys, L. and Beverland, D. E. (2006). "Comparison of Gait Kinematics in Patients Receiving Minimally Invasive and Traditional Hip Replacement Surgery: A Prospective Blinded Study." Gait and Posture **23**(3): 374-382.

Benoit, D. L., Ramsey, D. K., Lamontagne, M., Xu, L., Wretenberg, P. and Renström, P. (2006). "Effect of Skin Movement Artifact on Knee Kinematics During Gait and Cutting Motions Measured in Vivo." Gait and Posture **24**(2): 152-164.

Berger, R. A. (2006). "Minimally Invasive Total Hip Arthroplasty with Two Incisions." Operative Techniques in Orthopaedics **16**(2): 102-111.

Bergmann, G. (2008). "Orthoload." from www.orthoload.com.

Bergmann, G., Deuretzbacher, G., Heller, M., Graichen, F., Rohlmann, A., Strauss, J. and Duda, G. (2001). "Hip Contact Forces and Gait Patterns from Routine Activities." Journal of Biomechanics **34**(7): 859-871.

Bergmann, G., Graichen, F. and Rohlmann, A. (1993). "Hip Joint Loading During Walking and Running, Measured in Two Patients." Journal of Biomechanics **26**(8): 969-980.

Berry, D. J., Berger, R. A., Callaghan, J. J., Dorr, L. D., Duwelius, P. J., Hartzband, M. A., Lieberman, J. R. and Mears, D. C. (2003). Minimally Invasive Total Hip Arthroplasty. Development, Early Results, and a Critical Analysis. Annual Meeting of the American Orthopaedic Association. Charleston, South Carolina, USA, Journal of Bone and Joint Surgery (Am.). **85(11):** 2235-2246.

Bicanic, G., Delimar, D., Delimar, M. and Pecina, M. (2009). "Influence of the Acetabular Cup Position on Hip Load During Arthroplasty in Hip Dysplasia " International Orthopaedics (SICOT) **33**(2): 397-402.

Biegler, F. B., Reuben, J. D., Harrigan, T. P., Hou, F. J. and Akin, J. E. (1995). "Effect of Porous Coating and Loading Conditions on Total Hip Femoral Stem Stability." The Journal of Arthroplasty **10**(6): 839-847.

Birrell, F., Johnell, O. and Silman, A. (1999). "Projecting the Need for Hip Replacement over the Next Three Decades: Influence of Changing Demography and Threshold for Surgery." Annals of the Rheumatic Diseases **58**(9): 569-572.

Bitsakos, C., Kerner, J., Fisher, I. and Amis, A. A. (2005). "The Effect of Muscle Loading on the Simulation of Bone Remodelling in the Proximal Femur." Journal of Biomechanics **38**(1): 133-139.

Bobyn, J. D., Pilliar, R. M., Cameron, H. U. and Weatherly, G. C. (1981). "Osteogenic Phenomena across Endosteal Bone-Implant Spaces with Porous Surfaced Intramedullary Implants." Acta Orthopaedica **52**(2): 145-153.

Brand, R. A., Crowninshield, R. D., Wittstock, C. E., Pederson, D. R., Clark, C. R. and van Krieken, F. M. (1982). "A Model of Lower Extremity Muscular Anatomy." Journal of Biomechanical Engineering **104**(4): 304-310.

Brand, R. A., Pedersen, D. R., Davy, D. T., Kotzar, G. M., Heiple, K. G. and Goldberg, V. M. (1994). "Comparison of Hip Force Calculations and Measurements in the Same Patient." The Journal of Arthroplasty **9**(1): 45-51.

Brand, R. A., Pedersen, D. R. and Friederich, J. A. (1986). "The Sensitivity of Muscle Force Predictions to Changes in Physiologic Cross-Sectional Area." Journal of Biomechanics **19**(8): 589-596.

Bressler, B. H. and Clinch, N. F. (1974). "The Compliance of Contracting Skeletal Muscle." Journal of Physiology **237**(3): 477-493.

Bryan, R., Nair, P. B. and Taylor, M. (2009). "Use of a Statistical Model of the Whole Femur in a Large Scale, Multi-Model Study of Femoral Neck Fracture Risk." Journal of Biomechanics **42**(13): 2171-2176.

Callaghan, J., Salvati, E., Pellicci, P., Wilson, P. and Ranawat, C. (1985). "Results of Revision for Mechanical Failure after Cemented Total Hip Replacement, 1979 to 1982. A Two to Five-Year Follow-Up." Journal of Bone and Joint Surgery (Am.) **67**(7): 1074-1085.

Callister, W. D. (2000). Materials Science and Engineering. An Introduction., John Wiley and Sons.

Cappozzo, A., Catani, F., Leardini, A., Benedetti, M. G. and Croce, U. D. (1996). "Position and Orientation in Space of Bones During Movement: Experimental Artifacts." Clinical Biomechanics **11**(2): 90-100.

Carter, D. and Hayes, W. (1977). "The Compressive Behavior of Bone as a Two-Phase Porous Structure." Journal of Bone and Joint Surgery (Am.) **59**(7): 954-962.

Cerveri, P., Pedotti, A. and Ferrigno, G. (2003). "Robust Recovery of Human Motion from Video Using Kalman Filters and Virtual Humans." Human Movement Science **22**(3): 377-404.

Charnley, J. (1972). "The Long-Term Results of Low-Friction Arthroplasty of the Hip Performed as a Primary Intervention." Journal of Bone and Joint Surgery (Br.) **54**(1): 61-76.

Cheal, E. J., Spector, M. and Hayes, W. C. (1992). "Role of Loads and Prosthesis Material Properties on the Mechanics of the Proximal Femur after Total Hip Arthroplasty." Journal of Orthopaedic Research **10**(3): 405-422.

Cholewicki, J. and Mcgill, S. M. (1994). "Emg Assisted Optimization: A Hybrid Approach for Estimating Muscle Forces in an Indeterminate Biomechanical Model." Journal of Biomechanics **27**(10): 1287-1289.

Cowin, S. C. (2001). Bone Mechanics Handbook.

Crow, B. D., Haltom, D. J., Carson, W. L., Greene, W. B. and Cook, J. L. (2007). "Evaluation of a Novel Biomaterial for Intrasubstance Muscle Laceration Repair." Journal of Orthopaedic Research **25**(3): 396-403.

Crowinshield, R. D., Brand, R. A. and Johnston, R. C. (1978). "The Effects of Walking Velocity and Age on Hip Kinematics and Kinetics." Clinical Orthopaedics and Related Research **132**: 140-144.

Crowninshield, R. D. and Brand, R. A. (1981). "A Physiologically Based Criterion of Muscle Force Prediction in Locomotion." Journal of Biomechanics **14**(11): 793-801.

Crowninshield, R. D., Brand, R. A., Johnston, R. C. and Milroy, J. C. (1980). "The Effect of Femoral Stem Cross-Sectional Geometry on Cement Stresses in Total Hip Reconstruction." Clinical Orthopaedics and Related Research **146**: 71-77.

Crowninshield, R. D., Johnston, R. C., Andrews, J. G. and Brand, R. A. (1978). "A Biomechanical Investigation of the Human Hip." Journal of Biomechanics **11**(1-2): 75-85.

Dalton, J., Cook, S., Thomas, K. and Kay, J. (1995). "The Effect of Operative Fit and Hydroxyapatite Coating on the Mechanical and Biological Response to Porous Implants." Journal of Bone and Joint Surgery (Am.) **77**(1): 97-110.

Damborg, F., Nissen, N., JÃ¸rgensen, H. R. I., Abrahamsen, B. and Brixen, K. (2008). "Changes in Bone Mineral Density (Bmd) around the Cemented Exeter Stem: A Prospective Study in 18 Women with 5 Years Follow-Up." Acta Orthopaedica **79**(4): 494 - 498.

Davy, D. T. and Audu, M. L. (1987). "A Dynamic Optimization Technique for Predicting Muscle Forces in the Swing Phase of Gait." Journal of Biomechanics **20**(2): 187-201.

Davy, D. T., Kotzar, G. M., Brown, R. H., Heiple, K. G., Goldberg, V. M., Heiple, K. G., Berilla, J. and Burstein, A. H. (1988). "Telemetric Force Measurements across the Hip after Total Arthroplasty." Journal of Bone and Joint Surgery (Am.) **70**(1): 45-50.

Dearborn, J. T. and Harris, W. H. (1999). "High Placement of an Acetabular Component Inserted without Cement in a Revision Total Hip Arthroplasty. Results after a Mean of Ten Years." Journal of Bone and Joint Surgery (Am.) **81**(4): 469-480.

Della Valle, C., Berger, R., Rosenberg, A., Jacobs, J., Sheinkop, M. and Paprosky, W. (2003). "Extended Trochanteric Osteotomy in Complex Primary Total Hip Arthroplasty. A Brief Note." Journal of Bone and Joint Surgery (Am.) **85**(12): 2385-2390.

Delp, S. L. (1990). "Parameters for the Lower Limb." 2008, from http://isbweb.org/data/delp/Muscle_parameter_table.txt.

Delp, S. L., Komattu, A. V. and Wixson, R. L. (1994). "Superior Displacement of the Hip in Total Joint Replacement: Effects of Prosthetic Neck Length, Neck-Stem Angle, and Anteversion Angle on the Moment-Generating Capacity of the Muscles." Journal of Orthopaedic Research **12**(6): 860-870.

Delp, S. L. and Loan, J. P. (1995). "A Graphics-Based Software System to Develop and Analyze Models of Musculoskeletal Structures." Computers in Biology and Medicine **25**(1): 21-34.

Delp, S. L. and Maloney, W. (1993). "Effects of the Hip Center Location on the Moment-Generating Capacity of the Muscles." Journal of Biomechanics **26**(4/5): 485-499.

DePuy Orthopaedics (2010). "Aml: Total Hip System." 2010, from www.depuyorthopaedics.com.

DePuy Orthopaedics (2010). "S-Rom Modular Hip System." 2010, from http://www.depuy.com.

Doehring, T. C., Rubash, H. E., Shelley, E. J., Schwendeman, L. J., Donaldson, T. K. and Navalgund, Y. A. (1996). "Effect of Superior and Superolateral Relocations of the Hip Center on Hip Joint Forces." The Journal of Arthroplasty **11**(6): 693-703.

Dopico-González, C., New, A. M. and Browne, M. (2010). "Probabilistic Finite Element Analysis of the Uncemented Hip Replacement--Effect of Femur Characteristics and Implant Design Geometry." Journal of Biomechanics **43**(3): 512-520.

Dostal, W. F. and Andrews, J. G. (1981). "A Three-Dimensional Biomechanical Model of Hip Musculature." Journal of Biomechanics **14**(11): 803-812.

Downing, N. D., Clark, D. I., Hutchinson, J. W., Colclough, K. and Howard, P. W. (2001). "Hip Abductor Strength Following Total Hip Arthroplasty: A Prospective Comparison of the Posterior and Lateral Approach in 100 Patients." Acta Orthopaedica **72**(3): 215 - 220.

Duda, G. N., Brand, D., Freitag, S., Lierse, W. and Schneider, E. (1996). "Variability of Femoral Muscle Attachments." Journal of Biomechanics **29**(9): 1183-1190.

Duda, G. N., Heller, M. O., Albinger, J., Schulz, O., Schneider, E. and Claes, L. (1998). "Influence of Muscle Forces on Femoral Strain Distribution." Journal of Biomechanics **31**(9): 841-846.

Dujardin, F. H., Roussignol, X., Mejjad, O., Weber, J. and Thomine, J. M. (1997). "Interindividual Variations of the Hip Joint Motion in Normal Gait." Gait & Posture **5**(3): 246-250.

Dumbleton, J. H. and Manley, M. T. (2005). "Metal-on-Metal Total Hip Replacement: What Does the Literature Say?" The Journal of Arthroplasty **20**(2): 174-188.

Ebacher, V., Tang, C., McKay, H., Oxland, T. R., Guy, P. and Wang, R. (2007). "Strain Redistribution and Cracking Behavior of Human Bone During Bending." Bone **40**(5): 1265-1275.

El'Sheikh, H. F., MacDonald, B. J. and Hashmi, M. S. J. (2003). Finite Element Simulation of the Hip Joint During Stumbling: A Comparison between Static and Dynamic Loading. International Conference on the Advanced Materials Processing Technology, Journal of Materials Processing Technology. **143-144:** 249-255.

Engh, C., Bobyn, J. and Glassman, A. (1987). "Porous-Coated Hip Replacement. The Factors Governing Bone Ingrowth, Stress Shielding, and Clinical Results." Journal of Bone and Joint Surgery (Br.) **69**(1): 45-55.

Engh, C., O'Connor, D., Jasty, M., McGovern, T., Bobyn, J. and Harris, W. (1992). "Quantification of Implant Micromotion, Strain Shielding, and Bone Resorption with Porous-Coated Anatomic Medullary Locking Femoral Prostheses." Clinical Orthopaedics and Related Research **285**: 13-29.

Erceg, M. (2009). "The Influence of Femoral Head Shift on Hip Biomechanics: Additional Parameters Accounted." International Orthopaedics (SICOT) **33**(1): 95-100.

Erdemir, A., McLean, S., Herzog, W. and van den Bogert, A. J. (2007). "Model-Based Estimation of Muscle Forces Exerted During Movements." Clinical Biomechanics **22** (2): 131-154.

Essner, A., Sutton, K. and Wang, A. (2005). Hip Simulator Wear Comparison of Metal-on-Metal, Ceramic-on-Ceramic and Crosslinked Uhmwpe Bearings. 15th International Conference on Wear of Materials, Wear. **259**: 992-995.

Folgado, J., Fernandes, P. R., Jacobs, C. R. and Pellegrini, V. D. (2009). "Influence of Femoral Stem Geometry, Material and Extent of Porous Coating on Bone Ingrowth and Atrophy in Cementless Total Hip Arthroplasty: An Iterative Finite Element Model." Computer Methods in Biomechanics and Biomedical Engineering **12**(2): 135 - 145.

Fraysse, F., Dumas, R., Cheze, L. and Wang, X. (2009). "Comparison of Global and Joint-to-Joint Methods for Estimating the Hip Joint Load and the Muscle Forces During Walking." Journal of Biomechanics **42**(14): 2357-2362.

Fuller, J., Liu, L. J., Murphy, M. C. and Mann, R. W. (1997). "A Comparison of Lower-Extremity Skeletal Kinematics Measured Using Skin- and Pin-Mounted Markers." Human Movement Science **16**(2-3): 219-242.

Gao, B. and Zheng, N. (2008). "Investigation of Soft Tissue Movement During Level Walking: Translations and Rotations of Skin Markers." Journal of Biomechanics **41**(15): 3189-3195.

Garrett, W. E. and Duncan, P. W. (1988). Muscle Injury and Rehabilitation, Williams & Wilkins.

Garrett, W. E., Seaber, A. V., Boswick, J., Urbaniak, J. R. and Goldner, J. L. (1984). "Recovery of Skeletal Muscle after Laceration and Repair." Journal of Hand Surgery (Am.) **9**(5): 683-693.

Georgiades, G., Babis, G. C., Kourlaba, G. and Hartofilakidis, G. (2010). "Effect of Cementless Acetabular Component Orientation, Position, and Containment in Total Hip Arthroplasty for Congenital Hip Disease." The Journal of Arthroplasty **In Press, Corrected Proof**.

Gibson, L. J. (2005). "Biomechanics of Cellular Solids." Journal of Biomechanics **38**(3): 377-399.

Girard, J., Lavigne, M., Vendittoli, P.-A. and Roy, A. G. (2006). "Biomechanical Reconstruction of the Hip: A Randomised Study Comparing Total Hip Resurfacing and Total Hip Arthroplasty." Journal of Bone and Joint Surgery (Br.) **88**(6): 721-726.

Glaser, D., Dennis, D. A., Komistek, R. D. and Miner, T. M. (2008). "In Vivo Comparison of Hip Mechanics for Minimally Invasive Versus Traditional Total Hip Arthroplasty." Clinical Biomechanics **23**(2): 127-134.

Glitsch, U. and Baumann, W. (1997). "The Three-Dimensional Determination of Internal Loads in the Lower Extremity." Journal of Biomechanics **30**(11-12): 1123-1131.

Glyn-Jones, S., Alfaro-Adrian, J., Murray, D. W. and Gill, H. S. (2006). "The Influence of Surgical Approach on Cemented Stem Stability: An Rsa Study." Clinical Orthopaedics and Related Research **448**: 87-91.

Gore, D. R., Murray, M. P., Sepic, S. B. and Gardner, G. M. (1982). "Anterolateral Compared to Posterior Approach in Total Hip Arthroplasty: Differences in Component Positioning, Hip Strength, and Hip Motion." Clinical Orthopaedics and Related Research **165**: 180-187.

Gracia, L., Ibarz, E., Puértolas, S., Cegoñino, J., López-Prats, F., Panisello, J. J. and Herrera, A. (2010). "Study of Bone Remodeling of Two Models of Femoral Cementless Stems by Means of Dexa and Finite Elements." Biomedical Engineering Online **9**.

Gray, H. (1918). "Anatomy of the Human Body." 2007, from www.bartleby.com/107/.

Gruen, T. A., McNeice, G. M. and Amstutz, H. C. (1979). ""Modes of Failure" of Cemented Stem-Type Femoral Components: A Radiographic Analysis of Loosening." Clinical Orthopaedics and Related Research **141**: 17-27.

Haddad, F. and Adams, G. R. (2006). "Aging-Sensitive Cellular and Molecular Mechanisms Associated with Skeletal Muscle Hypertrophy." Journal of Applied Physiology **100**(4): 1188-1203.

Hardinge, K. (1982). "The Direct Lateral Approach to the Hip." Journal of Bone and Joint Surgery (Br.) **64**(1): 17-19.

Harris, W. H., Mulroy, R. D., Maloney, W. J., Burke, D., Chandler, H. P. and Zalenski, E. B. (1991). "Intraoperative Measurement of Rotational Stability of Femoral Components of Total Hip Arthroplasty." Clinical Orthopaedics and Related Research **266**: 119-126.

Hedlundh, U., Ahnfelt, L., Hybbinette, C.-H., Weckström, J. and Fredin, H. (1996). "Surgical Experience Related to Dislocations after Total Hip Arthroplasty." Journal of Bone and Joint Surgery (Br.) **78**(2): 206-209.

Hedlundh, U., Hybbinette, C.-H. and Fredin, H. (1995). "Influence of Surgical Approach on Dislocations after Charnley Hip Arthroplasty." The Journal of Arthroplasty **10**(5): 609-614.

Helgason, B., Perilli, E., Schileo, E., Taddei, F., Brynjólfsson, S. and Viceconti, M. (2008). "Mathematical Relationships between Bone Density and Mechanical Properties: A Literature Review." Clinical Biomechanics **23**(2): 135-146.

Heller, M., Bergmann, G., Deuretzbacher, G., Durselen, L., Pohl, M., Claes, L., Haas, N. and Duda, G. (2001). "Musculo-Skeletal Loading Conditions at the Hip During Walking and Stair Climbing." Journal of Biomechanics **34**(7): 883-893.

Heller, M. O., Bergmann, G., Kassi, J. P., Claes, L., Haas, N. P. and Duda, G. N. (2005). "Determination of Muscle Loading at the Hip Joint for Use in Pre-Clinical Testing." Journal of Biomechanics **38**(5): 1155-1163.

Heller, M. O., Perka, C., Wilke, K., Haas, N. P., Zippel, H. and Duda, G. N. (2003). Surgical Approach in Total Hip Arthroplasty Causes Long Term Differences in Periprosthetic Femoral Bone Densities. 49th Annual Meeting of the Orthopaedic Research Society, New Orleans, LA, USA.

Hill, A. V. (1926). "The Viscous Elastic Properties of Smooth Muscle." Proceedings of the Royal Society of London. Series B, Containing Papers of a Biological Character **100**(701): 108-115.

Hill, A. V. (1938). "The Heat of Shortening and the Dynamic Constants of Muscle." Proceedings of the Royal Society of London. Series B, Biological Sciences **126**(843): 136-195.

Hill, A. V. (1950). "The Series Elastic Component of Muscle." Proceedings of the Royal Society of London. Series B, Biological Sciences **137**(887): 273-280.

Hill, A. V. (1953). "The Mechanics of Active Muscle." Proceedings of the Royal Society of London. Series B, Biological Sciences **141**(902): 104-117.

Hirakawa, K., Mitsugi, N., Koshino, T., Saito, T., Hirasawa, Y. and Kubo, T. (2001). "Effect of Acetabular Cup Position and Orientation in Cemented Total Hip Arthroplasty." Clinical Orthopaedics and Related Research **388**: 135-142.

Hodgskinson, R. and Currey, J. D. (1992). "Young's Modulus, Density and Material Properties in Cancellous Bone over a Large Density Range." Journal of Materials Science: Materials in Medicine **3**(5): 377-381.

Hoek van Dijke, G. A., Snijders, C. J., Stoeckart, R. and Stam, H. J. (1999). "A Biomechanical Model on Muscle Forces in the Transfer of Spinal Load to the Pelvis and Legs." Journal of Biomechanics **32**(9): 927-933.

Holt, C. A. and Whatling, G. M. (2009). Unversity of Cardiff.

Hoy, M. G., Zajac, F. E. and Gordon, M. E. (1990). "A Musculosketal Model of the Human Lower Extremity: The Effect of Muscle, Tendon and Moment Arm on the Moment-Angle Relationship of Musculotendon Actuators at the Hip, Knee and Ankle." Journal of Biomechanics **23**(2): 157-169.

Hu, K., Zhang, X., Zhu, J., Wang, C., Ji, W. and Bai, X. (2009). "Periprosthetic Fractures May Be More Likely in Cementless Femoral Stems with Sharp Edges." Irish Journal of Medical Science **Epub ahead of print**.

Huard, J., Li, Y. and Fu, F. H. (2002). "Muscle Injuries and Repair: Current Trends in Research." Journal of Bone and Joint Surgery (Am.) **84**(5): 822-832.

Huiskes, R. (1990). "The Various Stress Patterns of Press-Fit, Ingrown and Cemented Femoral Stems." Clinical Orthopaedics and Related Research **261**: 27-38.

Huiskes, R. (1993). "Failed Innovation in Total Hip Replacement: Diagnosis and Proposals for a Cure." Acta Orthopaedica **64**(6): 699-716.

Huiskes, R., Weinans, H., Grootenboer, H. J., Dalstra, M., Fudala, B. and Slooff, T. J. (1987). "Adaptive Bone-Remodeling Theory Applied to Prosthetic-Design Analysis." Journal of Biomechanics **20**(11-12): 1135-1150.

Hung, J.-P., Chen, J.-H., Chiang, H.-L. and Wu, J. S.-S. (2004). "Computer Simulation on Fatigue Behavior of Cemented Hip Prostheses: A Physiological Model." Computer Methods and Programs in Biomedicine **76**(2): 103-113.

Iglic, A., Antolic, V. and Srakar, F. (1993). "Biomechanical Analysis of Various Operative Hip Joint Rotation Center Shifts." Archives of Orthopaedic and Trauma Surgery **112**(3): 124-126.

Ingham, E. and Fisher, J. (2000). "Biological Reactions to Wear Debris in Total Joint Replacement." Proceedings of the Institution of Mechanical Engineers, Part H: Journal of Engineering in Medicine **214**(1): 21-37.

Jasty, M., Maloney, W. J., Bragdon, C. R., O'Connor, D. O., Haire, T. and Harris, W. H. (1991). "The Initiation of Failure in Cemented Femoral Components of Hip Arthroplasties." Journal of Bone and Joint Surgery (Br.) **73**(4): 551-558.

Jerosch, J., Steinbeck, J., Stechmann, J. and Güth, V. (1997). "Influence of a High Hip Center on Abductor Muscle Function." Archives of Orthopaedic and Trauma Surgery **116**(6): 385-389.

Johnston, R., Brand, R. and Crowninshield, R. (1979). "Reconstruction of the Hip. A Mathematical Approach to Determine Optimum Relationships." Journal of Bone and Joint Surgery (Am.) **61**(5): 639-652.

Johnston, R. and Smidt, G. (1969). "Measurement of Hip-Joint Motion During Walking: Evaluation of an Electrogoniometric Method." Journal of Bone and Joint Surgery (Am.) **51**(6): 1083-1094.

Jonkers, I., Sauwen, N., Lenaerts, G., Mulier, M., Van der Perre, G. and Jaecques, S. (2008). "Relation between Subject-Specific Hip Joint Loading, Stress Distribution in the Proximal Femur and Bone Mineral Density Changes after Total Hip Replacement." Journal of Biomechanics **41**(16): 3405-3413.

Kääriäinen, M., Kääriäinen, J., Järvinen, T., Sievänen, H., Kalimo, H. and Järvinen, M. (1998). "Correlation between Biomechanical and Structural Changes During the Regeneration of Skeletal Muscle after Laceration Injury." Journal of Orthopeadic Research **16**(2): 197-206.

Kadir, M. R. A. and Kamsah, N. (2009). "Interface Micromotion of Cementless Hip Stems in Simulated Hip Arthroplasty." American Journal of Applied Sciences **6**(9): 1682-1689.

Karachalios, T., Hartofilakidis, G., Zacharakis, N. and Tsekoura, M. (1993). "A 12- to 18-Year Radiographic Follow-up Study of Charnley Low-Friction Arthroplasty. The Role of the Center of Rotation." Clinical Orthopaedics and Related Research **296**: 140-147.

Kärrholm, J., Garellick, G. and Herberts, P. (2007). Swedish Hip Arthroplasty Register. Annual Report 2006, Department of Orthopaedics, Sahlgrenska University Hospital.

Kärrholm, J., Garellick, G., Rogmark, C. and Herberts, P. (2008). Swedish Hip Arthroplasty Register. Annual Report 2007, Department of Ortopaedics, Sahlgrenska University Hospital.

Kayabasi, O. and Ekici, B. (2008). "Probabilistic Design of a Newly Designed Cemented Hip Prosthesis Using Finite Element Method." Materials and Design **29**(5): 963-971.

Kayabasi, O. and Erzincanli, F. (2006). "Finite Element Modelling and Analysis of a New Cemented Hip Prosthesis." Advances in Engineering Software **37**: 477-483.

Keaveny, T. M. and Bartel, D. L. (1993). "Effects of Porous Coating, with and without Collar Support, on Early Relative Motion for a Cementless Hip Prosthesis." Journal of Biomechanics **26**(12): 1355-1368.

Keaveny, T. M. and Bartel, D. L. (1995). "Mechanical Consequences of Bone Ingrowth in a Hip Prosthesis Inserted without Cement." Journal of Bone and Joint Surgery (Am.) **77**(6): 911-923.

Kennon, R. E., Keggi, J. M., Wetmore, R. S., Zatorski, L. E., Huo, M. H. and Keggi, K. J. (2003). "Total Hip Arthroplasty through a Minimally Invasive Anterior Surgical Approach." Journal of Bone and Joint Surgery (Am.) **85**(Suppl. 4): 39-48.

Keyak, J. H. and Rossi, S. A. (2000). "Prediction of Femoral Fracture Load Using Finite Element Models: An Examination of Stress- and Strain-Based Failure Theories." Journal of Biomechanics **33**(2): 209-214.

Kingston, B. (1996). Understanding Muscles: A Practical Guide to Muscle Function, Stanley Thornes (Publishers) Ltd.

Kiyama, T., Naito, M., Shitama, H. and Maeyama, A. (2009). "Effect of Superior Placement of the Hip Center on Abductor Muscle Strength in Total Hip Arthroplasty." The Journal of Arthroplasty **24**(2): 240-245.

Klein Horsman, M. D., Koopman, H. F. J. M., van der Helm, F. C. T., Prose, L. P. and Veeger, H. E. J. (2007). "Morphological Muscle and Joint Parameters for Musculoskeletal Modelling of the Lower Extremity." Clinical Biomechanics **22**(2): 239-247.

Kluess, D., Martin, H., Mittelmeier, W., Schmitz, K.-P. and Bader, R. (2007). "Influence of Femoral Head Size on Impingement, Dislocation and Stress Distribution in Total Hip Replacement." Medical Engineering and Physics **29**(4): 465-471.

Kopperdahl, D. L. and Keaveny, T. M. (1998). "Yield Strain Behavior of Trabecular Bone." Journal of Biomechanics **31**(7): 601-608.

Lanyon, L. E., Hampson, W. G. J., Goodship, A. E. and Shah, J. S. (1975). "Bone Deformation Recorded in Vivo from Strain Gauges Attached to the Human Tibial Shaft." Acta Orthopaedica **46**(2): 256-268.

Lecerf, G., Fessy, M. H., Philippot, R., Massin, P., Giraud, F., Flecher, X., Girard, J., Mertl, P., Marchetti, E. and Stindel, E. (2009). "Femoral Offset: Anatomical Concept, Definition, Assessment, Implications for Preoperative Templating and Hip Arthroplasty." Orthopaedics and Traumatology: Surgery & Research **95**(3): 210-219.

Lenaerts, G., Bartels, W., Gelaude, F., Mulier, M., Spaepen, A., Van der Perre, G. and Jonkers, I. (2009). "Subject-Specific Hip Geometry and Hip Joint Centre Location Affects Calculated Contact Forces at the Hip During Gait." Journal of Biomechanics **42**(9): 1246-1251.

Lenaerts, G., De Groote, F., Demeulenaere, B., Mulier, M., Van der Perre, G., Spaepen, A. and Jonkers, I. (2008). "Subject-Specific Hip Geometry Affects Predicted Hip Joint Contact Forces During Gait." Journal of Biomechanics **41**(6): 1243-1252.

Lengsfeld, M., Bassaly, A., Boudriot, U., Pressel, T. and Griss, P. (2000). "Size and Direction of Hip Joint Forces Associated with Various Positions of the Acetabulum." The Journal of Arthroplasty **15**(3): 314-320.

Lewis, C. L., Sahrmann, S. A. and Moran, D. W. (2007). "Anterior Hip Joint Force Increases with Hip Extension, Decreased Gluteal Force, or Decreased Iliopsoas Force." Journal of Biomechanics **40**(16): 3725-3731.

Little, J. P., Gray, H. A., Murray, D. W., Beard, D. J. and Gill, H. S. (2008). "Thermal Effects of Cement Mantle Thickness for Hip Resurfacing." The Journal of Arthroplasty **23**(3): 454-458.

Lloyd, D. G. and Besier, T. F. (2003). "An Emg-Driven Musculoskeletal Model to Estimate Muscle Forces and Knee Joint Moments in Vivo." Journal of Biomechanics **36**(6): 765-776.

Lotz, J. C., Cheal, E. J. and Hayes, W. C. (1991). "Fracture Prediction for the Proximal Femur Using Finite Element Models: Part I - Linear Analysis." Journal of Biomechanical Engineering **113**(4): 353-360.

Low, J. and Reed, A. (1996). Basic Biomechanics Explained. Oxford, Butterworth-Heinemann.

Lu, T.-W., O'Connor, J. J., Taylor, S. J. G. and Walker, P. S. (1998). "Validation of a Lower Limb Model with in Vivo Femoral Forces Telemetered from Two Subjects." Journal of Biomechanics **31**(1): 63-69.

Lundberg, A. (1996). "On the Use of Bone and Skin Markers in Kinematics Research." Human Movement Science **15**: 411-422.

Mackenzie, J. R., Kelley, S. S. and Johnston, R. C. (1996). "Total Hip Replacement for Coxarthrosis Secondary to Congenital Dysplasia and Dislocation of the Hip. Long-Term Results." Journal of Bone and Joint Surgery (Am.) **78**(1): 55-61.

Madsen, M. S., Ritter, M. A., Morris, H. H., Meding, J. B., Berend, M. E., Faris, P. M. and Vardaxis, V. G. (2004). "The Effect of Total Hip Arthroplasty Surgical Approach on Gait." Journal of Orthopaedic Research **22**(1): 44-50.

Mahomed, N. N., Arndt, D. C., McGrory, B. J. and Harris, W. H. (2001). "The Harris Hip Score: Comparison of Patient Self-Report with Surgeon Assessment." The Journal of Arthroplasty **16**(5): 575-580.

Malchau, H., Herberts, P., Garellick, G., Soderman, P. and Eisler, T. (2002). Prognosis of Total Hip Replacement. Update of Results and Risk-Ratio Analysis for Revision and Re-Revision from the Swedish National Hip Arthroplasty Register 1979-2000, Department of Orthopaedics. Goteborg University, Sweden: 1-18.

Malik, A. and Dorr, L. D. (2007). "The Science of Minimally Invasive Total Hip Arthroplasty." Clinical Orthopaedics and Related Research **463**: 74-84.

Marieb, E. N. (2006). Essentials of Human Anatomy and Physiology. San Francisco; London, Pearson/Benjamin Cummings.

Masonis, J. L. and Bourne, R. B. (2002). "Surgical Approach, Abductor Function, and Total Hip Arthroplasty Dislocation." Clinical Orthopaedics and Related Research **405**: 46-53.

Mayr, E., Nogler, M., Benedetti, M.-G., Kessler, O., Reinthaler, A., Krismer, M. and Leardini, A. (2009). "A Prospective Randomized Assessment of Earlier Functional Recovery in Tha Patients Treated by Minimally Invasive Direct Anterior Approach: A Gait Analysis Study." Clinical Biomechanics **24**(10): 812-818.

McCollum, D. E. and Gray, W. J. (1990). "Dislocation after Total Hip Arthroplasty Causes and Prevention." Clinical Orthopaedics and Related Research **261**: 159-170.

Meneghini, R. M., Pagnano, M. W., Trousdale, R. T. and Hozack, W. J. (2006). "Muscle Damage During Mis Total Hip Arthroplasty: Smith-Peterson Versus Posterior Approach." Clinical Orthopaedics and Related Research **453**: 293-298.

Menon, P. C., Griffiths, W. E. G., Hook, W. E. and Higgins, B. (1998). "Trochanteric Osteotomy in Total Hip Arthroplasty : Comparison of 2 Techniques." The Journal of Arthroplasty **13**(1): 92-96.

Milner-Brown, H. S. and Stein, R. B. (1975). "The Relation between the Surface Electromyogram and Muscular Force." Journal of Physiology **246**(3): 549-569.

Mjöberg, B., Hansson, L. I. and Selvik, G. (1984). "Instability of Total Hip Prostheses at Rotational Stress: A Roentgen Stereophotogrammetric Study." Acta Orthopaedica **55**(5): 504-506.

Mjöberg, B., Selvik, G., Hansson, L. I., Rosenqvist, R. and Onnerfält, R. (1986). "Mechanical Loosening of Total Hip Prostheses. A Radiographic and Roentgen Stereophotogrammetric Study." Journal of Bone and Joint Surgery (Br.) **68**(5): 770-774.

Morgan, E. F., Bayraktar, H. H. and Keaveny, T. M. (2003). "Trabecular Bone Modulus-Density Relationships Depend on Anatomic Site." Journal of Biomechanics **36**(7): 897-904.

Morgan, E. F. and Keaveny, T. M. (2001). "Dependence of Yield Strain of Human Trabecular Bone on Anatomic Site." Journal of Biomechanics **34**(5): 569-577.

Morlock, M., Schneider, E., Bluhm, A., Vollmer, M., Bergmann, G., Muller, V. and Honl, M. (2001). "Duration and Frequency of Every Day Activities in Total Hip Patients." Journal of Biomechanics **34**(7): 873-881.

Morse, C. I., Thom, J. M., Reeves, N. D., Birch, K. M. and Narici, M. V. (2005). "In Vivo Physiological Cross-Sectional Area and Specific Force Are Reduced in the Gastrocnemius of Elderly Men." Journal of Applied Physiology **99**(3): 1050-1055.

Mow, V. C. and Huiskes, R. (2005). Basic Orthopaedic Biomechanics and Mechano-Biology. Philadelphia, Lippincott Williams and Wilkins.

Mulroy, R. and Harris, W. (1990). "Failure of Acetabular Autogenous Grafts in Total Hip Arthroplasty. Increasing Incidence: A Follow-up Note." Journal of Bone and Joint Surgery (Am.) **72**(10): 1536-1540.

National Joint Registry (2005). National Joint Registry for England and Wales. 3rd Annual Clinical Report.

National Joint Registry (2009). National Joint Registry for England and Wales. 6th Annual Clinical Report.

New, A. M. (2008). Hip Implanter, University of Southampton.

Nistor, L., Blaha, J. D., Kjellström, U. and Selvik, G. (1991). "In Vivo Measurements of Relative Motion between an Uncemented Femoral Total Hip Component and the Femur by Roentgen Stereophotogrammetric Analysis." Clinical Orthopaedics and Related Research **269**: 220-227.

Pagnano, M., Hanssen, A., Lewallen, D. and Shaughnessy, W. (1996). "The Effect of Superior Placement of the Acetabular Component on the Rate of Loosening after Total Hip Arthroplasty. Long-Term Results in Patients Who Have Crowe Type-Ii Congenital Dysplasia of the Hip." Journal of Bone and Joint Surgery (Am.) **78**(7): 1004-1014.

Pancanti, A., Bernakiewicz, M. and Viceconti, M. (2003). "The Primary Stability of a Cementless Stem Varies between Subjects as Much as between Activities." Journal of Biomechanics **36**(6): 777-785.

Park, Y., Choi, D., Hwang, D. S. and Yoon, Y.-S. (2009). "Statistical Analysis of Interfacial Gap in a Cementless Stem Fe Model." Journal of Biomechanical Engineering **131**(2): 021016.

Park, Y., Shin, H., Choi, D., Albert, C. and Yoon, Y.-S. (2008). "Primary Stability of Cementless Stem in Tha Improved with Reduced Interfacial Gaps." Journal of Biomechanical Engineering **130**(2): 021008.

Parks, M. and Macaulay, W. (2000). "Operative Approaches for Total Hip Replacement." Operative Techniques in Orthopaedics **10**(2): 106-114.

Patriarco, A. G., Mann, R. W., Simon, S. R. and Mansour, J. M. (1981). "An Evaluation of the Approaches of Optimization Models in the Prediction of Muscle Forces During Human Gait." Journal of Biomechanics **14**(8): 513-525.

Paul, J. P. (1966). "Biomechanics. The Biomechanics of the Hip-Joint and Its Clinical Relevance." Proceeding Of The Royal Society Of Medicine **59**(10): 943-948.

Paul, J. P. (1966). "Forces Transmitted by Joints in the Human Body." Proceedings of the Institution of Mechanical Engineers **181**(3J): 8-15.

Pedersen, D. R., Brand, R. A. and Davy, D. T. (1997). "Pelvic Muscle and Acetabular Contact Forces During Gait." Journal of Biomechanics **30**(9): 959-965.

Perka, C., Heller, M., Wilke, K., Taylor, W. R., Haas, N. P., Zippel, H. and Duda, G. N. (2005). "Surgical Approach Influences Periprosthetic Femoral Bone Density." Clinical Orthopaedics and Related Research **432**: 153-159.

Perron, M., Malouin, F., Moffet, H. and McFadyen, B. J. (2000). "Three-Dimensional Gait Analysis in Women with a Total Hip Arthroplasty." Clinical Biomechanics **15**(7): 504-515.

Pettersen, S. H., Wik, T. S. and Skallerud, B. (2009). "Subject Specific Finite Element Analysis of Implant Stability for a Cementless Femoral Stem." Clinical Biomechanics **24**(6): 480-487.

Phillips, A. T. M. (2009). "The Femur as a Musculo-Skeletal Construct: A Free Boundary Condition Modelling Approach." Medical Engineering and Physics **31**(6): 673-680.

Pilliar, R. M., Lee, J. M. and Maniatopoulos, C. (1986). "Observations on the Effect of Movement on Bone Ingrowth into Porous-Surfaced Implants." Clinical Orthopaedics and Related Research **208**: 108-113.

Polgár, K., Gill, H., Viceconti, M., Murray, D. and O'Connor, J. (2003). "Strain Distribution within the Human Femur Due to Physiological and Simplified Loading: Finite Element Analysis Using the Muscle Standardized Femur Model." Proceedings of the Institution of Mechanical Engineers, Part H: Journal of Engineering in Medicine **217**(3): 173-189.

Pospischill, M., Kranzl, A., Attwenger, B. and Knahr, K. (2010). "Approach for Total Hip Arthroplasty: A Comparative Gait Analysis Minimally Invasive Compared with Traditional Transgluteal." Journal of Bone and Joint Surgery (Am.) **92**(2): 328-337.

Rasmussen, J., Damsgaard, M. and Voigt, M. (2001). "Muscle Recruitment by the Min/Max Criterion - a Comparative Numerical Study." Journal of Biomechanics **34**(3): 409-415.

Reggiani, B., Cristofolini, L., Taddei, F. and Viceconti, M. (2008). "Sensitivity of the Primary Stability of a Cementless Hip Stem to Its Position and Orientation." Artificial Organs **32**(7): 555-560.

Restrepo, C., Parvizi, J., Pour, A. E. and Hozack, W. J. (2010). "Prospective Randomized Study of 2 Surgical Approaches for Total Hip Arthroplasty." The Journal of Arthroplasty **In Press, Corrected Proof**.

Rice, J. C., Cowin, S. C. and Bowman, J. A. (1988). "On the Dependence of the Elasticity and Strength of Cancellous Bone on Apparent Density." Journal of Biomechanics **21**(2): 155-168.

Robertson, D. G. E., Caldwell, G. E., Hamill, J., Kamen, G. and Whittlesey, S. N. (2004). Research Methods in Biomechanics, Human Kinetics.

Robinson, R. P., Robinson Jr., H. J. and Salvati, E. A. (1980). "Comparison of the Transtrochanteric and Posterior Approaches for the Total Hip Replacement." Clinical Orthopaedics and Related Research **147**: 143-147.

Rohlmann, A., Mossner, U. and Bergmann, G. (1983). "Finite-Element-Analysis and Experimental Investigation in a Femur with Hip Endoprosthesis." Journal of Biomechanics **16**(9): 727-742.

Rotem, A. (1994). "Effect of Implant Material Properties on the Performance of a Hip Joint Replacement." Journal of Medical Engineering & Technology **18**(6): 208-217.

Russotti, G. M. and Harris, W. H. (1991). "Proximal Placement of the Acetabular Component in Total Hip Arthroplasty. A Long-Term Follow-up Study " Journal of Bone and Joint Surgery (Am.) **73**(4): 587-592.

Rydell, N. W. (1966). "Forces Acting on the Femoral Head-Prosthesis." Acta Orthopaedica **37**(Supplement 88): 1-132.

Sakai, R., Sato, Y., Itoman, M. and Mabuchi, K. (2010). "Initial Fixation of a Finite Element Model of an Ai-Hip Cementless Stem Evaluated by Micromotion and Stress." Journal of Orthopaedic Science **5**(1): 132-139.

Schileo, E., Dall'Ara, E., Taddei, F., Malandrino, A., Schotkamp, T., Baleani, M. and Viceconti, M. (2008). "An Accurate Estimation of Bone Density Improves the Accuracy of Subject-Specific Finite Element Models." Journal of Biomechanics **41**(11): 2483-2491.

Schileo, E., Taddei, F., Cristofolini, L. and Viceconti, M. (2008). "Subject-Specific Finite Element Models Implementing a Maximum Principal Strain Criterion Are Able to Estimate Failure Risk and Fracture Location on Human Femurs Tested in Vitro." Journal of Biomechanics **41**(2): 356-367.

Scovil, C. Y. and Ronsky, J. L. (2006). "Sensitivity of a Hill-Based Muscle Model to Perturbations in Model Parameters." Journal of Biomechanics **39**(11): 2055-2063.

Seireg, A. and Arvikar, R. J. (1973). "A Mathematical Model for Evaluation of Forces in Lower Extremeties of the Musculo-Skeletal System." Journal of Biomechanics **6**(3): 313-326.

Seireg, A. and Arvikar, R. J. (1975). "The Prediction of Muscular Load Sharing and Joint Forces in the Lower Extremities During Walking." Journal of Biomechanics **8**(2): 89-102.

Shih, K. S., Tseng, C. S., Lee, C. C. and Lin, S. C. (2008). "Influence of Muscular Contractions on the Stress Analysis of Distal Femoral Interlocking Nailing." Clinical Biomechanics **23**(1): 38-44.

Simões, J. A., Vaz, M. A., Blatcher, S. and Taylor, M. (2000). "Influence of Head Constraint and Muscle Forces on the Strain Distribution within the Intact Femur." Medical Engineering and Physics **22**(7): 453-459.

Siopack, J. S. and Jergesen, H. E. (1995). "Total Hip Arthroplasty." Western Journal of Medicine **162**(3): 243-249.

Søballe, K., Hansen, E. S., Brockstedt-Rasmussen, H. and Bünger, C. (1993). "Hydroxyapatite Coating Converts Fibrous Tissue to Bone around Loaded Implants." Journal of Bone and Joint Surgery (Br.) **75**: 270-278.

Speirs, A. D., Heller, M. O., Duda, G. N. and Taylor, W. R. (2007). "Physiologically Based Boundary Conditions in Finite Element Modelling." Journal of Biomechanics **40**(10): 2318-2323.

Speirs, A. D., Heller, M. O., Taylor, W. R., Duda, G. N. and Perka, C. (2007). "Influence of Changes in Stem Positioning on Femoral Loading after Thr Using a Short-Stemmed Hip Implant." Clinical Biomechanics **22**(4): 431-439.

Stagni, R., Leardini, A., Cappozzo, A., Grazia Benedetti, M. and Cappello, A. (2000). "Effects of Hip Joint Centre Mislocation on Gait Analysis Results." Journal of Biomechanics **33**(11): 1479-1487.

Stansfield, B. W., Nicol, A. C., Paul, J. P., Kelly, I. G., Graichen, F. and Bergmann, G. (2003). "Direct Comparison of Calculated Hip Joint Contact Forces with Those Measured Using Instrumented Implants. An Evaluation of a Three-Dimensional Mathematical Model of the Lower Limb." Journal of Biomechanics **36**(7): 929-936.

Stolk, J., Verdonschot, N. and Huiskes, R. (2001). "Hip-Joint and Abductor-Muscle Forces Adequately Represent in Vivo Loading of a Cemented Total Hip Reconstruction." Journal of Biomechanics **34**(7): 917-926.

Suh, J.-K., Scherping, S., Mardi, T., Richard Steadman, J. and Woo, S. L. Y. (1995). "Basic Science of Articular Cartilage Injury and Repair." Operative Techniques in Sports Medicine **3**(2): 78-86.

Szmukler-Moncler, S., Salama, H., Reingewirtz, Y. and Dubruille, J. H. (1998). "Timing of Loading and Effect of Micromotion on Bone-Dental Implant Interface: Review of Experimental Literature." Journal of Biomedical Materials Research **43**(2): 192-203.

Taddei, F., Pani, M., Zovatto, L., Tonti, E. and Viceconti, M. (2008). "A New Meshless Approach for Subject-Specific Strain Prediction in Long Bones: Evaluation of Accuracy." Clinical Biomechanics **23**(9): 1192-1199.

Taylor, M., Tanner, K. E., Freeman, M. A. R. and Yettram, A. L. (1995). "Cancellous Bone Stresses Surrounding the Femoral Component of a Hip Prosthesis: An Elastic-Plastic Finite Element Analysis." Medical Engineering and Physics **17**(7): 544-550.

Taylor, M. E., Tanner, K. E., Freeman, M. A. and Yettram, A. L. (1996). "Stress and Strain Distribution within the Intact Femur: Compression or Bending?" Medical Engineering and Physics **18**(2): 122-131.

Taylor, S. J. G., Perry, J. S., Meswania, J. M., Donaldson, N., Walker, P. S. and Cannon, S. R. (1997). "Telemetry of Forces from Proximal Femoral Replacements and Relevance to Fixation." Journal of Biomechanics **30**(3): 225-234.

Taylor, S. J. G. and Walker, P. S. (2001). "Forces and Moments Telemetered from Two Distal Femoral Replacements During Various Activities." Journal of Biomechanics **34**(7): 839-848.

Tensi, H. M., Gese, H. and Ascherl, R. (1989). "Non-Linear Three-Dimensional Finite Element Analysis of a Cementless Hip Endoprosthesis." Proceedings of the Institution of Mechanical Engineers, Part H: Journal of Engineering in Medicine **203**(4): 215-222.

Thaller, S. and Wagner, H. (2004). "The Relation between Hill's Equation and Individual Muscle Properties." Journal of Theoretical Biology **231**(3): 319-332.

Traina, F., De Fine, M., Biondi, F., Tassinari, E., Galvani, A. and Toni, A. (2009). "The Influence of the Centre of Rotation on Implant Survival Using a Modular Stem Hip Prosthesis." International Orthopaedics (SICOT) **33**(6): 1513-1518.

Ulrich, S. D., Seyler, T. M., Bennett, D., Delanois, R. E., Saleh, K. J., Thongtrangan, I., Kuskowski, M., Cheng, E. Y., Sharkey, P. F., Parvizi, J., Stiehl, J. B. and Mont, M. A. (2008). "Total Hip Arthroplasties: What Are the Reasons for Revision?" International Orthopaedics (SICOT) **32**(5): 597-604.

van Bolhuis, B. M. and Gielen, C. C. A. M. (1999). "A Comparison of Models Explaining Muscle Activation Patterns for Isometric Contractions." Biological Cybernetics **81**(3): 249-261.

van der Helm, F. C. T. and Veenbaas, R. (1991). "Modelling the Mechanical Effect of Muscles with Large Attachment Sites: Application to the Shoulder Muscle." Journal of Biomechanics **24**(12): 1151-1163.

Van Wynsberghe, D. V., Noback, C. R. and Carola, R. (1995). Human Anatomy & Physiology, WCB/McGraw-Hill.

Vasavada, A. N., Delp, S. L., Maloney, W. J., Schurman, D. J. and Zajac, F. E. (1994). "Compensating for Changes in Muscle Length in Total Hip Arthroplasty." Clinical Orthopaedics and Related Research **302**: 121-133.

Vaughan, C. L., Davis, B. L. and O'Connor, J. C. (1992). Dynamics of Human Gait. Cape Town, South Africa, Kiboho Publishers.

Verdonschot, N. J., Huiskes, R. and Freeman, M. A. (1993). "Pre-Clinical Testing of Hip Prosthetic Designs: A Comparison of Finite Element Calculations and Laboratory Tests." Proceedings of the Institution of Mechanical Engineers, Part H: Journal of Engineering in Medicine **207**(3): 149-154.

Vicar, A. J. and Coleman, C. L. (1984). "A Comparison of the Anterolateral, Transtrochanteric and Posterior Surgical Approaches in Primary Total Hip Arthroplasty." Clinical Orthopaedics and Related Research **188**: 152-159.

Viceconti, M., Brusi, G., Pancanti, A. and Cristofolini, L. (2006). "Primary Stability of an Anatomical Cementless Hip Stem: A Statistical Analysis." Journal of Biomechanics **39**(7): 1169-1179.

Viceconti, M., Monti, L., Muccini, R., Bernakiewicz, M. and Toni, A. (2001). "Even a Thin Layer of Soft Tissue May Compromise the Primary Stability of Cementless Hip Stems." Clinical Biomechanics **16**(9): 765-775.

Viceconti, M., Muccini, R., Bernakiewicz, M., Baleani, M. and Cristofolini, L. (2000). "Large-Sliding Contact Elements Accurately Predict Levels of Bone-Implant Micromotion Relevant to Osseointegration." Journal of Biomechanics **33**(12): 1611-1618.

Viceconti, M., Pancanti, A., Varini, E., Traina, F. and Cristofolini, L. (2006). "On the Biomechanical Stability of Cementless Straight Conical Hip Stems." Proceedings

of the Institution of Mechanical Engineers, Part H: Journal of Engineering in Medicine **220**(3): 473-480.

Wan, Z., Boutary, M. and Dorr, L. D. (2008). "The Influence of Acetabular Component Position on Wear in Total Hip Arthroplasty." The Journal of Arthroplasty **23**(1): 51-56.

Watanabe, Y., Shiba, N., Matsuo, S., Higuchi, F., Tagawa, Y. and Inoue, A. (2000). "Biomechanical Study of the Resurfacing Hip Arthroplasty: Finite Element Analysis of the Femoral Component." The Journal of Arthroplasty **15**(4): 505-511.

Whatling, G. M., Dabke, H. V., Holt, C. A., Jones, L., Madete, J., Alderman, P. M. and Roberts, P. (2008). "Objective Functional Assessment of Total Hip Arthroplasty Following Two Common Surgical Approaches: The Posterior and Direct Lateral Approaches." Proceedings of the Institution of Mechanical Engineers, Part H: Journal of Engineering in Medicine **222**(6): 897-905.

Whatling, G. M., Holt, C. A., Jones, L., Madete, J. K., Dabke, H., Alderman, P. M. and Roberts, P. (2006). Investigating the Effects of Surgical Approach on Total Hip Arthroplasty Recovery Using 3d Gait Analysis. Ninth Symposium on 3-D Analysis of Human Movement, Valenciennes, France.

Whiting, W., C. and Zernicke, R. F. (1998). Biomechanics of Musculoskeletal Injury, Human Kinetics.

Wickiewicz, T. L., Roy, R. R., Powell, P. L. and Reggie Edgerton, V. (1983). "Muscle Architecture of the Human Lower Limb." Clinical Orthopaedics and Related Research **179**: 275-283.

Witzleb, W.-C., Ziegler, J., Krummenauer, F., Neumeister, V. and Guenther, K.-P. (2006). "Exposure to Chromium, Cobalt and Molybdenum from Metal-on-Metal Total Hip Replacement and Hip Resurfacing Arthroplasty." Acta Orthopaedica **77**(5): 697-705.

Wong, A. S., New, A. M., Isaacs, G. and Taylor, M. (2005). "Effect of Bone Material Properties on the Initial Stability of a Cementless Hip Stem: A Finite Element Study." Proceedings of the Institution of Mechanical Engineers, Part H: Journal of Engineering in Medicine **219**(4): 265-275.

Woo, R. Y. G. and Morrey, B. F. (1982). "Dislocations after Total Hip-Arthroplasty." Journal of Bone and Joint Surgery (Am.) **64**(9): 1295-1306.

Worsley, P. (2009). Bioengineering Sciences Research Group and Physiotherapy, Univerisity of Southampton.

Wright Medical Technology (2010). "Profemur Total Hip Modular Neck." [Accessed 2010], from http://www.wmt.com/Physicians/Products/Hips/PROFEMURTotalHipSystem.asp .

Wroblewski, B. M. and Siney, P. D. (1993). "Charnley Low-Friction Arthroplasty of the Hip: Long-Term Results." Clinical Orthopaedics and Related Research **292**: 191-201.

Yoder, S. A., Brand, R. A., Pedersen, D. R. and O'Gorman, T. W. (1988). "Total Hip Acetabular Position Affects Component Loosening Rates." Clinical Orthopaedics and Related Research **228**: 79-87.

Young, J. L., Fritz, A., Liu, G., Thoburn, K., Kres, J. and Roffers, S. (2000). "Muscular System: Structure of a Skeletal Muscle." [Accessed 2007], from http://training.seer.cancer.gov/module_anatomy/unit4_2_muscle_structure.html.

Zajac, F. E., Neptune, R. R. and Kautz, S. A. (2002). "Biomechanics and Muscle Coordination of Human Walking Part I: Introduction to Concepts, Power Transfer, Dynamics and Simulations." Gait and Posture **16**(3): 215-232.

Zannoni, C., Mantovani, R. and Viceconti, M. (1998). "Material Properties Assignment to Finite Element Models of Bone Structures: A New Method." Medical Engineering and Physics **20**(10): 735-740.

Zimmerman, S., Hawkes, W. G., Hudson, J. I., Magaziner, J., Richard Hebel, J., Towheed, T., Gardner, J., Provenzano, G. and Kenzora, J. E. (2002). "Outcomes of Surgical Management of Total Hip Replacement in Patients Aged 65 Years and Older: Cemented Versus Cementless Femoral Components and Lateral or Anterolateral Versus Posterior Anatomical Approach." Journal of Orthopaedic Research **20**(2): 182-191.

Zioupos, P., Cook, R. B. and Hutchinson, J. R. (2008). "Some Basic Relationships between Density Values in Cancellous and Cortical Bone." Journal of Biomechanics **41**(9): 1961-1968.